CAVITATION AND OTHER FREE SURFACE PHENOMENA.

by

C.BRENNEN , B.A.

Thesis submitted for the degree of
Doctor of Philosophy at Oxford
University , September 1966.

Balliol College,
Oxford.

Dept. of Engineering Science,
Oxford University.

PREFACE

The work presented in this thesis was carried out in the Department of Engineering Science , Oxford University , between the autumns of 1963 and 1966 under the supervision of Dr. L.C.Woods.

The author is deeply indebted to Dr. Woods for his help , both moral and technical , throughout, not only the duration of this work , but also during an undergraduate career under his auspices.

The author would also like to express his graditude ; to Professor L.Fox of the University Computing Laboratory and Dr. R.N.Franklin of the Engineering Department for valuable assistence ; to the Oxford Computing Department for the use of both their Ferranti Mercury and English Electric KDF9 computers ; to the Ministry of Education for Northern Ireland and to Balliol College for their financial support ; to the Ship Hydrodynamics Division of N.P.L. for an extremely useful vacation studentship ; to Miss E.J.McD.Kerr for her accurate typing and Mr. C.J.Brennen for the careful tracing of numerous diagrams ; and , finally , to my wife for her sympathy and devotion throughout the last three years.

CONTENTS

Page No.

CHAPTER 5 (Continued)

ABSTRACT

This thesis develops a method of solving axisymmetric cavity flow problems using a relaxation or numerical technique.

Chapter 1 contains a general review of the phenomenon of cavitation in fluids. Special reference is then made to fully developed cavities in an Euler or ideal fluid for both plane and axisymmetric flow. The basic theorems and equations are presented , with the various types of mathematical model which have been suggested. Details of the fundamental feature of this type of flow , namely the phenomenon of flow separation , are given. At the conclusion of the chapter the analytic methods of solution of plane cavitating flow and , in particular , those using the Riabouchinsky model , are outlined. The numerical results of a pertinant example of this type of flow are included in Appendix A with some additional comments on the phenomenon of choked cavity flow.

Chapter 2 provides a brief account of the previous approaches to the problem of axisymmetric cavitating flow. These include ; empirical results ; theories based on source-sink and vortex sheet distributions ; theories based on correlation with the corresponding plane flow solutions ; previous applications of relaxation methods.

Chapter 3 develops the basic equations for axisymmetric cavity flow in the transformed φ, Ψ plane in which it is proposed to solve for the dependent variable f (equal to r^2 , where r is the radial variable in the physical plane) . The equations prove to be of the non-linear elliptic type. Relations for the boundary conditions , and certain other relevant physical quantities , are then evolved in terms of the derivatives of f. . The determinacy of the problem in this plane requires careful investigation. Special reference is made to two important phenomena ; (i) that of the limiting condition of choked flow , for which certain important relations are developed and (ii) that of the two distinct types of separation in cavity flow. The derivation of expansions describing the singular behaviour of the flow in that region of the transformed plane is given in each case.

Chapter 4 describes the adaptation of the results of chapter 3 to provide a numerical or relaxation method of solving axisymmetric cavity flows. The finite difference forms of the field equation and boundary conditions in the φ, Ψ plane are first derived. Their application is then discussed with special attention being paid to the separation point and to the free streamline , the treatment of which provides the crux of the problem. Details are then given of the treatment of the singular points , a subject which has commanded little attention in the literature for the case of non-linear partial differential equations. Finally the application of the methods developed is summarized.

Chapter 5 presents the results obtained by the author ,both for the convergence of the methods and for the resulting cavity flows. Comparison is made with previous results , with the corresponding plane flow solutions and with experiment. Special reference is made to the behaviour of cavity flows near the choked flow condition , results which have an added significance in view of the fact that most experiments are carried out in the restricted environment of a water tunnel. In the final section some analysis of the errors is given.

CHAPTER 1

CHAPTER 1

1.1 INTRODUCTION.

The phenomenon of cavitation was first given publicity during the sea trials of H.M.S.Daring in 1885. It was noticed that in the region of the propellor blades, "cavities were being formed in the water.....and these were the source of the great waste of power and other difficulties which were encountered." This was, in the main, due to the fact that the vessel had been equipped with a new type of steam turbine engine giving higher blade velocities than had been previously reached. Only by increasing the blade area by about half as much again did the designers find it possible to approach the design speed of the craft. Not long after this incident it was found that the instability and collapse of these cavities on a particular part of the blade was the cause of considerable pitting and erosion in that region. Thus cavitation showed itself initially as a particularly harmful effect.

Since that time much research has gone into the phenomenon of cavitation , which could be defined as the formation of the vapour phase of a liquid that has been subjected to reduced pressures at more or less constant temperatures. This definition would include ordinary boiling and in fact the processes of boiling and cavitation have , as will be seen later , many things in common. As well as the vapour of the liquid , cavities may also contain gas which may have been introduced either

artificially or because the liquid contained absorbed gas. It is therefore not neccessarily true that the pressure within the cavity is the vapour pressure of the liquid at the operating temperature.

The object of this chapter is to describe in brief some of the factors known to influence cavitation , to give outlines of previous approaches to the problem and further , to isolate and define the particular problem whose solution is the main aim of this thesis.
[The terms "cavity" and "bubble" are interchangeable in this thesis both referring to the vapour or gas filled regions.]

1.2 NOTATION,TERMINOLOGY,AND GENERAL CHARACTERISTICS OF CAVITATING FLOWS.

1.2.1 Notation.

The basic quantities used in describing cavitating flows are listed below. A complete nomenclature may be found at the end of this thesis.

p	Pressure
p_v	Vapour pressure
ρ	Density,usually assumed constant in time and space
q	Fluid velocity magnitude
c	As a subscript to denote values in or on the surface of the cavity
∞	As a subscript to denote values at a reference point,taken as the point at infinity for a uniform stream

[1.1] $Q = (p_a - p_c) / \frac{1}{2}\rho q_a^2$,the cavitation number.

[1.2] $C_p = (p - p_a) / \frac{1}{2}\rho q_a^2$,the pressure coefficient.

The number Q proves to be a fundamental parameter in cavitating flows. As has been mentioned before p_c will be equal to p_v only if all gas has been excluded from the liquid and cavity. Surface tension and other factors such as the presence of thermal gradients may also prevent p_c from being equal to p_v. If gas is present then p_c will be the sum of p_v and the partial pressure of that gas in the cavity. From the above definitions,[1.1] and [1.2], we can say that on the liquid/vapour interface where $p = p_c$, $C_p = -Q$.

1.2.2 An Example.

In order to define some of the terms used in referring to cavitating flows,we shall now take a particular example and describe what happens in practice as we increase the velocity of the flow while maintaining p_c and p_a at constant values. From equation [1.1] this is equivalent to decreasing the cavitation number. Since this thesis will be mainly concerned with the cavitation around bodies in a uniform stream we will take the flow of water past a cylinder as our illustration.

For $Q > 1.5$, at normal temperatures, the cylinder has a completly liquid wake of turbulent form. As Q is decreased below about 1.2 ,tiny bubbles begin to form in the water at a point such as A (Fig. 1,1) near the surface of the cylinder. These bubbles then travel into the wake and

FIG.11 (Q~1.2)

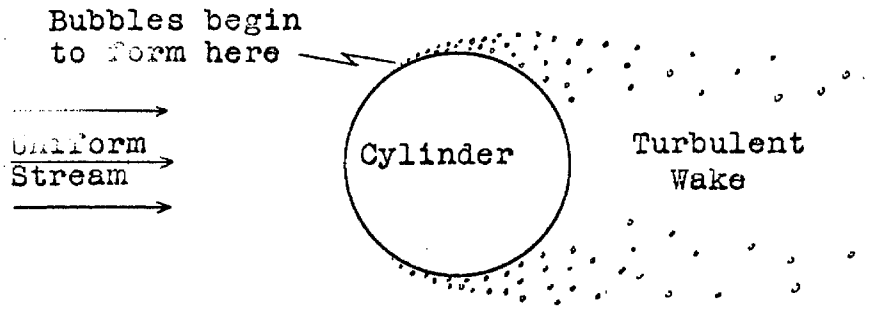

FIG.12 (Q~1.0)

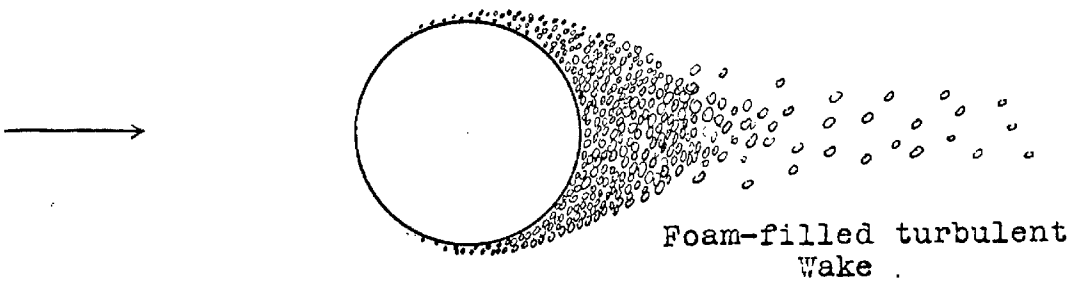

FIG.13 (Q~0.7)

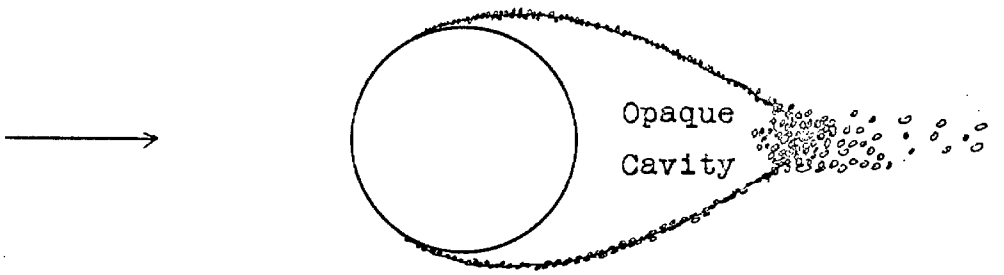

FIG.14 (Q~0.5)

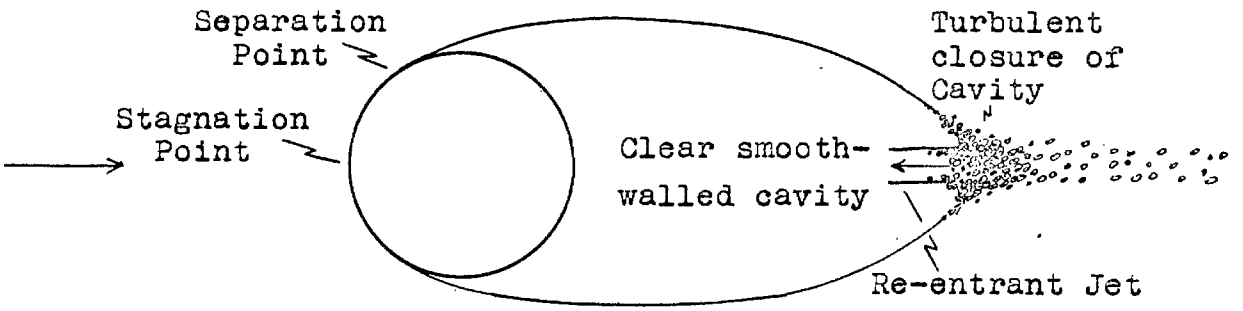

are convected away downstream.(Fig.1.1) This phenomenon, known as incipient cavitation , is very similar to nucleate boiling. It requires the growth of tiny nuclei in this region on the surface of the body into observable bubbles. The value of Q at which this begins to happen , Q_i, is known as the incipient cavitation number. Due to the near impossibility of measuring the pressure within these nucleate bubbles, p_c is always taken as being equal to p_v when describing incipient cavitation, whether dissolved gas is present in the liquid or not. It is the sudden collapse of these bubbles, when convected to regions of higher pressure , that is thought to cause the erosion of the body in the area of collapse. Both chemical and physical theories have been put forward to try to explain this damage. The actual process is likely to be explained in a complex combination of the two. Most physical theories are based on the factor of the release of energy due to bubble collapse.

At further reduction of Q these bubbles fill the whole wake, which then takes the appearance of a reasonably well defined region of white foam behind the cylinder (Fig. 1.2). This is termed partial cavitation and is an intermediate state. By lowering Q still further we find that the bubbles in this region of foam combine to form one large , reasonably steady bubble behind the cylinder. This stage is called full cavitation and the bubble known as a fully developed cavity. The surface of the cavity is still opaque and bubbly and the rear end remains very foamy and turbulent. (Fig. 1.3)

A further change takes place as we reduce Q to about 0.6. The cavity surface seems instantaneously to

become completely transparent and smooth for the greater part of its length. The end however remains turbulent. This change has been observed by Gadd and Grant (Ref. 15). The actual value at which this occurs may be dependent on the experimental set up. Although cavities for Q below this value seem to the naked eye to have this very steady,glassy appearance,high-speed photographs,with an exposure of a few microseconds,reveal a serrated but still transparent surface in this region.

As we reduce Q fully developed cavities grow in breadth and length and the coefficient of drag falls. Approximate power relationships were noticed for these variations,principally by Reichardt. (Ref. 34) These relations are :

[A] For planar flow around,for example, an infinitely long cylinder :

B ,the maximum height of the cavity above the plane of symmetry $\propto Q^{-1}$

L ,the half-length of the cavity $\propto Q^{-2}$

[B] For axisymmetric flow around ,for example,a sphere :

B ,the maximum radius of the cavity $\propto Q^{-\frac{1}{2}}$

L ,the half-length of the cavity $\propto Q^{-1}$

[C] For both planar and axisymmetric flow :

C_D ,the coefficient of drag on the body $\propto 1 + Q$

1.2.3 Further effects.

Another effect which has been observed in fully developed cavities is that of the re-entrant jet. This jet of fluid seems to emerge from the closure

region of the cavity,to be directed into the cavity and towards the body. This phenomenon can be taken into account when setting up mathematical models of the flow. (See section 1.4.5) Other points which we shall refer to are the "separation points" and the "stagnation points". The stagnation points are , as usual , the points of zero velocity relative to the body. The separation points are the points at which the flow separates from the body surface. The area of the body surface which is in contact with the liquid is known as the wetted surface ; that is to say the part of the body surface upstream of the separation points.

For Q below 0.2 cavities may become very large,and indeed it will be shown later that for flows in a straight walled channel there will be a minimum positive Q which can be reached. In theory,for this value of Q the cavities become infinitely long , and ,as the width of the channel tends to infinity,this minimum value of Q tends to zero.

These then are the general characteristics of simple cavitating flows. Usually cavitation occurs in practice in more complex flows,such as that around a revolving propellor blade in water,but these flows are so complex as to have,so far,resisted everything but an empirical approach. It will therefore be more advantageous to concentrate our attention here on the cavitating flow around simple bodies such as cylinders, discs and spheres. These are the bodies most frequently used in experiments to measure the drags,sizes and other effects of cavity flows in water tunnels. There is , therefore , some experimental data with which we can

compare,for these simple bodies,theoretical and numerical results.

1.3 CAVITATION RESEARCH.

1.3.1 General.

The research,both theoretical and practical,which has been done in cavitation ,can be divided roughly into two categories. The first has been concerned with the phenomenon of incipient cavitation,how and when it is initiated,and with the effects of the liquid and surface properties on the inception and growth of the minute bubbles. These researchers are concerned with the damage caused by the sudden collapse of the bubbles and therefore, in some applications , with the prevention of their appearance ; hence the term "cavitation suppression".

The other category is involved with fully developed cavities,their shape,drag and consequent wake. The theoretical research in this category,for the most part,assumes the flow of the liquid to be idealized with a smooth free streamline interface and a definite and unique separation point. A considerable number of two dimensional plane flows of this type have now been solved by what is known as the "hodograph" method. These will be discussed in section 1.5 .

This thesis is concerned with the second category, but in order to give a more complete picture it will be useful,first,to deal briefly with incipient cavitation and the effects of fluid properties upon it.

1.3.2 Incipient Cavitation.

As pointed out in section 1.2.2, when we reduce the cavitation number of the flow past a body in a stream, there comes a point at which minute bubbles are formed in the regions of reduced pressure near the surface of the body. The cavitation number at which this occurs is known as the incipient cavitation number or index, denoted by Q_i. Generally, it is assumed that this effect is due to the fact that, under these conditions, microscopic nuclei, ever present in the stream, are able to grow at a rate fast enough to make their presence felt or seen before being convected downstream to regions of higher pressure. Van der Walle (Ref. 44) made a detailed analytic approach to this problem, in which he showed that an initially stable nucleus, presumeably of undissolved gas, will not grow rapidly as it moves in the direction of a negative pressure gradient until C_p is less than $-Q_i$ by an amount $4/3\eta$ where η is a parameter directly proportional to bubble size.

Up to the point, $C_p = -Q_i$, the growth of the bubble will depend upon the diffusion of any absorbed gas present but beyond it will be limited only by heat conduction or dynamic effects as the bubble fills with vapour. In most experiments, the time for which the bubble is in the regime $C_p < -Q_i$ is much less than the typical time for gas diffusion and much greater than the typical time for heat diffusion. Hence the rapid growth after the point $C_p = -Q_i$. Many other factors may influence the rate of growth ; dissolved and undissolved gas content, pressure gradient forces on the bubble, viscosity, surface tension and surface roughness are some factors which command consideration. Silverleaf

(Ref. 40) gives a good account of these lines of research. The effect of total gas content has been studied analytically by van der Walle (Ref. 44) and Holl (Ref. 21) and experimentally by Ripken and Killen (Ref. 37) and Silverleaf and Berry (Ref. 41) among others. These authors seem to agree that Q_i increases with total air content. Ripken and Killen also found that Q_i was significantly increased by a reduction in surface tension. Thermal effets due to the latent heat of vapourisation and the consequent temperature gradients are discussed by van der Walle and Silverleaf. The former concludes that these effects are only important when the latent heat is large compared with that of water at normal temperatures, since heat diffusion is much more rapid than gas diffusion.

Holl and van der Walle have studied the effect of the Reynolds number, Re, of the flow. Here it appears the effect varies according to the shape of the body or, what amounts to the same thing, the shape of the pressure distribution. For long, smooth bodies such as hydrofoils the bubbles when formed tend to travel parallel to the surface of the body in their initial movement. In this case increasing Re tends to decrease Q_i. But for the flow around a bluff body such as a disc, cavitation occurs in the separated flow away from the body, and Q_i markedly increases with Re. The effect of the boundary layer will thus have to be taken into account in considering the viscous effects on Q_i.

This then is the form which research into incipient cavitation has taken. Although most of what has been done concerns only this initial stage of cavitation, the effects

could probably be extended with only slight modification to the flow in the region prior to and at separation for fully developed cavities. In actual flows of this type nucleate bubbles still form in this region,but it is probable that they have very little effect on the cavity as a whole,though they may influence the position of the separation point. Indeed as Silverleaf (Ref. 40) points out,it is probable that the relative effects of viscosity, surface tension,etc.,as concerning Q_i and incipient cavitation are very different from their effects for fully developed cavities. Most research,to date,shows that these "scale effects" are very small for fully developed cavitation in water at normal temperatures. It is therefore reasonable to consider initially the cavities in an "ideal" fluid (see next section) and to consider afterwards the effects and differences involved in having a real fluid.

1.4 FULLY DEVELOPED CAVITY FLOWS.

1.4.1 Basic Equations.

As with most other cases of fluid flow,the complete solution would be extremely complex,but can be simplified considerably by discounting some of the less significant properties of the fluid. So it is here in cavitating flow where theoretical solution is only possible by idealizing the fluid and the flow ; we define an ideal flow as one which is inviscid,incompressible and irrotational.

The assumption that the fluid is inviscid and incompressible means that we can apply Euler's equation

of motion :

$$[1.3] \qquad \frac{\partial}{\partial t}(\underline{q}) + \underline{q}.\nabla \underline{q} = -\frac{1}{\rho}\nabla p - \nabla G$$

where G is the gravitational potential. Also, by definition, the flow is irrotational if it has a velocity potential function, $\varphi(x,y,z,t)$, such that :

$$[1.4] \qquad u = \frac{\partial \varphi}{\partial x} \quad , \quad v = \frac{\partial \varphi}{\partial y} \quad , \quad w = \frac{\partial \varphi}{\partial z}$$

or :

$$[1.5] \qquad \underline{q} = \nabla \varphi$$

Hence, if the flow is incompressible :

$$[1.6] \qquad \nabla^2 \varphi = 0$$

Such flows are known as potential flows. Combining [1.3] and [1.4] it can easily be shown that a homogeneous, potential flow must satisfy the Bernoulli equation :

$$[1.7] \qquad p + \frac{1}{2}\rho \nabla\varphi.\nabla\varphi + \rho \frac{\partial q}{\partial t} + \rho G = P(t)$$

where P(t) is dependent only on time. Further, if the flow is steady, $\frac{\partial q}{\partial t} = 0$, and therefore :

$$[1.8] \qquad p + \frac{1}{2}\rho q^2 + \rho G = \text{Constant in time and space}$$

If we assume gravitational forces to be zero, then we have :

$$[1.9] \qquad p + \frac{1}{2}\rho q^2 = \text{Constant in time and space}$$

More rigorous treatment and proof of these basic equations is given in most standard texts. (See References 5,6,30 and 48 for example.)

1.4.2 Basic Theorems.

From the assumptions of the steady, irrotational flow of an ideal liquid we can draw a number of important

conclusions. The first , and most important , deduction is the fact that from [1.9],since the pressure on the interface or free streamline is constant and equal to p_c ,then the velocity magnitude of the free streamline is constant. By equation [1.9] and definition [1.1] :

[1.10] $$q_c^2 / q_a^2 = 1 + Q$$

There are a number of other important properties which can be deduced from these simple equations. Birkhoff and Zarantonello (Ref. 6) set out these properties in terms of theorems,their corollaries and proofs,so it will suffice simply to state them here along with some observations.

[A] In any irrotational Euler flow of an ideal fluid the point of minimum pressure occurs on the boundary. Kirchhoff (Ref. 23) first showed this, by taking the Laplacian of [1.7]. This gives the result that $\nabla^2 p \leqslant 0$. Thus,in an ideal fluid, cavitation must first occur on the boundary and p_c be the minimum pressure in the flow field. On the other hand this result is not neccessarily true in non-irrotational flow,as demonstrated by the phenomenon of "vortex cavitation" ,in which cavitation occurs in the region of reduced pressure at the centre of a vortex. Viscous effects may also prevent this theorem from being true. In actual flows past a cylinder the point of minimum pressure occurs on the surface of the cylinder just upstream from separation.

[B] From [A] it follows that since $p_c \leqslant p_a$, $Q \geqslant 0$.

The following are true of the steady,irrotational

Euler flow of an ideal liquid,ignoring the gravitational forces.

[C] Cavities must be convex. Since p_c is the minimum pressure,q_c must be the maximum velocity occuring in the flow by virtue of equation [1.9]. Hence the velocity gradient perpendicular to the interface and towards the cavity must be positive. But it is easily shown that the centre of curvature of a streamline at any point is on the same side of the streamline as that to which the velocity gradient is directed at that point. Therefore the free streamline must be convex , viewed from the fluid.

[D] Because the velocity,q_c,is constant the cavity cannot have a stagnation point at the rear end , since this would involve a point of different,namely zero, velocity.

1.4.3 Plane and Axisymmetric flows.

Cavitating flows around two basic types of body in a uniform stream have been considered in the literature.

Plane flows are defined as those which are uniform, in one cartesian direction,say Oz, perpendicular to the direction of the uniform stream,Ox. For example the flow past an infinitely long cylinder whose axis is set perpendicular to the direction of the uniform stream. All other surfaces, such as a channel wall , must obviously have the same property, so that every x,y, plane is identical and a point in the flow completely described by the two co-ordinates x,y.

Axisymmetric flows are defined as those that are

axisymmetric about an axis, Ox, parallel to the direction of the uniform stream. For example the flow past a disc set normal to the stream. All other boundaries must again be identical in every x,r plane where r is the radial direction measured perpendicular to Ox. A point in the flow is therefore completely defined by the two co-ordinates x,r .

In steady ideal plane flows we define the stream function, Ψ, such that :

[1.11] $$\frac{\partial \varphi}{\partial x} = u = \frac{\partial \Psi}{\partial y}$$

[1.12] $$\frac{\partial \varphi}{\partial y} = v = -\frac{\partial \Psi}{\partial x}$$

From these equations it follows that both φ and Ψ obey the Laplace equation. i.e.

[1.13] $\nabla^2 \varphi = 0$ [1.14] $\nabla^2 \Psi = 0$

Then it is easily shown that $\frac{\partial \Psi}{\partial s} = 0$ where s is measured along a streamline, that is in the direction of fluid velocity at any point. Thus Ψ is constant on each streamline and the difference in the numerical value of Ψ on two streamlines is a measure of the volume rate of flow/unit width between them.

In steady ideal axisymmetric flow Stokes' stream function, Ψ, is given by :

[1.15] $$\frac{\partial \varphi}{\partial x} = u = \frac{1}{r}\frac{\partial \Psi}{\partial r}$$

[1.16] $$\frac{\partial \varphi}{\partial r} = v = -\frac{1}{r}\frac{\partial \Psi}{\partial x}$$

Here again it is easily shown (Ref. 30 , p.432) that Ψ is constant on a streamline. The equations corresponding to [1.13] and [1.14] are :

$$[1.17] \qquad \frac{\partial^2\phi}{\partial x^2} + \frac{\partial^2\phi}{\partial r^2} + \frac{1}{r}\frac{\partial\phi}{\partial r} = 0$$

$$[1.18] \qquad \frac{\partial^2\psi}{\partial x^2} + \frac{\partial^2\psi}{\partial r^2} - \frac{1}{r}\frac{\partial\psi}{\partial r} = 0$$

Thus in this case, although ϕ obeys Laplaces equation, ψ does not.

In either case a knowledge of the values of ϕ or ψ at every point in the flow will provide a complete solution to that flow problem. This entails solving one of the differential equations [1.13],[1.14] or [1.17],[1.18] within the appropriate boundary conditions for that problem.

1.4.4 Boundary Conditions.

Comment is required here on the terminology used in referring to types of boundary condition. In order to solve a second order differential equation of the types exemplified by equations [1.13],[1.14],[1.17] and [1.18],it is neccessary to impose a condition for the dependent variable,be it ϕ,ψ or any other,on every part of the boundary. Three types will be referred to in this thesis.

[A] The Dirichlet boundary condition for which the value of the dependent variable is known at every point. This,therefore,is the condition on a "fixed" boundary,body or wall for a fluid flow in the physical plane.

[B] The Neumann boundary condition for which the normal derivative of the variable is known. This normally

means,in fluid flow,the physical plane,that one component of the velocity is known on this boundary.

[C] A complex boundary condition which consists of an identity connecting some or all of the variable,its tangential and normal derivatives. It will be seen later that the condition of constant velocity on a boundary leads to such a condition.

A problem in which different types of condition hold on different parts of the boundary is termed a "mixed" boundary condition problem. Should there be only two parts with different types of condition , the problem becomes "simply mixed".

1.4.5 Mathematical Models of Cavity Closure.

It was pointed out in section 1.2.2 that actual cavities exhibit considerable turbulence at their downstream end. Thus if we are to make an attempt at mathematical solution,in terms of a potential flow, we must idealize this region considerably. In fact we must assume the cavity to have,everywhere,a steady,smooth surface. From [C] of the section 1.4.2,the cavity must be convex at every point and this would imply a closure of the form sketched in figure 1.5,which would neccessarily mean a stagnation point at the point A. But this would give in turn,a point of zero velocity on the free streamline which,as pointed out in [D] , is incompatible with the condition of constant cavity pressure.

MATHEMATICAL MODELS OF CAVITY CLOSURE

FIG.1.5 SINGULARITY MODEL

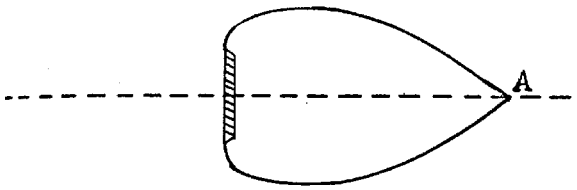

FIG.1.6 MODEL WITH CUSPED END

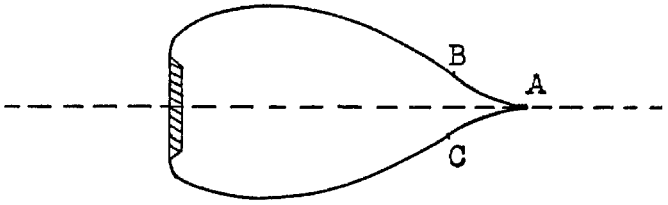

FIG.1.7 RIABOUCHINSKY FLOW MODEL

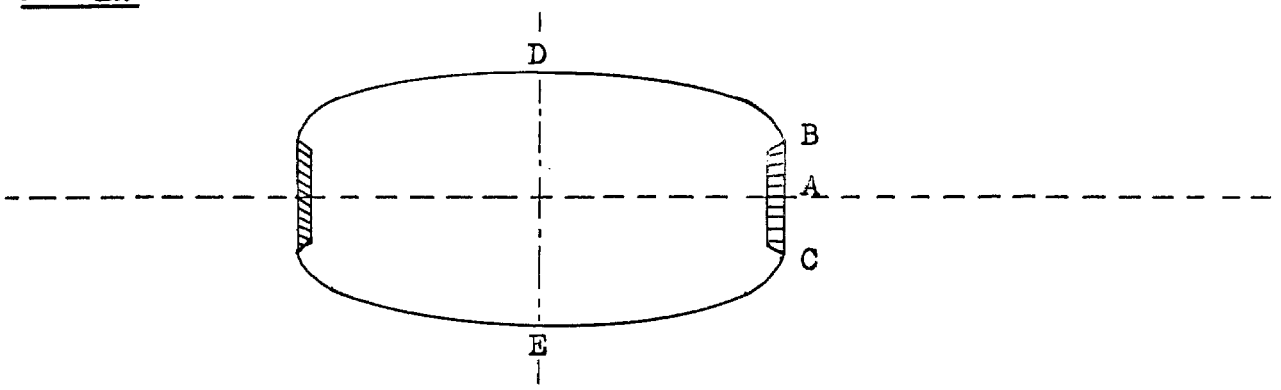

FIG.1.8 RE-ENTRANT JET MODEL

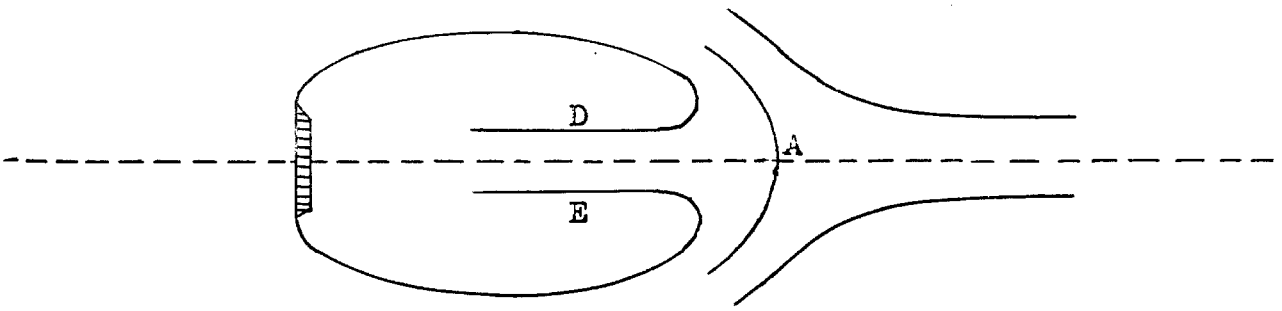

FIG.1.9 PARALLEL STREAMLINE MODEL

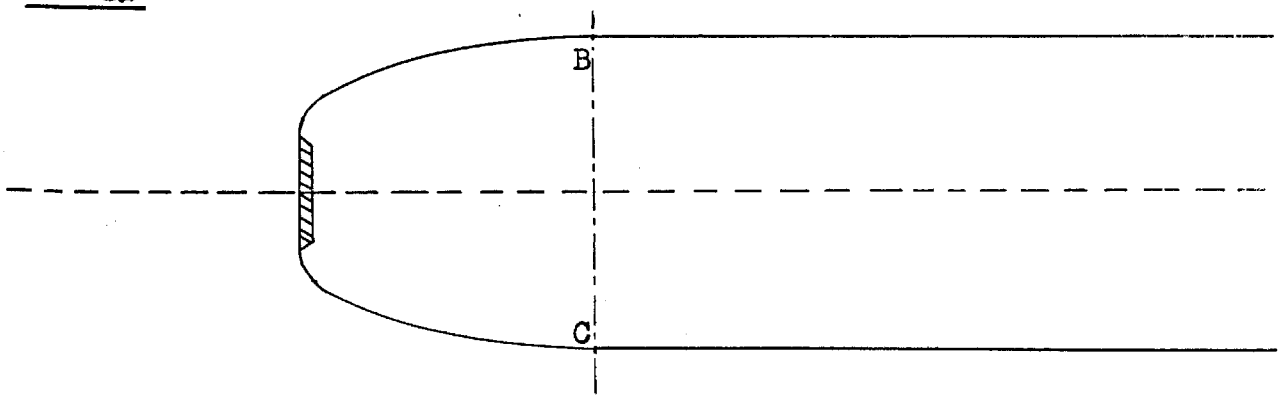

It is worth noting at this point, that experimental pressure measurements at intervals along the length of a cavity show a marked rise as the closure region is approached. (See Ref. 10)

A number of mathematical models have been designed to avoid or surmount the dilemma detailed above. One such model involves the introduction of a singularity at A (figure 1.5) in such a way that the velocity along the free streamline remained constant. There would be no justification for such a singularity, in terms of real flows, but the main difficulty with this model is the fact that it introduces a new variable to the solution of the flow, namely the value of the strength of the singularity. The type of singularity can be imagined as a double "rolling-up" of the end of the free surface.

A different type of model, the cusp-ended cavity is given in Figure 1.6. Here we introduce two cusps BA and CA whose curvature is concave but whose presence disposes of the stagnation point. Such a model, however, means that p_c is not the minimum pressure encountered in the flow by the converse of [A] of section 1.4.2. The question also arises as to how the cusps are "matched" into the flow.

A somewhat similar model was designed by Riabouchinsky (Ref. 36) and is shown in figure 1.7. He suggested the use of an "image" plate, BC, in such a way that the flow was symmetric about the plane EF. This has the advantage of halving the size of the flow field to be solved and dispenses with the unknowns of the first two models. A more complex problem would be the non-symmetric Riabouchinsky flow where the image plate is reduced in size to approach the actual flow.

Their observation of the re-entrant jet led Gilbarg and Rock (Ref. 17) to the fourth model. Figure 1.8 shows the mathematical re-entrant jet model they designed, taking into account this jet of liquid coming into the cavity from the closure point. The rear stagnation point in this model thus occurs away from the interface at a point such as A. A notable feature of this model is that the cavity is not only entirely convex but that q_c can be constant without leading to the original difficulty. However this model involves a permanent and continuous removal of liquid from the flow. The jet is assumed to continue through the body to an upstream infinity , giving a doubly covered region of flow. Both these properties are unrealistic. In practical experiments the jet seems to break up and the remains to be sprinkled onto the main cavity wall,although for small cavities the jet may actually impinge on the rear of the body. Nevertheless the re-entrant jet model is perhaps more realistic than the other models,though more complex to deal with than Riabouchinsky's.

Further models have been suggested,among them the parallel streamline model of figure 1.9, in which q_c is considered constant up to the point of maximum diameter or breadth and the free streamlines to be parallel to the axis of symmetry beyond this point. The pressure on the latter part therefore rises asymptotically to a uniform stream value. Gadd (Ref. 14) compares the validity of these models for a flat plate set normal to a uniform stream and introduces a further "converging streamline" model.

Since,for most purposes,the interest lies in the

upstream half of the flow,these artificial models do not,as might be imagined,so drastically alter the results required. In plane flows,where exact solution for simple bodies is possible,the indication is that for large cavities (or small Q) the two most significant models,Riabouchinsky and the re-entrant jet,give results very close to those of experiment,for the drag on the body and main dimensions of the cavity. As Q is increased above about 0.6 ,the results begin to diverge. (See Refs. 14,6 and 48.)

Figure 1.10 shows a mathematical model which contravenes the condition of convexity completely and which could only occur in practice at physically unrealistic negative cavitation numbers. However it avoids the presence of a rear stagnation point and has been used by Lighthill (Ref. 29) and Southwell and Vaisey (Ref. 43). The latter use a relaxation technique for their solution of the plane flow case and their results will be referred to later (section 2.5).

All these models are applicable to both plane and axisymmetric flows.

1.4.6 Separation Points.

When the flow past a body separates from that surface it will obviously do so along a line which is a closed contour on the surface of the body,providing this is finite. Where the body is infinite this contour may go off to infinity,but must nevertheless be closed through the point at infinity. In both plane and axisymmetric flow this contour appears as two points

FIG. 1.10 CUSPED CAVITY MODEL

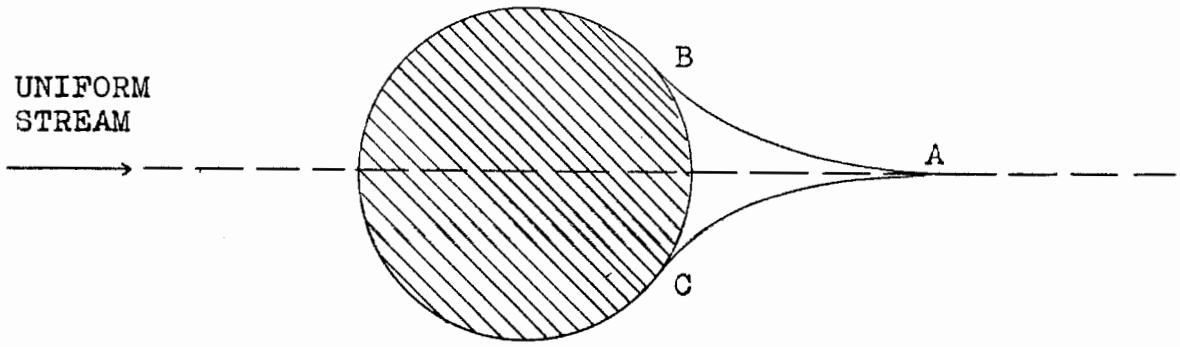

in, respectively, the longitudinal and axial planes. These points are referred to as the "separation points" since they completely define the contour in both cases. In axisymmetric flow one point is sufficient.

In the flow of a viscous fluid, the points of separation in cavity flow, as in non-cavity flow, will be determined by boundary layer theory knowing the pressure distribution just outside the layer. But in the flow of an ideal fluid separation is assumed to take place at the point $C_p = -Q$. It is therefore a necessary condition in determining the points of flow separation for an ideal fluid that, at all other points on the wetted surface, $1 > C_p > -Q$, unity being the value of C_p at the stagnation point and therefore its maximum value. This condition can be proved by assuming that there are points at which $C_p < -Q$. Then since $C_p = 1$ at the stagnation point there must be some other point at which $C_p = -Q$. But this is the condition for separation and thus the flow would separate at this point. With some irregular shapes of body there may be what is known as "flow re-attachment", in which the flow after separation impinges again on the body and thus gives another region of wetted surface. Nevertheless the identity $1 > C_p > -Q$ must still hold on all portions of wetted surface. There may also be more than one stagnation point. If s is the distance measured along the surface of the body then a typical $C_p(s)$ curve would be that of figure 1.11.

Another important conclusion can be reached using property [C] of section 1.4.2. This is that the curvature of the free streamline must always be convex,

FIGURE 1.11

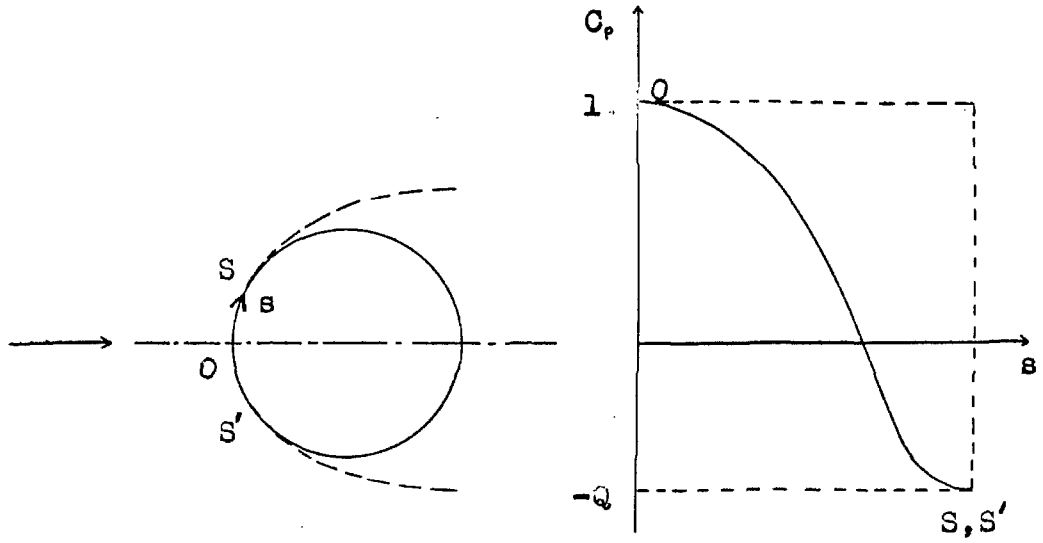

FIGURE 1.12

ABRUPT SEPARATION

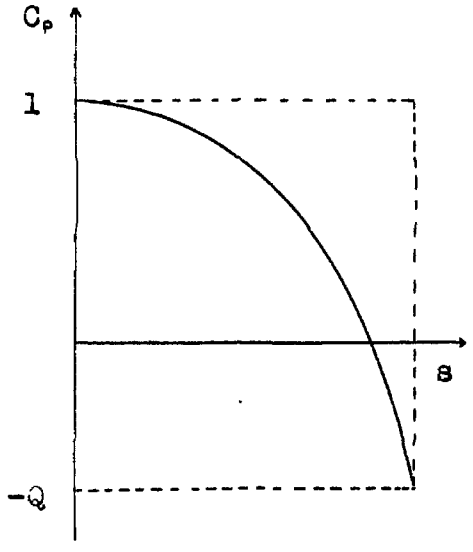

FIGURE 1.13

SMOOTH SEPARATION

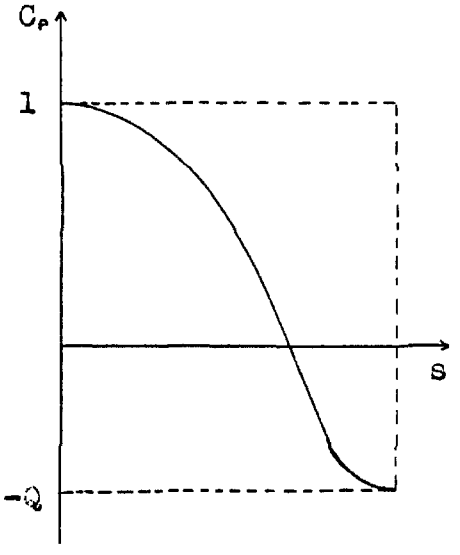

viewed from the fluid. If such a curvature is defined as positive the radius of curvature of the free streamline at the separation point, R_{FS}, must lie within the limits:

$$0 < \frac{1}{R_{FS}} < \frac{1}{R_{BS}}$$

where R_{BS} is the radius of curvature of the body at separation. If this were not true and $R_{BS} > R_{FS}$ then the solution would be unreal, since this would mean that the free streamline would cut into the body.

A special case of separation occurs when there is a sharp projecting corner on the body. The flow must separate at this point, since to negotiate the corner would entail an infinite velocity and therefore a point $Cp = -\infty$ which violates our first condition. This type of separation, exemplified by the separation from a disc, is termed abrupt . Since in this case $R_{BS} = 0$, R_{FS} could also be zero, and in fact this is the case in both plane and axisymmetric flow as is shown by Armstrong (Ref. 2). He also shows that there will be an infinite pressure gradient on the body at an abrupt separation point.

Separation which occurs at a point at which the curvature of the body is finite is termed smooth separation. As has been previously indicated this will only occur if the curvature of the body is everywhere finite on the wetted surface. (Milne Thomson, Ref. 30 , p.302 refers to smooth separation as proper cavitation). It has been shown [Armstrong, Ref. 2] that in the case of smooth separation:

$$R_{BS} = R_{FS}$$

and thus the radius of curvature and the second derivatives

such as $\frac{\partial^2\varphi}{\partial r^2}$, $\frac{\partial^2\psi}{\partial r^2}$ are continuous through a point of smooth separation. (Ref. 48 ,p.435 for the plane case and Ref. 2 for both plane and axisymmetric) Thus the appropriate Cp(s) functions in the two distinct methods of separation would have the forms sketched in figures 1.12 and 1.13.

The results obtained by Armstrong and refered to here will be dealt with in greater detail in subsequent sections. [1.5.6 for planar and 3.4 for axisymmetric flow.]

1.5 SOLUTION OF IDEAL PLANE FLOWS BY THE HODOGRAPH METHOD.

1.5.1 Complex Variable.

In an ideal plane flow,a point in the physical plane is completely defined by the complex variable, $z = x + iy$. If we define a complex velocity potential, w, such that

$$w = \varphi + i\psi$$

then it is easily seen,since equations [1.11],[1.12] are the Cauchy-Riemann conditions for z to be single valued in w :

[1.18] $$\frac{dw}{dz} = \zeta = \frac{\partial\varphi}{\partial x} + i\frac{\partial\psi}{\partial x} = u - iv = qe^{-i\theta}$$

where ζ is therefore the conjugate of the complex velocity, $u + iv$. From the equation [1.18] :

[1.19] $$z = \int \zeta^{-1}\, dw \qquad \underline{\text{and}} \qquad \left|\frac{dw}{dz}\right| = q$$

It is also useful to introduce the complex variable γ where :

$$\gamma = \Omega + i\theta$$

$\Omega = \ln (q_\infty / q)$

θ = The angle between the directions of q and q_∞.

Thus in uniform stream problems when $\Omega = \ln(U/q)$ we have:

[1.20] $$e^{\gamma} = U.\zeta = U. \frac{dz}{dw}$$

and

[1.21] $$z = \int U.e^{-\gamma} \, dw$$

1.5.2 Conformal Mapping.

Figure 1.14 represents a general plane case of an infinitely long cavity flow. The outer boundaries $D_\infty E_\infty$ and $D'_\infty E'_\infty$ may be extended to infinity to give the flow in an infinite uniform stream. Figure 1.15 represents the corresponding w-plane. On the body surface, AOA', z and θ are known functions and w is required in order to find the pressure and velocity distributions , whereas on the free surfaces, AC_∞ and $A' C'_\infty$ w and Ω are known but z and hence the shape of the cavity is to be found.

The required solution is therefore of the form $w = f(z)$ giving the required results on the free and fixed surfaces. This type of problem is among those more generally termed, mixed boundary condition problems. Here we have two types of boundary condition;

θ or z specified on the fixed boundaries, $D_\infty E_\infty$, AOA', $D'_\infty E'_\infty$. Normally the problem is symmetric about the stagnation streamline $B_\infty O$ in which case only one half of the flow need be considered. $B_\infty O$

FIGURE 1.14 z - Plane.

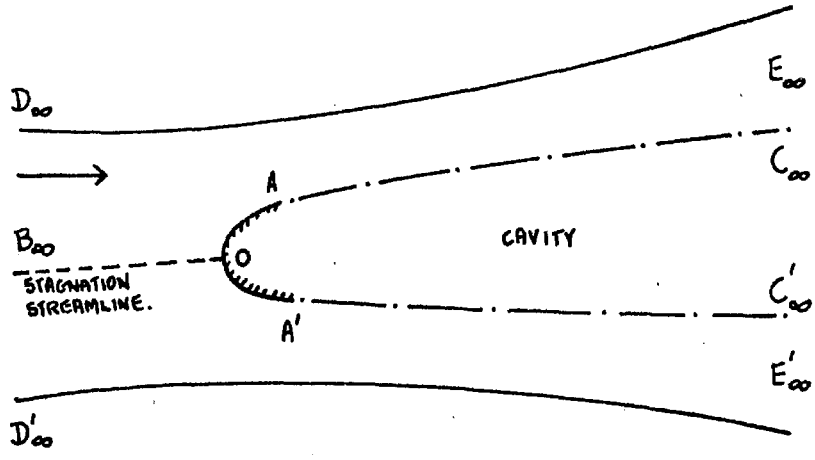

FIGURE 1.15 w - Plane.

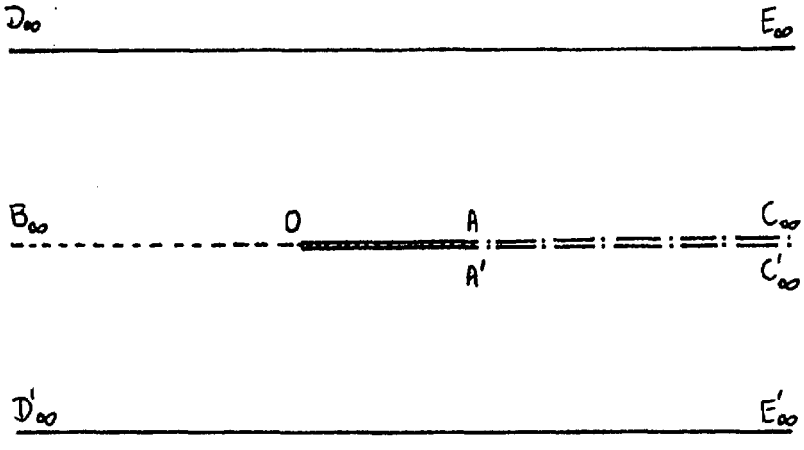

FIGURE 1.16 w - Plane.

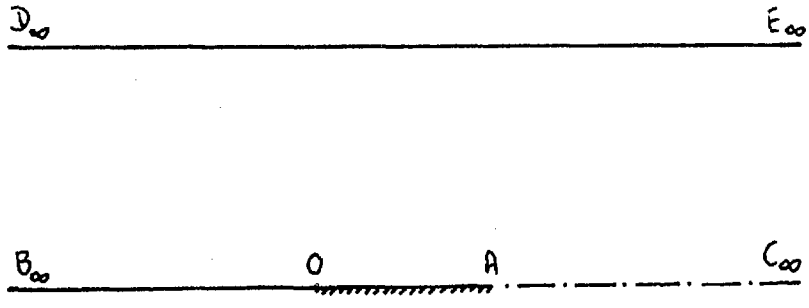

then becomes a "boundary" of this type.

Ω or q and therefore $\frac{\partial \varphi}{\partial s}$ is specified on the free boundaries $A'C'_\infty$ and AC_∞.

In the case of symmetry about the stagnation streamline, $\psi = 0$, the w-plane becomes that of figure 1.16. This type of problem is known as a simply mixed boundary condition problem since there is only one boundary region of each type, B_∞ and D_∞ being the same point, the point at infinity.

Thus conformal mapping suggests itself as an implicit part of plane flow and the basic principle of solution is to transform the flow into a plane for which the solution is known. For this we introduce a convenient complex variable t, where the solution is known in the t-plane and where we can find mapping relations between this plane and both the z and w planes. Then knowing w(t) and $\Upsilon(t)$ we can find by elimination the function $\Upsilon(w)$. The solution will then follow by substitution in and integration of equation [1.21] and give the required z(w).

1.5.3 Solution of Simply Mixed boundary condition problems.

A vast number of problems in plane flow have been solved by the method outlined above, and much has been written on the peculiar t-planes and substitutions involved in each particular type. [See for example Refs. 18 and 48 among others]. We will concern ourselves here only with the problems of cavitating plane flows in a uniform stream. It was shown in the last

section that, provided the uniform stream is either infinite in the y-direction or bounded by "fixed" surfaces and provided it is symmetric about the stagnation streamline, the problem becomes one with simply mixed boundary conditions. Figures 1.17a and 1.17b give two examples of problems of this type.

It is worth noting at this point that if the uniform stream were in fact a free jet, such that $F_\infty E_\infty$ in figures 1.17a , 1.17b were free streamlines, then 1.17a would remain simply mixed but 1.17b would become doubly mixed since there would now be two separated sections of free boundary. Doubly mixed boundary condition problems will not be dealt with here. Woods (Ref. 48) deals with this more complex class of problems.

Most texts (e.g. Ref. 6) give full details of the solutions of simply mixed boundary condition problems, so it will suffice here merely to give the outlines of the types of solution with the results we shall need.

It is evident that the w-plane in all problems of this type will be polygonal since all boundaries, providing that none of them are porous, will lie on lines of constant Ψ . Thus it will be relatively simple to transform this plane to a t-plane in which the solution is known. The major part of the problem therefore lies in finding $\Upsilon(t)$ if we are to proceed as indicated above. This step may only be possible using numerical techniques but can be effected analytically in some simple cases. By far the most useful result in all this type of work is the Schwarz-Christoffel mapping theorem. Proofs of this result can be found in most standard texts.

Simply Mixed Boundary Condition Problems

FIGURE 1.17 a

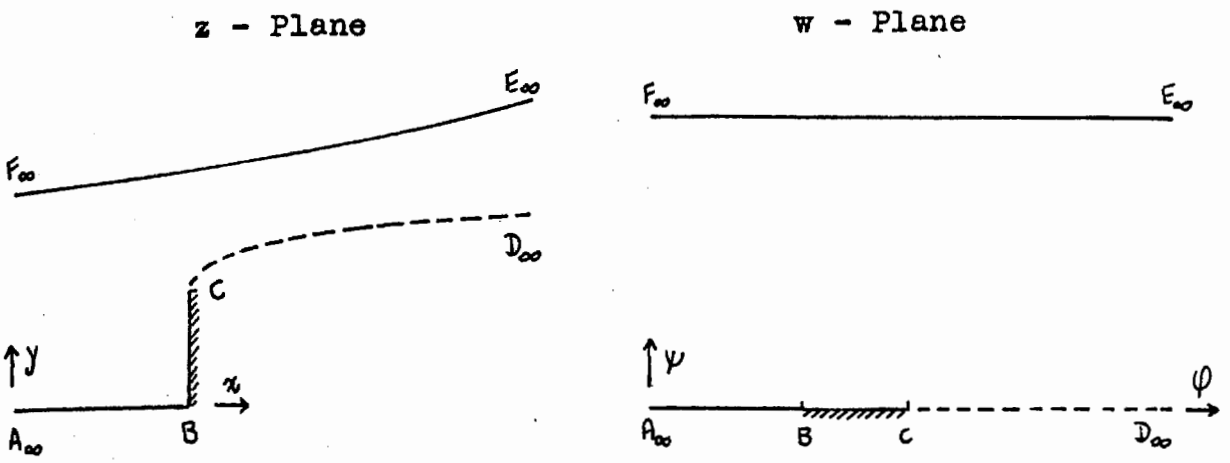

FIGURE 1.17 b

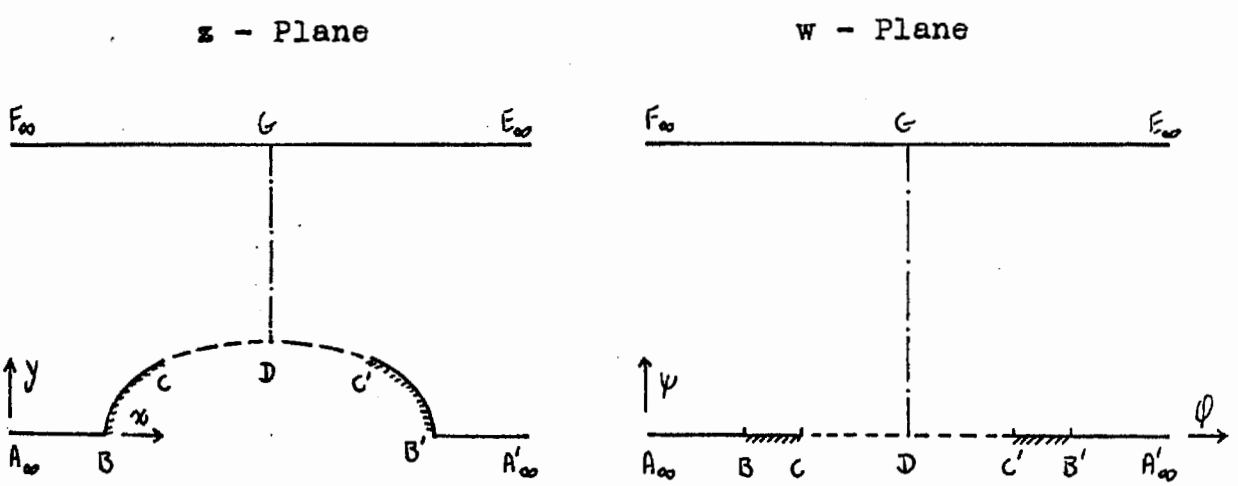

FIGURE 1.18

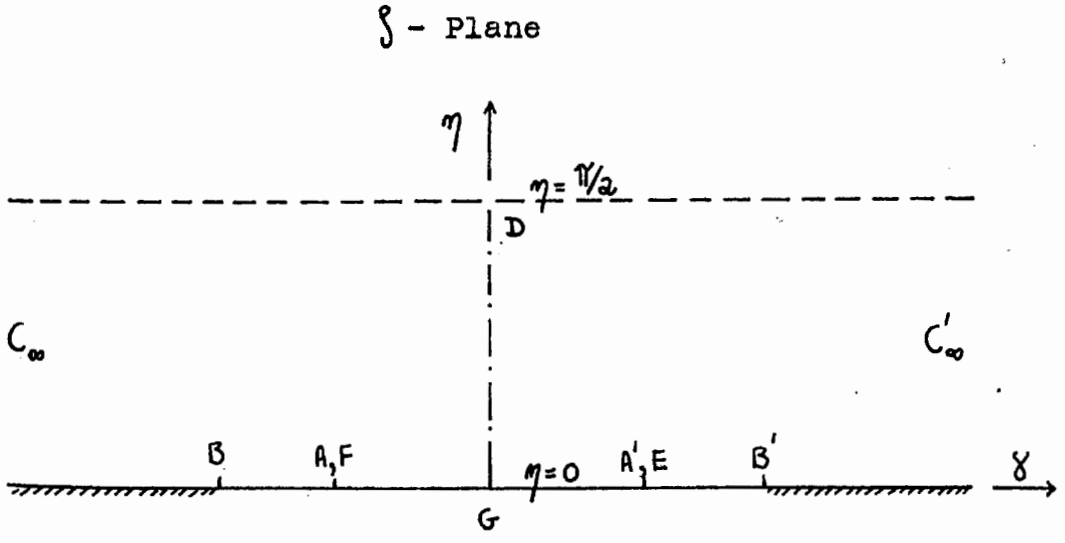

It states that if the boundaries in the z-plane are polygonal, the corners or discontinuities in Θ having the values α_n at the points $\varphi = \varphi_n$ where n=1, 2, 3, ...N then :

$$[1.22] \qquad \frac{dz}{dw} = K.\prod_{n=1}^{N} (w - \varphi_n)^{-\frac{\alpha_n}{\pi}}$$

where K is a constant of integration which can be found providing two corresponding points in the z and w planes are known.

Woods (Ref. 48) gives a more general form of this theorem which can be applied to curved boundaries in the z-plane. This form is :

$$[1.23] \qquad \frac{dz}{dw} = K.\exp\left\{ -\frac{1}{\pi} \int_{-\infty}^{+\infty} \ln(w - \varphi)\, d[\Theta(\varphi)] \right\}$$

When the boundaries are polygonal the integral degenerates to give the sum involving the discontinuities in Θ in equation [1.22]. The consequence of this theorem is that we need only to find $\Theta(\varphi)$ on the boundaries in the z-plane to effect solution.

Woods (Ref. 48, page 249) shows that the first step in a simply mixed boundary problem is to map Υ into $\zeta = \gamma + i\eta$ (Figure 1.18) in such a way that the interval in which Θ is known is mapped onto $\eta = 0$, $-\infty < \gamma < \infty$ and the interval in which Ω is known is mapped onto $\eta = \pi/2$, $-\infty < \gamma < \infty$. Using Schwarz-Christoffel, this is done by:

$$[1.24] \qquad \Upsilon(\zeta) = \frac{1}{\pi} \int_{-\infty}^{+\infty} [\Theta(\gamma)_{\eta=0}]\operatorname{cosech}(\gamma - \zeta) + [\Omega(\gamma)_{\eta=\frac{\pi}{2}}]\operatorname{sech}(\gamma - \zeta)\, d\gamma$$

On integrating by parts a more useful form of this equation can be found:

$$[1.25]\quad \gamma(\zeta) = \gamma_{\zeta=\infty} + \frac{2}{\pi}\int_{-\infty}^{+\infty} \tanh^{-1}(e^{\gamma-\zeta})\, d\,[\theta(\gamma)_{\eta=0}] + \frac{2}{\pi}\int_{-\infty}^{+\infty} \tan^{-1}(e^{\gamma-\zeta})\, d\,[\Omega(\gamma)_{\eta=\frac{\pi}{2}}]$$

All that is required to complete the theory therefore is the $\zeta(w)$ relation for the particular w-plane. Woods (Ref. 48, page 250) gives examples of these $\zeta(w)$ relations which, as anticipated above, turn out quite simple.

1.5.4 General Riabouchinsky flow in a channel.

Since the major part of this thesis is concerned with axisymmetric Riabouchinsky flows, it will be useful to deal in greater detail with the corresponding plane flows. The general Riabouchinsky flow in a channel is shown in figure 1.20a and the particular flow around a flat plate in figure 1.20b. In both cases we know that $(\Omega)_{\eta=\frac{\pi}{2}}$ is constant since $\eta = \frac{\pi}{2}$ is the free streamline on which the velocity is constant. Equation [1.25] then becomes:

$$[1.26]\quad \gamma(\zeta) = \gamma_{\infty} + \frac{2}{\pi}\int_{-\infty}^{+\infty} \tanh^{-1}\left[\exp(\gamma-\zeta)\right] d[\theta(\gamma)_{\eta=0}]$$

where $\theta(\gamma)_{\eta=0}$ is the equation for θ on the "fixed" boundary. The w-plane of figure 1.20c is mapped into this ζ-plane (figure 1.20d) by

$$[1.27]\quad \coth(\zeta) = -\coth\left[\frac{\pi\varphi_0}{2h}\right]\tanh\left[\frac{\pi w}{2h}\right]$$

where φ_0 is as shown in figure 1.20c and h is the value of Ψ on the channel wall.

To simplify the solution Woods introduces a further variable $\tau = \zeta + i\epsilon$ such that

Riabouchinsky Flows.

FIGURE 1.20 a z-Plane

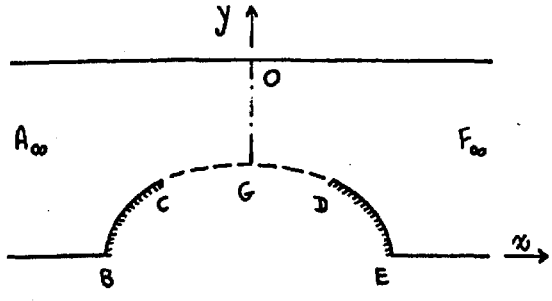

FIGURE 1.20 b z-Plane

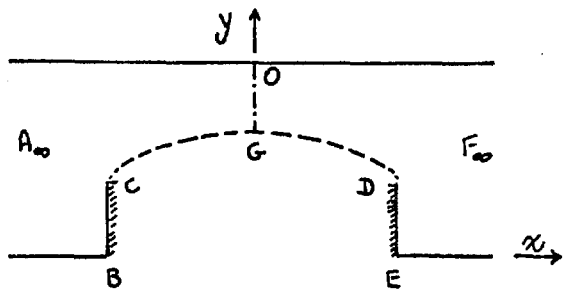

FIGURE 1.20 c w-Plane

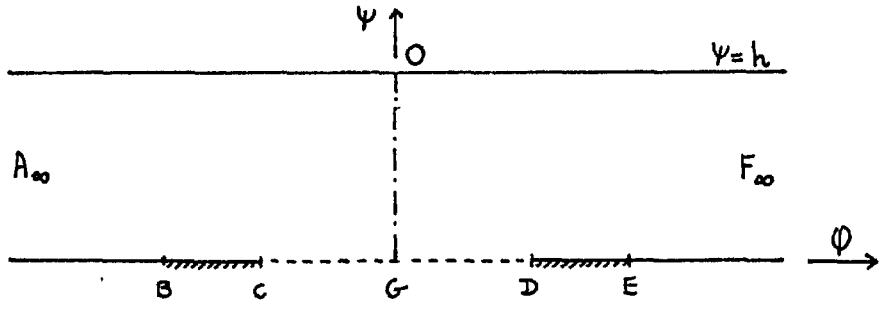

FIGURE 1.20 d ζ-Plane

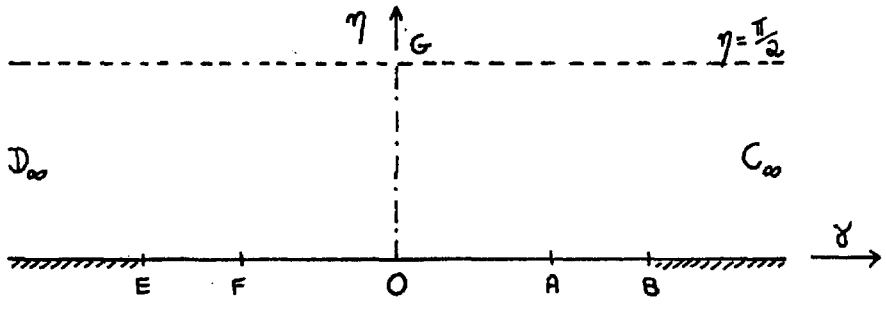

FIGURE 1.20 e χ-Plane

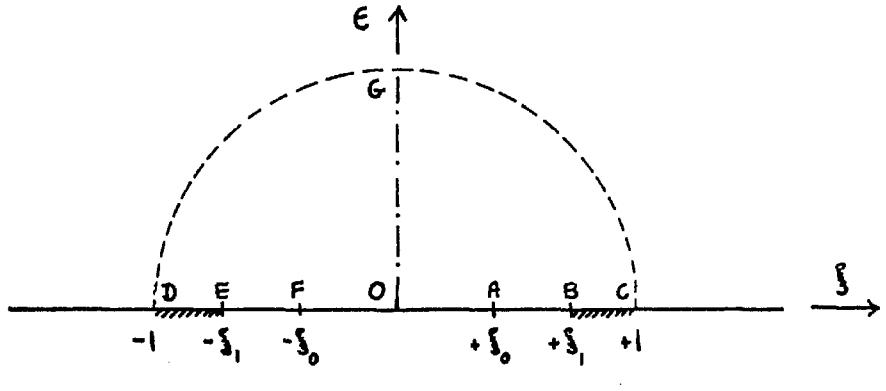

[1.28] $$\coth \zeta = \frac{1}{2}\left[\frac{1}{\chi} + \chi\right]$$

[N.B. The notation here is different from that used by Woods. It is altered so that ζ always relates to the same plane in which $\eta = \pi/2$ is the free streamline and $\eta = 0$, the solid boundary]. The χ-plane then assumes the form shown in figure 1.20e and from [1.26],[1.28] is related to the γ-plane by :

[1.29] $$\gamma(\chi) = \Omega_s + i\theta_s + \frac{1}{\pi}\int_{-1}^{+1} \ln\left[\frac{1 - \chi\xi}{\chi - \xi}\right] d\theta(\xi)$$

where Ω_s, θ_s are the values of Ω, θ at the separation point. The point upstream at infinity maps onto $\chi = \xi_0$, so that from [1.27] and [1.28] :

[1.30] $$\xi_0 = \tanh \frac{\pi\phi_0}{4h}$$

At this point we put $q = U$, $\theta = 0$ and $\gamma(\xi_0) = \gamma(-\xi_0) = 0$ and by substitution in [1.29], taking the real part of the integral :

[1.31] $$\Omega_s = \frac{1}{\pi}\int_{-1}^{+1} \ln\left|\frac{\xi - \xi_0}{1 - \xi\xi_0}\right| d\theta(\xi)$$

$$= \frac{1}{\pi}\int_{-1}^{+1} \ln\left|\frac{\xi + \xi_0}{1 + \xi\xi_0}\right| d\theta(\xi)$$

Hence

$$\int_{-1}^{+1} \ln\left|\frac{\xi - \xi_0}{\xi + \xi_0} \cdot \frac{1 + \xi\xi_0}{1 - \xi\xi_0}\right| d\theta(\xi) = 0$$

Then, since $q_c^2/U^2 = 1 + Q = e^{-\Omega_s}$

[1.32] $$Q = \exp\left\{-\frac{1}{\pi}\int_{-1}^{+1} \ln\left|\frac{\xi^2 - \xi_0^2}{1 - \xi^2\xi_0^2}\right| d\theta(\xi)\right\} - 1$$

Equations [1.29] and [1.32] represent the solution of the problem.

However, in order to solve a particular problem where the function $s(\theta)$, the equation of the wetted surface (where s is measured along that surface), is known, an iterative procedure of the following type

is required. This may consist of the following sequence of operations :

[1] A guess is made for the distribution $q\ (\varphi)$, denoted by $q_0(\varphi)$.

[2] From the equation $s = \int \frac{d\varphi}{q}$, we find $s_1(\varphi)$ and $\theta_1(\varphi)$.

[3] Thus equation [1.27] and [1.28] give $\theta_1(\xi)$.

[4] Then substituting this in [1.29] , taking the real part of that equation , $q_1(\chi)$ and therefore $q_1(\xi)$ results.

[5] Using $s = \int \frac{d\varphi}{d\xi}\frac{d\xi}{q}$ we get $s_2(\xi)$ and therefore $\theta_2(\xi)$.

The steps [3],[4] and [5] are then repeated until the process converges. The final value of Q will be found from the equation [1.32].

1.5.5 Riabouchinsky Flow past a Normal Plate in a Channel.

A relevant example of the last section is the Riabouchinsky flow past a flat plate in a channel. This is the simplest example since on the wetted surface $\theta = \pi/2$ and the solution does not require an iterative procedure. Woods (Ref. 48,p. 480) solves this as an example of the general type , whereas Birkhoff and Zarantonello (Ref. 6,p. 115) treat it as a particular case of "U-shaped" obstacles , where the "U" is in this case CBED of figure 1.21.

For the flat plate , since there are discontinuities

of $\pi/2$ in θ at B and E , [1.29] and [1.31] become

$$[1.33]\quad \gamma(\zeta) = \Omega_s + \frac{1}{2} i\pi + \frac{1}{2} \ln\left[\frac{1-\zeta\xi_1}{\zeta-\xi_1}\right] + \frac{1}{2} \ln\left[\frac{1+\zeta\xi_1}{\zeta+\xi_1}\right]$$

$$[1.34]\quad \Omega_c = \frac{1}{2} \ln\left[\frac{\xi_1^2 - \xi_0^2}{1 - \xi_1^2\xi_0^2}\right]$$

where $\pm\xi_1$ are the values of ξ at B and E , the stagnation points. Thus

$$e^{\gamma} = U\frac{dz}{dw} = e^{\Omega_c}\cdot\left[\frac{1-\zeta^2\xi_1^2}{\xi_1^2-\zeta^2}\right]^{\frac{1}{2}}$$

Woods then integrates this using the substitution

$$\zeta = \frac{k\, sn(u,k)}{1 + dn(u,k)}$$

where , therefore

$$\xi_1^2 = \frac{1-k'}{1+k'}$$

$$ns\, u = -\, ns\, u_0 \tanh\frac{\pi w}{2h}$$

$$k\, sn\, u_0 = \tanh\frac{\pi\varphi_0}{2h} = \frac{2\xi_0}{1+\xi_0^2}$$

The solution is then given by Woods as

$$[1.35]\quad z = \frac{HU}{2\pi q_c k}\left[-\frac{2u}{sn\, u_0} + \frac{k'}{cn\, u_0}\ln\left[\frac{cs\, u - cs\, u_0}{cs\, u + cs\, u_0}\right] + 2dc\, u_0\Pi(u, u_0+iK')\right]$$

the origins of z and u being the point J of figure 1.21.

The result given by Birkhoff and Zarantonello (Ref.6,p.117,eqn. (32)) differs essentially from this in the sign of the term upon which the logarithm acts. As a result of the computations of Appendix A the author concluded that the version given by Woods was correct.

From equation [1.35] and equation [1.34] the following identities are fairly easily obtained :

$$[1.36]\quad Q = \frac{2k'}{dn\, u_0 - k'}$$

$$[1.37]\quad \frac{L}{H} = \frac{2KU}{\pi k q_c}\left[k^2 sn\, u_0 - dc\, u_0 Z_4(u_0)\right]$$

FIGURE 1.21

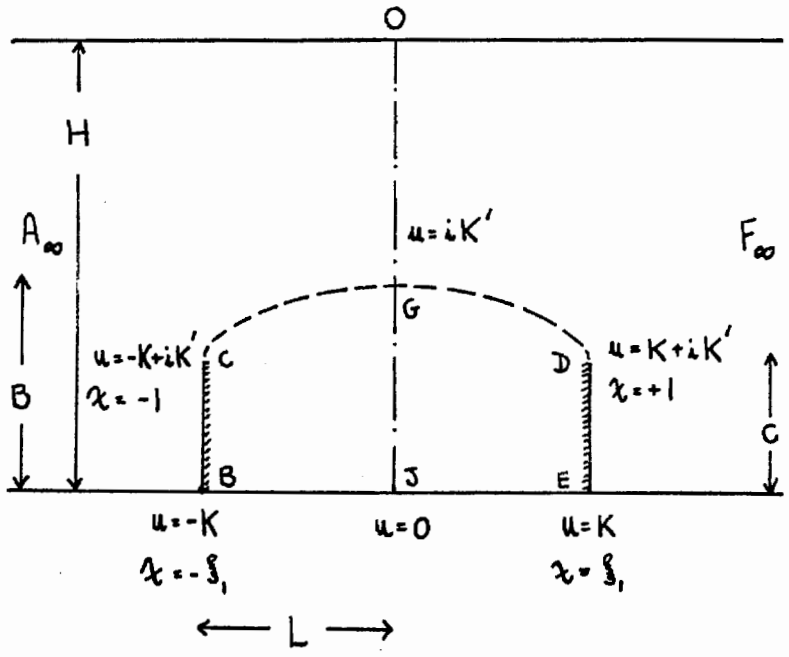
O
H
A_∞
$u = iK'$
F_∞
G
$u = -K + iK'$
C
D
$u = K + iK'$
$x = -1$
$x = +1$
B
C
B
J
E
$u = -K$
$u = 0$
$u = K$
$x = -\xi_1$
$x = \xi_1$
L

[1.38]

$$\frac{C}{H} = \frac{2U}{\pi k q_c}\left[\frac{\pi u_0 dc\ u_0}{2K} + K' dc\ u_0 Z_4(u_0) - K'k^2\, sn\ u_0 + k'\, nc\ u_0 \tan^{-1}(k'\, sc\ u_0)\right]$$

[1.39]

$$\frac{B}{H} = \frac{2U}{\pi k q_c}\left[\frac{\pi u_0 dc\ u_0}{2K} + K' dc\ u_0 Z_4(u) - K'k^2\, sn\ u_0 + k'\, nc\ u_0 \tan^{-1}(sc\ u_0)\right]$$

[1.40] $$C_D = \left(\frac{4q_c}{\pi U k}\right)\left(\frac{H}{C}\right)\left[\frac{\pi u_0 dc\ u_0}{2K} - K'k^2\, sn\ u_0 + K'\, dc\ u_0 Z_4(u_0)\right]$$

[In all these equations the elliptic functions are as given in Ref. 48, Chapter 4]

The case $H = \infty$ requires special treatment. Here the results of references 6 and 48 are identical. The results given by Woods (Ref. 48) contain the parameter k and φ_0, the latter not appearing in any of the dimensionless ratios.

[1.41] $$Q = \frac{2k'}{1 - k'}$$

[1.42] $$L = \frac{2\varphi_0}{k^2 q_c}\left(E - K k'^2\right)$$

[1.43] $$C = \frac{2\varphi_0}{k^2 q_c}\left(E' - K'k^2 + k'^2\right)$$

[1.44] $$B = \frac{2\varphi_0}{k^2 q_c}\left(E' - K'k^2 + k'\right)$$

[1.45] $$C_D = 2\left(\frac{q_c}{U}\right)^2\left(\frac{E' - K'k^2}{E' - K'k^2 + k'^2}\right)$$

When Q is small these can be approximated by :

[1.46] $$\frac{L}{C} = \frac{16}{4 + \pi}\,\frac{1}{Q^2}$$

[1.47] $$\frac{B}{C} = \frac{8}{4 + \pi}\,\frac{1}{Q}$$

[1.48] $$C_D = \frac{2\pi}{4 + \pi}\,(1 + Q)$$

Computations based on these formulae are carried out in Appendix A .

1.5.6 Separation in Plane Flow.

In section 1.4.6 we quoted some results given by Armstrong (Ref. 2) for the nature of the flow in the neighbourhood of a separation point. His results for the axisymmetric flow case are discussed in section 3.4 where they are developed to suit the particular requirements of this thesis. But, since Armstrong concludes that the nature of the flow in the region of abrupt or smooth separation is independent of whether the flow is planar or axisymmetric , it will be useful to give a brief outline of the results obtained for the plane case. [Armstrongs notation and sign convention have been altered here for the sake of uniformity.]

He introduces a complex variable t where

$$w = \frac{1}{2} t^2$$

so that t is real on the free streamline and imaginary on the wetted surface , the origin being taken at the separation point and the x axis as tangential to the streamline at this point. A more useful form of Υ (section 1.5.1) in this application is Υ^* where

$$\Upsilon^* = \log\left(\frac{q_c}{q}\right) + i\theta$$

This means that on the free streamline where t is real, Υ^* is purely imaginary, since $q = q_c$, and that $\Upsilon^* = 0$ at the origin. Armstrong therefore proposes that the general relation between Υ^* and t ,in the neighbourhood of the origin where t is small, will be :

[1.49] $$-\Upsilon^* = i \sum_{n=p}^{\infty} a_n t^n$$

Here the coefficients a_n are real and p is a non-zero positive integer. Also using the technique of complex variable , we have :

$$\frac{dz}{dw} = q_c \cdot e^{-\gamma^*}$$

Thus

$$\frac{dz}{dt} = q_c \cdot t \cdot e^{-\gamma^*} \qquad [1.50]$$

He then considers two cases; p = 1 and p = 2, and shows that the former corresponds to abrupt , the latter to smooth separation. Putting $\epsilon = |t|$, he shows that:

For p = 1 On the free streamline where $t = \epsilon$,

$$\frac{dy}{dx} = a_1\epsilon + O(\epsilon^2)$$

$$\frac{d^2y}{dx^2} = a_1\epsilon^{-1} + O(1) \qquad [1.51a]$$

On the wetted surface where $t = -i\epsilon$,

$$\frac{dy}{dx} = -a_2\epsilon^2 + O(\epsilon^3)$$

$$\frac{d^2y}{dx^2} = 2a_2 + O(\epsilon) \qquad [1.51b]$$

From equations [1.51] we see that the curvature of the free streamline tends to infinity as $\epsilon \to 0$. But this point of infinite curvature does not constitute a "corner" since the slope , from the equations for $\frac{dy}{dx}$,is continuous through the origin. It can also be seen that p = 1 leads to an infinite velocity gradient on the wetted surface at the origin. Thus p = 1 gives the case of abrupt separation.

For p = 2 On the free streamline,

$$\frac{dy}{dx} = a_2\epsilon^2 + a_3\epsilon^3 + O(\epsilon^4)$$

$$\frac{d^2y}{dx^2} = 2a_2 + O(\epsilon) \qquad [1.52a]$$

On the wetted surface,

$$\frac{dy}{dx} = -a_2\epsilon^2 + O(\epsilon^4)$$

[1.52b]

$$\frac{d^2y}{dx^2} = 2a_2 + O(\epsilon^2)$$

This, therefore, corresponds to smooth separation since $\frac{d^2y}{dx^2}$ (and hence the curvature) is continuous through the origin and, as Armstrong also shows, the velocity gradient approaches zero on the wetted surface as $\epsilon \to 0$. It also follows from [1.52a] and [1.52b] that the radius of curvature of both the wetted surface and the free streamline at the origin is $1/2a_2$.

Woods (Ref. 48, p. 435) arrives at similar results for smooth separation by a slightly different approach. He quotes the results as conditions for the correct positioning of a smooth separation point.

CHAPTER 2

CHAPTER 2

2.1 OUTLINE OF PREVIOUS APPROACHES TO THE SOLUTION OF AXISYMMETRIC CAVITY FLOWS.

The object of this thesis is the development of a relaxation technique for the numerical solution of axisymmetric cavity flows. This technique will take as its starting point a method suggested by Woods (Ref. 46) for the solution of flows in axisymmetric ducts.

However , before this method is developed , an outline of previous approaches to the problem of axisymmetric cavity flow will be given. This type of flow is of considerable practical importance and , in the absence of exact solutions , numerous efforts have been made at useful approximations. These previous approaches can be split very roughly into four types which will be dealt with in turn in the following sections.

[A] At an early stage in the consideration of this problem the idea of simulating cavity flows by means of distributed sources and sinks was conceived. Initially axial distributions were used and various authors have successively improved the method with other distributions.

[B] Using the exact solutions for the corresponding plane

flows a number of authors have developed methods for their adaption to the axisymmetric case.

[C] Relaxation methods for the solution of fluid flows have been developed for application in flows with free surfaces.

An excellent review of these methods , and those for planar flow , is given by Gilbarg (Ref. 16).

2.2 EMPIRICAL RESULTS.

2.2.1 Flow on the wetted surface. The drag of the body.

Reichardt (Ref. 34) , in his experiments on bodies of revolution, noticed the linear dependence of the coefficient of drag, C_D , on the cavitation number. Thus he put forward an approximate equation for the drag of a body in cavitating flow:

[2.1] $$C_D(Q) = (1 + Q)\, C_D(0)$$

where $C_D(0)$ is the drag on the same body under similar conditions, but at zero cavitation number.

We can relate the coefficient of drag to the equation for C_p in terms of y or r for a body of given shape and known point of separation. In the case of a plane flow

[2.2] $$C_D(Q) = \int_{\text{Wetted Surface}} (Q + C_p)\, \frac{dy}{Y}$$

where Y is the maximum y ordinate of the body surface. In the axisymmetric case:

$$[2.3] \qquad C_D(Q) = \int_{\text{Wetted Surface}} (Q + C_p) \frac{2r\,dr}{r^2_{MAX}}$$

where r_{MAX} is the maximum radius of the body. Reichardt surmised that for bodies with a fixed separation point, his result was due to the similarity of the $(C_p - 1)$ against y curves for different values of Q and a given profile ; that these were reducible to a single typical curve by adjustment in the $(C_p - 1)$ scale, so that all curves of $\frac{(C_p - 1)}{(1 + Q)}$ against y were identical.

Then putting

$$[2.4] \qquad \frac{(C_p - 1)}{(1 + Q)} = -1 + f(y)$$

we get, in plane flow

$$[2.5] \qquad C_D = (1 + Q) \int_{W.S.} \frac{f(y)}{Y}\,dy$$

and in axisymmetric flow

$$[2.6] \qquad C_D = (1 + Q) \int_{W.S.} \frac{f(r)}{r^2_{MAX}}\,2r\,dr$$

The integral is now independent of Q and hence leads to equation [2.1] in each case.

In the case of flows with smooth separation the y scale must also be reduced since y_s may vary with Q . Assuming that the curve of $\frac{(C_p - 1)}{(1 + Q)}$ against $\frac{y}{y_s}$ is the same in each case, then

$$[2.7] \qquad C_D \overset{\text{PLANE}}{=\!=} (1 + Q) \int_{W.S.} f'\left(\frac{y}{y_s}\right) \frac{dy}{Y}$$

$$[2.8] \qquad C_D \overset{\text{AXISYM.}}{=\!=\!=} (1 + Q) \int_{W.S.} f'\left(\frac{r}{r_s}\right) \frac{2r\,dr}{r^2_{MAX}}$$

Due to the variation of y_b we would expect equation [2.1] to be less accurate in the case of smooth separation if the basic premise of reducibility is reasonably correct.

Equation [2.1] has been shown to be remarkably accurate for plane and axisymmetric flow in both experiment and theory. The reader is referred to Waid (Ref. 45) for experiments on plane flows ; Reichardt (Ref. 34) , Eisenberg and Pond (Ref. 10) and Hsu and Perry (Ref. 19) for experiments on axisymmetric flow ; the exact and approximate relations given in section 1.5.5 ; the numerous theoretical results obtained for axisymmetric flow which are outlined in the following sections and to the graphs of section 5.4 . However , as has been anticipated , it is more accurate in the case of flows with abrupt separation as is demonstrated by a comparison of the results of sections 5.4.1 and 5.4.3 .

2.2.2 The Main dimensions of the Cavity.

The notation used when referring to the main dimensions of a cavity is defined in figure 2.1. The author defines the half-length , L , as the axial distance from the front stagnation point to the point of maximum radius of the cavity. Reichardt (Ref. 34) , from his experimental results for bodies of revolution , deduced the following empirical relations for the half-length and maximum radius of the cavities.

[2.9] $$\frac{L}{C} = \frac{(Q + 0.008)\sqrt{C_D}}{(0.066 + 1.70\,Q)\,Q^{\frac{1}{4}}}$$

FIGURE 2.1

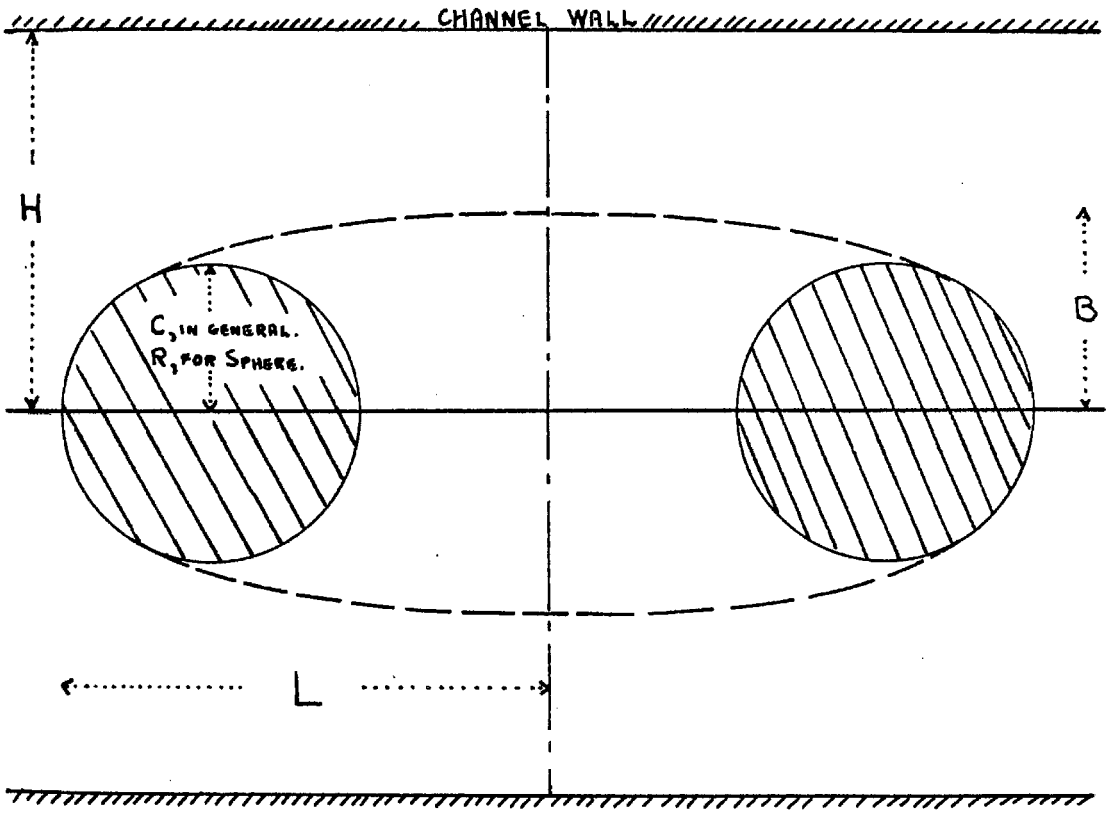

[2.10] $$\frac{B}{C} = \left(\frac{C_D}{Q}\right)^{\frac{1}{2}}$$

His experiments were carried out in the range of Q between 0 and 0.1 and the empirical relations are thus designed for this range. They do , however , demonstrate the power relations of section 1.2.2 ; the approximate formulae of section 1.5.5 confirm the power relations for the plane case. It has therefore become fairly normal when plotting results for the dimensions of a cavity to plot $\frac{C}{L}$ and $\left(\frac{C}{B}\right)^2$ against Q in the axisymmetric case and $\left(\frac{C}{L}\right)^{\frac{1}{2}}$ and $\frac{C}{B}$ against Q for the plane case since these curves should be , very roughly , straight lines through the origin.

2.3 THEORIES BASED ON SOURCE-SINK DISTRIBUTIONS.

2.3.1 Axial Distributions.

The first attempt to be made at simulating axisymmetric cavity flow by setting up "Rankine" bodies using source-sink distributions was made by Reichardt and Munzner (Ref. 35) . The solution of the flow in an infinite medium due to a point source , strength M , at the point $x = x_1$, $y = 0$ namely,

[2.11] $$\phi = \frac{M}{[(x - x_1)^2 + r^2]^{\frac{1}{2}}}$$
$$\psi = M\left[-1 + \frac{x - x_1}{[(x - x_1)^2 + r^2]^{\frac{1}{2}}}\right]$$

provides the basis of all these methods. Reichardt and Munzner used five different axial asymmetric line

distributions and by adjusting the five parameters governing the relative strengths of each distribution produced Rankine flows in which the pressure on the line $\Psi = 0$ was fairly constant over the major part of the body surface ; that is to say except for the surface close to the stagnation point. Since the distributions were all asymmetric , theirs was essentially a Riabouchinsky type flow. However this method only produced head shapes of a small aspect ratio. The equation of the Rankine body surface is a Fredholm integral of the first kind :

[2.12]
$$\int_a^b \frac{m(t)\,dt}{[(x-t)^2 + r^2]^{\frac{1}{2}}} = \frac{1}{2}$$

where the axial source strength / unit length is a function of x , m(x); that function is limited to the interval , $a \leqslant x \leqslant b$.

Methods of solution of this integral equation and others , such as that given by a doublet distribution , under conditions to simulate cavity flows have been further developed by Landweber (Ref. 26) , Munk (Ref. 31) and Armstrong and Tadman (Ref. 3) among others.

2.3.2 Theories based on Vortex Sheet Distributions.

Since the distributions of the last section are analytic off the axis they cannot simulate the singularity at the separation point which is a very important feature of cavity flows , especially those with abrupt separation. To overcome this other types of

distributed singularity have been used. Of these, distributed source rings have been employed but , more profitably , a number of authors have used vortex sheets to make up the body surface and free streamline. The body and cavity are considered to be replaced by a mass of liquid completely at rest. Then the only singularities in the flow are the doublet at infinity , producing the infinite uniform stream , and the vortex sheet along the closed stream surface which produces the velocity difference across that surface. The strength / unit arc length of the vortex sheet at any point is then equal to the velocity of the flow on , and external to , the sheet at that point since the internal velocity is zero. The reader is referred to Landweber (Ref. 26) and Armstrong and Dunham (Ref. 1) among others. We will denote the strength / unit arc length , therefore , by the function q(s). The key to the method is the fact that the solution of the flow due to a single vortex ring , of strength q ds , is known. [For the actual equations , see Ref. 1] Then the flow due to the vortex sheet q (s) can be found by superposition of its elements to give the solution in the form of an integral for any of φ , ψ , u or v .

The value of the function q is known on part of the vortex sheet (the free streamline) and the function x(s) or r(s) on the rest (the wetted surface). Thus it is required to find q (s) on the wetted surface and x(s) or r(s) on the free streamline.

Two approaches have been made to the iterative numerical solution of the integral equations obtained by this method. Armstrong and Dunham (Ref. 1) alternately

recalculated the distributions q(s) and x(s) for the flow past a disc , taking as their starting point the velocity distribution , $q_0(s)$, on the wetted surface of the corresponding planar flow past a flat plate. Landweber (Ref. 26) employs a slightly different method which only requires the repeated recalculation of the single function, q(s). The results of Armstrong and Dunham provide a useful comparison to the results of this thesis.

One limitation of these methods is that they only produce results for the cavitating flows in an infinite stream. Also , the computation required is considerable.

Using this type of method , Levinson (Ref. 28) determined the approximate shape of the infinite cavity at $Q = 0$ as $x \to \infty$.

2.4 THEORIES BASED ON PLANE FLOW SOLUTIONS.

2.4.1 Velocity Distributions.

Several authors have calculated approximate values for the coefficient of drag on axisymmetric bodies using the analytic velocity distributions on the surface of the corresponding planar body. Since the two distributions , for plane and axisymmetric profiles , will have the same end conditions it is reasonable to assume that they will not differ widely in between. Thus , for a disc and flat plate ,

$$(C_p)_{\frac{r}{r_b}=0} = 1 \quad , \quad \left(\frac{\partial C_p}{\partial r}\right)_{\frac{r}{r_b}=0} = 0 \quad , \quad (C_p)_{\frac{r}{r_b}=1} = -Q \quad , \quad \left(\frac{\partial C_p}{\partial r}\right)_{\frac{r}{r_b}=1} = -\infty$$

in both cases.

Plesset and Shaffer (Ref. 33) calculated C_D for cones using the velocity distributions on wedges with the same vertex angle and at the same cavitation number. Their results and those for other authors mentioned in this section are presented in section 5.4.1 . Plesset and Shaffer's results appear in comparison with others to be best for the disc (180° cone) and poorest for cones of small vertex angle and low Q.

Fisher (Ref. 11) refined this method by suggesting that a better approximation to the velocity distribution in the axisymmetric case at $Q = Q_2$ is the distribution of the plane flow at $Q = Q_3$ where the uniform stream velocity of the former is $\pi/2$ times that of the latter. He bases this assumption on the fact that the velocity distributions for the Dirichlet flows around a flat plate and a disc are identical when $U_2 = \pi U_3/2$. Thus putting

$$1 + Q_2 = \frac{\pi^2}{4} (1 + Q_3)$$

Fisher obtained better agreement with other computed results.

Armstrong and Dunham (Ref. 1) suggest yet another correspondence relation in connection with their work , outlined in section 2.3.2 .

2.4.2 The Perturbation Method of Garabedian.

Garabedian (Ref. 13) has devised an ingenious method for the solution of the axisymmetric problem using the results of its plane flow equivalent. In order to draw a parallel between the two he considers the concept

of the flow in $\epsilon + 2$ dimensions where $\epsilon = 0$ gives the planar equations and $\epsilon = 1$ the axisymmetric. Thus equations [1.14] and [1.18] become

$$[2.13] \qquad \frac{\partial^2\psi}{\partial x^2} + \frac{\partial^2\psi}{\partial y^2} - \frac{\epsilon}{y}\cdot\frac{\partial\psi}{\partial y} = 0$$

The flow is denoted by $\Omega(\epsilon)$ and its boundary as $T_1(\epsilon)$ and $T_2(\epsilon)$, being the fixed and free parts respectively. The condition on the free streamline becomes

$$[2.14] \qquad \frac{1}{y^\epsilon}\frac{\partial\psi}{\partial n} = 0$$

Now Garabedian proposes that the solution is a regular function of ϵ, convergent for $Re(\epsilon) > -1$ and thus the stream function can be written as

$$[2.15] \qquad \psi(x,y;\epsilon) = \psi_0(x,y) + \epsilon.\psi_1(x,y) + \epsilon^2.\psi_2(x,y) + \ldots$$

He shows that by expansion in the variable, δ, where

$$[2.16] \qquad \delta = \frac{\epsilon}{\epsilon + 2} \qquad (\text{thus } \epsilon = 1,\ \delta = 1/3)$$

convergence can be produced in the entire region of $Re(\epsilon) > -1$. From equation [2.15] it is clear that $\psi_0(x,y)$ is the known solution of the two dimensional problem and it remains to estimate the perturbations, ψ_i.

From [2.15] these terms satisfy the recurrence relation

$$[2.17] \qquad \nabla^2\psi_i = \frac{1}{y}\frac{\partial\psi_{i-1}}{\partial y}$$

At this point Garabedian introduces the function $U_i = \frac{\psi_i}{y^\epsilon}$ which he considers more convenient than ψ_i. However for ψ_i the boundary condition on $T_{1,2}$ is

$$\psi_i = 0$$

and that on T_2 after some considerable calculation and the substitution $\epsilon = 0$ becomes

$$\frac{\partial \Psi_i}{\partial n} + R_0 \Psi_i = B_i$$

where $R_0(\epsilon)$ is the curvature of $T_2(\epsilon)$ and B_i are known expressions involving only earlier coefficients of Ψ_{i-m}. Thus all the solutions for Ψ_i are given progressively as solutions of linear mixed boundary value problems starting initially with Ψ_0.

Garabedian gives considerable detail of this method of solution for infinite cavities ($Q = 0$) with special reference to the coefficient of drag behind a disc. In this case he estimates

[2.18] $$C_D = 0.8798 - 0.14838\,\delta - 0.02818\,\delta^2$$

in which 0.8798 is the value of $(C_D)_{Q=0}$ for the flat plate. (See Appendix A.) Thus for $\delta = 1/3$, the axisymmetric case, he finds

[2.19] $$(C_D)_{Q=0} = 0.8272$$

and estimates his error at less than 1/2 per cent.

This method, however, proves to be much less accurate in the case of finite cavities ($Q > 0$) and Garabedian devises a different method of successive approximation to be used by itself or along with the perturbation method. From this method he derives the value of $\frac{C_D}{1+Q} = 0.865$ for $Q = 0.22$. He concludes however that these results are less accurate than those for $Q = 0$. The computation involved in either case is considerable.

2.5 RELAXATION METHODS.

Relaxation methods , a general outline of which is given , appropriately , in section 4.1.1 , were first developed for the solution of elliptic partial differential equations by Southwell (Ref. 42 among others). Southwell and Vaisey (Ref. 43) have also succeeded in the solution of certain flows with free surfaces. Without exception their solutions were carried out in the physical plane and therefore involved an unknown boundary shape with irregular stars (Ref. 12).

Southwell and Vaisey make a distinction between "stable" and "unstable" free streamline problems of which the cavity problem is the unstable type. They employ a method similar to that mentioned in section 4.3.5 of successive fixed boundary solutions interspersed with free streamline boundary adjustments according to the condition required on that boundary. The latter adjustments , since their methods were designed for desk calculators , would seem to have been based on physical reasoning , any other method apparently giving divergence for unstable free surfaces. Using this method they solve such problems as the axisymmetric Borda mouthpiece and a free jet falling through an orifice.

At the conclusion of that work they solve one axisymmetric cavity problem though this is of the unrealistic , cusped cavity behind a sphere. (See section 1.4.5 and figure 1.10 .) This would appear , in the authors experience , a much simpler solution than that of the Riabouchinsky flow.

Brunauer (Ref. 9) has also used a relaxation technique for the solution of one cavity behind a disc.

The author , unfortunately , found considerable difficulty in obtaining details of this method. His result (section 5.4.1) is taken from Armstrong and Dunham (Ref. 1).

Birkhoff and Zarantonello (Ref. 6) also mention some unpublished work by Young and Varga.

CHAPTER 3

CHAPTER 3

3.1 APPLICATION OF WOODS METHOD TO AXISYMMETRIC CAVITY FLOW.

3.1.1 Basic Equations.

Woods (Ref. 46) suggests that,if relaxation methods are to be applied to the solution of axisymmetric flows, then instead of dealing with the problem in the x,r plane where boundaries are not only curved but also,in the case of cavity flow,must be free to move,it would be much more convenient to use the transformed φ,Ψ plane where boundaries are polygonal. This involves interchanging the roles of the dependent and independent variables in the equations of section 1.4.3 ,the basic equations of ideal and steady axisymmetric flow. These were :

[3.1] $$\frac{\partial \varphi}{\partial x} = u = \frac{1}{r}\frac{\partial \Psi}{\partial r}$$

[3.2] $$\frac{\partial \varphi}{\partial r} = v = -\frac{1}{r}\frac{\partial \Psi}{\partial x}$$

In order to find the inverted differentials , Woods evaluates the Jacobian of φ and Ψ with respect to x and r :

$$\frac{\partial(\varphi,\Psi)}{\partial(x,r)} = \frac{\partial \varphi}{\partial x}\frac{\partial \Psi}{\partial r} - \frac{\partial \varphi}{\partial r}\frac{\partial \Psi}{\partial x}$$

$$= u(ru) - v(-vr)$$

[3.3] $$= rq^2$$

Then the differentials in the φ,Ψ plane become :

[3.4]
$$\frac{\partial x}{\partial \varphi} = \frac{1}{rq^2}\frac{\partial \psi}{\partial r}$$
$$\frac{\partial x}{\partial \psi} = -\frac{1}{rq^2}\frac{\partial \varphi}{\partial r}$$
$$\frac{\partial r}{\partial \varphi} = -\frac{1}{rq^2}\frac{\partial \psi}{\partial x} = \frac{1}{2f^{\frac{1}{2}}}\frac{\partial f}{\partial \varphi} = \frac{v}{q^2}$$
$$\frac{\partial r}{\partial \psi} = \frac{1}{rq^2}\frac{\partial \varphi}{\partial x} = \frac{1}{2f^{\frac{1}{2}}}\frac{\partial f}{\partial \psi} = \frac{u}{q^2 f^{\frac{1}{2}}}$$

where $f = r^2$. Hence in the φ, ψ plane the equations corresponding to [3.1] and [3.2] are :

[3.5]
$$\frac{\partial x}{\partial \varphi} = r\frac{\partial r}{\partial \psi}$$

[3.6]
$$\frac{\partial x}{\partial \psi} = -\frac{1}{r}\frac{\partial r}{\partial \varphi}$$

Then the equations corresponding to the equations for φ and ψ in the x,r plane(equations [1.17] and [1.18] of section 1.4.3) namely the equations which x and r must obey in the φ, ψ plane are found by differentiating equations [3.5] and [3.6]. Equating the cross-differentials we get :

[3.7]
$$\frac{\partial}{\partial \varphi}\left[\frac{1}{r}\frac{\partial r}{\partial \varphi}\right] + \frac{\partial}{\partial \psi}\left[r\frac{\partial r}{\partial \psi}\right] = 0$$

[3.8]
$$\frac{\partial}{\partial \varphi}\left[\frac{1}{r}\frac{\partial x}{\partial \varphi}\right] + \frac{\partial}{\partial \psi}\left[r\frac{\partial x}{\partial \psi}\right] = 0$$

Since the object is to solve for either x or r in the φ, ψ plane,of the two equations [3.7] and [3.8] , [3.7] is obviously preferable containing as it does only one dependent variable,r. Thus we choose to solve equation [3.7] to find r as a function of φ and ψ . Equation [3.7] can in fact be simplified by the introduction of the variable $f = r^2$ so that it becomes :

[3.9]
$$\frac{\partial}{\partial \varphi}\left[\frac{1}{f}\frac{\partial f}{\partial \varphi}\right] + \frac{\partial^2 f}{\partial \psi^2} = 0$$

or
$$\frac{\partial^2}{\partial \varphi^2}(\ln f) + \frac{\partial^2 f}{\partial \psi^2} = 0$$

This is the equation we propose to solve. Having found r as a function of φ and ψ , x will then follow.

$$dx = \frac{\partial x}{\partial \varphi} d\varphi + \frac{\partial x}{\partial \psi} d\psi$$

[3.10] $$dx = \frac{1}{2}\frac{\partial f}{\partial \psi} d\varphi - \frac{1}{2f}\frac{\partial f}{\partial \varphi} d\psi$$

using equations [3.4]. Relations for the velocities u, v, q will also follow from [3.1], [3.2] and [3.4] :

[3.11] $$v = \frac{q^2}{2r}\frac{\partial f}{\partial \varphi} = \frac{(u^2 + v^2)}{2r}\frac{\partial f}{\partial \varphi}$$

[3.12] $$u = \frac{q^2}{2}\frac{\partial f}{\partial \psi} = \frac{(u^2 + v^2)}{2}\frac{\partial f}{\partial \psi}$$

Therefore

$$q^2 = u^2 + v^2$$

$$= \frac{q^4}{4}\left(\frac{\partial f}{\partial \psi}\right)^2 + \frac{q^4}{4f}\left(\frac{\partial f}{\partial \varphi}\right)^2$$

Hence the equation for the velocity, q , is :

[3.13] $$\frac{4}{q^2} = \frac{1}{f}\cdot\left(\frac{\partial f}{\partial \varphi}\right)^2 + \left(\frac{\partial f}{\partial \psi}\right)^2$$

From the above equations for u and v we can find the angle, θ , which the vector $\underline{q}$ makes with the axis of symmetry.

[3.14] $$\tan\theta = \frac{\partial f}{\partial \varphi} \Big/ f^{\frac{1}{2}}\left(\frac{\partial f}{\partial \psi}\right)$$

The velocities u and v then follow since $u = q\cos\theta$ and $v = q\sin\theta$.

A relation connecting the second derivatives of the x, r and φ , ψ planes will also prove useful. From [3.1] and [3.2] we already know that the following relations hold in the x, r plane.

[3.15] $$-\frac{1}{r}\frac{\partial^2 \psi}{\partial x^2} = \frac{\partial^2 \varphi}{\partial x \partial r} = -\frac{1}{r^2}\frac{\partial \psi}{\partial r} + \frac{1}{r}\frac{\partial^2 \psi}{\partial r^2}$$

$$r\frac{\partial^2 \varphi}{\partial x^2} = \frac{\partial^2 \psi}{\partial x \partial r} = -\frac{\partial \varphi}{\partial r} - r\frac{\partial^2 \varphi}{\partial r^2}$$

These equations are simply a fuller version of those stated in section 1.4.3 for axisymmetric flow. In particular we shall need an expression for $\frac{\partial^2 f}{\partial \psi^2}$ in terms

of the second derivatives of equations [3.15]. This involves taking a further Jacobian, but since only one derivative is required it is simpler to start from first principles. By considering the changes in $\frac{\partial f}{\partial \psi}$ in both the x,r and ϕ , Ψ planes and also the changes in x and r in the ϕ , Ψ plane we find :

$$d\left(\frac{\partial f}{\partial \psi}\right) = \frac{\partial}{\partial \phi}\left(\frac{\partial f}{\partial \psi}\right) d\phi + \frac{\partial}{\partial \psi}\left(\frac{\partial f}{\partial \psi}\right) d\Psi$$

Also

$$d\left(\frac{\partial f}{\partial \psi}\right) = \frac{\partial}{\partial x}\left(\frac{\partial f}{\partial \psi}\right) dx + \frac{\partial}{\partial r}\left(\frac{\partial f}{\partial \psi}\right) dr$$

$$= \left(\frac{\partial x}{\partial \phi} d\phi + \frac{\partial x}{\partial \psi} d\Psi\right) \cdot \frac{\partial}{\partial x}\left(\frac{\partial f}{\partial \psi}\right) + \left(\frac{\partial r}{\partial \phi} d\phi + \frac{\partial r}{\partial \psi} d\Psi\right) \cdot \frac{\partial}{\partial r}\left(\frac{\partial f}{\partial \psi}\right)$$

Comparing the first and third of these equations and equating the coefficients of $d\Psi$:

$$[3.16] \qquad \frac{\partial^2 f}{\partial \psi^2} = \frac{\partial x}{\partial \psi} \frac{\partial}{\partial x}\left(\frac{\partial f}{\partial \psi}\right) + \frac{\partial r}{\partial \psi} \cdot \frac{\partial}{\partial r}\left(\frac{\partial f}{\partial \psi}\right)$$

But from [3.4]

$$\frac{\partial f}{\partial \psi} = \frac{2}{q^2} \frac{\partial \phi}{\partial x} = 2 \frac{\partial \phi}{\partial x} \Big/ \left[\left(\frac{\partial \phi}{\partial x}\right)^2 + \left(\frac{\partial \phi}{\partial r}\right)^2\right]$$

Then the partial derivatives of $\frac{\partial f}{\partial \psi}$ with respect to x and r become after simplification :

$$\frac{\partial}{\partial x}\left(\frac{\partial f}{\partial \psi}\right) = \frac{2}{q^4}\left[(v^2 - u^2) \frac{\partial^2 \phi}{\partial x^2} - 2uv \frac{\partial^2 \phi}{\partial x \partial r}\right]$$

$$\frac{\partial}{\partial r}\left(\frac{\partial f}{\partial \psi}\right) = \frac{2}{q^4}\left[(v^2 - u^2) \frac{\partial^2 \phi}{\partial x \partial r} - 2uv \frac{\partial^2 \phi}{\partial r^2}\right]$$

Substituting these expressions in [3.16] and for $\frac{\partial x}{\partial \psi}$ and $\frac{\partial r}{\partial \psi}$ from [3.4] we find :

$$[3.17] \qquad \frac{\partial^2 f}{\partial \psi^2} = \frac{2}{rq^2}\left[(vu^2 - v^3)\frac{\partial^2 \phi}{\partial x^2} + (3uv^2 - u^3)\frac{\partial^2 \phi}{\partial x \partial r} - 2vu^2 \frac{\partial^2 \phi}{\partial r^2}\right]$$

This expression for $\frac{\partial^2 f}{\partial \psi^2}$ can of course be rephrased in terms of the other second derivatives in the x,r plane by using

equations [3.15].

3.1.2 Description of the Problem.

Before any attempt is made to apply numerical or relaxation techniques to axisymmetric cavitating flows all the boundary conditions and determinate parameters must be specified. In this and the next section we will discuss appropriate boundary conditions and the determinacy of a particular problem.

The author decided that the simplest model which would prove useful would be that of a Riabouchinsky flow in a straight channel or tube. As has been previously mentioned in section 1.4.5 ,one advantage of the Riabouchinsky model is that it halves the size of the flow field to be solved,the flow being symmetric about the line BC of figure 3.1. This is particularly desirable in relaxation methods in which the field has to be covered with a mesh or net,the value of the dependent variable being estimated at the intersection points.

The figure 3.1 represents the flow field of such a problem in the x,r plane. Since the flow is symmetric about the line BC in the Riabouchinsky model the boundary condition on this line will be that all streamlines intersect it orthogonally. Thus v = 0 at all points on BC and BC is in fact a line ψ = constant. The curved line CD represents the free streamline or cavity wall whose position is unknown and the boundary condition on which is one of constant velocity. DE is the wetted

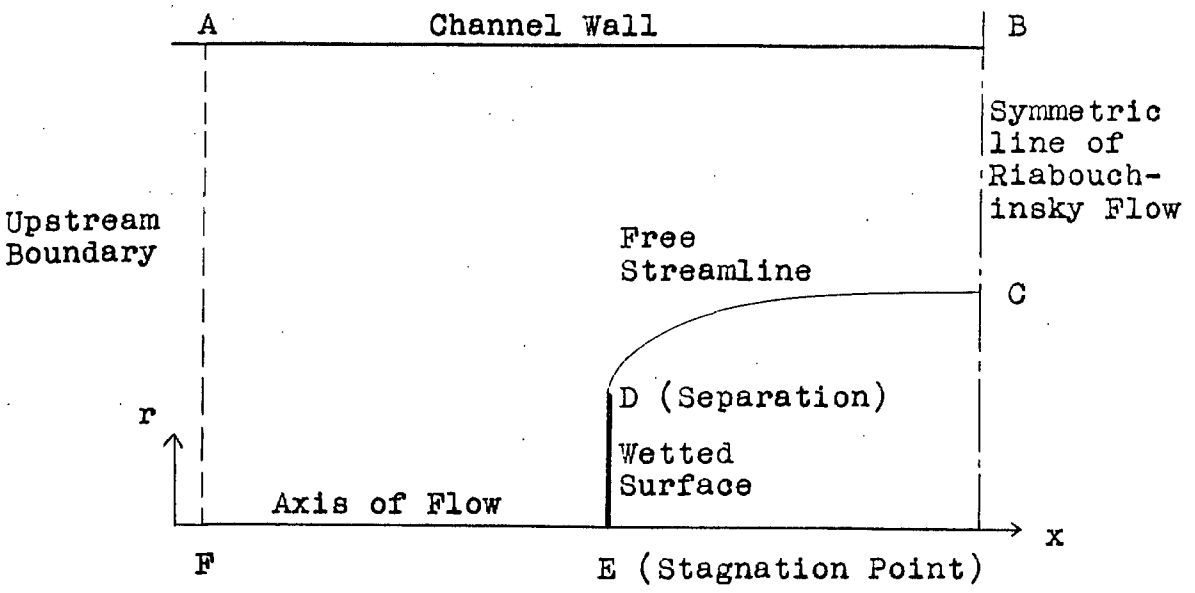

Figure 3.1 x , r Plane

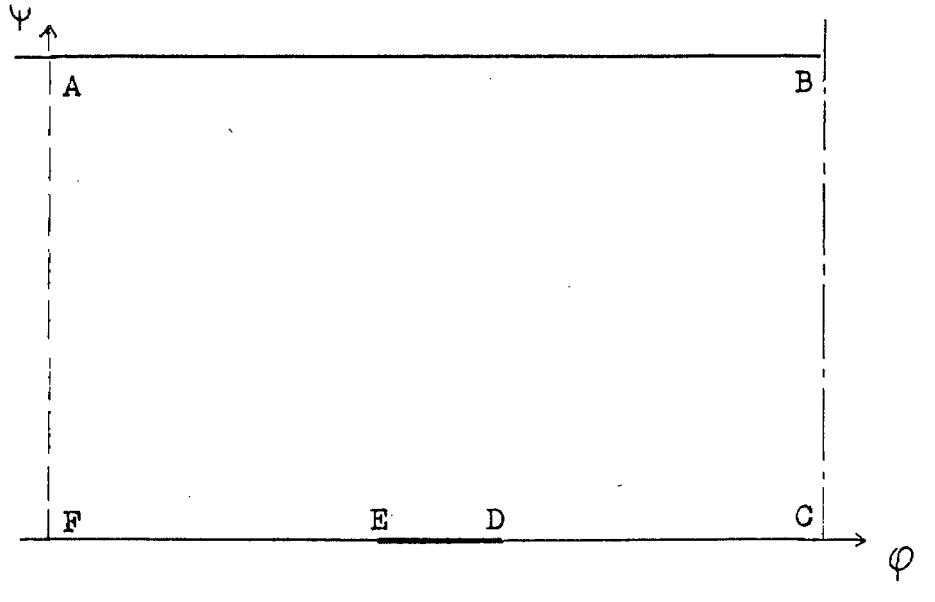

Figure 3.2 φ , Ψ Plane

surface on which θ is known as a function of x and r, D being the separation point and E the stagnation point. On the axis of the flow, EF, and the channel wall, AB, r is constant, being zero on the former. The lines AB and FEDC must also be streamlines on which Ψ = constant, the constant being zero on FEDC.

In order to use relaxation methods, the field must be finite and boundary conditions specified on every boundary. Thus, although the actual upstream condition of the flow depicted in figure 3.1 is that the flow tends to a uniform stream as x tends to $-\infty$, a condition will have to be found on a line such as AF at a finite value of x, so that the field to be solved will be finite and enclosed by the boundary ABCDEF. The simplest approximation on this boundary would assume uniform stream values, the position of AF being adjusted so that any further movement of it in the direction of $x = -\infty$ made no appreciable difference in the required results. However a more complex but more accurate condition will be introduced in section 3.3.2.

As to the choice of body profile, it was decided to use two different types in the calculations; one which exhibited abrupt separation and one with smooth separation. The obvious choices were a disc and a sphere since these gave simple boundary conditions on DE and experimental data existed for both. The solution for the Dirichlet flow around each in an infinite stream is also known and these solutions proved very useful when attempt was made tc treat the singularity at the stagnation point.

3.1.3 Boundary conditions in the transformed plane.

It is easily seen that the corresponding ϕ, Ψ plane to the x,r plane of figure 3.1 ,given the conditions that ϕ is constant on AF and BC ,is as shown in figure 3.2.

In this plane the boundary conditions outlined in section 3.1.2 become :

AB The channel wall is a streamline on which Ψ=constant and f = constant = r_H^2.

BC The condition on the line of symmetry is v = 0. By equation [3.11] this leads to $\frac{\partial f}{\partial \phi} = 0$; a Neumann boundary condition since $\frac{\partial f}{\partial \phi}$ is the normal gradient.

CD The free streamline. Thus :

$$q = \text{constant} = U\left(1 + Q\right)^{\frac{1}{2}}$$

From equation [3.13] this becomes,in terms of the normal and tangential gradients of f :

[3.18] $$\frac{1}{f}\left(\frac{\partial f}{\partial \phi}\right)^2 + \left(\frac{\partial f}{\partial \Psi}\right)^2 = \frac{4}{U^2(1+Q)}$$

where $\frac{\partial f}{\partial \Psi}$ is now the normal gradient and $\frac{\partial f}{\partial \phi}$ the tangential gradient. This is therefore a complex boundary condition.

DE The body surface. For a given profile, θ will be specified as a function of f , $\theta(f)$. Therefore,by virtue of equation [3.14] , the boundary condition becomes :

[3.19] $$f^{\frac{1}{2}}\left(\frac{\partial f}{\partial \Psi}\right)\tan\left[\theta(f)\right] - \frac{\partial f}{\partial \phi} = 0$$

Here the normal and tangential gradients are as for CD. We have , then , a complex boundary condition on DE.

For a disc this boundary condition becomes, since $\theta = \pi/2$.

[3.20] $$\frac{\partial f}{\partial \psi} = 0 \quad , \quad f \neq 0$$

This is equivalent to assuming $u = 0$ by equation [3.12]. The singular point, $f = 0$, the stagnation point, will require special treatment (sections 3.3.3 and 4.4).

For a sphere, given the radius, R, we know that on the wetted surface :

$$\cos\theta = \sqrt{f}/R \quad , \quad \tan\theta = \sqrt{R^2 - f}/\sqrt{f}$$

and therefore the condition becomes :

[3.21] $$\frac{\partial f}{\partial \psi}\sqrt{R^2 - f} = \frac{\partial f}{\partial \varphi}$$

EF The axis of symmetry : $f = 0$, and $\psi = 0$.

FA A more elaborate condition for this boundary will be given in section 3.3.2 , but a simpler condition used in the rough solutions, is to assume uniform stream conditions. The stream will of course be uniform only at $\varphi = -\infty$. We will assume that on a particular streamline the value of $f \to f_U$ as $\varphi \to -\infty$. Then since the stream is uniform at $\varphi = -\infty$,

$$\left(\frac{\partial^2 f}{\partial \varphi^2}\right)_{\varphi=-\infty} = \left(\frac{\partial f}{\partial \varphi}\right)_{\varphi=-\infty} = 0$$

Then by equations [3.9] and [3.4]

$$\left(\frac{\partial^2 f}{\partial \psi^2}\right)_{\varphi=-\infty} = 0 \qquad \text{and} \qquad \left(\frac{\partial f}{\partial \psi}\right)_{\varphi=-\infty} = \frac{2u}{q^2} = \frac{2}{U}$$

And thus:

[3.21a] $$\psi = \frac{1}{2}.U.f_U$$

since ψ is taken as zero on the axis. Thus the simple approximate boundary condition for FA would assume f to be linear with ψ on this boundary and if

f_H is given, f is known at all points on it.

It is worth noting at this point that one thing which must be borne in mind when dealing with Stokes stream function, Ψ, is that its dimensions, unlike those of ϕ, Ψ in planar flow and ϕ in axisymmetric flow, are velocity × (distance)^2 instead of velocity × distance for the other functions. In axisymmetric flow Ψ/ϕ is therefore not dimensionless, but has the dimension of distance.

3.1.4 Considerations of Determinacy.

Figure 3.3 depicts a cavity flow about a disc in a straight walled tube. In such a flow the position and shape of the free boundary CD is uniquely determined by the two dimensionless parameters Q and H/r_s, providing that the boundary AF on which the flow is uniform is at an infinite distance upstream. Then the flow is uniquely determined by the choice of two scales; a distance and a velocity scale. If, on the other hand, the boundary AF is at a finite distance upstream, and the boundary condition given on it, then the position of CD is uniquely determined by the specification of the parameters Q, H/r_s, and the dimensionless parameter L_1/r_s. Thus, given the condition on AF, the flow, in terms of dimensionless quantities, is completely determined by fixing the three parameters :

[3.22] $\qquad r_s/H \;,\; L_1/H \;,\; Q$

Then, in order to find the solution to the case $L_1 = \infty$, the object will be to increase the value of the

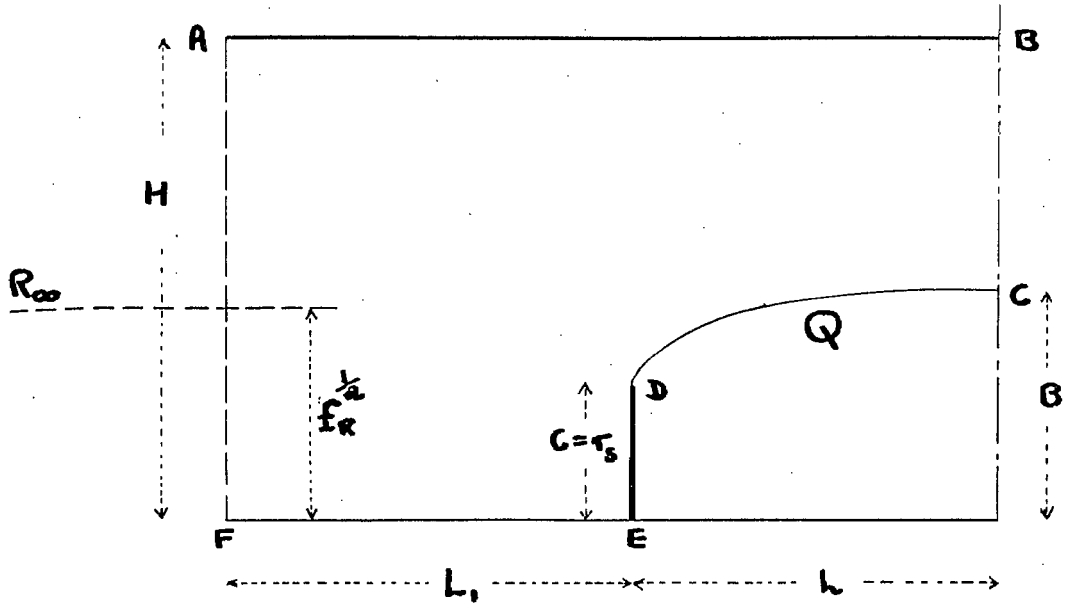

FIGURE 3.3

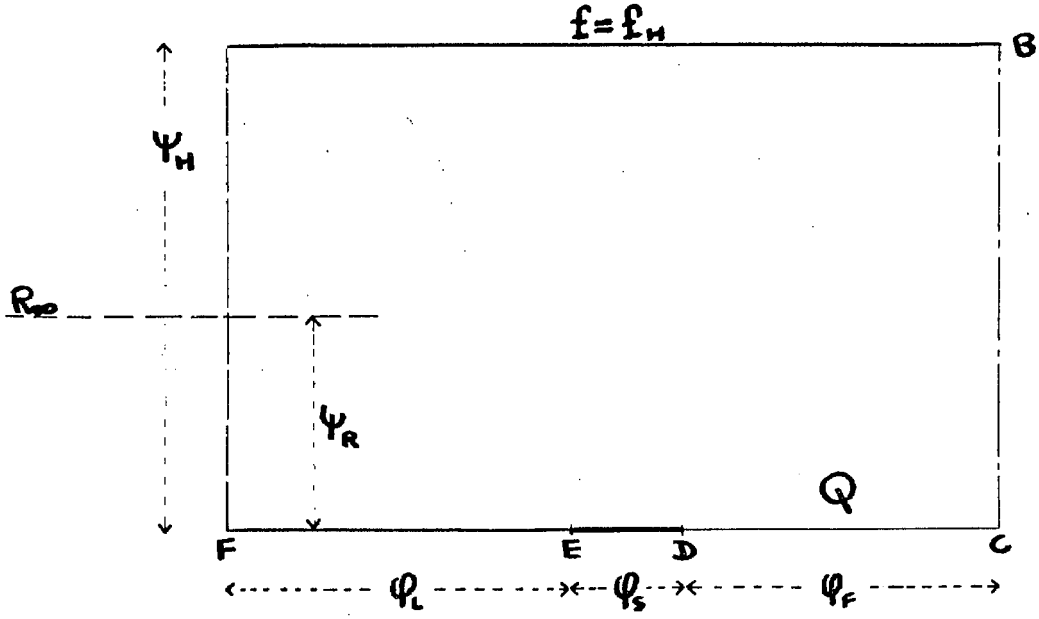

FIGURE 3.4

parameter L_1/H until any further increase has no significant effect on the position of CD in the solution for fixed values of r_s/H and Q.

It follows that the problem in the transformed plane (figure 3.4) will be uniquely determined for all dimensionless quantities by three parameters one of which will have the same function and effect as L_1/H in the x,r plane. All the quantities which could be specified are shown in figure 3.4. The quantity φ_L will be analogous to L_1 in the x,r plane, so that the dimensionless parameter φ_L/φ_S can be used in the same way as L_1/H. It will also be convenient to retain Q as one of the parameters to be specified in the φ, ψ plane. We are therefore left with only one other dimensionless quantity to specify in order to make the solution uniquely determined for all dimensionless quantities. This third parameter will clearly have to include some function of the position of the channel wall, say ψ_H or f_H. Various forms could be used but the author found the parameter $\psi_H^2 / \varphi_S^2 f_H$ the most easily applicable. Therefore, for a given boundary condition on AF, specifying the three parameters

[3.23] $$\frac{\varphi_L}{\varphi_S} \quad , \quad \left[\frac{\psi_H}{\varphi_S f_H}\right]^2 f_H \quad , \quad Q$$

will uniquely determine the value of f/f_H at any point $(\varphi/\varphi_S, \psi/\psi_H)$ in the φ, ψ plane. The coefficient of pressure C_p, will also be uniquely determined at any point.

One of the most important facts to emerge from this investigation is that the quantity φ_E is not included in the parameters [3.23]. Therefore, if [3.23] are specified, the boundary BC must be free to move in the φ

direction while, of course, remaining an equipotential. On the other hand one of [3.23], say Q, could be left unspecified and φ_F/φ_S used as a parameter , but the author found [3.23] the most convenient system. The way in which the position of this floating boundary is determined in the solution cannot be discussed until the nature of the flow on the free streamline and, in particular, at the separation point has been more fully investigated. (See sections 4.3.5 , 4.3.6 , 4.3.7 .)

Besides the parameters [3.22] or [3.23] we are of course free to choose both a length and a velocity scale in a particular problem. It is convenient to have numerical values of f at any point in the solution and so a numerical value could be assigned to f_H for the purposes of computation. But it will be noticed that the quantity $(\Psi_H/\varphi_S f_H)^2$ in the second of parameters [3.23] has the dimension $(1/f)$. It will prove more convenient if the distance scale is set by assigning a numerical value to this quantity rather than f_H. Thus we set

$$X = \frac{\Psi_H}{\varphi_S f_H}$$

and to avoid confusion this quantity X is held fixed throughout the complete set of solutions. Then in a particular problem the value of the second parameter gives a numerical value for f_H ,and therefore numerical values of f throughout the field. Alternatively we could ,by retaining the same value of X,find a complete set of solutions by varying the quantities :

[3.23a] $$\frac{\varphi_S}{\varphi_L} \quad , \quad f_H \quad , \quad Q$$

Every different set of these parameters defines a different problem, provided, in every case, X takes the same numerical value. It is not neccessary to set a velocity scale.

3.2 RELATIONS IN THE ϕ, Ψ PLANE FOR PHYSICAL QUANTITIES IN THE x,r PLANE.

3.2.1 General.

Certain properties of the flow at a point in the x,r plane will be required either as results or for purposes of computation as functions of the variables at the corresponding point in the ϕ, Ψ plane. For example a relation giving the radius of curvature of a streamline in the x,r plane will be needed in terms of the derivatives in the ϕ, Ψ plane. It will therefore be most convenient to develop all such relations in one section so that reference can be made to them later without digression. Some of these relations, for velocity direction and magnitude, have already been found in section 3.1.1.

3.2.2 The exact solutions for the Dirichlet flows around a sphere and a disc.

These are classic results involving particular solutions of the Laplace equation in three dimensions. The ideal steady flow solution for a sphere in an infinite uniform stream is a result quoted in most standard texts (e.g. Milne-Thomson, Ref. 30, p. 443) and is equivalent to the flow due to a doublet in an infinite stream. The solution is :

$$\psi = \frac{Ur^2}{2}\left[1 - \frac{R^3}{(r^2 + x^2)^{\frac{3}{2}}}\right]$$

$$\varphi = Ux\left[1 + \frac{R^3}{(r^2 + x^2)^{\frac{3}{2}}}\right] \qquad [3.24]$$

where x is measured from the centre of the sphere whose radius is R.

The solution for the flow of an infinite uniform stream around an infinitely thin disc is not so well known but is given by Lamb (Ref. 25, p. 144) as a special case of the motion due to a planetary ellipsoid moving with velocity U parallel to its axis in an infinite mass of liquid. Adjusting the solutions for φ, ψ to give the flow of an infinite stream past a disc set normal to the stream we get:

$$\varphi = \frac{2CU}{\pi}\mu\left[1 + \xi \tan^{-1}\xi\right]$$

$$\psi = \frac{UC^2}{\pi}(1 - \mu^2)\left[\xi + (1 + \xi^2)\tan^{-1}\xi\right] \qquad [3.25]$$

where C is the radius of the disc and μ, ξ are given by:

$$x = C.\xi.\mu$$

$$r = C(1 - \mu^2)^{\frac{1}{2}}(1 + \xi^2)^{\frac{1}{2}} \qquad [3.25a]$$

x being measured from the centre of the disc, which coincides with both the front and rear stagnation points since the disc is infinitesmally thin.

In this solution, since the flow negotiates the 180^0 corner at the edge of the disc, the velocity at this point is infinite.

Given the co-ordinates (φ, Ψ) of a point in the φ, Ψ plane in either of these flows we can then calculate the position (x,r) of the point in the physical plane.

3.2.3 The radius of curvature of a streamline.

In the physical plane the radius of curvature of a line through a point is given by:

[3.26] $$\frac{1}{R} = -\frac{d\theta}{ds}$$

where s is measured along that line and θ is the direction of its tangent that any point. If the line is a streamline, Ψ = constant , then we can say that

[3.27] $$\frac{1}{R} = -\frac{\partial s}{\partial \varphi}\frac{\partial \theta}{\partial \varphi} = -q\frac{\partial \theta}{\partial \varphi}$$

where q is the velocity magnitude at the point under consideration. But from equation [3.14] we know that,

[3.28] $$\tan\theta = \frac{\frac{\partial f}{\partial \varphi}}{f^{\frac{1}{2}}\frac{\partial f}{\partial \Psi}}$$

and hence :

[3.29] $$\sec^2\theta \cdot \frac{\partial \theta}{\partial \varphi} = -\frac{\left(\frac{\partial f}{\partial \varphi}\right)^2}{2f^{\frac{3}{2}}\frac{\partial f}{\partial \Psi}} + \frac{\frac{\partial^2 f}{\partial \varphi^2}}{f^{\frac{1}{2}}\frac{\partial f}{\partial \Psi}} - \frac{\frac{\partial f}{\partial \varphi}\cdot\frac{\partial^2 f}{\partial \varphi \partial \Psi}}{f^{\frac{1}{2}}\left(\frac{\partial f}{\partial \Psi}\right)^2}$$

From [3.28] we also find that

$$\sec^2\theta = \frac{f\left(\frac{\partial f}{\partial \psi}\right)^2 + \left(\frac{\partial f}{\partial \varphi}\right)^2}{f\left(\frac{\partial f}{\partial \psi}\right)^2} = \frac{4}{q^2\left(\frac{\partial f}{\partial \psi}\right)^2}$$

using the equation [3.13], for the velocity magnitude.

Then eliminating $\sec^2\theta$ from [3.29] and substituting the resultant equation for $\frac{\partial \theta}{\partial \varphi}$ in [3.27] we obtain an expression for the radius of curvature of a streamline in terms of the derivatives of f in the φ, ψ plane.

[3.30] $$\frac{1}{R} = -\frac{q^3}{4f^{\frac{1}{2}}}\left[\frac{\partial f}{\partial \psi}\left(\frac{\partial^2 f}{\partial \varphi^2} - \frac{1}{2f}\left(\frac{\partial f}{\partial \varphi}\right)^2\right) - \frac{\partial f}{\partial \varphi}\frac{\partial^2 f}{\partial \varphi \partial \psi}\right]$$

3.2.4 The radius of curvature of a free streamline.

The above result, for the curvature of any streamline, can be simplified if that streamline is free .

Consider again the expression for the velocity magnitude :

[3.31] $$\frac{4}{q^2} = \frac{1}{f}\left(\frac{\partial f}{\partial \varphi}\right)^2 + \left(\frac{\partial f}{\partial \psi}\right)^2$$

Since the velocity, q, is constant on the free streamline it is therefore invariant in the direction φ on this line. Therefore, differentiating with respect to φ :

$$\frac{2}{f}\frac{\partial f}{\partial \varphi}\frac{\partial^2 f}{\partial \varphi^2} - \frac{1}{f^2}\left(\frac{\partial f}{\partial \varphi}\right)^3 + 2\frac{\partial f}{\partial \psi}\frac{\partial^2 f}{\partial \varphi \partial \psi} = 0$$

This provides us with a relation for the second order cross differential, $\frac{\partial^2 f}{\partial \varphi \partial \psi}$, at a point on the free streamline :

[3.32] $$\frac{\partial^2 f}{\partial \varphi \partial \psi} = \frac{\frac{\partial f}{\partial \varphi}}{2f.\frac{\partial f}{\partial \psi}}\left[\frac{1}{f}\left(\frac{\partial f}{\partial \varphi}\right)^2 - 2\frac{\partial^2 f}{\partial \varphi^2}\right]$$

Substituting this in equation [3.30] we find after simplification by using [3.31] and setting $q = U(1+Q)^{\frac{1}{2}}$:

$$[3.33] \qquad \frac{1}{R} = - \frac{U\sqrt{1+Q}}{f^{\frac{1}{2}} \frac{\partial f}{\partial \psi}} \left[\frac{\partial^2 f}{\partial \varphi^2} - \frac{1}{2f}\left(\frac{\partial f}{\partial \varphi}\right)^2 \right]$$

This can be rewritten in the form :

$$[3.34] \qquad \frac{1}{R} = - \frac{U\sqrt{1+Q}}{f^{\frac{1}{2}} \frac{\partial f}{\partial \psi}} \left[f \frac{\partial^2 \ln f}{\partial \varphi^2} + \frac{1}{2f}\left(\frac{\partial f}{\partial \varphi}\right)^2 \right]$$

It is also useful to have relations for u and v on the free streamline. Since $u = q \cos\theta$, $v = q \sin\theta$, from equations [3.13] and [3.14] it follows that on the free streamline:

$$[3.35] \qquad \begin{aligned} u &= \frac{q^2}{2} \frac{\partial f}{\partial \psi} = \frac{U^2}{2}(1+Q) \frac{\partial f}{\partial \psi} \\ v &= \frac{q^2}{2f^{\frac{1}{2}}} \frac{\partial f}{\partial \varphi} = \frac{U^2}{2f^{\frac{1}{2}}} (1+Q) \frac{\partial f}{\partial \varphi} \end{aligned}$$

One important conclusion can be drawn from these equations regarding the signs which the derivatives for f should take on the free streamline. Since, in a physically realistic solution, both u and v must be positive on free streamline section of the boundary, CD, of figure 3.1. this means that in the solution in the φ , ψ plane both the tangential and normal gradients of f must be positive to give a realistic solution.

i.e. On the boundary CD of figure 3.2

$$\frac{\partial f}{\partial \varphi} \geqslant 0$$

$$\frac{\partial f}{\partial \psi} \geqslant 0$$

At the point C where v = 0, then $\frac{\partial f}{\partial \varphi} = 0$.

Now consider the radius of curvature. We have already stipulated (section 1.4.2) that a solution is only realistic if this is such that the free surface is everywhere

convex, viewed from the fluid. The sign in the initial equation for R, [3.26], has been carefully selected so that such a curvature is positive; if θ is falling with s it gives a positive value for R. Therefore in equation [3.34] the radius of curvature calculated from the derivatives of f must be positive. Hence on the free streamline :

$$f \frac{\partial^2 \ln f}{\partial \varphi^2} + \frac{1}{2f}\left(\frac{\partial f}{\partial \varphi}\right)^2 \leqslant 0$$

But $\frac{\partial f}{\partial \varphi}$, we have already shown, must be positive. Therefore at any point on the free streamline, using the basic field equation [3.9] :

$$f \frac{\partial^2 \ln f}{\partial \varphi^2} \leqslant - \frac{1}{2f}\left(\frac{\partial f}{\partial \varphi}\right)^2$$

$$\leqslant 0$$

And

$$\frac{\partial^2 f}{\partial \psi^2} \geqslant 0$$

Clearly $\frac{\partial^2 f}{\partial \psi^2}$ and $\frac{\partial^2 \ln f}{\partial \varphi^2}$ can only be equal to zero when $\frac{\partial f}{\partial \varphi} = 0$; that is to say at the point C of figures 3.1, 3.2.

3.2.5 Properties of the flow on the wetted surface.

On the wetted surface , since we know $\theta = \theta(f)$ we can find from equations [3.13] and [3.14] the velocities u and v as functions of f and its derivatives in the φ , ψ plane.

Using [3.14] we found (section 3.1.3) that the boundary condition on a fixed surface was :

[3.36] $$f^{\frac{1}{2}} \frac{\partial f}{\partial \psi} \tan[\theta(f)] - \frac{\partial f}{\partial \varphi} = 0$$

Then, from the solution, using [3.13] and $u = q\cos\theta$, $v = q\sin\theta$, we can find q, u, v, at any point. In particular :

For a disc we found (section 3.1.3), equation [3.36] reduced to :

$$\frac{\partial f}{\partial \psi} = 0$$

Hence equation [3.13] gives:

[3.37] $$\frac{4}{q^2} = \frac{1}{f}\left(\frac{\partial f}{\partial \varphi}\right)^2$$

and thus

[3.37a] $$u = 0$$
$$v = q = 2f^{\frac{1}{2}} \Big/ \left(\frac{\partial f}{\partial \varphi}\right)$$

For a sphere we found (section 3.1.3), equation [3.36] gave:

$$\frac{\partial f}{\partial \psi} \cdot (R^2 - f)^{\frac{1}{2}} = \frac{\partial f}{\partial \varphi}$$

Thus substituting in [3.13] we get

$$\frac{4}{q^2} = \left(\frac{\partial f}{\partial \psi}\right)^2 \frac{R^2}{f}$$

Therefore

[3.38] $$q = \frac{2\, f^{\frac{1}{2}}}{R\ \frac{\partial f}{\partial \psi}} = \frac{2f^{\frac{1}{2}}(R^2 - f)^{\frac{1}{2}}}{R\left(\frac{\partial f}{\partial \varphi}\right)}$$

and since $\tan\theta = (R^2 - f)^{\frac{1}{2}} / f^{\frac{1}{2}}$, it is easily shown that:

$$u = q\cos\theta = \frac{2f\,(R^2 - f)^{\frac{1}{2}}}{R^2\left(\frac{\partial f}{\partial \varphi}\right)}$$

[3.38a] $$v = q\sin\theta = \frac{2f^{\frac{1}{2}}(R^2 - f)}{R^2\left(\frac{\partial f}{\partial \varphi}\right)}$$

From these results we can find an expression for the coefficient of pressure at any point and hence, by equation [2.3] of section 2.2.1, the coefficient

of drag of the body.

From the definition of the coefficient of pressure it is easily shown (by Bernoulli's theorem applied to the infinite stream) :

$$1 - C_p = q^2/U^2$$

and hence :

For the disc using equation [3.37]

[3.39] $$C_p = 1 - \frac{4f}{\left(U.\frac{\partial f}{\partial \varphi}\right)^2}$$

For the sphere using equation [3.38]

[3.40] $$C_p = 1 - \frac{4f(R^2 - f)}{R^2\left(U.\frac{\partial f}{\partial \varphi}\right)^2}$$

Then the coefficient of drag in both cases is found by integration , using equation [2.3] :

[3.41] $$C_D = \int_{\text{Wetted Surface}} \frac{(Q + C_p)}{f_M}\, df$$

where f_M is the square of the maximum radius of the body; C^2 in the disc, R^2 in the sphere.

3.3 NATURE OF THE FLOW IN THE REGION OF SPECIAL POINTS.

3.3.1 On the line of symmetry.

Some important conclusions can be reached by considering the flow over the line of symmetry of the Riabouchinsky flow ; BC of figures 3.1 and 3.2. The streamlines are all perpendicular to this line so that in section 3.1.3 we drew the conclusion that the

boundary condition on this line was:

$$\frac{\partial f}{\partial \varphi} = 0$$

But the point C also lies on the free streamline and therefore, using equation [3.13] at this point:

$$\frac{4}{q^2} = \left(\frac{\partial f}{\partial \psi}\right)_c^2 = \frac{4}{U^2(1+Q)}$$

and therefore

[3.42] $$\left(\frac{\partial f}{\partial \psi}\right)_c = \frac{2}{U\sqrt{1+Q}}$$

Also, in section 3.2.4 , we drew the conclusion that at the point C :

$$\left(\frac{\partial^2 f}{\partial \psi^2}\right)_c \geqslant 0$$

The radius of curvature of any streamline (equation[3.30]) provides further information. Substituting $\frac{\partial f}{\partial \varphi} = 0$ in that equation we find the radius of curvature of the streamline at any point on this line of symmetry.

$$\frac{1}{R} = -\frac{q^3}{4f^{\frac{1}{2}}} \frac{\partial f}{\partial \psi} \frac{\partial^2 \ln f}{\partial \varphi^2}$$

or using the field equation [3.9]

[3.43] $$\frac{1}{R} = \frac{q^3}{4f^{\frac{1}{2}}} \frac{\partial f}{\partial \psi} \frac{\partial^2 f}{\partial \psi^2}$$

We shall base the conclusions of this section on two assumptions, both physically reasonable:

[1] That on the line BC of figure 3.1 , the velocity u is always positive. That is to say everywhere in the same direction as the uniform stream velocity.

[2] That the radius of curvature of the streamline through any point on BC is either positive or zero. Since the curvature at C is positive and that at B is zero this is reasonable.

If these assumptions are accepted then from equations [3.12] and [3.43] then we can say that at every point on BC :

$$\frac{\partial f}{\partial \psi} > 0$$

$$\frac{\partial^2 f}{\partial \psi^2} \geqslant 0$$

And since φ is constant on BC we can write

$$\frac{\partial^2 f}{\partial \psi^2} = F(\psi) \quad , \quad F(\psi) \geqslant 0$$

where $F(\psi) = 0$ at B.

Integrating :

$$\frac{\partial f}{\partial \psi} = A_1 + \int_0^{\psi} F(\psi)\, d\psi$$

At the point C , where $\psi = 0$, by equation [3.42] we find A_1. Then integrating again:

$$(f)_{\text{on BC}} = \frac{2}{U\sqrt{1+Q}}\psi + A_2 + \int_0^{\psi}\int_0^{\psi} F(\psi)\, d\psi\, d\psi$$

And hence, eliminating A_2 using the values of f at A and B :

$$f_B = \frac{2}{U\sqrt{1+Q}}(\psi)_B + f_C + \int_0^{\psi_B}\int_0^{\psi} F(\psi)\, d\psi\, d\psi$$

But $(\psi)_B = (\psi)_A$ and by virtue of equation [3.21a]

$$(\psi)_A = \frac{1}{2} U f_A = \frac{1}{2} U f_B \quad \underline{\text{since}} \quad f_{U,A} = f_A = f_B = f_H$$

Substituting for ψ_B we get :

[3.43]
$$f_B\left[1 - \frac{1}{\sqrt{1+Q}}\right] = f_C + \Delta$$

where

$$\Delta = \int_0^{\psi_B}\int_0^{\psi} F(\psi)\, d\psi\, d\psi$$

But since $F(\psi) > 0$ for all points, Δ must always have a positive value. When the curvature of the free streamline takes its lowest possible value of zero, then by virtue of our second assumption and the fact that $[F(\psi)_B] = 0$, $F(\psi)$ is everywhere zero and $\Delta = 0$. In this limiting case :

[3.44] $$\frac{f_c}{f_B} = 1 - \frac{1}{\sqrt{1+Q}}$$

and since Δ is positive this must be the maximum value of f_c / f_B. Since $f_c = B^2$, $f_B = H^2 = f_H$,

[3.44a] $$\left(\frac{B}{H}\right)_{max} = \left[1 - \frac{1}{\sqrt{1+Q}}\right]^{\frac{1}{2}}$$

The conclusion to be drawn from this is that for a given cavitation number, Q, and a given channel radius, H, there is a maximum cavity radius, B, which can be achieved by any variation of C.

Since B/C will be some function of Q we can restate this by saying that for a given blockage ratio, H/C, there will be a minimum cavitation number which can be achieved. If the cavity pressure remains constant this in turn is equivalent to saying that there is a maximum velocity which can be reached in the cavitating flow around a disc in a circular channel. This phenenomenon is known as "choked flow". When B/H takes this maximum value we have shown that the curvature of the free streamline at the point of maximum diameter of the cavity is zero. Although it cannot easily be proved from the above derivation the conclusion could be drawn that in this case the cavity is infinite in length.

A similar result can be obtained for the equivalent planar flow around a flat plate in a channel. In this case the limiting result is:

[3.44b] $$\left(\frac{B}{H}\right)_{MAX} = 1 - \frac{1}{\sqrt{1+Q}}$$

The assumption of infinite length in a choked flow leads to the conclusion of a uniform stream around the cavity far downstream of the body. Thus the coefficient

of drag is easily found in this situation , by simple momentum considerations. These give the choked flow limits for C_D as follows :

[3.44c] Plane flow : $$(C_D)_{C.F.} = \left(\frac{H}{C}\right)_{C.F.} \left[(1+Q)^{\frac{1}{2}} - 1 \right]$$

[3.44d] Axisymmetric flow : $$(C_D)_{C.F.} = \left(\frac{H}{C}\right)^2_{C.F.} \left[(1+Q)^{\frac{1}{2}} - 1 \right]$$

Further comments can be made on the nature of this limit :

[A] If the values of H/C and Q for a particular finite cavity are substituted in the right hand side of either of the above equations , the resulting value will be greater than the actual C_D , since $(H/C)_{C.F.} < (H/C)$ for a finite cavity at given Q. The value of $\left(\frac{H}{C}\right)^2 \left[(1+Q)^{\frac{1}{2}} - 1 \right]$ is denoted by $(C_D)_{MAX}$ in this situation.

[B] By a similar investigation to that given for f_c/f_B the conclusion can be drawn that , for a given Q , C_D will decrease as the choked flow condition is approached by increasing H/C ; a determination of the sign of the error integral demonstrates this as before.

The validity of the conclusions of this section is demonstrated in Appendix A for the results of the planar Riabouchinsky flow around a flat plate. As anticipated above, the cavity becomes infinitely long in the limit and therefore the validity of the theory is independent of the model chosen , the rear end no longer effecting the flow.

Birkhoff and Zarontonello (Ref. 6) mention this result though their simple analysis does not show the nature of the limiting case.

3.3.2 An improved upstream boundary condition.

In section 3.1.3 we stated that a simple approximate boundary condition which could be applied on the boundary FA of figures 3.1 and 3.2 would assume uniform stream conditions on this boundary. Since this is only true exactly at $\phi = -\infty$ (figure 3.2) or $L_1 = \infty$ (figure 3.1) we stated that the object would be to increase L_1/H, or the equivalent ϕ_L/ϕ_S of section 3.1.4, until no appreciable change in the required results took place. This may require quite a large section of the flow upstream of the disc to be taken into acccunt. A more refined boundary condition would reduce the size of this section of the flow to give the same accuracy in the results. This may be obtained by considering the Dirichlet flow around a sphere or disc (section 3.2.2). A streamline will have a limiting upstream value of f which will be the uniform stream value, denoted by f_U. We will denote the difference between the value of f at any point on the streamline and f_U by a, where

$$a = f - f_U$$

As shown in section 3.1.3 the Ψ value on the streamline will be:

[3.45] $$\Psi = \frac{1}{2} U f_U$$

Eliminating x from the equation for the Dirichlet flow around a sphere in an infinite uniform stream (equations [3.24]) we get:

[3.46] $$\left(\frac{\phi}{U}\right)^2 = 2\,(1 - \Psi/Uf)^2 \left[\frac{R^2}{(1 - 2\Psi/Uf)^{\frac{2}{3}}} - f\right]$$

Then substituting for Ψ from [3.45] and for $f = a + f_U$

$$\left[1 + \frac{a}{f_U}\right]^2 \left(\frac{\phi}{U}\right)^2 = \left[1 + \frac{2a}{f_U}\right]^2 \left[\frac{R^2}{f_U}\left(1 + \frac{f_U}{a}\right)^{\frac{2}{3}} - 1 - \frac{a}{f_U}\right] f_U$$

Then if we assume that we are considering points sufficiently far upstream so that terms $O(a/f_U)$ are negligible compared with terms $O(1)$ or higher this becomes:

$$\left(\frac{\phi}{U}\right)^2 = \frac{R^2 f^{\frac{2}{3}}}{a^{\frac{2}{3}}} - f_U$$

or

[3.47] $$\frac{a}{f_U} = R^3 \Big/ \left[f_U + \left(\frac{\phi}{U}\right)^2\right]^{\frac{3}{2}}$$

This is therefore an approximate equation for $a = f - f_U$ in terms of ϕ for a streamline in the region upstream from the sphere where a/f_U is small compared with unity.

The equations for a disc (equations[3.25]) cannot be treated as simply since it is impossible to reach an exact equation for ϕ in terms of ψ and f ,of the type [3.46]. But using the equations [3.25] and [3.25a] we can find in this case:

$$f = C^2(1 - \mu^2)(1 + \xi^2)$$

[3.48] $$f_U = \frac{2\psi}{U} = \frac{2C^2}{\pi}(1 - \mu^2)[\xi + (1 + \xi^2)\tan^{-1}\xi]$$

Hence

[3.49] $$\frac{a}{f_U} = \frac{-\xi + (1 + \xi^2)\tan^{-1}(1/\xi)}{\xi + (1 + \xi^2)\tan^{-1}\xi}$$

μ conveniently being eliminated. By inspection of equations [3.25] [3.25a] we can see that $-1 < \mu < 1$ since otherwise r would be imaginary. Thus as $x \to \infty$, $\xi \to \infty$. Now expanding the $\tan^{-1}(1/\xi)$ term of equation [3.49] we get after simplification :

$$\frac{a}{f_U} = \frac{-\frac{1}{3\xi} + \frac{1}{5\xi^3} - \frac{1}{7\xi^5} + \cdots}{\xi + (1 + \xi^2)\tan^{-1}\xi}$$

For $\xi \gg 1$ this becomes (putting $\tan^{-1}\xi = \pi/2$, and taking simply the first term in the numerator series) :

[3.50] $$\frac{a}{f_v} \simeq -\frac{2}{3\pi\xi^3} \quad , \quad \xi \gg 1$$

Also for $\xi \gg 1$ we can write the first of equations [3.25] as :

$$\frac{\varphi}{U} = C\mu\xi = x$$

Eliminating μ between this and equation [3.48] we find

$$\left(\frac{\varphi}{U}\right)^2 = C^2\xi^2\left[1 - \frac{\pi f_v}{2C^2\left[\xi + (1+\xi^2)\tan^{-1}\xi\right]}\right]$$

so that for $\xi \gg 1$ this becomes:

$$\left(\frac{\varphi}{U}\right)^2 = C^2\xi^2 - f_v$$

Substituting for ξ from equation [3.50] and rearranging we find:

[3.51] $$\frac{a}{f_v} = 2C^3 \Big/ 3\pi\left[\left(\frac{\varphi}{U}\right)^2 + f_v\right]^{\frac{3}{2}}$$

where $\xi \gg 1$, or from equation [3.50] , $a/f_v \ll 1$. Comparing equation [3.47] for the sphere with equation [3.51] for the disc we see that they are exactly the same provided

$$R^3 = \frac{2C^3}{3\pi}$$

Due to this similarity we can conclude with reasonable accuracy that approximate upstream solution for any axisymmetric body in an infinite uniform stream is:

[3.52] $$\frac{a}{f_v} = (kD)^3 \Big/ \left[\left(\frac{\varphi}{U}\right)^2 + f_v\right]^{\frac{3}{2}}$$

where D is some typical length of the body and k is a constant for all sizes of body.

We could therefore adapt this formula to give us a better upstream boundary condition. But first a term will

be inserted to take account of the fact that the stream is not infinite but enclosed in a straight walled channel, in order that a is zero everywhere on this boundary. It will be assumed that in this case equation [3.52] becomes :

$$[3.53] \qquad \frac{a}{f_U} = X\,(kD)^3 \Big/ \left[\left(\frac{\varphi}{U}\right)^2 + f_U\right]^{\frac{3}{2}}$$

where $X = X(f_U)$ so that $X(f_H) = 0$.

Now consider one of the streamlines cutting AF of figure 3.5. The value of f at $\varphi = -\infty$ will be f_U as before. Since the origin of φ in the equation [3.47] is the front stagnation point we shall take E, the stagnation point of the body, as the origin of φ . Then the value of a at the point H on AF will be

$$\frac{a_H}{f_U} = X(f_U)\,(kD)^3 \Big/ \left[\left(\frac{\varphi_L}{U}\right)^2 + f_U\right]^{\frac{3}{2}}$$

φ_L being negative. Also at a point K on the streamline where $\varphi = \varphi_L + \delta\varphi$ the value of a is given by

$$\frac{a_K}{f_U} = X(f_U)\,(kD)^3 \Big/ \left[\left(\frac{\varphi_L + \delta\varphi}{U}\right)^2 + f_U\right]^{\frac{3}{2}}$$

Hence

$$[3.54] \qquad \frac{a_H}{a_K} = \left[\frac{\left(\frac{\varphi_L + \delta\varphi}{U}\right)^2 + f_U}{\left(\frac{\varphi_L}{U}\right)^2 + f_U}\right]^{\frac{3}{2}}$$

Thus we eliminate the awkard typical length D and the function $X(f_U)$ which , being dependent only on f_U , therefore takes the same value at the points H and K.

This equation, [3.54], can then be applied at any point on the boundary AF, the value of $a = f - f_U$ and therefore f being dependent on the value of a or f at a point on the same streamline within the field , where the distance between these points is $\delta\varphi$. Alternatively we could consider

Figure 3.5

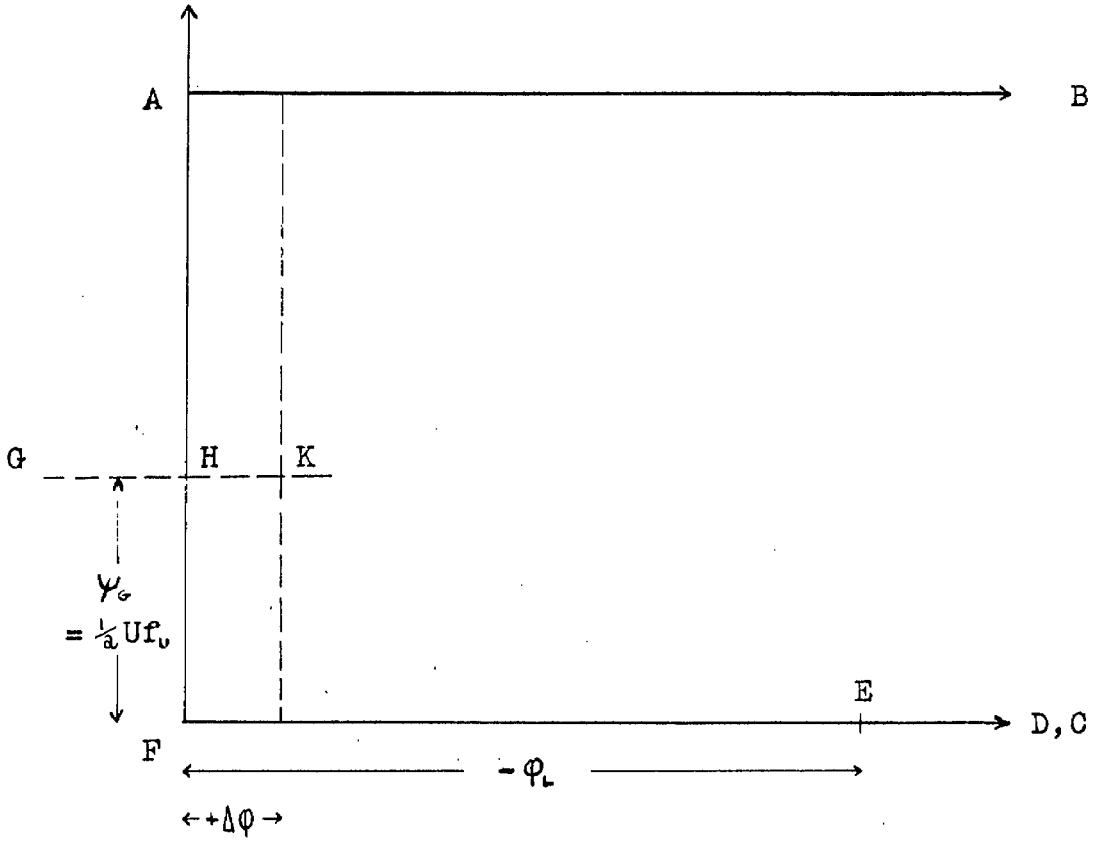
A
B
G
H
K
ψ_G
$= \frac{1}{a} U f_v$
E
D, C
F
$-\varphi_L$
$\leftarrow +\Delta\varphi \rightarrow$

$D^* = D.[X(f_v)]^{\frac{1}{3}}$ where D^* is the effective typical length of the body at a particular point on AF. Thus the effective typical length, D^*, is zero on the streamline AB. This line AB is thus equivalent to the line at infinity in the infinite stream case.

Although this boundary condition is still an approximation it is certainly better than the original assumption of uniform stream flow over AF.

3.3.3 The nature of the flow on the axis and at the stagnation point.

Since the basic equation [3.9] contains f in the denominator when written in the non-logarithmic form, we must consider what happens to the derivatives near the axis f = 0. Since

$$\frac{1}{f}\frac{\partial f}{\partial \varphi} = \frac{\partial \ln f}{\partial \varphi} = \frac{2v}{rq^2}$$

and both v and r are zero on the axis the question arises as to how the functions $\frac{\partial \ln f}{\partial \varphi}$ and $\frac{\partial^2 \ln f}{\partial \varphi}$ (and therefore $\frac{\partial^2 f}{\partial \psi^2}$) behave in the neighbourhood of the axis. If these derivatives were infinite on the axis, and it is our purpose here to show that they are not, then a very difficult situation would arise since the axis would then be in effect a line of singularity. Intuitively , of course , we could guess that this is not the case since there is no indication that the flow is in any way ill-behaved on the axis.

The author could, however, find no way of proving this except by assuming that the behaviour of these derivatives in

the general case did not differ, in type, to their behaviour in the case of the Dirichlet flows. For the Dirichlet flow around a sphere [equations [3.24], section 3.2.2] it can easily be shown that on the axis :

$$\frac{\partial \ln f}{\partial \varphi} = \frac{3R^3(R - x)^2}{U[(R - x)^3 - R^3]^2}$$

and

$$\frac{\partial^2 \ln f}{\partial \varphi^2} = \frac{6R^3(R - x)^4[R^3 + 2(R - x)^3]}{U^2[(R - x)^3 - R^3]^4}$$

$$= - \frac{\partial^2 f}{\partial \psi^2}$$

where x is now measured from the front stagnation point and is positive downstream. Both these derivatives are therefore finite on the axis, providing $x \neq 0$. As $x \to 0$ (i.e as we approach the stagnation point) both $\frac{\partial \ln f}{\partial \varphi}$ and $\frac{\partial^2 \ln f}{\partial \varphi^2}$ tend to $+\infty$. As $x \to -\infty$ both derivatives tend to zero. Hence in this case the only upstream singularity on the axis is at the stagnation point, $x = 0$. It is reasonable to assume that this is true for all axisymmetric flows since at a great distance upstream, the actual shape of the body will have little effect on the flow. We shall also assume that both derivatives tend to infinity as $x \to 0$ for all blunt nosed bodies.

The results given above are also useful in determining the type of singularity at the stagnation point. Using the assumption outlined above we can say that on the axis ;

$f = 0$

$v = 0$

$u = q \to 0$ as $x \to 0$
$\to U$ as $x \to -\infty$

$$\frac{\partial f}{\partial \varphi} = \frac{vr}{q^2} = 0$$

$$\frac{\partial f}{\partial \psi} = \frac{2}{u} = \frac{2}{q} \qquad \begin{array}{l} \to \infty \quad \text{as} \quad x \to 0 \\ \to 2/U \quad \text{as} \quad x \to -\infty \end{array}$$

$$\frac{\partial \ln f}{\partial \varphi} = \frac{v}{rq^2} = \text{finite}(x \neq 0) \qquad \begin{array}{l} \to +\infty \quad \text{as} \quad x \to 0 \\ \to 0 \quad \text{as} \quad x \to -\infty \end{array}$$

$$\frac{\partial^2 \ln f}{\partial \varphi^2} = -\frac{\partial^2 f}{\partial \psi^2} = \text{finite}(x \neq 0) \qquad \begin{array}{l} \to +\infty \quad \text{as} \quad x \to 0 \\ \to 0 \quad \text{as} \quad x \to -\infty \end{array}$$

making use of equations [3.4].

When investigating the behaviour on the wetted surface side of the stagnation point (E in figure 3.2) we shall again make use of the Dirichlet flow solution for the two particular profiles, the disc and the sphere.

For the sphere , rearranging the second of equations [3.24] so that both x and φ are zero at the front stagnation point and then substituting for variable x from the equation of the wetted surface x(r) , we find:

[3.55a] $$f = \frac{4R\varphi}{3U} - \frac{4\varphi^2}{9U^2}$$ on the wetted surface.

Thus

[3.55b] $$\frac{\partial f}{\partial \varphi} = \frac{4R}{3U} - \frac{8\varphi}{9U^2}$$

$$\frac{\partial^2 f}{\partial \varphi^2} = -\frac{8}{9U^2}$$

Assuming that the limits of these functions as we approach the stagnation point are the same in the case of cavitating flow and using equations [3.38] and [3.21], we can say that the behaviour of the derivatives in this region is :

$$\frac{\partial f}{\partial \varphi} = \frac{2f^{\frac{1}{2}}\sqrt{R^2 - f}}{qR} \to \left[\frac{4R}{3U}\right]_{\text{Dirichlet}} \text{as } f \to 0$$

$$\frac{\partial f}{\partial \psi} = \frac{2f^{\frac{1}{2}}}{qR} \to \left[\frac{4}{3U}\right]_{\text{Dirichlet}} \text{as } f \to 0$$

[3.55]
$$\frac{\partial \ln f}{\partial \varphi} = \frac{2\sqrt{R^2 - f}}{qRf^{\frac{1}{2}}} \rightarrow \infty \quad \text{as } f \rightarrow 0$$
$$\frac{\partial^2 \ln f}{\partial \varphi^2} = -\frac{\partial^2 f}{\partial \psi^2} \rightarrow \infty \quad \text{as } f \rightarrow 0$$

It is interesting to note that the tangent to the equipotential, $\varphi = 0$, at the stagnation point makes an angle of $\tan^{-1}(1.5) \approx 56.2^0$ with the axis in the Dirichlet solution. In any planar flow of course this tangent always bisects the angle between the tangent to the body surface and the tangent to the stagnation streamline at the stagnation point. Thus in the equivalent planar flow around a cylinder the angle is 45^0.

For a disc , using the equations [3.25] , it can be shown that on the wetted surface in the Dirichlet flow :

[3.56]
$$f = \frac{\pi C \varphi}{2U} - \frac{\pi^2 \varphi^2}{4U^2}$$

and

[3.56a]
$$\frac{\partial f}{\partial \varphi} = \frac{\pi C}{2U} - \frac{\pi^2 \varphi}{2U^2}$$
$$\frac{\partial^2 f}{\partial \varphi^2} = -\frac{\pi^2}{2U^2}$$

Thus on the wetted surface side of the stagnation point for a disc, making the same assumption as for a sphere, we can say that :

[3.57]
$$\frac{\partial f}{\partial \psi} = \frac{2u}{q^2} = 0$$
$$\frac{\partial f}{\partial \varphi} = \frac{2rv}{q^2} = \frac{2r}{v} \rightarrow \left[\frac{\pi C}{2U}\right]_{\text{Dirichlet}} \text{ as } f \rightarrow 0$$
$$\frac{\partial \ln f}{\partial \varphi} = \frac{2}{v f^{\frac{1}{2}}} \rightarrow \infty \text{ as } f \rightarrow 0$$
$$\frac{\partial^2 \ln f}{\partial \varphi^2} = -\frac{\partial^2 f}{\partial \psi^2} \rightarrow [\infty]_{\text{Dirichlet}} \text{ as } f \rightarrow 0$$

The results of this section are summarised in figure 3.6 which shows the general shape of the curves found if the

FIGURE 3.6 DIAGRAM OF STAGNATION SINGULARITY

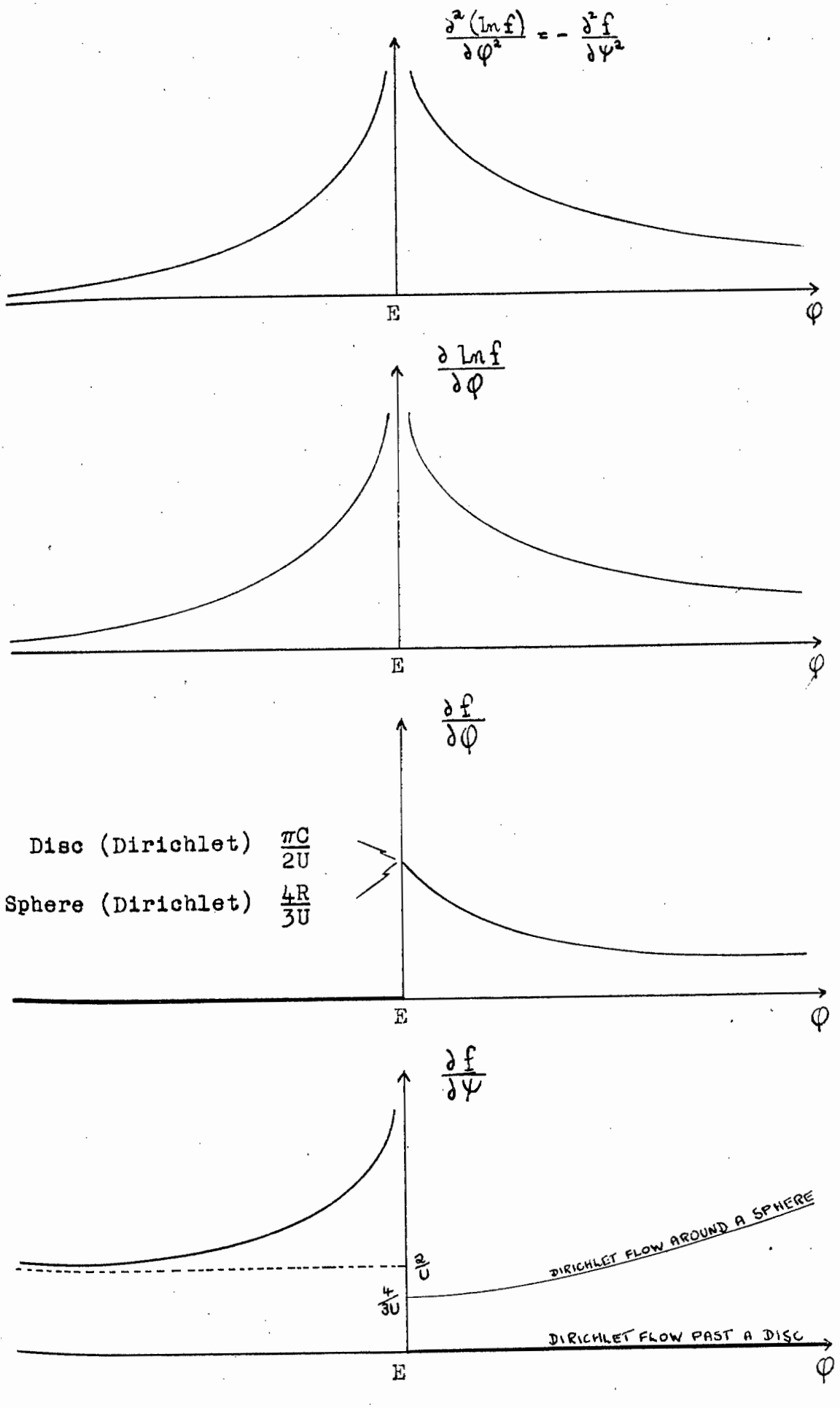

various derivatives were plotted against ϕ for $\psi = 0$. As in figure 3.2 , the point E represents the stagnation point.

3.4 SEPARATION.

3.4.1 General.

The separation point, in general, has been dealt with in section 1.4.6 , and for the plane case in section 1.5.6. Armstrong (Ref.2) also deals with the nature of the flow in the region of a separation point in axisymmetric flow and his method and results will be outlined here and further developed to suit our purposes.

The method is essentially the same as for plane flow (section 1.5.6) although the powerful complex variable methods cannot be used. Figure 3.7a and 3.7b show the notation used in this and the following two sections. The coordinates (s,n) are chosen with the origin at the separation point, the s-axis being tangential to the body streamline. DE represents the wetted surface and DC the free streamline. As in the plane case, a transformed plane t_1 , t_2 is used where DE transforms into the axis , $t_1 = 0$, and DC into $t_2 = 0$. A perturbation velocity potential, w, is defined such that

$$w = -\phi + s$$

where the free streamline velocity is taken as unity and the origins of ϕ and w are at D. It is then assumed, following the example of plane flow, that the three functions

FIGURE 3.7 a

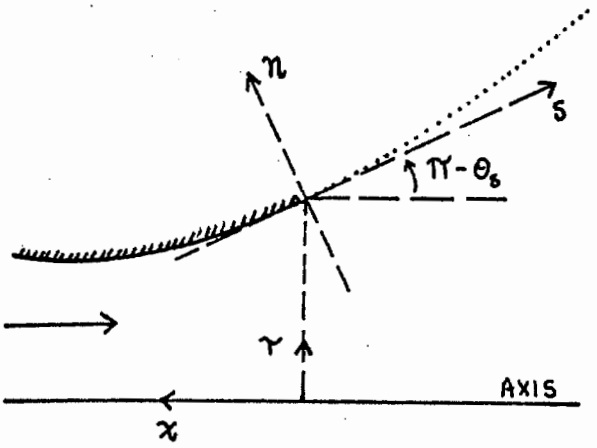

FIGURE 3.7 b

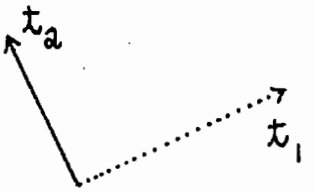

FIGURE 3.8

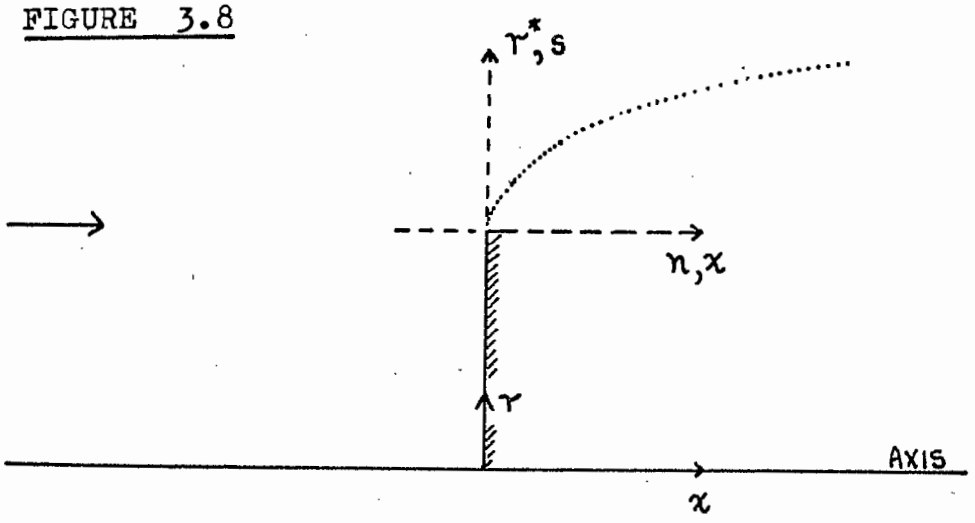

FIGURE 3.9

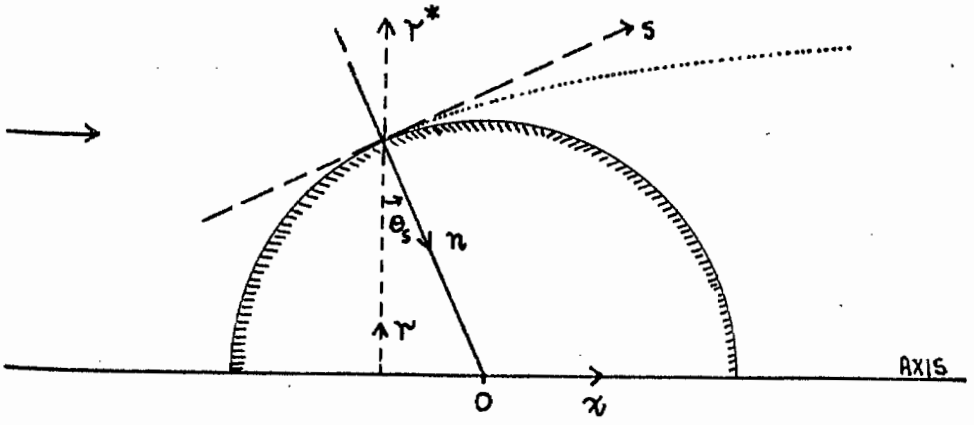

s,n and w can be written in the form :

$$[3.58] \qquad s = \sum_{j=0}^{\infty}\sum_{k=0}^{\infty} S_{j,k}\,\frac{t_1^j}{\lfloor j}\,\frac{t_2^k}{\lfloor k}$$

$$n = \sum_{j=0}^{\infty}\sum_{k=0}^{\infty} N_{j,k}\,\frac{t_1^j}{\lfloor j}\,\frac{t_2^k}{\lfloor k}$$

$$w = \sum_{j=0}^{\infty}\sum_{k=0}^{\infty} W_{j,k}\,\frac{t_1^j}{\lfloor j}\,\frac{t_2^k}{\lfloor k}$$

[In the following sections we will use similar expansions for φ , Ψ and a perturbation streamfunction , $w^* = \Psi + n$, with coefficients $Y_{j,k}$, $Z_{j,k}$ and $W^*_{j,k}$ respectively.]

We will denote the velocity in the n direction by v^* and that in the s direction by $1 + u^*$. Thus :

$$[3.59] \qquad u^* = -\frac{\partial w}{\partial s}$$

$$v^* = -\frac{\partial w}{\partial n}$$

Then if Δ represents the operator $\frac{\partial}{\partial(t_1, t_2)}$, Armstrong shows that :

$$[3.60] \qquad u^* = \Delta(n,w) \,/\, \Delta(s,n)$$

$$v^* = \Delta(w,s) \,/\, \Delta(s,n)$$

And

$$[3.61] \quad [\Delta(s,n)]^3\left(\frac{\partial u^*}{\partial s} + \frac{\partial v^*}{\partial n}\right)$$

$$= \Delta(s,n)[\Delta[\Delta(n,w),n] - \Delta[\Delta(w,s),s]]$$

$$- \Delta(n,w)\,\Delta[\Delta(s,n),n] + \Delta(w,s)\,\Delta[\Delta(s,n),s]]$$

Now , by definition of the positioning of the axes some of the first coefficients in the expansions [3.58] are known:

$$[3.62] \qquad N_{10} = N_{01} = S_{10} = S_{01} = N_{20} = N_{02} = 0$$

and S_{20} and S_{02} can be set equal to $+1$ and -1 respectively, since this only involves fixing the scales

of t_1 and t_2. Then, applying the resultant expansions, the Jacobian of transformation becomes

[3.63] $$\Delta(s,n) = N_{11}(S_{20}t_1^2 - S_{02}t_2^2) + O(t^3)$$

where t_1, t_2 are convergent in some region $t_1^2 + t_2^2 = t$. Thus $\Delta(s,n)$ is $O(t^2)$ and since u^* and v^* vanish at the origin both $\Delta(n,w)$ and $\Delta(w,s)$ must be $O(t^3)$. Thus:

[3.64] $$W_{10} = W_{01} = W_{11} = W_{02} = W_{20} = 0$$

The equation of continuity can be written as :

[3.65] $$\frac{\partial u^*}{\partial s} + \frac{\partial v^*}{\partial n} + \frac{(1+u^*)\sin\theta_s + v^*\cos\theta_s}{1 + s\sin\theta_s + n\cos\theta_s} = 0$$

Due to the above orders of magnitude, this becomes :

[3.66] $$\frac{\partial u^*}{\partial s} + \frac{\partial v^*}{\partial n} = -\sin\theta_s + O(t)$$

Then substituting this in equation [3.61], Armstrong finds

[3.67] $$\Delta(s,n)[\Delta[\Delta(n,w),n] - \Delta[\Delta(w,s),s]] - \Delta(n,w)\Delta[\Delta(s,n),n] + \Delta(w,s)\Delta[\Delta(s,n),s] = -\sin\theta_s[\Delta(s,n)]^3 + O(t^7)$$

This is clearly a form of the equation of continuity and is thus the condition that the perturbation potential, w, shall describe the flow in the neighbourhood of the origin, the separation point.

By substitution of the series [3.58] into this equation and equating the coefficients of like power terms Armstrong finds a set of simultaneous equations in the coefficients $S_{j,k}$, $N_{j,k}$ and $W_{j,k}$. He then investigates particular solutions of these equations, the number of unknowns being larger than the number of equations.

However this requires some lengthy simple algebra and since the stream function must also be investigated in our application, the author designed a slightly different approach giving, in addition, this

function. The algebra would seem to be reduced by this method.

3.4.2 Alternative Procedure.

This alternative procedure involves the use of the basic equations of axisymmetric flow :

$$\begin{aligned} \frac{\partial \varphi}{\partial x} &= \frac{1}{r}\frac{\partial \Psi}{\partial r} \\ \frac{\partial \varphi}{\partial r} &= -\frac{1}{r}\frac{\partial \Psi}{\partial x} \end{aligned} \qquad [3.68]$$

By definition we have

$$\begin{aligned} W_{j,k} &= -Y_{j,k} + S_{j,k} \\ W^*_{j,k} &= Z_{j,k} + N_{j,k} \end{aligned} \qquad [3.69]$$

From figure 3.7a

$$\begin{aligned} s &= r^* \cos\theta_s + x \sin\theta_s \\ n &= x \cos\theta_s - r^* \sin\theta_s \end{aligned} \qquad [3.69a]$$

where $r^* = r - 1$. Substituting for x and r in [3.68] and simplifying

$$(1 + s\sin\theta_s - n\cos\theta_s)\frac{\partial \varphi}{\partial s} = -\frac{\partial \Psi}{\partial n}$$

$$(1 + s\sin\theta_s - n\cos\theta_s)\frac{\partial \varphi}{\partial n} = \frac{\partial \Psi}{\partial s}$$

Substituting for the four derivatives as follows

$$\frac{\partial \varphi}{\partial s} = \frac{\partial \varphi}{\partial t_1}\frac{1}{\Delta(s,n)}\frac{\partial n}{\partial t_2} - \frac{\partial \varphi}{\partial t_2}\frac{1}{\Delta(s,n)}\frac{\partial n}{\partial t_1}$$

(and three similar equations) we get finally :

$$\begin{aligned} (1 + s\sin\theta_s - n\cos\theta_s)\left[\frac{\partial \varphi}{\partial t_1}\frac{\partial n}{\partial t_2} - \frac{\partial \varphi}{\partial t_2}\frac{\partial n}{\partial t_1}\right] &= \frac{\partial \Psi}{\partial t_1}\frac{\partial s}{\partial t_2} - \frac{\partial \Psi}{\partial t_2}\frac{\partial s}{\partial t_1} \\ (1 + s\sin\theta_s - n\cos\theta_s)\left[\frac{\partial \varphi}{\partial t_2}\frac{\partial s}{\partial t_1} - \frac{\partial \varphi}{\partial t_1}\frac{\partial s}{\partial t_2}\right] &= \frac{\partial \Psi}{\partial t_1}\frac{\partial n}{\partial t_2} - \frac{\partial \Psi}{\partial t_2}\frac{\partial n}{\partial t_1} \end{aligned} \qquad [3.70]$$

These two equations thus form the condition which was previously the property of [3.67]. They are much simpler

than that equation and the substitution of the series [3.58] involves less algebra in order to obtain the relations which must hold between the coefficients of those series.

Besides the lower power coefficient relations [3.62] and [3.64], used by Armstrong, we will clearly have

[3.71] $$Z_{j,0} = 0 \quad , \quad Z_{0,k} = 0$$

since $t_1 t_2 = 0$ is the body streamline.

Now substituting the expansions [3.58] in [3.70] and equating coefficients of like power terms the following emerges.

[A] The pairs of identities for the powers (j=0,k=0), (j=1,k=0) and (j=0,k=1) yield no new information since each term involves a coefficient which is zero by virtue of equation [3.62].

[B] The pairs of equations found by equating the coefficients of (j=2,k=0),(j=1,k=1) and (j=0,k=2) are, after substitution of the information of equations [3.62] and [3.71] :

$$\begin{aligned} Y_{02} + Y_{20} &= 0 \\ Y_{20} N_{11} + Z_{11} &= 0 \\ -Y_{20} S_{11} + Y_{11} &= 0 \end{aligned} \qquad [3.72]$$

But since $W_{11} = 0$, using [3.69] these become

$$\begin{aligned} Y_{20} &= -Y_{02} = 1 \\ N_{11} &= -Z_{11} \\ S_{11} &= Y_{11} \end{aligned} \qquad [3.73]$$

[C] The eight equations for the j+k=3 power terms become after simplification :

$$\begin{aligned} 2 N_{11} (S_{03} - Y_{03}) &= N_{30} + N_{11}^2 N_{30} \\ 2 (Z_{12} + N_{12}) &= -N_{30} - N_{30} N_{11}^2 \\ Z_{21} + N_{21} &= 0 \end{aligned} \qquad [3.74]$$

$$S_{21} - Y_{21} = - N_{11} N_{30}$$

$$S_{12} - Y_{12} = 0$$

the other three being already obeyed.

As mentioned before we are looking for a particular solution of these equations which is compatible with the problem being considered. The results so far are identical with those obtained by Armstrong (Ref. 2), and the same particular solution , namely that for which $S_{11} = 0$, $N_{11} = 1$ will now be investigated. We will also take $W_{30} = 0$, or $Y_{30} = S_{30}$, since as Armstrong points out u must be a higher order quantity than v on the axis $t_2 = 0$. Using these two identities equations [3.74] give the results

$$N_{03} = 0 \quad , \quad Z_{21} + N_{21} = 0$$

$$S_{03} - Y_{03} = N_{30} \quad , \quad S_{21} - Y_{21} = - N_{30}$$

$$S_{12} - Y_{12} = 0 \quad , \quad Z_{12} + N_{12} = - N_{30}$$

These are precisely the results given by Armstrong except that he does not deal with the Z coefficients.

Two separate cases are now considered. The first will be seen to correspond to abrupt separation , the second to smooth.

3.4.3 Abrupt Separation.

Consider the case in which $N_{30} \neq 0$. The resultant expansions , [3.58], become

$$n = t_1 t_2 + O(t^3)$$

$$s = \frac{t_1^2}{2} - \frac{t_2^2}{2} + O(t^3)$$

[3.76]

[3.76]
$$\varphi = s + \frac{N_{30}}{2} t_1^2 t_2 - \frac{N_{30}}{6} t_2^3 + O(t^4)$$
$$\psi = -n - \frac{N_{30}}{2} t_1 t_2^2 + O(t^4)$$

These expansions lead to the following velocity distributions.

On the free streamline , $t_2 = 0$ $\quad u^* = O(|s|)$
$$v^* = \frac{N_{30}}{2}(2s)^{\frac{1}{2}} + O(|s|)$$

On the wetted surface , $t_1 = 0$ $\quad u^* = \frac{N_{30}}{2}(-2s)^{\frac{1}{2}} + O(|s|)$
$$v^* = O(|s|)$$

Thus we have an infinite velocity gradient on the wetted surface as $s \to 0$ and an infinite radius of curvature on the free streamline as $s \to 0$. This then represents abrupt separation , providing $N_{30} \neq 0$.

We will now consider the application of these results , obtained by Armstrong , to our problem of the abrupt separation from a disc. The object is to find three expansions for $f^* = f - f_s$ in terms of φ, ψ and φ respectively to describe the behaviour of the function $f(\varphi, \psi)$ on the wetted surface , the line $\varphi = 0$ and the free streamline. That is to say for the three mesh lines emanating from the separation point , D , in the φ, ψ plane.

Thus , from the expansions [3.76] the behaviour of s on the wetted surface can be shown to be

[3.77]
$$s = \varphi + \sum_{j=3}^{\infty} P_j' (-\varphi)^{\frac{j}{2}}$$

where P_j' are unknown coefficients. Generalizing this result for $r_s \neq 1$ and $q_c \neq 1$ and putting $f^* = 2s + s^2$ in the case of the disc , [3.77] becomes

[3.78] $$\frac{f^*}{f_s} = -2\left(\frac{-\varphi}{q_c\sqrt{f_s}}\right) + \sum_{j=3}^{\infty} P_j^2 \left(\frac{-\varphi}{q_c\sqrt{f_s}}\right)^{j/2}$$

It is easily seen that this expansion gives the correct expression for $\frac{\partial f}{\partial \varphi}$ at the separation point (so that $v=q_c$) and that the singularity is of the correct type. A more useful form of this expansion is

[3.79] $$\ln\left(\frac{f}{f_s}\right) = -\frac{2}{f_s^{1/2}}\left(\frac{-\varphi}{q_c}\right) + K_1\left(\frac{-\varphi}{q_c f_s^{1/2}}\right)^{3/2} + \sum_{j=4}^{\infty} P_j^3 \left(\frac{-\varphi}{q_c\sqrt{f_s}}\right)^{j/2}$$

Similarly the expansion along the line $\varphi = 0$ is seen to be

[3.80] $$f = f_s + K_2\left(\frac{\Psi}{q_c}\right)^{3/2} + \sum_{j=4}^{\infty} P_j^4 \left(\frac{\Psi}{q_c}\right)^{j/2}$$

and that on the free streamline

[3.81] $$\ln\left(\frac{f}{f_s}\right) = \frac{2}{\sqrt{f_s}}\left(\frac{\varphi}{q_c}\right) + \sum_{j=4}^{\infty} P_j^5 \left(\frac{\varphi}{q_c}\right)^{j/2}$$

These expansions are used in the manner described in sections 4.3.7 and 4.4.5.

3.4.4 Smooth Separation.

In the special case , $N_{30} = 0$, it can be shown, using the equations [3.69a], that the following expansions must hold (after generalization) :

On the wetted surface :

[3.82] $$\ln\left(\frac{f}{f_s}\right) = -\frac{2\sin\theta_s}{f_s^{1/2}}\left(-\frac{\varphi}{q_c}\right) - C_3^*\left(-\frac{\varphi}{q_c}\right)^2 + \sum_{j=5}^{\infty} P_j^6 \left(-\frac{\varphi}{q_c}\right)^{j/2}$$

On the line $\varphi = 0$:

$$[3.83]\quad f = f_s + 2\cos\theta_s \left(\frac{\Psi}{q_c}\right) + C_2^* \left(\frac{\Psi}{q_c}\right)^2 + \sum_{j=5}^{\infty} P_j^7 \left(\frac{\Psi}{q_c}\right)^{\frac{j}{2}}$$

On the free streamline :

$$[3.84]\quad \ln\left(\frac{f}{f_s}\right) = \frac{2\sin\theta_s}{f_s^{1/2}} \left(\frac{\varphi}{q_c}\right) - C_1^* \left(\frac{\varphi}{q_c}\right)^2 + \sum_{j=5}^{\infty} P_j^8 \left(\frac{\varphi}{q_c}\right)^{\frac{j}{2}}$$

where $C_1^*, C_2^*, C_3^*, P_j^6, P_j^7, P_j^8$ are initially all unknown.

It can be seen that these expansions give the correct first derivatives and components of velocity at the separation point according to [3.35].

Armstrong (Ref. 2) goes further to show rigorously that the special solution , $S_{40} = Y_{40}$, leads to the flow at a smooth separation point. For this he finds a particular solution of the equations for the coefficients given by $j+k = 4$ power terms in section 3.4.1 (or 3.4.2).

It is intended to demonstrate here that the coefficients C_1^* , C_2^* and C_3^* are also known. This could , presumably , be shown by the solution of the equations for $j + k = 4$ and $j + k = 5$ as in section 3.4.2 but the algebra required is immense. A much simpler procedure will serve our purposes equally well.

If the expansion on the free streamline is considered in conjunction with Armstrongs result that the radius of curvature of the free streamline at the separation point is that of the sphere , then , using the result [3.34] , it follows that

$$\left(\frac{\partial^2 \ln f}{\partial \varphi^2}\right)_{\substack{\varphi=0 \\ \text{on F.S.}}} = -\frac{2}{q_c^2 f_s}$$

and $$C_1^* = \frac{1}{f_s}$$

Equally , for the wetted surface it can be shown that

$$\left(\frac{\partial^2 \ln f}{\partial \varphi^2}\right)_{\substack{\varphi=0 \\ \text{on W.S.}}} = -\frac{2}{q_c^2 f_s}$$

and $C_3^* = \frac{1}{f_s}$

and putting $\left(\frac{\partial^2 \ln f}{\partial \varphi^2}\right) = -\left(\frac{\partial^2 f}{\partial \psi^2}\right)$, we find that $C_2^* = 1/f_s$.

Hence , in the region of the smooth separation point on the surface of the sphere the following expansions hold on the wetted surface , the line $\varphi = 0$ and the free streamline respectively :

[3.85] $$\ln \frac{f}{f_s} = -\frac{2\sin\theta_s}{f_s^{3/2}}\left(-\frac{\varphi}{q_c}\right) - \frac{1}{f_s}\left(-\frac{\varphi}{q_c}\right)^2 + \sum_{j=5}^{\infty} P_j^6 \left(-\frac{\varphi}{q_c}\right)^{j/2}$$

[3.86] $$f = f_s + 2\cos\theta_s\left(\frac{\psi}{q_c}\right) + \frac{1}{f_s}\cdot\left(\frac{\psi}{q_c}\right)^2 + \sum_{j=5}^{\infty} P_j^7 \left(\frac{\psi}{q_c}\right)^{j/2}$$

[3.87] $$\ln \frac{f}{f_s} = \frac{2\sin\theta_s}{f_s^{3/2}}\left(\frac{\varphi}{q_c}\right) - \frac{1}{f_s}\left(\frac{\varphi}{q_c}\right)^2 + \sum_{j=5}^{\infty} P_j^8 \left(\frac{\varphi}{q_c}\right)^{j/2}$$

These expansions exhibit the required singularity at the separation point. They are used in the manner described in sections 4.3.7 and 4.4.6.

CHAPTER 4

CHAPTER 4

4.1 GENERAL NUMERICAL PROCEDURE.

4.1.1 The Relaxation Mesh.

In this chapter the results of chapter 3 will be applied to the numerical solution of the axisymmetric cavity problem by means of finite differences.

The basic principle of the relaxation technique is that the field is covered with a mesh or net and the numerical value of the dependent variable estimated at each of the intersection points. The differential equation relating the dependent variable with position coordinates or independent variables is translated , approximately , into a finite difference equation which relates the value of the dependent variable at a point with the values at surrounding points. Then at every intersection point we adjust or "relax" the value, keeping the values at surrounding points fixed, so that this equation is obeyed at that point. Working through every point in the field and then repeating the process, values are continuously relaxed until the finite difference equation is obeyed at every point,the values having converged. The resultant values of the dependent variable at each intersection point are then taken as an estimation of the values which would be found were the differential equation to be solved.

Relaxation methods , first developed by Southwell (Refs. 42 and 43) , are normally used in problems for

which analytical treatment has not been found or in which the boundary conditions are so complex as to render known methods impractical.

Both these limitations are found in the ϕ, Ψ plane described in chapter 3 (figure 3.2). The differential equation, [3.9], is non-linear and of the second order elliptic type. This type can only be solved analytically when one has the very simplest of boundary conditions. The boundary conditions described in section 3.1.3 are very complex. The ϕ, Ψ plane of figure 3.2 is shown in figure 4.1 covered with a mesh or net. This mesh is "graded" in such a way that the regions in which the flow experiences the most rapid changes are covered by a much finer mesh than the regions in which it is likely to change only very slowly and smoothly. Thus in the neighbourhood of the wetted surface and the free streamline the mesh length (i.e. the distance between the intersection points) is much smaller than that near the channel wall. Having obtained a solution the "grading" is then adjusted according to an error analysis, to achieve both accuracy and efficiency.

4.1.2 Boundary Conditions - General.

One of the advantages of using the ϕ, Ψ plane in a problem such as this is the polygonal shape of the closed contour of its boundary. The mesh can then easily be laid so that the boundaries are lines of the mesh. Thus at points such as N, P or Z of figure 4.1 the value of the

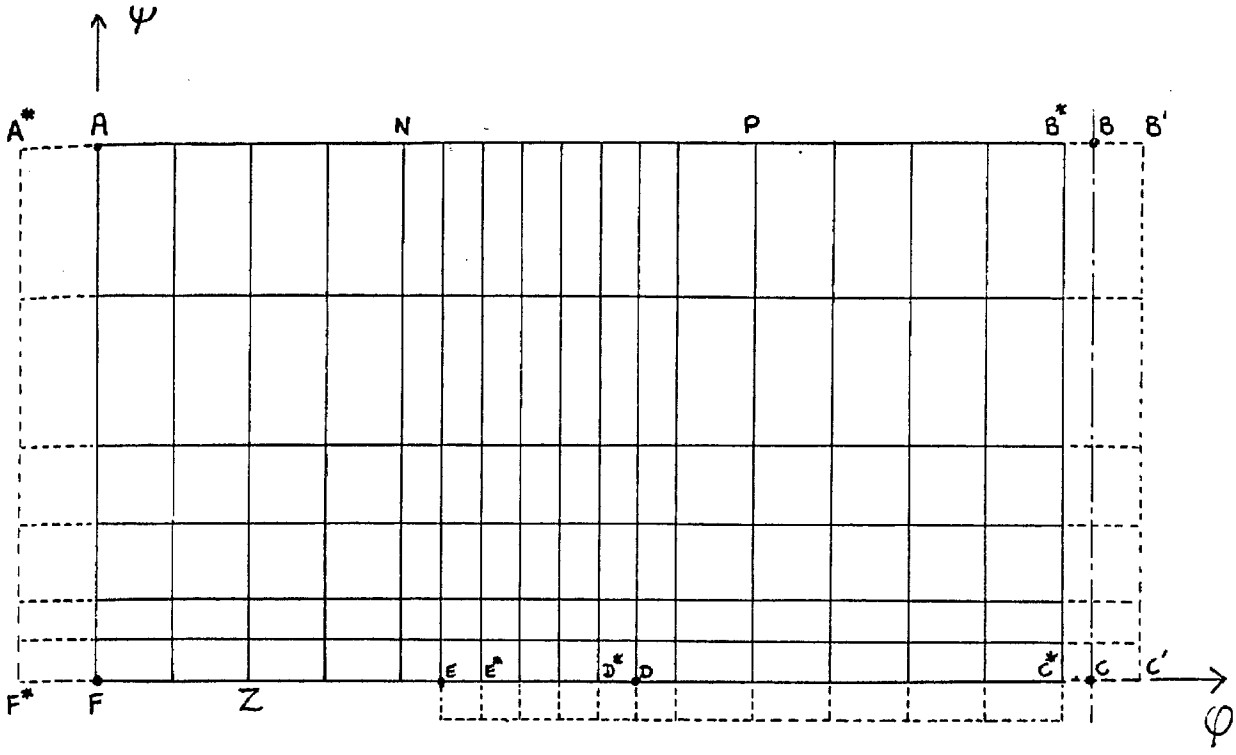

FIGURE 4.1

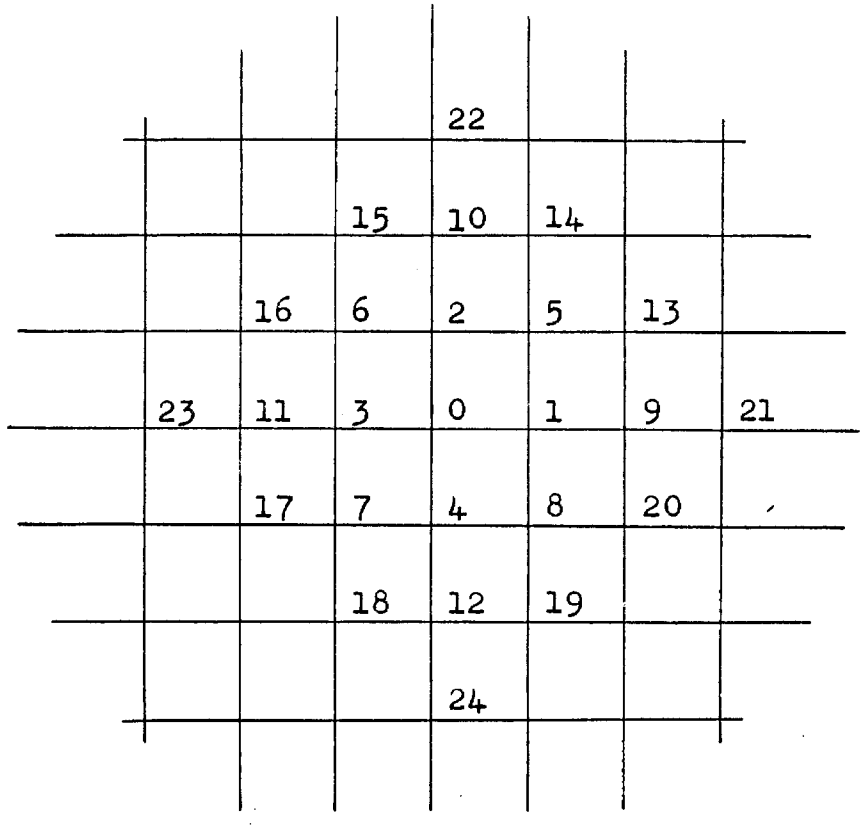

FIGURE 4.2

dependent variable is known and fixed and intersection points lying on Dirichlet or fixed boundaries need not be relaxed.

The equation to be applied at general points in the field, that is to say the finite difference form of [3.9], is known as the "field equation". Since the value of the dependent variable, in this case f, is unknown on the Neumann or complex boundaries the field equation will have to be applied on such boundaries. A simple way of doing this is to place a further line of mesh points outside the boundary so that every point on the boundary is surrounded. The values of f at "imaginary points" are then determined by applying the boundary condition at the nearby boundary points. The lines of "imaginary points" are dotted in figure 4.1, being required on the boundaries BC and CD , though not on the boundary FA , the condition there (equation [3.54]) not including gradients of f as such. The boundary DE may also have a line of imaginary points.

4.1.3 Point Identification.

In order to describe the position of a point in the field a system of identification by subscript is required. It is also useful to have a further system which, defines the relative position of a point to its neighbours in general.

[A] The Field System.

This identifies the position of a point in the

field by the address (j,k). The horizontal mesh lines, on which ψ = constant, are numbered from the body streamline outwards, a point on this streamline having the address (0,k). Thus the imaginary line of points outside CDE have addresses (-1,k). Since the value of f_υ (the f value at $\varphi = -\infty$) on any streamline is of considerable importance, a further line of points is placed upstream of, and parallel to the boundary AF. The value of f at a mesh point on this line, A* F* of figure 4.1 , is the f_υ value of the intersecting streamline at that point. The line A* F* is not an integral part of the mesh as such but is used merely to store the f_υ values. The equipotential mesh lines are therefore numbered from this line so that the f_υ value on the streamline j = J is given in (J,0) and the f value of the boundary point on FA in (J,1).

Thus the subscripted $f_{j,k}$ refers to the f value at the point (j,k) in the field.

[B] The Local System.

An abbreviated system is useful when referring, in general, to the points surrounding a particular point. In this "local" system the values at the points are denoted by the singly-subscripted f_p where p gives the position of the point relative to the point p = 0, the point under consideration. This system is shown in figure 4.2. Thus if

$$0 \equiv (j,k)$$

Then :

1 ≡ (j,k+1) , 2 ≡ (j+1,k) , 3 ≡ (j,k-1) , 4 ≡ (j-1,k)

5 ≡ (j+1,k+1), 6 ≡ (j+1,k-1), 7 ≡ (j-1,k-1), 8 ≡ (j-1,k+1)

9 ≡ (j,k+2) , 10 ≡ (j+2,k) , 11 ≡ (j,k-2) , 12 ≡ (j-2,k)

Normally , these are the only points to which reference need be made but others are included in figure 4.2 to take account of the exceptional cases. This local system is useful in that the subscripts are considerably shortened when dealing with general points. It is used in the manipulation and deduction of the finite difference forms of the equations,whereas the field system is used mostly in the computations or application of these equations. This particular numbering of points in the local system has become fairly standard being used for example in references 32, 39 and 47.

4.1.4 The Relaxation Mesh. Further Comment.

The notation used in this and the following sections is :

m The mesh length in the Ψ direction.

n The mesh length in the φ direction.

X The quantity $\Psi_H/\varphi_S f_H$. This has dimensions $(f)^{-\frac{1}{2}}$ as mentioned in section 3.1.4.

M^P The operator $\frac{\delta^P}{\delta\Psi^P}$

N^P The operator $\frac{\delta^P}{\delta\varphi^P}$

From the investigation carried out in section

3.1.4 it was found that the specification of the parameters [3.23] was necessary and sufficient for a unique solution in the ϕ, Ψ plane provided that for all solutions took the same value of $\Psi_H/\phi_S f_H$. We will now discuss how the particular mesh used in this problem was set up using these parameters. For this purpose reference will be made to figure 4.3. It was also shown in section 3.1.4 that the solution would be found in terms of the dimensionless co-ordinates ϕ/ϕ_S and Ψ/Ψ_H. Thus we would expect every distance in the ϕ or Ψ directions to be given in terms of multiples of ϕ_S and Ψ_H respectively. That is to say, at any point $n = n^*\phi_S$, $m = m^*\Psi_H$ where n* and m* are dimension-less parameters defined by the geometry of the mesh.

Thus if it is decided to have P equally spaced points on the wetted surface (ED of figure 4.3) then the mesh length, n, between points within that interval, DE, is ϕ_S/P. Hence every other mesh length in the horizontal direction is defined by the geometry of the net. If the mesh length is doubled in the grading at a point such as J, then the mesh length, n, between points such as L and M is $2\,\phi_S/P$.

In this problem it was decided that the most convenient values of P were those which were $P = 2^p$ where p was a positive integer. It is also convenient if, when at points such as K and N a larger mesh length is allowable, it is in fact doubled. Thus n* is always 2^s where s is an integer, positive, zero or negative. The last case rarely arises as the "doubling" in the ϕ direction is applied at the most, three times.

On the other hand it was found that the correct medium between efficiency and accuracy was achieved by massive grading in the Ψ direction. This will be

FIGURE 4.3

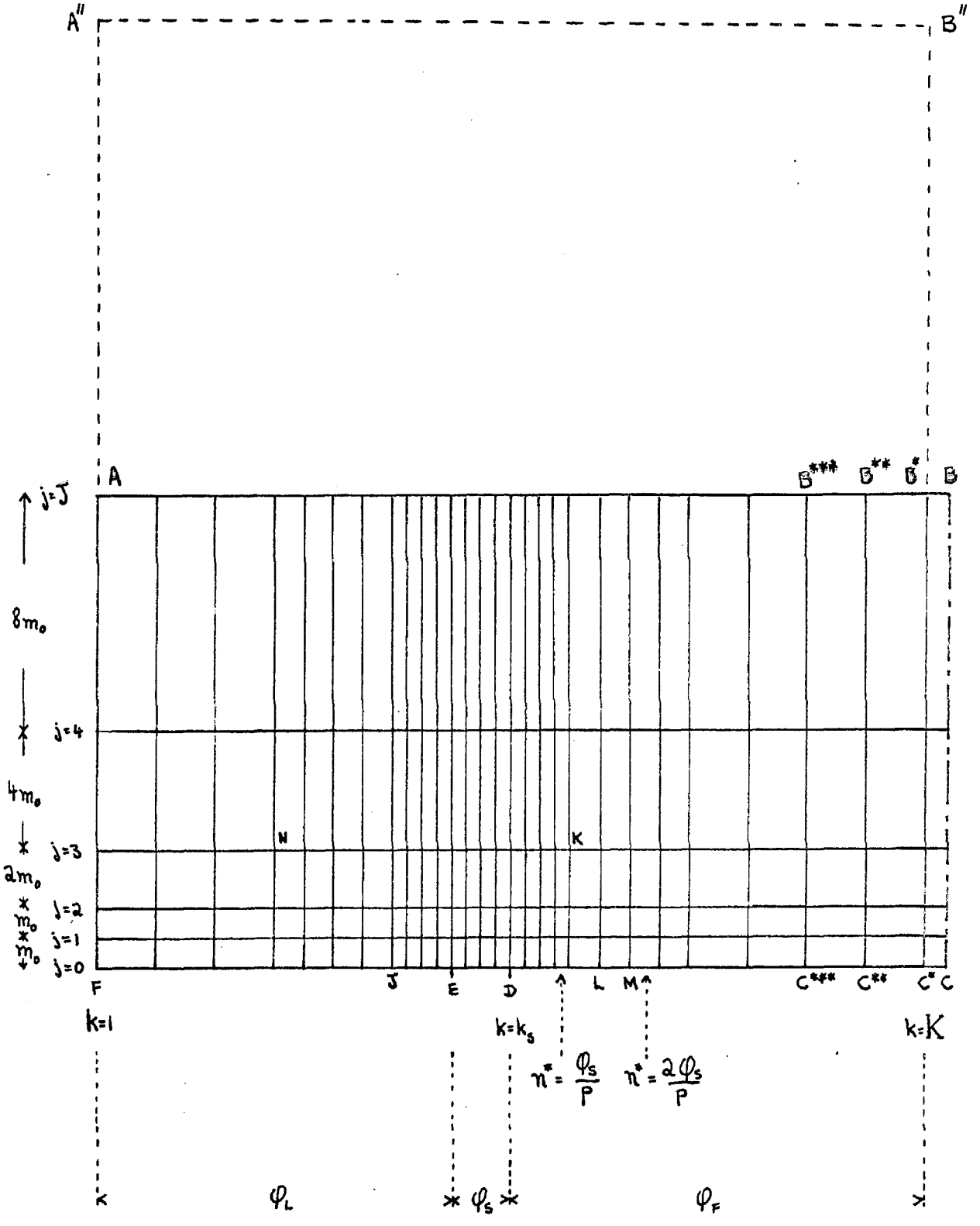
A''
B''
A
B
B***
B**
B*
j=J
8m₀
j=4
4m₀
N
K
j=3
2m₀
j=2
m₀
j=1
m₀
j=0
F
J
E
D
L
M
C***
C**
C*
C
k=1
k=k_s
k=K
π*= φ_s/P
π*= 2φ_s/P
φ_L
φ_s
φ_F

demonstrated numerically by the error analysis (section 5.5.2) but the same conclusion can be reached simply by considering the geometry of the physical plane. These results are anticipated here. The author found that the most convenient method of applying this large grading was to double the mesh length, m ,after each mesh line except the first, as shown in figure 4.3. i.e. If

$$\Psi_{1,k} - \Psi_{0,k} = A \text{ ,say}$$

Then :

$$\Psi_{2,k} - \Psi_{1,k} = A$$
$$\Psi_{3,k} - \Psi_{2,k} = 2A$$

and for other intervals

[4.1] $$\Psi_{j+1,k} - \Psi_{j,k} = 2^{(j-1)} .A$$

Thus :

[4.2] $$\Psi_{j,k} = 2^{(j-1)} .A \quad \text{for } j > 1 ,$$

the body streamline being taken as $\Psi = 0$.

It will be found that all the finite difference equations to be used can be written in a form which includes only the ratio of m/n. This is true, for example, of the various forms of the field equation, [4.18], [4.21]. But we know that, from equation [3.21a], the f_v value of any streamline is directly proportional to its Ψ value :

[4.3] $$\Psi = \frac{U}{2} . f_v$$

Thus the difference in the f_v values for two points is a measure of the increment, m. i.e.

$$\Psi_{j+1,k} - \Psi_{j,k} = m_j = \frac{U}{2} \left[(f_v)_{j+1,k} - (f_v)_{j,k} \right]$$

We shall put

$$(f_v)_{j+1,k} - (f_v)_{j,k} = g_j$$

But from [4.3] we also have

[4.4] $$\Psi_H = \frac{U}{2} . f_H$$

Therefore:

[4.5] $$m_j = \frac{\Psi_H}{f_H} \cdot g_j = \frac{U}{2} \cdot g_j$$

Now we are in a position to write the important ratio m/n as :

[4.6] $$\left(\frac{m}{n}\right)_{j,k} = \frac{m_j}{n_k} = \frac{\Psi_H}{\phi_s f_H} \frac{g_j}{n^*_k} = X \cdot \frac{g_j}{n^*_k}$$

Also

[4.6a] $$\left(\frac{n}{U}\right)_{\substack{\text{INTERVAL} \\ \phi_s}} = \frac{1}{2XP} \quad , \quad \frac{m_j}{U} = \frac{g_j}{2}$$

Hence the importance of the quantity $\Psi_H / \phi_s f_H$, whose relevance in section 3.1.4 may have seemed a little obscure.

4.1.5 The Parameter Specification in the Relaxation Mesh.

Having found the important relation [4.6] in the last section we are now in a position to discuss how the complete set of solutions may be obtained. The conclusion was reached in section 3.1.4 that by varying the quantities

[4.7] $$\frac{\phi_L}{\phi_s} \quad , \quad f_H \quad , \quad Q$$

we could get a complete set of unique solutions, provided the quantity, X , retained the same value throughout.

Having set up a net for one set of [4.7] and solved that particular problem the question arises as to how a change in one of these parameters effects the geometry of the net. A change in Q means merely a change in the boundary condition on DC. If an alteration is made

in φ_L/φ_s then the obvious course is to add or substract some mesh lines and move the boundary AF either up or downstream. However if a change is to be made in f_H then two courses of action are open to us. We can either alter the value of f_H on the mesh line AB, thus altering the values of $(f_v)_j$ and g_j on all the mesh lines, or lines can be added or substracted from the mesh so that the boundary streamline now lies on a different mesh line, say A"B", dotted in figure 4.3. The latter course is obviously preferable since it can be arranged so that mesh lines retain the same values of $(f_v)_j$ and g_j, and therefore the value of m/n at any point lying in both nets remains the same, by virtue of equation [4.6]. The f values on these lines may then be used as a first approximation to the solution of the new problem.

Also in section 3.1.4, the conclusion was reached that the specification of [4.7] demanded that the boundary BC (figure 4.1) be free to move, the length φ_r being determined as part of the solution to the problem. The position of BC will therefore change during an iterative process of solution and may not coincide with a mesh line. The mesh lines which straddle it are marked in figure 4.1 as B*C* and B'C', although their position may vary according to the position of BC; at a given moment in the iterative process the position of B*C* is described by k = K and that of BC by

$$\frac{(\varphi_{BC} - \varphi_{B^*C^*})}{\varphi_s \cdot n^*_K} = c \quad ;$$

or in other words

$$c = \text{LENGTH } C^*C \;/\; \text{LENGTH } C^*C'$$

4.1.6 Useful Approximate Formulae.

It is useful, in order to prevent trying to find solutions for sets of parameters for which no realistic solution exists, to develop some approximate formulae. In doing so we will also find convenient numerical values to assign to the scale value X in the case of the sphere and the disc.

[1] On the surface of the disc.

Let us assume that the velocity distribution on the surface of the disc in the solution will be closely related to the velocity distribution for the Dirichlet flow which achieves the velocity, q_c, at the same distance r_s from the axis, shown diagrammatically in figure 4.3a. Then from [3.56], [3.56a], [3.57]

$$r_s^2 = f_s = \frac{\pi \varphi_s C}{2U} - \frac{\pi^2 \varphi_s^2}{4U^2}$$

$$\left(\frac{\partial f}{\partial \varphi}\right)_s = \frac{\pi C}{U} - \frac{\pi^2 \varphi_s}{2U^2} = \frac{2r_s}{q_c} = \frac{2r_s}{U\sqrt{1+Q}}$$

Then eliminating C and solving the quadratic for r_s we find :

[4.8] $$r_s = \frac{1}{2X\sqrt{1+Q}}\left[1 + \left(1 + \frac{\pi^2(1+Q)}{4}\right)^{\frac{1}{2}}\right]$$

$$= \frac{\lambda}{X} \text{ , say}$$

after substituting for U from [4.3] and putting $X = \Psi_H / \varphi_s f_H$. This then is a simple guide to the approximate value of f_s which we would expect given the scale value, X, and the cavitation number. The author decided that values of r_s , f_s of the order of unity would be convenient. Typical values of λ are ; $Q = 0.2$, $\lambda = 1.412$;

$Q = 0.6$, $\lambda = 1.275$.

FIGURE 4.3 a

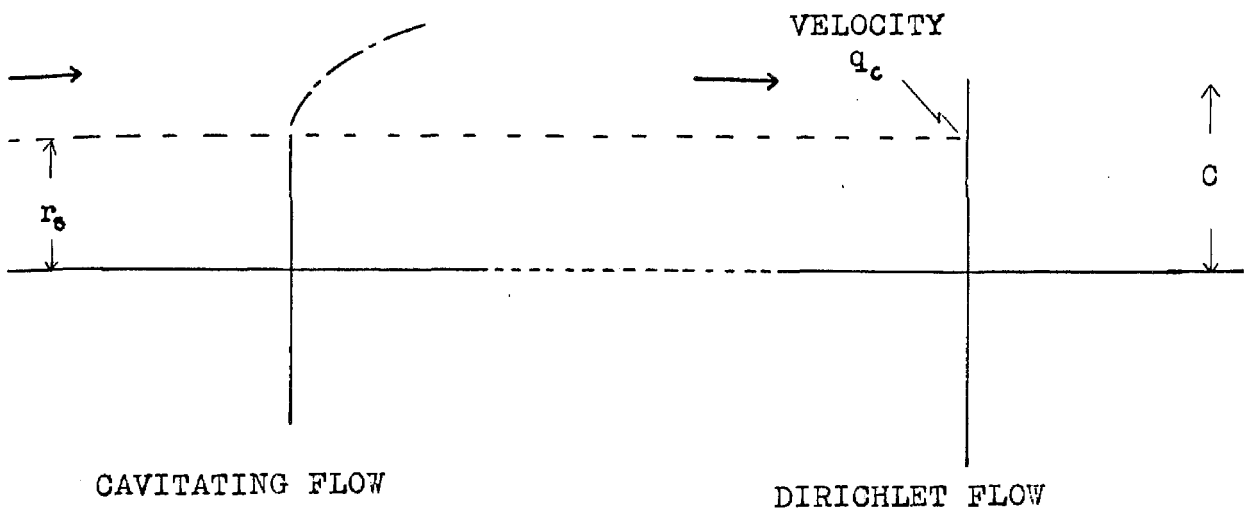

VELOCITY DISTRIBUTION

PROJECTION

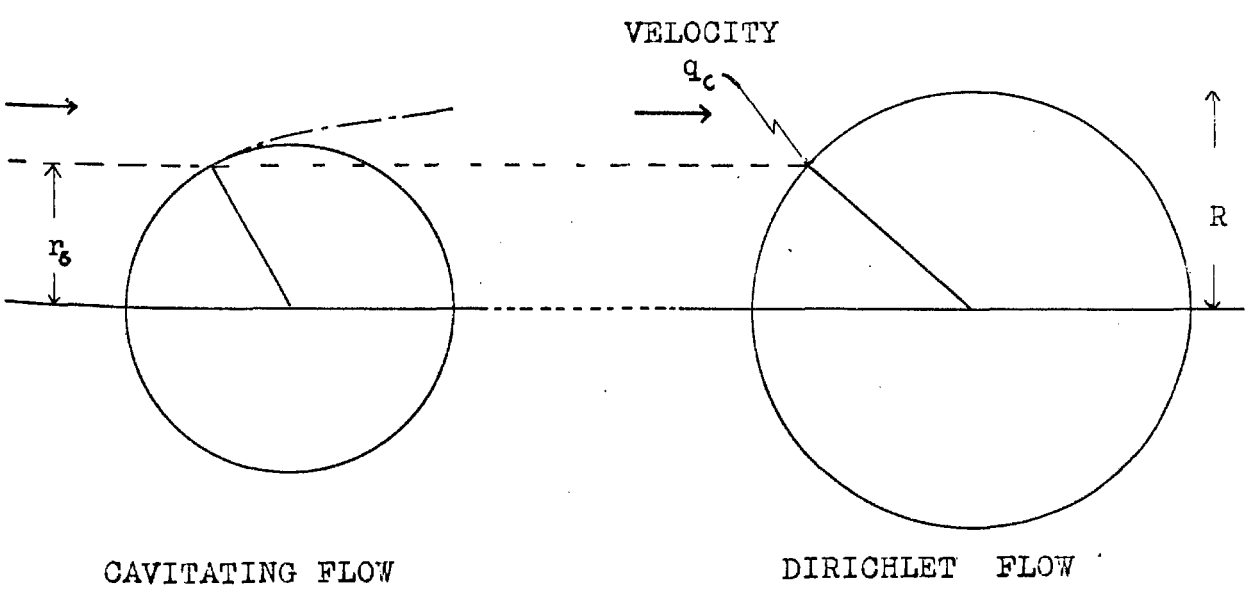

FIGURE 4.3 b

The value of X was, therefore, chosen to be 1.5 throughout the solutions for the disc. Although this would seem from these rough calculations, to give values r_s below unity, X = 1.5 in fact gives values of r_s ranging from about 1.1 to 1.2 in the actual solutions.

[2] On the surface of the sphere.

We will follow a similar procedure as that for the disc. In the Dirichlet flow (equations [3.24]) it is easily shown that the velocity, q, at any point on the surface of the sphere is given by :

[4.9] $$q = 1.5\, U\, f^{\frac{1}{2}} / R$$

Eliminating R from this and equation [3.55a] we find :

$$q = 2 f^{\frac{1}{2}} \varphi \Big/ \left[f + \frac{4\varphi^2}{9U^2} \right]$$

We will assume that the velocity distribution on the wetted surface in the cavitating flow is close to that for the Dirichlet flow past a sphere which achieves the velocity q_c at the same radius, r_s (figure 4.3b). The radius of the spheres need not be identical, though the free stream velocities are. Thus putting $q = q_c$, $f = f_s = r_s^2$, $\varphi = \varphi_s$ in the above equation and substituting for X we find :

$$r_s = \frac{\lambda}{X} \quad \text{, where } \lambda \text{ now becomes}$$

[4.10] $$\lambda = \frac{1}{2\sqrt{1+Q}} \left[1 + \left(1 - \frac{4(1+Q)}{9} \right)^{\frac{1}{2}} \right]$$

Typical values for λ are : $Q = 0.2$, $\lambda = 0.795$;

$Q = 0.6$, $\lambda = 0.608$.

For $Q > 1.25$, λ becomes unreal since the maximum Cp occurs on the wetted surface in the Dirichlet flow at the point $\theta = 0$, where Cp = - 1.25.

In order that r_s was greater than unity for the range $0 < Q < 0.8$ the value chosen for X was 0.45. In the actual solutions ,this gave typical values of r as follows ; $Q = 0.6$, $r_s \approx 1.15$; $Q = 0.2$, $r_s \approx 1.42$.

The parameter, λ , used above only varies to a small degree, increasing as Q decreases in both cases. It is therefore anticipated that f_s will increase slightly with Q, and that the other two parameters, φ_L / φ_s and f_H will have small effects. This is convenient since it means that the f values in the region of the disc or sphere for one solution, can be used to good effect as a first approximation for a new problem with an altered set of parameters.

[3] Upstream.

Although the value which φ_L / φ_s will take, will ultimately be decided by the process of increasing its value until further increase has a negligible effect on the required results, a reasonable value can be found by considering the nature of the upstream flow. From the investigation carried out in section 3.3.2, the conclusion was reached that, for values of $a/f_U \ll 1$ (equation[3.52]):

$$\frac{a}{f_U} = (kD)^3 \Big/ \left[f_U + \left(\frac{\varphi}{U} \right)^2 \right]^{\frac{3}{2}}$$

On the upstream boundary we substitute $\varphi = \varphi_L$ and $U = 2 X \varphi_s$. Since the boundary condition only holds for $a/f_U \ll 1$, in order to find a reasonable value for φ_L / φ_s we must have

$$\frac{a}{f_v} = (kD)^3 \Big/ \left[f_v + \left(\frac{\varphi_L}{2X \varphi_s} \right)^2 \right]^{\frac{3}{2}}$$

$$<< 1$$

The worst case is provided when f_v is small. The constant k is of the order of unity and so, for our choices of X, is D, the typical length, in the case of both the disc and the sphere. Thus we must have :

$$\left(\frac{1}{2X} \frac{\varphi_L}{\varphi_s} \right)^3 >> 1$$

For example:

In the disc, putting X = 1.5 and $\varphi_L / \varphi_s = 12$ we find that the largest value of a/f_v will be 1/64 ,approximately. For the sphere, with X = 0.45, $\varphi_L / \varphi_s = 4$, $(a/f_v)_{MAX} \approx 1/64$.

Thus for these values φ_L / φ_s , $a/f_v << 1$ and these values are,in fact, very close to those used initially for φ_L / φ_s . It subsequently proved that these initial values did not require alteration, an increase in them having very little effect on the results. This will be demonstrated in the error analysis.(Section 5.5.4)

[4] The Free Streamline.

The potential distance φ_F is, as was pointed out in section 3.1.4 , unknown. In section 4.3.6 we will discuss how this may be determined in the process of solution, but from the point of view of designing the relaxation mesh it is useful to have an idea of the values of φ_F / φ_s which may result.

We know that on any streamline, $\frac{\partial \varphi}{\partial s} = q$, where s is measured along that streamline. Since q is constant on

the surface of the cavity, the boundary CD of figure 4.1, then at the point C :

S = the distance measured along the surface of the cavity from the separation point to the point of maximum diameter, C.

$$= \frac{\phi_F}{q_C} = \frac{\phi_F}{\phi_S} \frac{1}{2X\sqrt{1+Q}}$$

Then, having some idea of the value of S, this exact equation enables us to find the corresponding value of ϕ_F/ϕ_S , knowing both X and Q. For example in the case of the disc , Reichardt's empirical formula (equation[2.9]) was used to estimate L, the half-length of the cavity, and this [or, say, $(L^2 + (B-C)^2)^{\frac{1}{2}}$] taken as an estimate of S. Thus the approximate final position of the boundary BC is known. This is helpful when setting up the relaxation net for a particular value of Q .

4.2 FINITE DIFFERENCE EQUATIONS.

4.2.1 The Field Equation.

The basis of all the finite difference equations in this thesis is Taylor's expansion. For example, the value of f at $\Psi = \Psi_1$, $\phi = \phi_1 + n$ will be related to the value of f at $\Psi = \Psi_1$, $\phi = \phi_1$ by :

$$(f)_{\phi_1+n} = \left[1 + nN + \frac{n^2N^2}{\lfloor 2} + \frac{n^3N^3}{\lfloor 3} + \ldots \right] (f)_{\phi_1}$$

This expansion will only hold provided there are no

singularities in the interval,

$$\varphi_1 \leqslant \varphi \leqslant \varphi_1 + n \quad ,$$

on the equipotential joining the two points. Care must be taken, therefore, not to apply a finite difference equation at a point, where the mesh length "tentacles" emanating from that point and used in the difference equation, cover or touch a singularity unless the presence of the singularity has been accounted for in that equation. Treatment of the singularities is given in section 4.4 .

Since the operator and the variable upon which it acts are often widely separated it is much more convenient to use the incorrect suffix notation $N^p f_0$ rather than its strict equivalent $(N^p f)_0$. Confusion will not arise from such a substitution and the simplification is considerable.

In order to translate the field equation, [3.9],

[4.11] $$\frac{\partial^2 \ln f}{\partial \varphi^2} + \frac{\partial^2 f}{\partial \psi^2} = 0$$

we could say :

[4.12] $$\ln(f_1) = \left[1 + nN + \frac{n^2 N^2}{\lfloor 2} + \frac{n^3 N^3}{\lfloor 3} + \ldots \right] \ln f_0$$

[4.13] $$\ln(f_3) = \left[1 - nN + \frac{n^2 N^2}{\lfloor 2} - \frac{n^3 N^3}{\lfloor 3} + \ldots \right] \ln f_0$$

[4.14] $$(f_2) = \left[1 + mM + \frac{m^2 M^2}{\lfloor 2} + \frac{m^3 M^3}{\lfloor 3} + \ldots \right] f_0$$

[4.15] $$(f_4) = \left[1 - mM + \frac{m^2 M^2}{\lfloor 2} - \frac{m^3 M^3}{\lfloor 3} + \ldots \right] f_0$$

using the local system shown in figure 4.4. Adding [4.12] to [4.13] we find :

$$\ln\left(\frac{f_1 f_3}{f_0^2}\right) = \frac{2n^2}{\lfloor 2}(N^2 \ln f_0) + \frac{2n^4}{\lfloor 4}(N^4 \ln f_0) + \ldots$$

But,

$$(N^2 \ln f_0) = \left(\frac{\partial^2 \ln f}{\partial \varphi^2}\right)_0$$

and therefore :

$$[4.16] \qquad n^2 \left(\frac{\partial^2 \ln f}{\partial \varphi^2}\right)_0 = \ln\left(\frac{f_1 f_3}{f_0^2}\right) - \sum_{p=2}^{\infty} \frac{2n^{2p}}{\lfloor 2p} (N^{2p} \ln f_0)$$

Similarly from [4.14],[4.15] :

$$[4.17] \qquad m^2 \left(\frac{\partial^2 f}{\partial \psi^2}\right)_0 = f_2 + f_4 - 2f_0 - \sum_{p=2}^{\infty} \frac{2m^{2p}}{\lfloor 2p} (M^{2p} f_0)$$

Hence substituting in [4.11] we can say that the equation,

$$[4.18] \qquad \frac{m^2}{n^2} \ln\left(\frac{f_1 f_3}{f_0^2}\right) + f_2 + f_4 - 2f_0 = 0$$

is a finite difference approximation to the field equation. If E is the error involved in substituting [4.18] for [4.11] then from the above analysis it follows that

$$[4.19] \qquad E = m^2 \sum_{p=2}^{\infty} \frac{2n^{2p-2}}{\lfloor 2p} (N^{2p} \ln f_0) + \frac{2m^{2p-2}}{\lfloor 2p} (M^{2p} f_0)$$

In other words the error is a function of n,m and the 4th and higher derivatives of f_0 at the point 0. Thus the smaller n and m the smaller the error of finite difference substitution.

Woods (Ref. 46) also gives another form of the field equation based on the first rather than the second of [3.9]. That is

$$[4.20] \qquad 2\left(\frac{m}{n}\right)^2 \left[\frac{f_1 - f_0}{f_1 + f_0} - \frac{f_0 - f_3}{f_0 + f_3}\right] + (f_2 + f_4 - 2f_0) = 0$$

This is based on rough approximations and is much less accurate than [4.18]. It is however useful in one case, as will be seen in section 4.4.3 , where [4.18] and [4.21] break down.

The form [4.18] of the field equation can only be used,of course, for the particular mesh system shown in figure 4.4. Figure 4.5 shows the other mesh system which is used. Taking the expansions of the form [4.14], [4.15]

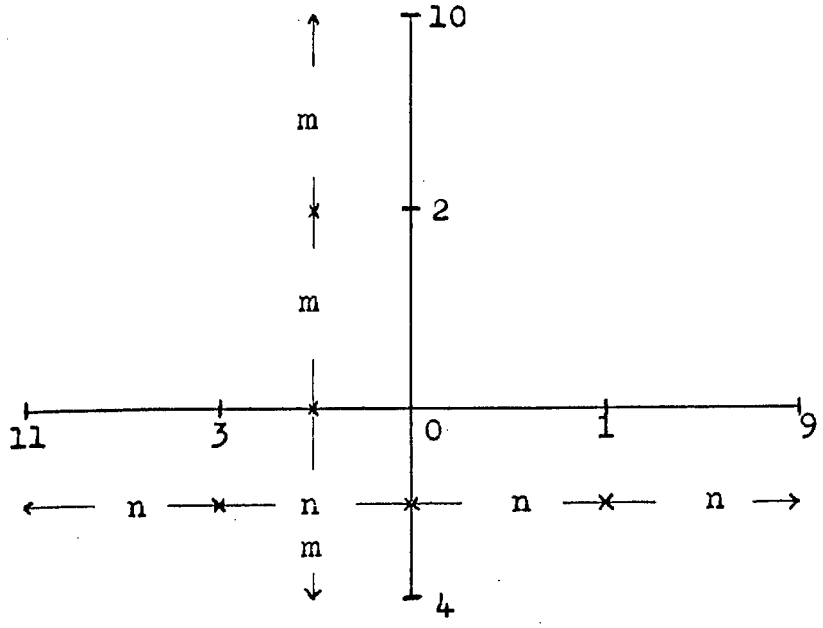

FIGURE 4.4

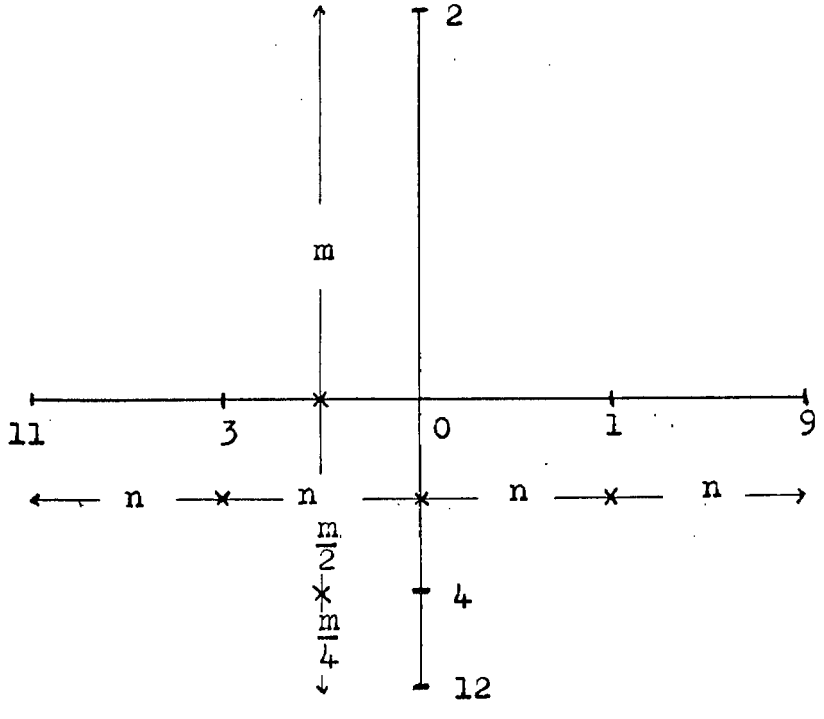

FIGURE 4.5

we find $M^2 f_0$ in this case is given by:

$$5.25m^2M^2f_0 = 16f_{12} - 14f_4 + 5f_2 - 7f_0 - \sum_{p=4}^{\infty}\left[5 + 16\left(-\frac{3}{4}\right)^p - 14\left(\frac{1}{2}\right)^p\right]\frac{m^pM^pf_0}{\lfloor p}$$

Thus we can write the field equation as:

$$[4.21] \quad 5.25\left(\frac{m}{n}\right)^2 \ln\left(\frac{f_1 f_3}{f_0^2}\right) + 16f_{12} - 14f_4 + 5f_2 - 7f_0 = 0$$

where the error is

$$[4.22] \quad E = 5.25m^2\sum_{p=2}^{\infty}\frac{2n^{2p-2}N^{2p}\ln f_0}{\lfloor 2p} + \sum_{p=4}^{\infty}\left[5 + 16\left(-\frac{3}{4}\right)^p - 14\left(\frac{1}{2}\right)^p\right]\frac{m^pM^pf_0}{\lfloor p}$$

Hence, again ,the error is of the order of the fourth derivative in f. Indeed it is the best policy to make all the finite difference equations to be applied accurate to the same order. Then the field is "refined" to give greater accuracy where the solution demands it. Thus we will try as far as possible to make all finite difference equations have errors not lower than the fourth derivatives in f . The author found this the best medium between an excessive number of points and excessive computation for a single point.

The form [4.18] of the field equation is, therefore, used on the lines $j = 1$ and $j = 2$ (figure 4.3) and the form [4.21] on all lines for $j \geqslant 3$.

A further complication arises at points in the regions of the mesh where the mesh length n* is doubled. Thus if we have

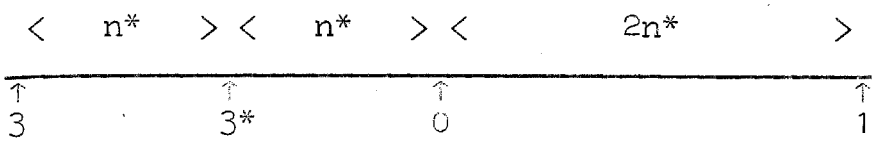

the value f in either [4.18] or [4.21] is now taken from the second point to the left of 0 rather than the first. This is simpler than involving the point 3* ,the presence of whose value would not improve the accuracy of the field equation anyway unless further points are involved.

4.2.2 The First Derivatives.

It is also useful to derive finite difference formulae for the first derivatives in f. These occur in the equations for the velocities and the distance, x both of which are required as results. In order that these formulae will have errors of not less than the 4th derivative in f we must introduce the points 9, 10 and 11 (figure 4.4). Writing

$$\ln f_9 = \left[1 + 2nN + \frac{(2n)^2 N^2}{\lfloor 2} + \frac{(2n)^3 N^3}{\lfloor 3} + \ldots\right] \ln f_0$$

and eliminating $N^2 \ln f_0$ and $N^3 \ln f_0$ using [4.12], [4.13] we find

$$[4.23a] \quad 6n\,N \ln f_0 = 6\ln f_1 - \ln f_9 - 2\ln f_3 - 3\ln f_0 - \sum_{p=4}^{\infty} [6 - 2^p - 2(-1)^p] \frac{n^p N^p \ln f_0}{\lfloor p}$$

Similarly writing $\ln f_{11}$ in terms of $\ln f_0$ and eliminating with [4.12],[4.13] we find:

$$[4.23b] \quad 6n\,N \ln f_0 = -6\ln f_3 + \ln f_{11} + 2\ln f_1 + 3\ln f_0 - \sum_{p=4}^{\infty} [6 - 2^p - 2(-1)^p] \frac{(-n)^p N^p \ln f_0}{\lfloor p}$$

Carrying out exactly similar procedures with f rather than ln f we find

$$[4.24a] \quad 6n\,N\,f_0 = 6f_1 - f_9 - 2f_3 - 3f_0 - \sum_{p=4}^{\infty} [6 - 2^p - 2(-1)^p]\,\frac{n^p N^p f_0}{\underset{\sim}{\lfloor p}}$$

$$[4.24b] \quad 6n\,N\,f_0 = -6f_3 + f_{11} + 2f_1 + 3f_0 - \sum_{p=4}^{\infty} [6 - 2^p - 2(-1)^p]\,\frac{(-n)^p N^p f_0}{\underset{\sim}{\lfloor p}}$$

The two alternative forms of N ln f_0 or N f_0 are used according to the situation. For example at a point near a boundary, say (j,1) the forms [4.23a] and [4.24a] must be used since there is no point 11. As mentioned in section 4.2.1 we cannot go "through" a singularity so that, for example, [4.23b] or [4.24b] must be used at the point D**(figure 4.6b) and [4.23a] or [4.24a] at the point E**.

A further slight complication is provided at or near points where the mesh length n* is doubled. This can,however, be overcome by the right choice of type of equation for Nf_0 or N ln f_0 . For example the following shows the combinations chosen when the point 0 takes three different positions in such a region.

	‹ n* ›	‹ n* ›	‹ n* ›	‹ 2n* ›	‹ 2n* ›	‹ 2n* ›	‹ 2n* ›
Case 1.	7	3	0	1			
Case 2.		3		0	1	5	
Case 3.				3	0	1	5

The other gradient of f, $\frac{\partial f}{\partial \psi}$, is only required on the boundary, j = 0 , in the solution of the field

problem. In this case, using figure 4.4 we have :

$$f_{10} = \left[1 + 2mM + \frac{(2m)^2 M^2}{\lfloor 2} + \frac{(2m)^3 M^3}{\lfloor 3} + \ldots\right] f_0$$

and eliminating between this and [4.14]:

$$8f_2 - f_{10} - 7f_0 = 6mMf_0 + 2m^2 M^2 f_0 + \sum_{p=4}^{\infty} \frac{(8-2^p)m^p M^p f_0}{\lfloor p}$$

Then substituting $N^2 \ln f_0 = - M^2 f_0$ and for $N^2 \ln f_0$ from [4.16]

$$[4.25] \quad 6m\, M\, f_0 = 8f_2 - f_{10} - 7f_0 + 2\left(\frac{m}{n}\right)^2 \ln\left(\frac{f_1 f_3}{f_0^2}\right) - E$$

where

$$[4.26] \quad E = 2\left(\frac{m}{n}\right)^2 \sum_{p=2}^{\infty} \frac{2n^{2p} N^{3p} \ln f_0}{\lfloor 2p} + \sum_{p=4}^{\infty} \frac{(8-2^p)m^p M^p f_0}{\lfloor p}$$

This, therefore, gives us an equation for $\frac{\partial f}{\partial \psi}$ (or Mf_0) on the boundaries DE or DC (figure 4.1) in terms of the values at the points 0, 1, 2, 3 and 10.

4.2.3 Upstream Boundary Condition.

On the upstream boundary, AF of figure 4.6a, the value of f is related to the value of f at a point within the mesh on the same streamline by equation [3.54]. We, therefore, relax a mesh point on this boundary by putting, simply

$$f_{j,1} = (f_U)_j + \left[\frac{\left(\frac{\psi_L - n_j^* \psi_s}{U}\right)^2 + (f_U)_j}{\left(\frac{\psi_L}{U}\right)^2 + (f_U)_j}\right]^{\frac{3}{2}} [f_{j,2} - (f_U)_j]$$

where the $(f_U)_j$ values are, as was mentioned in section 4.1.3, stored in (j,0). Putting $U/\psi_s = 2X$ this becomes :

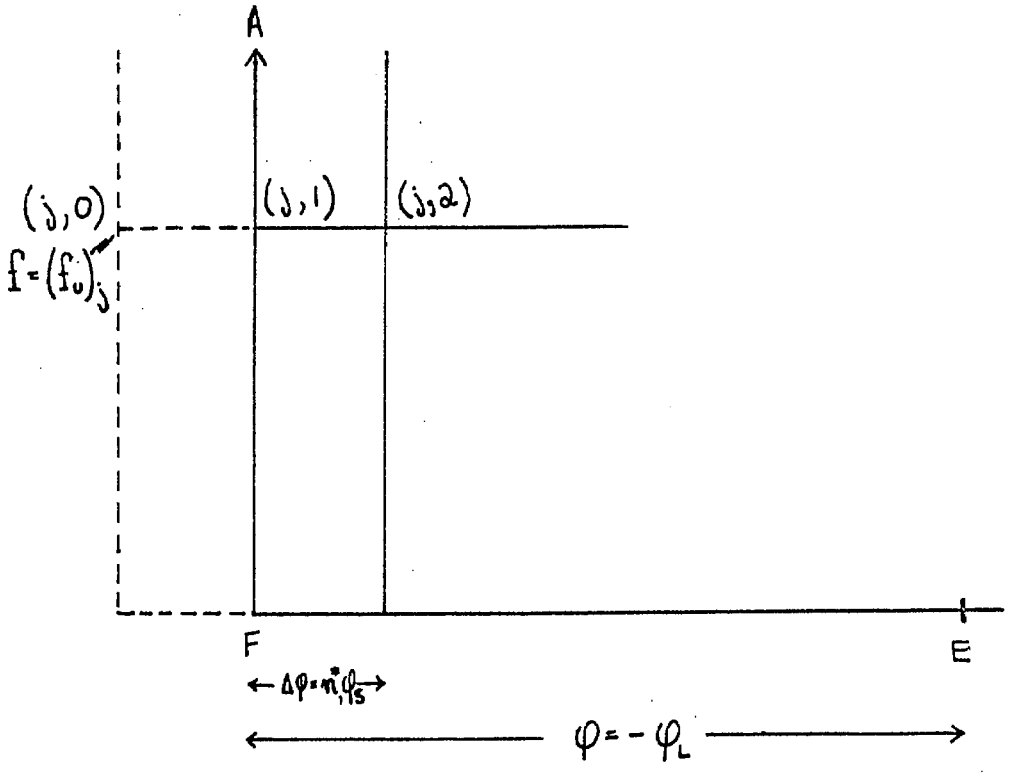

FIGURE 4.6 a

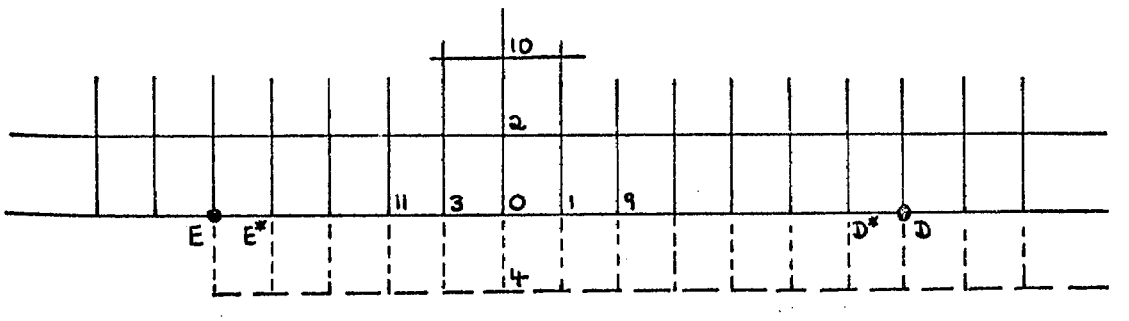

FIGURE 4.6 b

$$[4.27]\quad f_{j,1} = (f_U)_j + [f_{j,2} - (f_U)_j]\left[\frac{\left(\frac{\rho_L}{\rho_S} - n_1^*\right)^2 + 4X^2(f_U)_j}{\left(\frac{\rho_L}{\rho_S}\right)^2 + 4X^2(f_U)_j}\right]^{\frac{3}{2}}$$

Then in a given solution $f_{j,1}$, depends simply on the value of $f_{j,2}$ and the values of the parameter ρ_L/ρ_S, the scale X, and the relative mesh length n_1^*.

Once a solution has been obtained we can test the parameter ρ_L/ρ_S by calculating from the formula [3.54] and the values of $f_{j,1}$, $f_{j,2}$ values for the points (j,3), (j,4) etc. and comparing them with the actual values obtained. An example of this procedure can be found in section 5.5.4 .

4.2.4 The Stream Limiting Boundary and the Upstream Stagnation Streamline.

The values of f on the channel wall, AB of figure 4.1, are all fixed at $f = f_H$; the values on the axis, FE at zero. The relaxation process does not, therefore, deal with points on these boundaries.

4.2.5 The Wetted Surface Boundary Condition for the Disc.

In section 3.1.3 we found that the boundary condition on the surface of the disc ([3.20]) was :

$$\frac{\partial f}{\partial \Psi} = 0$$

or $$M f_0 = 0$$

for a point on ED of figure 4.6b. From this we have to find a finite difference equation connecting the

value of f at the imaginary point 4 (figure 4.6b), to the values at the corresponding points 0, 1, 2 and 3. Then the value of f_4 is known and can be used in the field equation, [4.18], to be applied at 0. This procedure can be carried out in the two stages indicated or, which is more convenient, f_4 can be eliminated from the two equations leaving a special form of the field equation for this boundary. This form of the field equation will, therefore, contain only f_0, f_1, f_2 and f_3.

Thus substituting $Mf_0 = 0$ in equation [4.25] we find the form to be applied on the wetted surface boundary in the case of the disc.

$$[4.28] \qquad \left(\frac{m}{n}\right)^2 \ln\left(\frac{f_1 f_3}{f_0^2}\right) + 4f_2 - 0.5f_{10} - 3.5f_0 = 0$$

where the error is that of [4.26] divided by two.

One unfortunate point that arises here is that the equation [4.28] clearly cannot be used at the point E* (figure 4.6b), where $f_3 = 0$. This is due to the effect of the presence of the stagnation singularity at the point 3 which means that equation [4.16] is no longer accurate or applicable. The form, [4.20], of the field equation is at least applicable though could hardly be any more accurate. The treatment of the singularity at the stagnation point (section 4.4.3) includes the process by which this difficulty is overcome. A special equation must also be used at the point D* since this is close to the separation point singularity. (See section 4.4.4 .)

4.2.6 The Wetted Surface Boundary Condition for the Sphere.

The condition on the boundary DE for the sphere is (section 3.1.3. equation [3.21]):

$$\frac{\partial f}{\partial \psi}\ (R^2 - f)^{\frac{1}{2}} = \frac{\partial f}{\partial \varphi}$$

This provides a more complex boundary form of the field equation than that for the disc. The derivative $\frac{\partial f}{\partial \varphi}$ is first estimated on the boundary. The above condition then gives a value of $\frac{\partial f}{\partial \psi}$ at the particular point under consideration from which the value of f_4, or the equivalent boundary form of the field equation can be obtained.

Clearly this amounts to substituting for Mf_0 and Nf_0 from [4.24a] or [4.24b] and [4.25]. Hence we find the form of the field equation to be applied on the wetted surface boundary in the case of the sphere.

$$[4.29]\quad \left(\frac{m}{n}\right)^2 \ln\left(\frac{f_1 f_3}{f_0^2}\right) + 4f_2 - 0.5f_{10} - 3.5f_0 - \left(\frac{m}{n}\right)\frac{6nNf_0}{2\sqrt{R^2 - f_0}} = 0$$

where , if

$$6nNf_0 = 6f_1 - f_9 - 2f_3 - 3f_0 \quad \underline{\text{then}}$$

$$[4.29a]\quad E = \left(\frac{m}{n}\right)^2 \sum_{p=2}^{\infty} \frac{2n^{2p} N^{3p} \ln f_0}{\lfloor 2p}$$

$$+ \frac{1}{2} \sum_{p=4}^{\infty} \frac{(8-2^p) m^p M^p f_0}{\lfloor p} - \left(\frac{m}{n}\right) \frac{[6-2^p-2(-1)^p] n^p N^p \ln f_0}{\sqrt{R^2 - f_0}\ \lfloor p}$$

Or if $6nNf_0 = -6f_3 + f_{11} + 2f_1 + 3f_0$ then the error is as [4.29a] except that the last term contains $(-n)^p$ rather than n^p .

The same comments obviously apply to the use of equation [4.29] near the singularities D and E as applied in the case of the disc.

It is relevant at this stage to comment on the

major difference between the solutions for the disc and those for the sphere , namely the additional unknown of the direction of flow at separation , θ_s . This is , of course , covered by the additional condition of smooth separation in which the second , as well as the first , derivatives of f are known at the separation. (See section 3.4.4)

The procedure followed in the solutions was that a guess was made as to the value of θ_s . The problem was then solved using this value (see sections 4.3.7 [2] and 5.2.7) which at any given moment in the iterative procedure provides the radius of the sphere, R, from the value of f at the separation point , f_s , as follows (see figure 4.7a)

[4.30a] $$R = \frac{\sqrt{f_s}}{\cos \theta_s}$$

The radius , R , is required for use in equation [4.29] for the boundary condition on the wetted surface.

The manner in which the correct θ_s was found is postponed until after the investigations of section 4.3.7 [2] and is contained in sections 5.2.7 with results in section 5.4.2.

4.2.7 The Free Streamline Boundary Condition.

In section 3.1.3 we found that the condition of constant velocity magnitude on the free streamline became:

$$\frac{1}{f}\left(\frac{\partial f}{\partial \varphi}\right)^2 + \left(\frac{\partial f}{\partial \psi}\right)^2 = \frac{4}{q_c^2} = \frac{4}{U^2(1+Q)}$$

Multiplying through by m^2 and setting $4m^2/U^2 = (g_j)^2 = (g_1)^2$ (from equation [4.5]) we find:

[4.30] $$\frac{1}{f_0}\left(\frac{m}{n}\right)^2 (nNf_o)^2 + (mMf_o)^2 = \frac{g_1^2}{(1+Q)}$$

In this case g_1 is simply the f_v value of the $j=1$ streamline.

On this boundary, as will be seen in section 4.3.6, a different relaxation procedure is employed to that used on the boundary DE. For the purposes of this procedure we have to estimate the "local" cavitation number at every point on this boundary. That is say the value of Q which would make equation [4.30] hold at the point 0 given the f values at the points 0, 1, 2, 3, 9, 10, 11 at that particular time in the relaxation process. This local cavitation number, denoted by the subscripted Q_k, must, in the solution be equal to the chosen Q at every point. From [4.30] :

[4.31] $$Q_k = \frac{g_1^2}{\left(\frac{1}{f}\right)_{0,k}\left(\frac{m}{n}\right)^2_{0,k} (nNf_{0,k})^2 + (mMf_{0,k})^2} - 1$$

where $nNf_{0,k}$ and $mMf_{0,k}$ are calculated using equations [4.24a or b] and [4.25] respectively. The process by which all the Q_k are made to converge to Q is described in section 4.3.6 .

4.2.8 The Boundary of symmetry of the Riabouchinsky flow.

In section 4.1.5 the position of the boundary BC at a given moment in the iterative process was described by k = K and the fractional mesh length , c. From section 3.1.3 the condition on this boundary is :

FIGURE 4.7 a

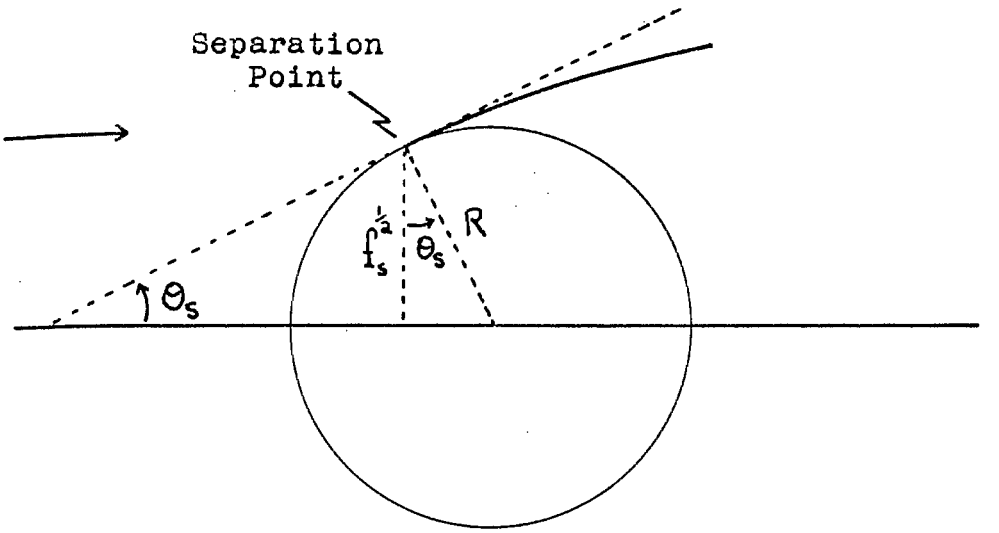

FIGURE 4.7 b

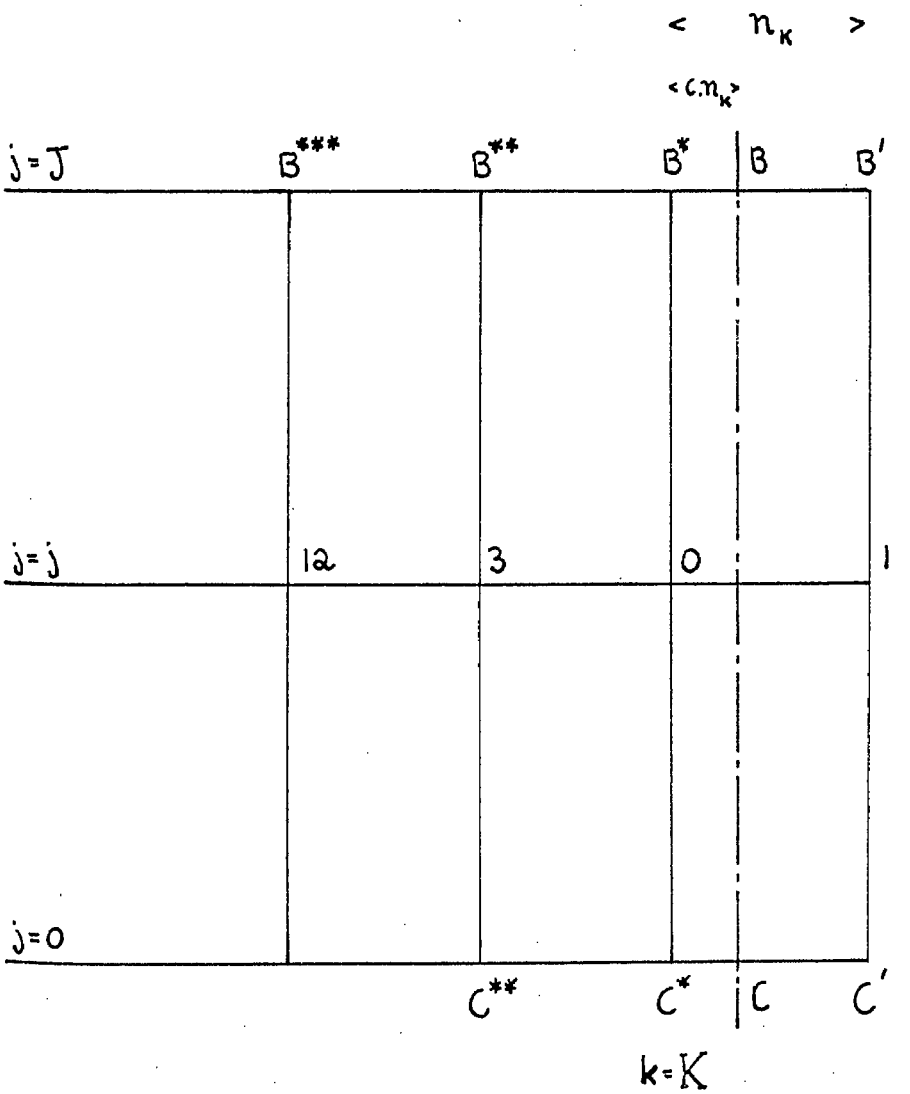

$$\frac{\partial f}{\partial \varphi} = 0$$

or $$(Nf)_{Bc} = 0$$

This condition will be used to find an expression for the values of f on $B'C'$ in terms of the values on the mesh lines B*C* and B**C** and the fraction c. (Figure 4.7b) Taking an expansion for Nf rather than f we get

[4.32] $$(Nf)_{\varphi+c.n} = \left[N + (cn)N^2 + \frac{(cn)^2 N^3}{\lfloor 2} + \ldots \right] (f)_{\varphi}$$

Substituting $(Nf)_{\varphi+c.n} = 0$, we find the condition in terms of c and the derivatives at 0. Now eliminating Nf_0 and $N^2 f_0$ from [4.32] using expansions for f_1 and f_3 in terms of the derivatives at 0 we find

[4.33] $$(2c + 1)f_1 = 4cf_0 + (1 - 2c)f_3 + E$$

[4.34] $$E = \sum_{p=2}^{\infty} \frac{n^{2p-1} N^{2p-1} f_0}{\lfloor 2p-1} + c.\frac{2n^{2p} N^{2p} f_0}{\lfloor 2p} - \sum_{p=3}^{\infty} c^{p-1} \frac{n^p N^p f_0}{\lfloor p-1}$$

This gives the relation for f_1 in terms of f_0 and f_3. The error term is, however, of the third order. An equation for f_1 can be developed whose error is of the fourth order by including a further value from the point 12 but this refinement is unneccessary in this case. It can be anticipated that the solution is well behaved in the neighbourhood of this boundary, so that E is small provided c is of an order not larger than unity. This is acheived by means of straddling the line of symmetry by the last two equipotential mesh lines. Thus the condition on this boundary is given by [4.33] which determines the values at all points on $B'C'$.

4.3 THE RELAXATION PROCESS.

4.3.1 The basic method.

If we denote the finite difference form of the field equation by

[4.35] $$F(f_0, f_1, f_2, f_3, f_4, f_{12} \ldots\ldots) = 0$$

then, as mentioned in section 4.1.1, the basic principle of the relaxation method is to treat each point of the field in turn, adjusting the value f_0 at that point so that [4.35] holds for the present values at 1,2,3,4,12, etc..(Figure 4.2) The value at a particular point after i iterations will be denoted by $f_0^i, f_1^i, f_2^i, f_3^i$; the final value after this process has converged by f_0^*, f_1^*, f_2^*, etc..

There are a number of ways in which the relaxation process can be carried out :

[1] The method of Jacobi sets the value f_0^{i+1} at a point using the values f_1^i, f_2^i, f_3^i .. from the last complete field iteration. The equation to be obeyed at 0 is therefore

[4.36] $$F(f_0^{i+1}, f_1^i, f_2^i, f_3^i \ldots) = 0$$

[2] The Gauss-Seidel method, however, uses the most recent values obtained at any point. If, for example, the point 3 has been treated prior to the point 0 then f_3^{i+1} is used in [4.35] rather than f_3^i. The condition will therefore depend on the order in which the points are relaxed. If this order is j=0,k=1,2,3 ... N, j=1, k=1,2,3 ... N, etc. then [4.35] becomes

[4.37] $$F(f_0^{i+1}, f_1^i, f_2^i, f_3^{i+1}, f_4^{i+1} \ldots) = 0$$

In both cases the value which F takes before the

relaxation of that point is termed the residual , denoted throughout by Y_0 or in the other system $Y_{j,k}$; the process will have converged when the residuals are reduced to zero.

4.3.2 Successive Relaxation by Points.

The finite difference forms corresponding to [4.35] which we shall use are [4.18] and [4.21] ; there are , in addition , the special forms for use on the boundaries. These are all non-linear equations and hence the step involved in finding f_0^{i+1} using [4.36] or [4.37] is less simple than in the case of a linear differential equation. In the latter case it is normally possible to write [4.36] , say , as

[4.38] $$f_0^{i+1} = F'(f_1^i, f_2^i, f_3^i, f_4^i \ \dots\ )$$

where the function F' is known. This is not possible with [4.18] or [4.21] in which an iterative process will be required at each point to solve for f_0^{i+1}. At this stage the residuals become an integral part of the calculations and we will use the simplest method,namely Newton's,to find the value of f_0^{i+1} which gives a zero residual. Thus , for example , the method of Jacobi becomes :

$$F(f_0^i, f_1^i, f_2^i, f_3^i \ \dots\ ) = (Y_0)^i$$

$$\left[\frac{\partial Y_0}{\partial f_0}\right]^i = \left[\frac{\partial F(f_0, f_1, f_2, f_3 \ \dots\ )}{\partial f_0}\right]^i$$

and we put,as a first approximation

[4.39] $$f_0^{i+1} = f_0^i + (-Y_0)^i \Big/ \left[\frac{\partial Y_0}{\partial f_0}\right]^i$$

Since this is an iterative process within an iterative process, namely the relaxation technique, it is normally sufficient to use Newton's method a single time at a particular point. Thus the change in value at a point is calculated as

$$\Delta f_0 = (-Y_0)^i \Big/ \left[\frac{\partial Y_0}{\partial f_0}\right]^i$$

If , for example , the field equation [4.18] is being used then

$$Y_0 = \left(\frac{m}{n}\right)^2 \ln \frac{f_1 f_3}{f_0^2} + f_2 + f_4 - 2f_0$$

$$\frac{\partial Y_0}{\partial f_0} = -2 - \frac{2}{f_0}\left(\frac{m}{n}\right)^2$$

An over-relaxation factor can be introduced to optimise the convergence of the relaxation process. (See , for example , Ref. 39) Denoted by ω , it is used as follows

[4.40] $$f_0^{i+1} = f_0^i + \omega . (-Y_0)^i \Big/ \left[\frac{\partial Y_0}{\partial f_0}\right]^i$$

That is to say the value at f is increased by ω times the required amount , where ω would normally be just greater than unity. Clearly certain limits exist as to the maximum value of ω which can be used though these limits depend very much on the particular problem. It will be seen in the next section that ω alters the rate of convergence according to a simple formula.

4.3.3 Convergence.

We will denote the difference between an intermediate value of f and the final value at the same point by e

where ,therefore

$$e^i = f^i - f^*$$

But we must finally have

$$F(f_0^*, f_1^*, f_2^*, f_3^* \ldots) = 0$$

so that

[4.41] $$F(f_0^i - e_0^i, f_1^i - e_1^i, f_2^i - e_2^i \ldots) = 0$$

or

[4.41a] $$F(f_0^{i+1} - e_0^{i+1}, f_1^i - e_1^i, f_2^i - e_2^i \ldots) = 0$$

This can be used in conjunction with [4.36] or [4.37] to give a relation between e^{i+1} and e^i (see example below) of the form

[4.42] $$\left\{e^{i+1}\right\} = \left[E\right]\left\{e^i\right\}$$

where $\left[E\right]$ is a matrix whose elements are usually known for a particular mesh and field arrangement.

Clearly,in order that the process be convergent the errors ,e,must be consistently reduced. It can be shown (Ref. 32) that the neccessary condition for this to be so is :

[4.43] $$(|\lambda|)_{\max.} < 1$$

where λ is the eigenvalue of $\left[E\right]$ with the largest spectral radius. In fact, $|\lambda|$ is a measure of the convergence of the relaxation process since , from [4.42] it follows that

$$\left\{e^{i+1}\right\} = \lambda \left\{e^i\right\}$$

Let us take the example of the field equation [4.18] in a Jacobi iterative procedure. Equation [4.36] becomes

[4.44] $$\left(\frac{m}{n}\right)^2 \ln\left(\frac{f_1^i f_3^i}{f_0^{i+1}}\right) + f_2^i + f_4^i - 2f_0^{i+1} = 0$$

Equation [4.41a] becomes

[4.45] $$\left(\frac{m}{n}\right)^2 \ln \frac{(f_1^i - e_1^i)(f_3^i - e_3^i)}{(f_0^{i+1} - e_0^{i+1})} + [f_2^i - e_2^i + f_4^i - e_4^i - 2(f_0^{i+1} - e_0^{i+1})] = 0$$

We shall assume that $e/f \ll 1$ at all points. Thus subtracting [4.45] from [4.44] we find

$$[4.46] \quad e_0^{i+1}\left[2 + \frac{2}{f_0^{i+1}}\left(\frac{m}{n}\right)^2\right] \simeq \frac{1}{f_1^i}\left(\frac{m}{n}\right)^2 e_1^i + \frac{1}{f_3^i}\left(\frac{m}{n}\right)^2 e_3^i + e_2^i + e_4^i$$

Thus we can write [4.42] where the elements of $[E]$ are known. Hence the matrix $[E]$ can be set up and its eigenvalue, λ, found. Clearly if $e/f \ll 1$ then the elements of $[E]$ do not change significantly during the relaxation process.

If an over-relaxation factor is used it is easily seen that equation [4.42] becomes

$$[4.47] \quad \left\{e^{i+1}\right\} = (1-\omega)\left\{e^i\right\} + \omega[E]\left\{e^i\right\} = [E^*]\left\{e^i\right\}$$

where the relevant eigenvalue, λ^*, of the matrix $[E^*]$ is therefore given by

$$[4.48] \quad 1 - \lambda^* = \omega(1-\lambda)$$

Thus the convergence of the process on the introduction of an O.R.F. (given by λ^*) can easily be anticipated knowing the convergence of the original process (given by λ). Further investigations are carried out in section 5.2, in relation to the actual meshes and field equations used.

4.3.4 Possible Semi-direct Method.

By expanding the method of section 4.3.2 it is possible to suggest a semi-direct method of solution. The field equation is applied at every point at which f is initially unknown. Thus we have a set of T equations for T unknowns, where T is the total number of such points.

In the case of a linear differential equation we therefore have T simple simultaneous equations , and the direct method involves the direct solution of these. i.e. If the equations can be written as

$$\{a\} = [M]\{f\}$$

then

$$\{f\} = [M]^{-1}\{a\}$$

where $\{a\}$ and $[M]$ are known.

This is not possible where the equations are non-linear since we cannot write the field equations in this matrix form. However,the following semi-direct method is possible.

If the approximate,or "guessed",values are substituted in the field equations,we have

$$F(f_0, f_1, f_2, f_3 \ldots) = Y_0$$

Then,to the first order

$$\Delta Y_0 = \Delta f_0 \frac{\partial Y_0}{\partial f_0} + \Delta f_1 \frac{\partial Y_0}{\partial f_1} + \Delta f_2 \frac{\partial Y_0}{\partial f_2} + \ldots$$

The required change, ΔY_0 ,is of course $-Y_0$. Thus the required changes in $f_0, f_1, f_2 \ldots$ are given by

$$\{-Y_{j,k}\} = [M]\{\Delta f_{j,k}\}$$

in matrix notation,where the elements of $[M]$ consist of the derivatives of the type $\frac{\partial Y}{\partial f}$. Thus

$$\{\Delta f_{j,k}\} = [M]^{-1}\{-Y_{j,k}\}$$

This process is then repeated since the elements of $[M]$ may change,some of the second derivatives , $\frac{\partial^2 Y}{\partial f^2}$, being non-zero.

Such a method would,no doubt,be more convergent than the successive relaxation by points , but,in practice, has a number of disadvantages. Consider the storage space required in a digital computer. The dimension of the

square matrix $[M]$ is equal to the number of points at which a field equation is applied. Usually if the number of such points exceeds 70 , storage of the whole of $[M]$ is impossible,since many other quantities must obviously be preserved. This matrix must then be inverted,a labourious,time-consuming task. However , many of the elements of $[M]$ are zero , the matrix having only a few non-zero diagonals. Fox (Ref. 12) gives methods of carrying out the inversion of such a matrix which save time by treating only significant non-zero sub-matrices and vectors. This cuts the labour considerably,though the storage and time required are still much greater than a single field relaxation by points.

4.3.5 Investigations on the Free Streamline.

The flow on and in the region of the free streamline and the separation point clearly constitutes the crux of the problem. Consider the following observations which can be made at this stage :

[1] The position of the boundary,BC,the plane of symmetry,is unknown ; it is determined by the position of the point of maximum radius of the cavity,a property of the free streamline.

[2] A great deal is known of the flow at the separation point.

[3] Intuitively we could say that the position of the free streamline will depend considerably on the flow at separation.

General though these observations may be, they do suggest that the lack of knowledge at the point C , the point of maximum radius, ought to be complemented by an excess of knowledge of the flow at separation.

Now consider the field equation for a point on the free streamline, given by [4.31].

$$[4.49] \qquad Q = \frac{g_1^2}{\frac{1}{f_{0,k}}\left(\frac{m}{n}\right)^2_{0,k}(nNf_{0,k})^2 + (mMf_{0,k})^2} - 1$$

Since this may not be obeyed, except in the final solution the numerical value of the right-hand side is denoted by Q_k refered to as the local cavitation number. The effective residual at any point is thus $\Delta Q_k = Q_k - Q$. Also from [4.25] and [4.24 a or b] :

$$6mMf_{0,k} = 8f_2 - f_{10} - 7f_0 + 2\left(\frac{m}{n}\right)^2 \ln \frac{f_1 f_3}{f_0^2}$$

$$6nNf_{0,k} = 6f_1 - f_9 - 2f_3 - 3f_0$$

$$= -6f_3 + f_{11} + 2f_1 + 3f_0$$

Then , if we are to follow the procedure given in section 4.3.2 at points on this boundary , $\partial \Delta Q_k / \partial f_0$ must be found.

$$[4.50] \qquad \frac{\partial \Delta Q_k}{\partial f_0} = -\frac{(Q_k+1)^2}{g_1^2}\left[\frac{1}{f_0^2}\left(\frac{m}{n}\right)^2 nNf_0\,(-nNf_0 \mp f_0) + \frac{mMf_0}{3}\left(-7-\frac{4}{f_0}\left(\frac{m}{n}\right)^2\right)\right]$$

The $\mp$ sign in the middle of this expression is a result of the two alternative expressions for nNf_0 . Irrespective of this , and given the provision that the approximate shape of the cavity always obeys the basic relations of section 3.2.4 ($Mf_0 > 0$, $Nf_0 > 0$, $N^2 \ln f_0 < 0$ providing $\varphi < \varphi_{Bc}$), $\partial \Delta Q_k / \partial f_0$ invariably takes a numerically positive value, in the authors experience. Thus , if at all points on DC the residuals are calculated as positive (i.e. Q_k larger than Q at all points) this requires us to put

$$f_o^{i+1} = f_o^i - (\Delta Q_k) \Big/ \frac{\partial \Delta Q_k}{\partial f_o}$$

That is to say , in this example , all the f values on the free streamline would be decreased.

But this is contrary to physical experience. Normally if the cavitation number is too large , we would have to <u>increase</u> the size of the cavity to reduce Q. Thus the use of the normal procedure would seem to be incorrect on the free streamline.

Consider the other derivative :

$$[4.51] \quad \frac{\partial \Delta Q_k}{\partial f_1} = - \frac{(Q_k+1)^2}{g_1^2} \cdot \frac{2}{3} \left(\frac{m}{n}\right)^2 \left[(2 \pm 1) \frac{nNf_o}{f_o} + \frac{mMf_o}{f_1} \right]$$

This,on the other hand,is always negative , given the same provision as before. If along the length of the free streamline the residual at the point O is dispersed by altering f_1 , the direction of movement would seem to be compatible with physical experience. Clearly one method would diverge the other,seemingly the latter,would converge.

This investigation,together with the initial observations led the author to conclude that one feasible treatment of the free streamline was as follows. Suppose, initially,that the values of f at the separation point, $k = k_s$,and the next point, $k = k_s + 1$, are fixed. Then if ΔQ_{k_s+1} is dispersed by altering f_{o,k_s+2} and this procedure followed for every point as we move down the free streamline,we find that $f_{o,K+1}$ is determined by ΔQ_K , $k = K$ being the last point at which Q_k can be calculated. Hence the position of the centre line,BC,is automatically determined by this process , since from [4.33] , c can be

calculated.

Thus, if the value of $f_{0,k_{s+1}}$ can be found by considerations other than the application of the field equation , [4.49] , at that point the solution of the problem acquires feasibility. The initial observation, that the lack of knowledge at C ought to be complemented by an excess at D , would seem to be the case. Thus a major part of the problem lies in an investigation of the flow at separation , in order to find a method of determining $f_{0,k_{s+1}}$. This will be carried out in section 4.3.7 for the cases of the disc and the sphere. In the next section the possibility of such a relation will be anticipated and the method of sclution adopted by the author will be developed, based on the method outlined above.

However, before the details of such a method are discussed , it is relevant to consider it in relation to the solution of the problem as a whole. Suppose an initial guess , based on approximate formulae , has been made for the values of f at all points on the free streamline and wetted surface and that the rest of the field has been filled in with guessed values , possibly taken from sketched equipotentials and streamlines in the physical plane. Clearly the Q_k values on which we must base any change of the f values on that boundary are those calculated from a Dirichlet solution in which the boundary values are kept fixed. These Q_k values may bear no relation to those calculated when all the values are guessed. A similar situation would arise after any change in the boundary values.

For this reason, and from experience, the

author found it neccessary to adopt a procedure which consisted , essentially , of alternately solving a Dirichlet problem and changing the boundary values on CD according to the resultant Q_k values. In finite difference terms , this amounts to relaxing all points except those on the boundary CD for a number of iterations, then relaxing the points on that boundary and repeating the process. Clearly it is sufficient to iterate in first operation until ΔQ_k values , indicative of the ΔQ_k values which would result were this process to be repeated to complete convergence , are obtained. This usually entails far fewer iterations than the complete Dirichlet solution.

Southwell and Vaisey (Ref. 43) recommended and used the latter type of procedure in their solutions with cusped cavities. (See section 2.5) They do not seem , however , to have developed any automatic method of free streamline adjustment such as that given above.

4.3.6 Method of Solution for the Free Streamline.

Since equation [4.49] is essentially a function of the first derivatives of f , it is easily shown that the value of Q_k at a point is more sensitive to changes in the differences $(f_1 - f_0), (f_2 - f_0), (f_3 - f_0)$ etc. than to uniform changes in the magnitudes of the f values. In fact the alteration in Q_k due to a small equal change in all the values $f_0, f_1, f_2, f_3 \ldots$ at a point is negligible compared with the alteration in Q_k for the

same change applied only to f_i , say.

With this and the derivatives , [4.50] and [4.51], in mind , we will examine particular methods of carrying out the procedure envisaged in the last section. It will be found that various restrictions and modifications must be placed on that general method. To simplify the investigations a situation will be used , in which all the residuals except one , at the point in question , are zero. This will give an idea of the behaviour of the particular process being envisaged.

[1] Gauss-Seidel. The first method which will be investigated is that in which the newest values are used at every point. Thus we must set

$$[4.52] \qquad f_{k+1}^{i+1} = f_{k+1}^{i} - (\Delta Q_k) \Big/ \frac{\partial Q_k}{\partial f_{k+1}}$$

Now f_{k+1} being altered , this will alter the value of ΔQ_{k+1} as follows ;

$$\delta(\Delta Q_{k+1}) = \delta f_{k+1} \cdot \frac{\partial \Delta Q_{k+1}}{\partial f_{k+1}}$$

$$= - \frac{\partial \Delta Q_{k+1}}{\partial f_{k+1}} \cdot \frac{\Delta Q_k}{\frac{\partial Q_k}{\partial f_{k+1}}}$$

Thus

$$[4.53] \qquad \frac{\delta(\Delta Q_{k+1})}{\Delta Q_k} = - \frac{\partial Q_{k+1}}{\partial f_{k+1}} \Big/ \frac{\partial Q_k}{\partial f_{k+1}}$$

Now , with the aid of [4.50] and [4.51] , provided the first derivatives of f at k and k+1 are reasonably close together , it can be seen that the numerical value of the right hand side of [4.53] is greater than +1 . Thus the residual ΔQ_k is removed to the next point, k+1 , and ,which is even more unsatisfactory , usually magnified in the transfer. This method must therefore

be discounted , in its present form , as unsatisfactory.

[2] Jacobi. On the other hand we could , in the calculations for δQ_k , use only the "old" values of f at every point. Thus [4.52] will still be applicable but δQ_{k+1} will be unaffected by the resultant change in f_{k+1} . The residuals are therefore not transferred and the unsatisfactory magnification of the Gauss-Seidel eliminated. This method would work but the author found it unsatisfactory , in that after the subsequent Dirichlet solution a residual equivalent to δQ_k invariably appeared as δQ_{k+1} . But based on this the following,more workable method was designed.

[3] Overall Downstream Displacement. This method presents a satisfactory compromise between [1] and [2]. The values of δQ_k are calculated as in [2] from the "old" values of f. But instead of making the requiste change only in f_{k+1} , all the downstream values are changed by the same amount , δf_{k+1} . Thus the whole free streamline downstream of the point in question is moved bodily to disperse the residual at that point. This is more simply carried out by representing the values on the free streamline by the recurrence relation

$$f_{k+1} = f_k + d'_k$$

If,then,the d'_k values are altered according to δQ_k we will get the desired effect. Clearly

$$\frac{\partial \delta Q_k}{\partial d'_k} = \frac{\partial \delta Q_k}{\partial f_{k+1}}$$

We will also use the notation

$$(f_3 - f_0)_{0=k} = d^3_k$$

$$(f_2 - f_0)_{0 \equiv k} = d^2_k$$

In designing the procedure for the free streamline it must be borne in mind that the object is to eliminate or successively reduce the residuals which occur at the end of the next internal or Dirichlet solution. The residuals occuring immediately after the boundary change are relatively unimportant. The issue will be complicated by the fact that changes will occur in the internal values , f_2 , f_{10} , during the next internal solution and these values are used in the calculations of the residuals. Clearly any change in f_1 or d'_k at a point will also alter the resulting values, f_2 , f_{10}. Thus equation [4.52] does not represent a true picture of the required change in the values and any method of solution attempted must include or take account of these unknown factors.

Due to these effects , if $\frac{\partial \Omega Q_k}{\partial d'_k}$ was estimated from [4.51] and the value substituted in

[4.54] $$(d'_k)^{i+1} = (d'_k)^i - \beta . \Omega Q_k \Big/ \frac{\partial \Omega Q_k}{\partial d'_k}$$

then with $\beta = 1$, the changes in d'_k which resulted were found (see section 5.2.5) to be too large. Thus some alteration was required in the basic method.

Two alternative methods were tried by the author. The first involved the use of [4.54] with the parameter β taking a value less than unity.

The second involved a trial and error procedure to find a numerical value , α_1 , for the gradient $\frac{\partial d'_k}{\partial \Omega Q_k}$ which would serve as follows

[4.55] $$\left(d'_k\right)^{(i+1)} = \left(d'_k\right)^{i} + \alpha_1 (P.n^*_k)(\partial Q_k)$$

where , since the gradient assumed ought to include a multiplier proportional to the relative mesh length, n^*_k , we introduce the term $n^*_k / n^*_s = P.n^*_k$. (See section 4.1.4)

The relative merits of these two methods , and the reasons for the second , apparently more empirical , are discussed in section 5.2.5.

Finally it must also be pointed out that, due to the condition $N^2 \ln f_o < 0$ on the free streamline (see section 3.2.4) it is easily seen that a physically realistic solution has at every point

$$d'_{k+1} < d'_k$$

provided the relative mesh-lengths n^*_{k+1} and n^*_k are the same. A constraint was introduced to the programme so that this could never fail to be the case. Naturally the constraint only came into action during earlier iterations. If,however,the constraint is not included divergence occasionally took place when d'_{k+1} became greater than d'_k , depending on the initial guessed values.

4.3.7 Investigation at the Separation Point.

The aim of this section is to discover whether and how the value f_{k_s+1} may be determined without the application of the boundary field equation at that point. For that purpose the series expansions of section 3.4 were derived. Since,as was pointed out in section 4.2.1 ,

we cannot apply a finite difference form of the field equation at the singular separation point itself , this question will also be investigated.

It will be assumed that the expansions must hold in the neighbourhood of the separation point. It will also be assumed that the field equation , or the relevant boundary type , can be applied at all points in this region except the separation point itself. This is not precisely the case since at points such as 1,2, 3 (figure 4.8) the presence of the singularity demands modified field equations with extra-residuals .(See sections 4.4.3 to 4.4.6) But for the purposes of the following discussion this embellishment can be neglected.

[1] Abrupt Separation from the Disc.

The expansions [3.79],[3.80] and [3.81] must obviously be truncated at some power in order that they may be applied. There will also be some limit to the number of points at which they can reasonably be expected to hold. Clearly these two limits must be interconnected. One major problem which arises out of this is how to determine , say , the range of points at which the expansions , truncated at a given power , can be applied. This problem will be demonstrated by an example. Suppose,initially, that the following truncated expansions are to be used :

$$[4.58] \qquad \ln(f) = \ln(f_0) - \frac{2}{f_0^{\frac{1}{2}}}\left(-\frac{\psi}{q_c}\right) + K_3\left(-\frac{\psi}{q_c}\right)^{\frac{3}{2}}$$

$$[4.59] \qquad f = f_0 + K_2\left(\frac{\psi}{q_c}\right)^{\frac{3}{2}}$$

$$[4.60] \qquad \ln(f) = \ln(f_0) + \frac{2}{f_0^{\frac{1}{2}}}\left(\frac{\psi}{q_c}\right)$$

FIGURE 4.8

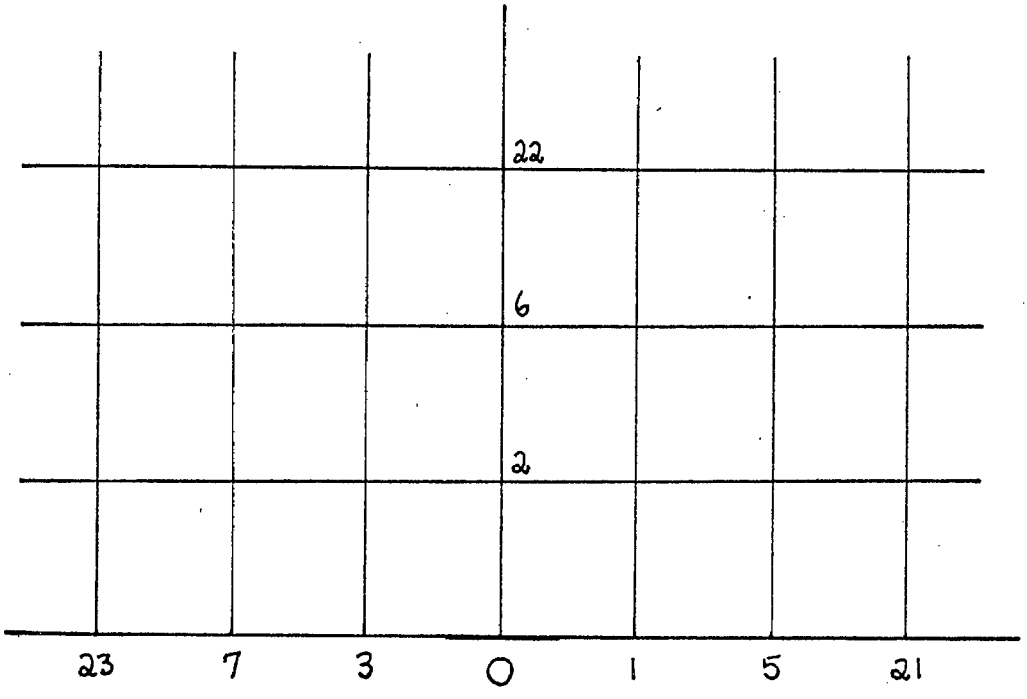

Terms with powers equal or greater than 2 have been neglected. [In these and all the following expansions φ is measured from the separation point , positive downstream. From section 4.1.4 we can write

$$\frac{\varphi}{q_c} = \frac{(k - k_s)}{2XP\sqrt{1 + Q}}$$

$$\frac{\Psi}{q_c} = \frac{(f_v)_j}{2\sqrt{1 + Q}}$$

where the address of the point is either $(0,k)$ or (j,k_s) .]

This introduces two new unknowns , K_2 and K_3 . Application of [4.58] at points 3 and 7 produces two equations which can be solved for K_3 and f_o ; [4.59] applied at 2 gives K_2 ; [4.60] at 1 finds f_1 . Thus neccessary and sufficient conditions for our purposes are the applications of the relevant expansions , [4.58],[4.59] or [4.60], at points 7,3,2 and 1. If more points are used the problem becomes over-determined for our purposes in this region ; if less then we cannot achieve our objective.

Alternatively , another term could be included in the expansions as follows :

[4.61] $$\ln (f) = \ln (f_o) - \frac{2}{f_o^{\frac{1}{2}}}\left(-\frac{\varphi}{q_c}\right) + K_3\left(-\frac{\varphi}{q_c}\right)^{\frac{3}{2}} + A_3\left(-\frac{\varphi}{q_c}\right)^2$$

[4.62] $$f = f_o + K_2\left(\frac{\Psi}{q_c}\right)^{\frac{3}{2}} + A_2\left(\frac{\Psi}{q_c}\right)^2$$

[4.63] $$\ln (f) = \ln (f_o) + \frac{2}{f_o^{\frac{1}{2}}}\left(\frac{\varphi}{q_c}\right) + A_1\left(\frac{\varphi}{q_c}\right)^2$$

Then substituting values from 23,7 and 3 in [4.61] enables us to solve for K_3,A_3 and f_o ; from 2 and 6 in [4.62] enables us to solve for K_2,A_2 ; from 1 and 5 in [4.63] finds A_1 and f_1 .

It is relevant to point out at this stage that

at least one point must be used in each of the three directions since the expansions ensure that the correct conditions are achieved at the separation point.

However the procedure outlined above is , of course , only one of a number of alternatives. In the second case , for example , we could substitute for the use of [4.61] at 23 , the use of [4.62] at 22. The process of finding f in any case is clearly equivalent to the application of the partial differential equation at the separation point ; the process of finding f could be imagined as the application of the extra information of the flow at separation.

In the solutions carried out by the author the second set of expansions and accompanying procedure was used , being ,presumably, more accurate.

The author could not , however , justify the the application of the expansions at the neccessary and sufficient number of points , except in so far as it was neccessary and sufficient for the solution of the problem in finite differences. Comparing the truncation errors of the expansions with the truncation errors involved in setting up the ordinary field equation leads nowhere , the series being of different types.

[2] Smooth Separation from the Sphere.

The expansions [3.85],[3.86] and [3.87] are truncated as follows :

$$[4.64]\quad \ln(f) = \ln(f_0) - \frac{2\sin\theta_s}{f_0^{1/2}}\left(-\frac{\varphi}{q_c}\right) - \frac{1}{f_0}\left(-\frac{\varphi}{q_c}\right)^2 + K_3^*\left(-\frac{\varphi}{q_c}\right)^{5/2}$$

$$[4.65]\quad f = f_0 + 2\cos\theta_s\left(\frac{\psi}{q_c}\right) + \frac{1}{f_0}\left(\frac{\psi}{q_c}\right)^2 + K_2^*\left(\frac{\psi}{q_c}\right)^{5/2}$$

$$[4.66]\quad \ln(f) = \ln(f_0) + \frac{2\sin\theta_s}{f_0^{1/2}}\left(\frac{\varphi}{q_c}\right) - \frac{1}{f_0}\left(\frac{\varphi}{q_c}\right)^2 + K_1^*\left(\frac{\varphi}{q_c}\right)^{5/2}$$

There is however an additional unknown in this case, namely the separation angle , θ_s . Suppose that a guess has been made for θ_s . Then the application of expansion [4.64] at 3 and 7 (refering to figure 4.8) will produce two equations , soluble for K_3^* and f_0, of [4.66] at 1 and 5 gives K_1^* and f_1 ,and of [4.65] at 2 and 6 will also produce two equations. But the last two equations will include only the unknown K_2^* ,known f values and θ_s . Thus eliminating K_2^* from these two will give an expression which will act as a test to our initial guess for θ_s . As in the case of the disc , this is only one of a number of ways in which the neccessary and sufficient number of equations can be obtained. The same problem of justification will also be relevant. The procedure given above was the one employed in the authors solutions.

Finally it remains to comment on one minor modification made to both procedures in the actual programme. In view of the importance of the d_k' differences, dealt with in section 4.3.6 , the procedure in the free streamline expansion application is slightly altered. Instead of regarding f_5 as being fixed , the value $(f_5 - f_1)$ is treated as constant. Thus $(f_1 - f_0)$, or since $(f_1 - f_0)/f_0 \ll 1$, $\ln f_1/f_0$, and K_1 (or K_1^*) are the unknowns.

4.4 THE SINGULARITIES.

4.4.1 General.

At the separation and stagnation points of the flow all derivatives of f above a certain order become infinite as indicated in sections 3.4 and 3.3.3 respectively. These are the only singular points in the field to be solved. In the neighbourhood of these points the higher derivatives included in the error terms of the finite difference equations are not insignificant and the errors may destroy the accuracy of any solution in this region. Clearly some effort must be made to modify the equations to be applied in these regions in order that the difference between the finite difference solution obtained and the solution of the differential equation is contained within required limits.

In problems where the differential equation is linear, much has been written on methods of treatment of singularities. [Southwell (Ref. 42), Russell (Ref. 39) and Woods (Ref. 47) among others.] The importance of the condition of linearity lies in the fact that if f is the dependent variable in the partial differential equation then we can write

[4.67] $$f = f^{A} + f'$$

where both f^{A} and f' also obey the differential equation when substituted for f.

Then the general method of treatment, given by Russell (Ref. 39), is as follows ;

[1] Identify the type of singularity. A type n is conventionally one in which the n th derivative of f is discontinuous.

[2] Find a suitable analytic function, say $f'(\varphi,\Psi)$, which has the same type of singularity and which also satisfies the partial differential equation and the boundary conditions in the vicinity of the singularity. This is arranged so that we can write [4 67] where f^A is well behaved in this region. The actual functions used in the linear case do not concern us here so it will suffice to say that they are usually of the type $r^{\frac{n}{2}}$ or $\ln(r)$ where r is a radial variable.

[3] Find some special numerical treatment so as to satisfy the analytical solution near the singularity. One such method suggested by Woods (Ref. 47) involves the use of "extra-residuals" in the neighbourhood of the singularity ; that is to say corrections to the standard difference equations in the vicinity of the singularity so that in this region the equation to be applied becomes

[4.68] $F(f_0, f_1, f_2, f_3 \ldots) = Z_{j,k}$

rather than [4.35].

Russell (Ref. 39) generalizes previous methods for the linear case as follows :

let f** represent the exact solution of the partial differential equation ;

f be an approximation to f**;

f' be the chosen analytic function $f'(\varphi,\Psi)$;

$f^{D*} = f^* - f'$;

$f^D = f - f'$;

∂ represent a differential operator ;

δ represent the finite difference equivalent of ∂ .

Then, in the linear case

$$\partial f^{**} = \partial f^{D*} + \partial f'$$

$$\delta f = \delta f^{D} + \delta f'$$

and since f^{D} is well-behaved we may write

$$\partial f^{D*} = \delta f^{D}$$

Thus

[4.69] $$\partial f^{**} = \delta f + (\partial f' - \delta f')$$

The term in brackets is therefore the extra-residual required. This is simply the difference between the analytic result, $\partial f'$, obtained by differentiating f' and its finite difference equivalent, $\delta f'$, obtained using f_0', f_1', f_2', etc. according to the operator δ.

4 4 2 The Non-linear Case.

When the partial differential equation is not linear a similar method can be applied given certain other conditions on f'. We will stipulate that f' obey the differential equation and the boundary conditions in the neighbourhood of the singularity as well having the same type of singularity. Then in general, using the notation of the last section

$$\partial f^{**} - \partial f' = \partial^*(F^{D*})$$

where F^{D*} is a function of f^{**} and f, and ∂^* a differential operator where, in general, $\partial \neq \partial^*$ Also

$$\delta f - \delta f' = \delta^*(F^{D})$$

F^{D} being an approximation to F^{D*} and δ^* the finite difference equivalent of ∂^* Subtracting

[4 70] $$\partial f^{**} = \delta f + (\partial f' - \delta f') + (\partial^* F^{D*} - \delta^* F^{D})$$

Thus [4 69] is still applicable provided F^{D*} is sufficiently

well-behaved so that

$$\gamma^* F^{D*} = \delta^* F^D$$

throughout the region in question.

Taking the partial differential equation , [3.9], as the relevant example we have

$$\frac{\partial^2 \ln f^{**}}{\partial \varphi^2} + \frac{\partial^2 f^{**}}{\partial \psi^2} = 0$$

and

$$\frac{\partial^2 \ln f'}{\partial \varphi^2} + \frac{\partial^2 f'}{\partial \psi^2} = 0$$

Thus

$$\gamma^*(F^{D*}) = \frac{\partial^2}{\partial \varphi^2} \ln\left[1 + \frac{f^{**} - f'}{f^{**}}\right] + \frac{\partial^2}{\partial \psi^2}\left(f^{**} - f'\right)$$

and we can say that the method [4.69] is applicable provided f' is chosen in such a way that both $(f^{**} - f')$ and $(f^{**} - f')/f^{**}$ are non-singular in the neighbourhood of the singularity. This clearly requires that f' very closely resemble the required solution f^{**}.

The major problem therefore lies in finding an analytic function f' whose behaviour we know to be exactly that of f^{**} at the singularity and very close to it elsewhere in the region in question.

4.4.3 The Stagnation Point Singularity.

In the case of this singularity,whether the flow be around a sphere or a disc,one obvious function must closely resemble the exact solution,namely a Dirichlet flow of the same type. As will be seen later the actual Dirichlet solution taken can be adjusted to fit,at any stage in the iterative solution,the actual flow as closely as possible. But it will ,of course,

obey the differential equation,the boundary conditions, the type of singularity and the flow at the singularity exactly . It must be mentioned at this stage that this singularity is of type one , a discontinuity in the first derivative,as was demonstrated in section 3.3.3. It is therefore a "strong" singularity and ,were not a special treatment provided,would make nonsense of the solution obtained in this region if not in the rest of field. The derivation and application of the extra-residuals was as follows :

[1] The coordinates φ/U and Ψ/U are known at every point in the mesh. (Equations [4.6a] and [4.3] respectively) Thus we can solve either [3.24] or [3.25] ,the Dirichlet flows around a sphere and a disc, provided R (or C) is known. The resultant solution,f' $(=r^2)$ would be dependent only on the additional variable , R (or C) , which is initially unknown. For reasons given below, it is more convenient to exchange the variable R (or C) for <u>one</u> of the results,f'. The particular result chosen was that for the point E* (figure 4.6b) in both cases.

Thus at any point in the solution the relevant analytic function,f',is that for which $f'_{E*} = f_{E*}$ and the variable R (or C) is discarded.

The reason for this interchange becomes apparent when we consider that it is required to match the Dirichlet and actual solutions only in the immediate vicinity of the stagnation point. Thus the converged results may be better matched in this region by a Dirichlet solution

whose equivalent "R" is different from the actual radius of the sphere obtained for the cavitating flow. Clearly this is even more relevant in the case of the disc.

[2] The second step involves the substitution of the relevant analytic solution, f', into the left hand side of the field equation to be applied at each point, be it [4 18] , [4 20] or [4 21]. The result obtained for each point is the extra-residual for that point, $Z_{j,k}$. The $Z_{j,k}$ values should, of course, be largest at the points immediately surrounding the singularity, tending to the negligible the further removed (j,k) is from that point. In fact, the limit of the points to which treatment must be given is best determined by the condition that for points outside this region the $Z_{j,k}$ values are negligible. (See section 5.5.3 .)

[3] Thus, knowing $Z_{j,k}$ for all the surrounding points these values are used as extra-residuals when the field equation is applied there ; that is to say in the manner of [4.68].

It would be laborious in the extreme to carry out this process, including the difficult solution of the Dirichlet flow, every time the value f_{ϵ^*} altered. A simpler procedure was found to serve equally well. Initially, using the approximate formulae of section 4 1 6 a rough estimate of the final value of f_{ϵ^*} can be obtained. Two values of f'_{ϵ^*} close to this are taken from which two sets of Z values are calculated. It is then a simple task to interpolate between these two sets

according to the value of f_{E^*} at any stage. The Z sets may be altered at some interval if the original estimate of f_{E^*} was insufficiently accurate. This, then, was the procedure used.

However, special attention besides the treatment given above, is required at the point E^*; here, as mentioned in sections 4.2.5 and 4.2.6 we cannot apply the normal form of the field equation since this would involve the logarithm of zero. A number of approaches could be made to this problem; the author decided to apply the alternative, though normally less accurate form, [4 20], of the field equation with the relevant extra-residual i.e. In the case of the disc it becomes :

$$[4\ 71] \qquad -4\left(\frac{m}{n}\right)^2 \frac{f_0}{f_1 + f_0} + 4f_2 - 0.5f_{10} - 3.5f_0 = Z_{E^*}$$

An alternative was to apply the simple relations which exist in the Dirichlet solution between the values at E^* and E^{**}. From section 3.3.3 we have

$$[4\ 72] \text{ For the Disc : } f_{E^*} = \frac{1}{2} \cdot f_{E^{**}} + \frac{\pi}{4}\left(\frac{n}{U}\right)^2$$

$$[4\ 73] \text{ For the Sphere: } f_{E^*} = \frac{1}{2} \cdot f_{E^{**}} + \frac{4}{9}\left(\frac{n}{U}\right)^2$$

Obviously an extra-residual is not required in this case.

The latter equations were used in the rougher solutions, since they proved more stable. In the final solutions for the sphere the difference between the values found using the two methods was negligible, though for the disc it was greater.

4.4.4 The Separation Point Singularities.

The expansions used in section 4.3.6 will form the basis of the analytic function , f',in the neighbourhood of the separation point. The extra-residuals will be seen to be directly proportional, as a first approximation , to the coefficient of the first odd half-power term ; that is to say to K_1,K_2 and K_3 in the case of the disc and K_1^*,K_2^* and K_3^* in the case of the sphere.

However , unlike the front stagnation point , the singularities at the separation point are comparatively weak. In the case of abrupt we have a type two , and in the case of smooth separation a type three singularity. This implies that the range of points at which we must apply some sort of correction will be smaller than the equivalent range for the stagnation point. In fact it was found that the only corrections which were neccessary in both cases were those to finite difference forms of derivatives which included the value at the separation point , 0 of figure 4.9 .

In the following two sections we will deal separately with abrupt separation from the disc and smooth separation from the sphere. The extra-residuals which will be obtained are those for use with the field equation or relevant boundary type , though corrections for other derivatives used in calculating results from the final field will be required. Since , however , the procedure is the same in any case it will suffice to deal only with that one example.

FIGURE 4.9

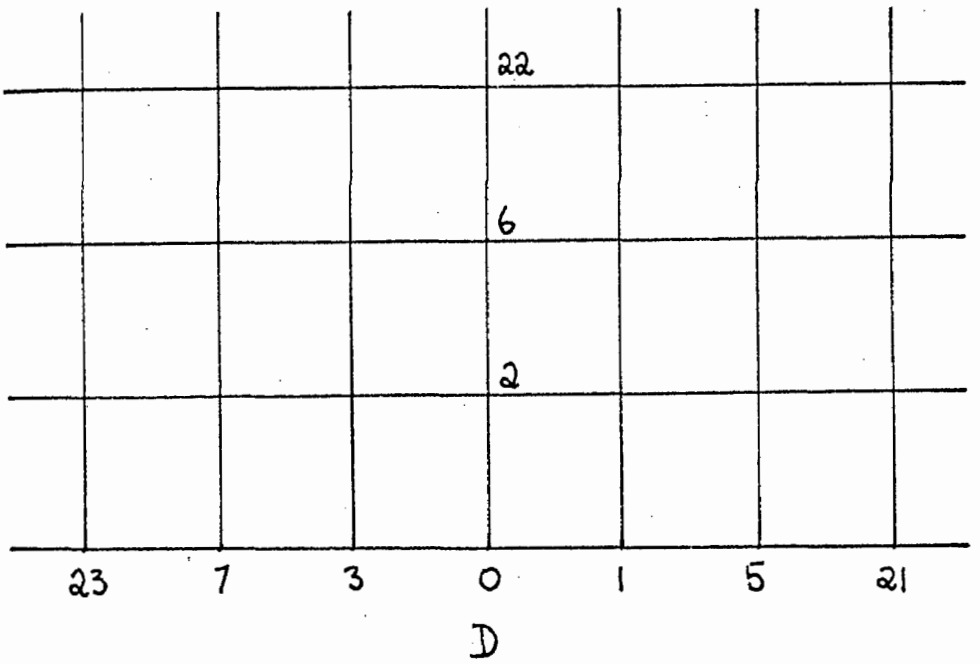

Separation
Point.

4.4.5 Abrupt Separation from the Disc.

The procedure outlined in section 4.4.1 will be followed. Refering to figure 4.9 and considering first the point 3 , from the expansion [4.61] it is found that, analytically ,

$$n^2\left(\frac{\partial^2 \ln f}{\partial \varphi^2}\right)_3 = \frac{3}{4} K_3 \left(\frac{n}{q_c}\right)^{\frac{3}{2}} + 2 A_3 \left(\frac{n}{q_c}\right)^2$$

Normally we used the finite difference approximation

$$n^2\left(\frac{\partial^2 \ln f}{\partial \varphi^2}\right)_3 = \ln \left(\frac{f_0 f_7}{f_3^2}\right)$$

But using the expansion [4.61]

$$\ln \left(\frac{f_0 f_7}{f_3^2}\right) = (2\sqrt{2} - 2) K_3 \left(\frac{n}{q_c}\right)^{\frac{3}{2}} + 2 A_3 \left(\frac{n}{q_c}\right)^2$$

[In these equations n/q_c and m/q_c will be given by the same identities as in section 4.3.7]

Then we find that for this derivative the extra-residual is given by

$$n^2 \left(\frac{\partial^2 \ln f}{\partial \varphi^2}\right)_3 - \ln \frac{f_0 f_7}{f_3^2} = \left[\frac{3}{4} - (2\sqrt{2} - 2)\right] K_3 \left(\frac{n}{q_c}\right)^{\frac{3}{2}}$$

Thus the extra-residual which we will use at the point 3 in the application of the field equation at that point will be

[4.74] $$Z_3 = - 0.07842712 K_3 \left(\frac{n}{q_c}\right)^{\frac{3}{2}} \left(\frac{m}{n}\right)^2$$

No first derivatives are estimated at this point so no other extra-residuals are required. Repeating the process for the point 1 we find $Z_1 = 0$ since the expansion [4.63] contains no 1/2 power term. This applies not only to the second derivative $\left(\frac{\partial^2 \ln f}{\partial \varphi^2}\right)_1$ but also to $\left(\frac{\partial f}{\partial \varphi}\right)_1$ which must also be estimated at this point. At the point 2 the extra-residual comes from the derivative $\frac{\partial^2 f}{\partial \psi^2}$ rather than $\frac{\partial^2 \ln f}{\partial \varphi^2}$, but otherwise the procedure is similar.

$$[4.75] \qquad Z_2 = m^2\left(\frac{\partial^2 f}{\partial \psi^2}\right)_2 - (f_0 + f_6 - 2f_2)$$

$$= \left[\frac{3}{4} - (2\sqrt{2} - 2)\right] K_2\left(\frac{m}{q_c}\right)^{\frac{3}{2}}$$

$$= -0.07842712\, K_2\left(\frac{m}{q_c}\right)^{\frac{3}{2}}$$

If the field equation at the point 6 includes the value at the point 0 a similar procedure is followed for that point.

It is noticeable that the difference between the two subtracting terms in any of these derivations is only one tenth , approximately , of the size of the terms themselves. This is indicative of the fact that the singularity is much weaker than that at the stagnation point.

4.4.6 Smooth Separation from the Sphere.

Taking the expansions , [4.64],[4.65] and [4.66] , and following the procedure used in the case of the disc it is easily shown that the extra-residuals for the second derivatives $\left(\frac{\partial^2 \ln f}{\partial \varphi^2}\right)_3$, $\left(\frac{\partial^2 f}{\partial \psi^2}\right)_2$, $\left(\frac{\partial^2 \ln f}{\partial \varphi^2}\right)_1$ are respectively :

$$[4.76] \qquad Z_3 = n^2\left(\frac{\partial^2 \ln f}{\partial \varphi^2}\right)_3 - \ln \frac{f_0 f_7}{f_3^2}$$

$$= \left[\frac{15}{4} - (4\sqrt{2} - 2)\right] K_3^*\left(\frac{n}{q_c}\right)^{\frac{5}{2}}$$

$$= 0.09314575\, K_3^*\left(\frac{n}{q_c}\right)^{\frac{5}{2}}$$

$$[4.77] \qquad Z_2 = m^2\left(\frac{\partial^2 f}{\partial \psi^2}\right)_2 - (f_0 + f_6 - 2f_2)$$

$$= 0.09314575\, K_2^*\left(\frac{m}{q_c}\right)^{\frac{5}{2}}$$

$$4.78] \qquad Z_1 = n^2 \left(\frac{\partial^2 \ln f}{\partial \varphi^2}\right)_1 - \ln \frac{f_0 f_5}{f_1^2}$$

$$= 0.09314575 \; K_1^* \left(\frac{n}{q_c}\right)^{\frac{5}{2}}$$

The two terms within the larger bracket of [4.76] give an idea of the relative magnitudes of the terms resulting from the analytic and finite difference factors. Due to the very weak singularity (type 3) the numerical value of the extra-residual is less than 1/30 th of the two subtracting terms.

We must also insert extra-residuals for the first derivative estimations since at the points 1 and 3 , $\frac{\partial f}{\partial \varphi}$ is found using the value at the point 0.

$$[4.79] \qquad n \left(\frac{\partial \ln f}{\partial \varphi}\right)_3 - \frac{1}{2} \ln \frac{f_0}{f_7} = (2\sqrt{2} - 2.5) \; K_3^* \left(\frac{n}{q_c}\right)^{\frac{5}{2}}$$

$$[4.80] \qquad n \left(\frac{\partial \ln f}{\partial \varphi}\right)_1 - \frac{1}{2} \ln \frac{f_5}{f_0} = -(2\sqrt{2} - 2.5) \; K_1^* \left(\frac{n}{q_c}\right)^{\frac{5}{2}}$$

The simple derivatives are easily found by multiplying by f_3 and f_1 respectively.

4.5 SUMMARY OF OPERATIONS AND SOME REFINEMENTS.

4.5.1 General.

In this section we will summarize the operations involved in the internal and external iterations. These terms are used to denote the field iterations carried out between the boundary changes and the boundary changes themselves , respectively.

Mention will also be made of some refinements made to speed the convergence of the processes.

Whereas , it is very difficult to anticipate the convergence of the method as a whole , some simple experiments can be carried out to test the convergence of the internal procedure when applied to a fixed boundary value problem. This also enables us to find an optimum over-relaxation factor (see section 4.3.3) which to use in the internal iterations. Some simple tests carried out by the author with various nets and field equations can be found in section 5.2 .

4.5.2 The Internal Iteration.

It is perhaps self-evident that the internal operation be given as much freedom as possible and yet still retain stability and convergence. Thus , for example it was found perfectly satisfactory to relax the points on the wetted surface every internal iteration. It will be convenient to list the sequence of operations which constituted an internal field iteration :

[1] The points on the wetted surface , up to $k = k_s - 1$, were relaxed with any relevant extra-residuals.

[2] The process of solution at the separation point was carried by the methods indicated in section 4.3.7 , giving new values of f_{k_s} and $(f_{k_{s+1}} - f_{k_s})$ and therefore $f_{k_{s+1}}$.

[3] The values of d'_k , $k=k_s+1, k_s+2 \ldots K$ from the last boundary change were used to create new values on the free streamline. Thus the free streamline was moved bodily during each internal iteration according to the change in $f_{k_{s+1}}$.

[4] The extra-residuals at the stagnation point are adjusted to conform to the new value of f_{E^*} .

[5] All other points (i.e. points on all lines except $j = 0$) are relaxed.

As stated above, the object was to relax as many quantities as possible during each internal iteration while still retaining stability and convergence. The values of d'_k , $k = k_s+1, k_s+2, \ldots K$, of course retain the same value thoughout the internal operation. So also does c , as it is easily seen from equation [4.33] that it is a function only of d'_{K-1} and d'_K . Unfortunately it was found neccessary to carry out a similar process with a few other , but relatively minor quantities. Divergence took place unless these were only treated "occasionally." That is to say every five or ten internal iterations. In this way all were found to converge so that , merely for convenience , they were relaxed or changed only at the same time as the external iteration. The following were the quantities which had to be treated in this way.

[1] Two alternative procedures were given in section 4.4.3 for the treatment of the point E* (the first point on the wetted surface downstream of stagnation). If the first of these , [4.71] , was used and the point relaxed <u>every</u> internal iteration divergence took place. By retaining the same value at this point and altering only during an external iteration it was found that the value converged fairly rapidly. This may be due to the fact that by far the largest extra-residual is encountered

at this point. If, however, the second equations , [4.72] or [4.73], are used no such divergence took place and it was possible to alter f_{E^*} every internal iteration.

[2] A somewhat similar difficulty was encountered at the separation point. As a direct consequence of part [2] of an internal iteration , values are found for K_2, K_3 (or K_1^*, K_2^* and K_3^*). If these were immediately used in the calculation of new extra-residuals for the points surrounding the separation point , divergence often occured. If , however , these extra-residuals were only altered every external iteration convergence was achieved. Thus although K_2, K_3 (or K_1^*, K_2^* and K_3^*) varied with each internal iteration , the extra-residuals were only altered according to those values every external iteration.

Before the sequence of events occuring during an external iteration are listed three refinements to the method as it stands must be mentioned. These are given in the following 3 sections.

4.5.3 Linearization of the late Free Streamline Differences.

Here we will anticipate the numerical results of section 5.2.5 , in order to outline a harmful effect which arises and the steps taken to overcome it. In that section it will be demonstrated that under the present scheme of solution we get a "whiplash" effect at the end of the free streamline ; the latter part , during successive

boundary changes , tends to exhibit a weaving , oscillating motion , the position of the boundary BC oscillating about a certain position. This was deleterious to the convergence of the method. However it was noticed that if a diagram were drawn in which the d_k' differences were plotted against φ ,or the position of the point k , the mean of the oscillations was almost exactly a straight line,cutting the axis at the mean value of c. This "whiplash effect" only occured over the last five or six d_k' values. The obvious solution was to impose linearity on these last few d_k' values after each boundary change. This was done by linearizing the d_k' values from k = K - 5 ,say, to k = K. Thus in the calculation of c , the value found immediately after the boundary change (and therefore the value retained throughout the next internal solution) corresponded to the point of intersection of the mean straight line with the axis.

This was very successful in damping out the whiplash effect. Clearly , however , it is only justified if the ΔQ_k values on this linearized portion are able to approach zero in the solution. This was found to be the case. It is evidence of the well known fact that the shape of the free streamline close to the line of symmetry and remote from the separation point is very close to elliptic. (See Ref. 35 , for example.)

In fact it was found (see section 5.2.5) that providing the linearized portion is confined to points at which

$$\frac{\varphi_\infty - \varphi}{\varphi - \varphi_s} < 0.2$$

the method worked satisfactorily.

4.5.4 Adjustment of internal values following an external iteration.

The last refinement aided the convergence of the method as a whole ; the following is an aid to the internal solution.

The new values on the free streamline are generated immediately after each boundary alteration. To help the subsequent internal solution , the internal values can be roughly adjusted according to the change between the boundary values before and after the external iteration. If the difference is denoted by $\delta f_{0,k}$, then the author found the following change in the internal values reduced the neccessary number of subsequent internal iterations.

$$\delta f_{j,k} = \left[1 - \frac{(f_v)_j}{(f_v)_J} \right]^2 \delta f_{0,k} \quad , \quad k > k_s$$

where $j = J$ is the channel wall.

4.5.5 Alternate Points.

The density of equipotential mesh lines in the region near the wetted surface needs to be greater than elsewhere in the field. But as the mesh stands at present the same density occurs on the channel wall opposite the wetted surface. This is uneconomical and the programme was so written that on the streamlines, $j > J^*$, only alternate mesh points are used. This requires K to be odd. The limit J^* was a programme parameter.

4.5.6 The External Iteration.

The sequence of operations making up an external iteration can now be listed.

[1] The ΔQ_k values are calculated and the d'_k values adjusted accordingly by one of the methods indicated in section 4.3.6 . The following constraints are present.

(A) If the identity

$$d'_k < d'_{k-1} \quad \text{for} \quad n^*_k = n^*_{k-1}$$

is not obeyed then d'_k is set as follows

$$d'_k = 2d'_{k-1} - d'_{k-2}$$

and the programme prints the letter G. Normally once G occurs at a point it does so for all downstream points but this was found preferable to distorting the shape. It only occurs , in any case , during the early iterations.

(B) The author also inserted a maximum change constraint where

$$\left|(d'_k)^{i+1} - (d'_k)^i\right| < \alpha_2$$

This proved useful during the earlier iterations. It printed M when called into action.

[2] The linearized portion is confined to

$$K_L \leqslant k \leqslant K$$

where K_L is inserted as a programme parameter. The new d'_k values are printed out with the letters LIN. next the value d'_{K_L}.

[3] The fractional mesh length c is calculated. The value of K is adjusted so that c cannot be negative.

The following steps are separate :

[4] The separation point residuals are adjusted according to the values of K_2 and K_3 (or K_1^*, K_2^* and K_3^*).

[5] If , refering to section 4.4.3 , the first type of equation is used at the point E* then this point is relaxed.

[6] In the case of the sphere , the separation angle test equation is applied and the "test" value printed. It was unneccessary to do this every internal iteration. [Further comment on this testing of the separation angle is left until section 5.2.7 .]

4.5.7 Conclusion.

In this chapter a method has been developed for the solution of the axisymmetric cavitating flow problem. The methods described were those which were found to work. This could , in many cases , only be discovered by trial , many other methods having been developed only to be found wanting , usually through divergence.

The next chapter includes one of the programmes used , the results and other relevant computations. The author began his work with the Ferranti Mercury computer of the Oxford University Computing Laboratory; it was continued on their English Electric KDF9

CHAPTER 5

CHAPTER 5

5.1 MESH POINT DISTRIBUTIONS.

5.1.1 Streamline mesh point distribution.

In this and the next section the precise geometry of the mesh used is discussed. Comments on the equipotential mesh point distribution are contained in the next section.

In section 4 1.4 we defined the relative mesh length n* as n/ϕ_s Thus the relative mesh length between points on the wetted surface was $1/P$, P being the number of equally spaced points on that part of the boundary (DE of figure 5.1). In view of this , the number and spacing of points on the boundary FEDC (figure 5.1,5.2 from figure 4.1) and therefore the number and spacing on every streamline mesh line , will be outlined for both types of body.

[A] The Disc.

Intially P was chosen to be 8 in the case of the disc , but was later refined to 16. These 16 points were equally spaced in DE(figure 5.1). But using the recommended result of section 4.1.6 [3] :

$$\phi_L/\phi_s = 12$$

for the chosen value of X for the disc (1.5) , we clearly cannot use the same spacing in the entire interval EF without having an excessive number of points. Bearing in mind the alternate point treatment of section 4.5.5 , even numbers of equal

FIGURE 5.1 A Streamline Mesh Point Distribution For The Disc.

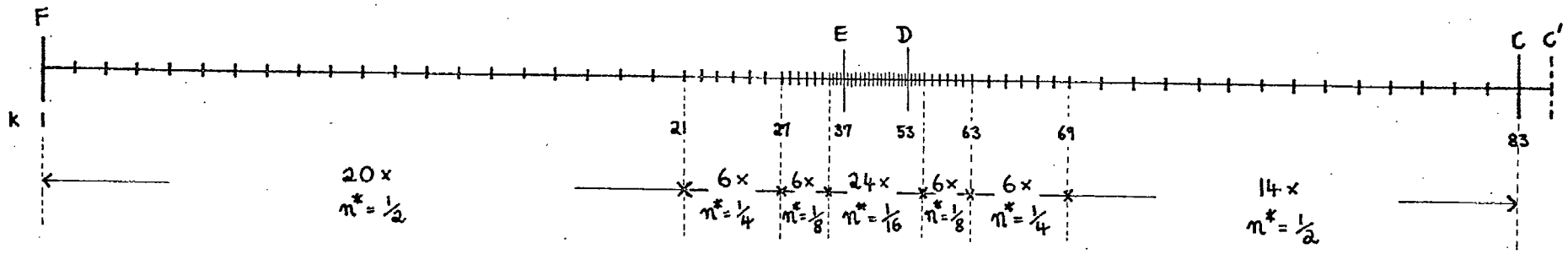

FIGURE 5.2 A Streamline Mesh Point Distribution For The Sphere.

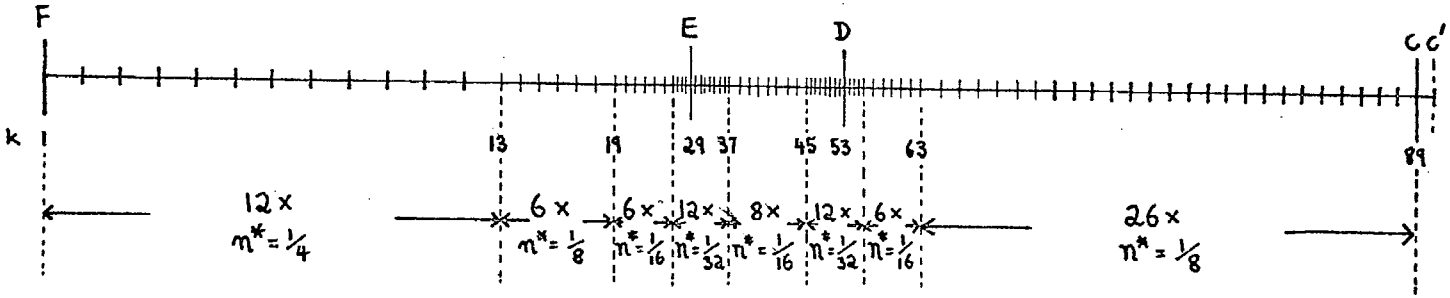

intervals are used and a suitable distribution (figure 5.1) designed for the interval EF. The maximum value of n* occuring is 1/2 and the minimum , 1/16 . This distribution in EF was used for all disc solutions. However the distribution on the free streamline part , DC , varied with cavitation number , although in all cases a similar type of design , to that in the interval EF , was used. Thus figure 5.1 was designed for Q = 0.5 where $\phi_F/\phi_S \simeq 8$. For cavitation numbers below 0.2 it was required to use the larger spacing , n* = 1 , in the interval DC in order that the total number of points per line was contained within the programming limit of 100. Note that $k_S = 53$.

[B] The Sphere.

The situation is slightly easier in the case of the sphere where , from section 4.1.6 [3] , ϕ_L/ϕ_S need only be of the order of 4 (X = 0.45). The cavities are shorter so that ϕ_F/ϕ_S is smaller than for the disc for the same Q . For example , $\phi_F/\phi_S \simeq 7.5$ for Q = 0.3 . The distribution chosen is shown in figure 5.2 , that particular free streamline distribution having been designed for Q = 0.3 . The distribution of the 24 points on the wetted surface was also different from that used in the disc. Normally $(n^*)_{MIN} = 1/32$ and $(n^*)_{MAX} = 1/4$ though for cavitation numbers below 0.3 , n* = 1/2 had to be used. Again $k_S = 53$.

5.1.2 Equipotential Mesh Point Distribution.

The number and spacing of points on a streamline was dictated by (i) the nature of the problem (ii) the neccessity of having a minimum number of points on the wetted surface and (iii) the limit to the total number of points per line. The consequent distributions are the fairly obvious types to choose. On the other hand the equipotential distributions are much more difficult.

It was found that in order to get any reasonable rate of convergence per unit time , it was neccessary to limit J to something of the order of 15. (See section 5.2) In section 4.1.6 the X values for the disc and the sphere (1.5 and 0.45 respectively) were chosen in such a way that the resultant f_S values would be close to unity. Clearly , then , $(f_U)_{j=1}$ must be considerably less than unity. The value eventually taken was 1/16. But in section 3.3.1 it was found that , for a given Q ,a minimum value of f_H/f_C existed given by equation [3.44]. Thus for a given f_S there is a minimum value which f_H must take in order that a solution exist. For Q = 0.3 ,for example, equation [3.44] gives $(f_H/f_C)_{MIN} \simeq 8.15$. Thus , if we say $f_C = 2f_S$, then this implies that the limit occurs at about $(f_H)_{MIN} = 16.3$. Comparing this with the chosen value of $(f_U)_{j=1}$ it is clear that massive grading is required in the Ψ direction. Figures 5.3 and 5.4 show two alternative schemes , with the field equations which would be applied on each line. Both are investigated for convergence in the next section. The former was chosen in view of the convergence / unit time it gave for both the internal and external iterations.

Equipotential Mesh Point Distributions.

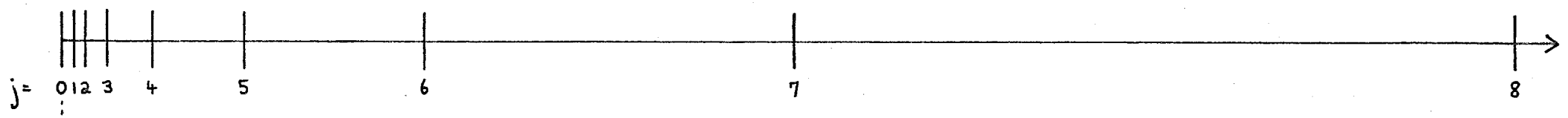

FIGURE 5.3 Distribution uses field equations [4.18] at j = 0,1,2 , [4.21] for j > 2

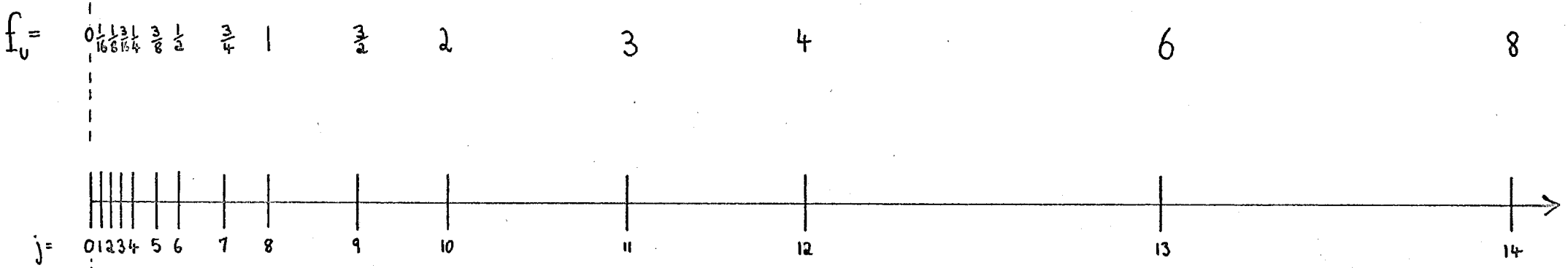

FIGURE 5.4 Distribution uses the field equation [4.18] for all j .

It must be borne in mind that , since $f = r^2$, the relative spacing is less drastic in the physical plane.

The design criterion of the error distribution also showed that the extra accuracy involved in the use of the distribution 5.4 did not warrant the much greater time required to find a solution.

5.2 CONVERGENCE.

5.2.1 Test Meshes and Equations.

The matrix $[E]$ of section 4.3.3 is clearly of the same size as the matrix $[M]$ of section 4.3.4 for a given net. Thus the same problems of space and time arise. However , by carrying out convergence tests on much smaller , but similar , nets , we will hope to anticipate the convergence of the internal iterations.

As mentioned in section 4.5.1 , it is almost impossible to predict the convergence of the method as a whole. This can only be discovered by actually carrying out the solutions. The convergence of the internal iterations can , however , be investigated by considering the same equations and type of mesh applied to a fixed boundary value problem. In the following sections the results given are for the convergence of this type of problem.

The eigenvalue , $|\lambda|$, is found for each matrix $[E]$ set up , by the simple method of continuous

multiplication starting with a random vector. [See Ref.32, p.24] This is essentially the same process as that which takes place during relaxation since the initial guessed values have unknown , or random , errors. Thus, if $\{b\}^0$ is a random vector of the same dimension as $[E]$, we put

$$\{b\}^{i+1} = [E]\{b\}^i$$

The ratios of corresponding elements in $\{b\}^{i+1}$ and $\{b\}$ should converge to the required eigenvalue , λ .

The matrix $[E]$ is given by equation [4.42] , where the elements are determined from equation [4.46] or the corresponding equation for the other form of the field equation , [4.21]. Taking [4.46] as an example , it is clear that the elements are functions of f_0^{i+1} , f_1^i and f_3^i , which are unknown. In order to carry out this investigation we will assume that these can be replaced by their upstream values , f_U, without serious error. These values are known for a given equipotential mesh point distribution (e.g. figure 5.3 or 5.4) , given the value for one streamline , say $(f_U)_{j=1}$.

All the test meshes will , for simplicity , have an equally spaced streamline distribution though the actual interval , n* , will be a variable. For a given equipotential distribution the variation of λ with the following quantities will be required :

(1) K and J , the dimensions.

(2) $(f_U)_{j=1}$. Therefore defines all other f_U values.

(3) X

(4) n*

However , by inspection of [4.46] , the number

of parameters can be reduced. It is clear from that equation , substituting $f_0 = f_1 = f_3 = f_U$,that only variation in $\frac{1}{f_U}\left(\frac{m}{n}\right)^2$ will effect the matrix $[E]$. Thus we define the parameter

[5.1] $$\eta = \left(\frac{m}{n}\right)^2_{j=1} \Big/ (f_U)_{j=1}$$

$$= X^2 (f_U)_{j=1} \Big/ (n^*)^2$$

using section 4.1.4. Thus η replaces the variables X, n* and $(f_U)_{j=1}$.

With nets for the Laplace and Poisson equations, it can be shown (See Ref. 39) that if one dimension (K in this case) is much larger than the other (J) , the variation of $|\lambda|$ with K is small compared with that with J. In that case , $|\lambda|$ is given by

[5.2] $$|\lambda| = \frac{1}{4}\left[\cos\frac{\pi}{K} + \cos\frac{\pi}{J}\right]^2$$

Thus the problem will reduce to finding the variation of $|\lambda|$ with η and J , with a few tests to show the relative unimportance of the variation with K.

5.2.2 Types of Mesh Investigated.

The field equation [4.18] gives the approximate error equation (from [4.46]) :

[5.3] $$e_0^{i+1}[2 + 2b\eta] = b\eta e_1^i + b\eta e_3^i + e_2^i + e_4^i$$

Where b is a multiplier depending on the value of j for a given equipotential distribution.

Similarly , the field equation [4.21] gives

[5.4] $$e_0^{i+1}\left[2 + \frac{4}{3} b\eta\right] = b\eta\, e_1^i + b\eta\, e_3^i + \frac{20}{21} e_2^i - \frac{8}{3} e_4^i + \frac{64}{21} e_{12}^i$$

In both cases the factors $[2 + 2\, b\eta]$ and $[2 + 4\, b\eta/3]$ correspond to the derivatives , $\frac{\partial Y_0}{\partial f_0}$, used in equation [4.39] when relaxing a point.

Three types of matrix $[E]$ were investigated.

Type [A] The form given using the equipotential distribution of figure 5.4 with the error equation [5.3] (E1) since only the field equation [4.18] is used with that distribution.

Type [B] The form given using the equipotential distribution of figure 5.3 with the relevant error equation , [5.3] or [5.4] , at every point.

Type [C] As type [B] except that where the error equation [5.4] is used the factor $[2 + 4b\eta/3]$ is replaced by $[2 + 2b\eta]$. This corresponds to using the value of $\left[10.5 + 10.5 \left(\frac{m}{n}\right)^2 \frac{1}{f_0}\right]$ as $\frac{\partial Y_0}{\partial f_0}$ in the relaxation process rather than $\left[7 + 10.5 \left(\frac{m}{n}\right)^2 \frac{1}{f_0}\right]$ at points at which the field equation [4.21] is applied. The reasons for this substitution will become apparent in section 5.2.4.

5.2.3 The Over-Relaxation Factor , ω .

Thus far , we have referred only to a relaxation process in which $\omega = 1$. (See section 4.3.3) If ω is non-zero then the rate of convergence , λ^* , is given by

[5.5] $$1 - \lambda^* = \omega\,(1 - \lambda)$$

It is now relevant to discuss the differences occuring in the behaviour of the relaxation process with variation in ω . This can be compared with the response of a position control system to a step input where the damping corresponds to $1/\omega$. Thus $\omega = 0$ gives no change in any of the values. As ω increases the rate of approach to the correct position gradually increases. An "optimum" value of ω , denoted by ω_0 (e.g. Ref. 39) , is the maximum value at which no overshoot or oscillation of the dependent variable values occurs. For ω greater than ω_0 the process oscillates but may still converge unless ω is greater than another critical value above which convergence never takes place. Russell (Ref. 39) recommends , for Laplace and Poisson equations , that ω should take a value smaller than ω_0 rather than larger for reasons of convergence.

In some tests carried out with each of the types , [A],[B],[C] , ω was varied to observe these effects. Oscillation of values invariably first occured on the line $j = 1$ as ω was increased , though the value varied both with η and with type. In the solutions for the major problem it was found these oscillations on $j = 1$ had a serious effect on the convergence of the method as a whole since they effected the ΔQ_k values. This implied that a value of ω not greater than ω_0 had to be used. The value of ω_0 was found to behave as follows.

[1] It increased with η . Thus the ω_0 which was used in any solution was that for the minimum η occuring in the mesh. The minimum η occurs at the extremes of the streamline distribution where n* takes its

maximum value.

[2] It varied considerably with type.

[3] It did not depend appreciably on the dimensions K and J.

These variations are demonstrated in figure 5.6 , though the actual values are only roughly correct. On average , these values are lower than those permissable in Laplace and Poisson fields.

In the actual solutions carried out the following minimum values of η occured :

[1] Disc

$(f_v)_{j=1} = 0.0625$, $X = 1.5$, $(n^*)_{MAX} = 0.5$

then $(\eta)_{MIN} = 0.5625$

or if $(n^*)_{MAX} = 1.0$ then $(\eta)_{MIN} = 0.140625.$

[2] Sphere

$(f_v)_{j=1} = 0.0625$, $X = 0.45$, $(n^*)_{MAX} = 0.25$

then $(\eta)_{MIN} = 0.2025$

or if $(n^*)_{MAX} = 0.5$ then $(\eta)_{MIN} = 0.050625$

5.2.4 Conclusions of Convergence Tests.

Clearly the relevant comparison between the results for type [A] and those for [B] and [C] are for the same f dimension of the field , namely f_H. Thus K = 10, J = 10 in type [A] corresponds to K = 10, J = 6 for types [B] and [C]. Figure 5.5 shows the results of a logarithmic plot of $|\lambda|$ against η using the types indicated and the dimensions , (K × J). In passing it may be remarked that these values are substantially

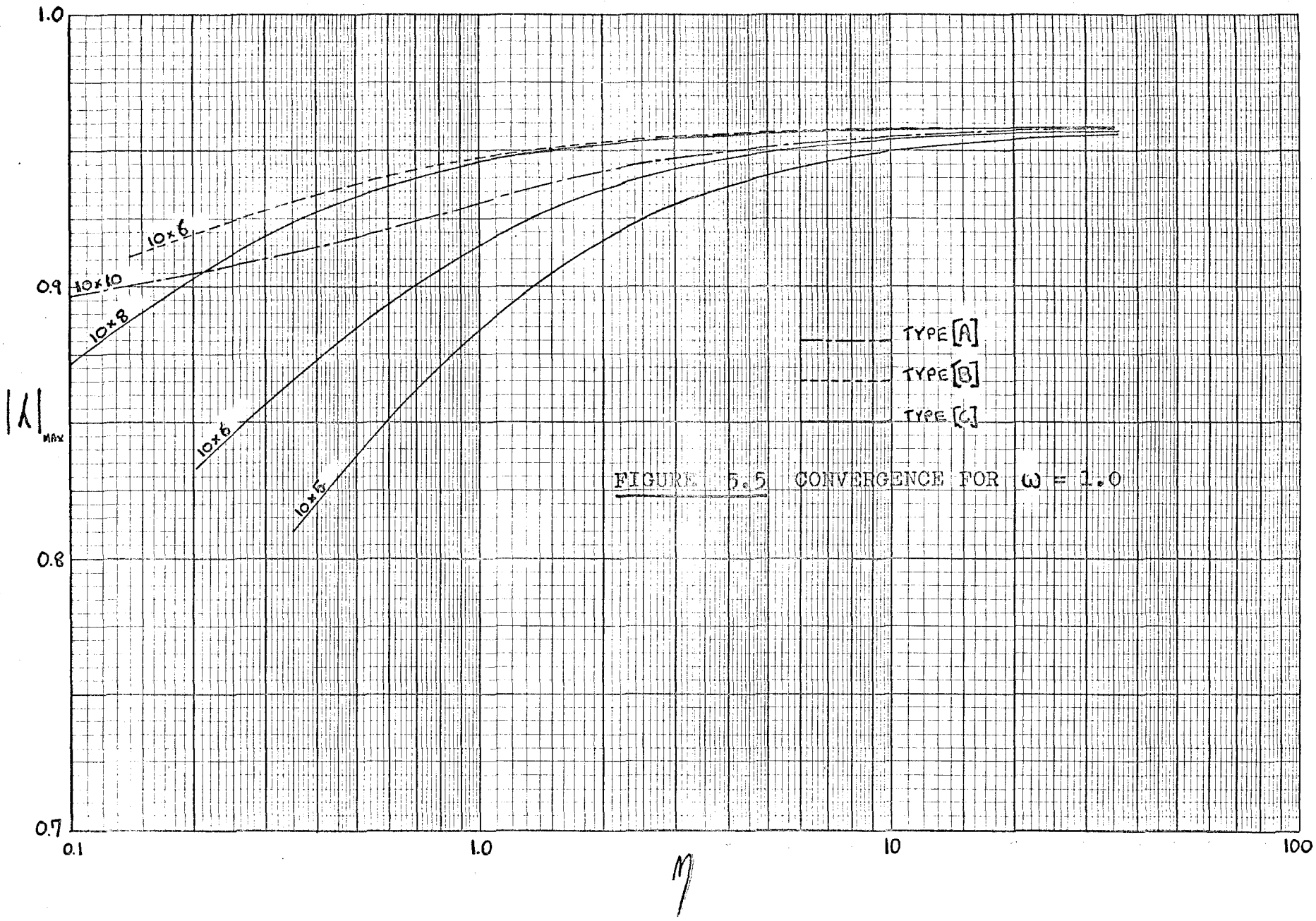

FIGURE 5.5 CONVERGENCE FOR $\omega = 1.0$

FIGURE 5.6 ROUGH RELATION BETWEEN ω_o AND η FOR THE THREE TEST MESH TYPES.

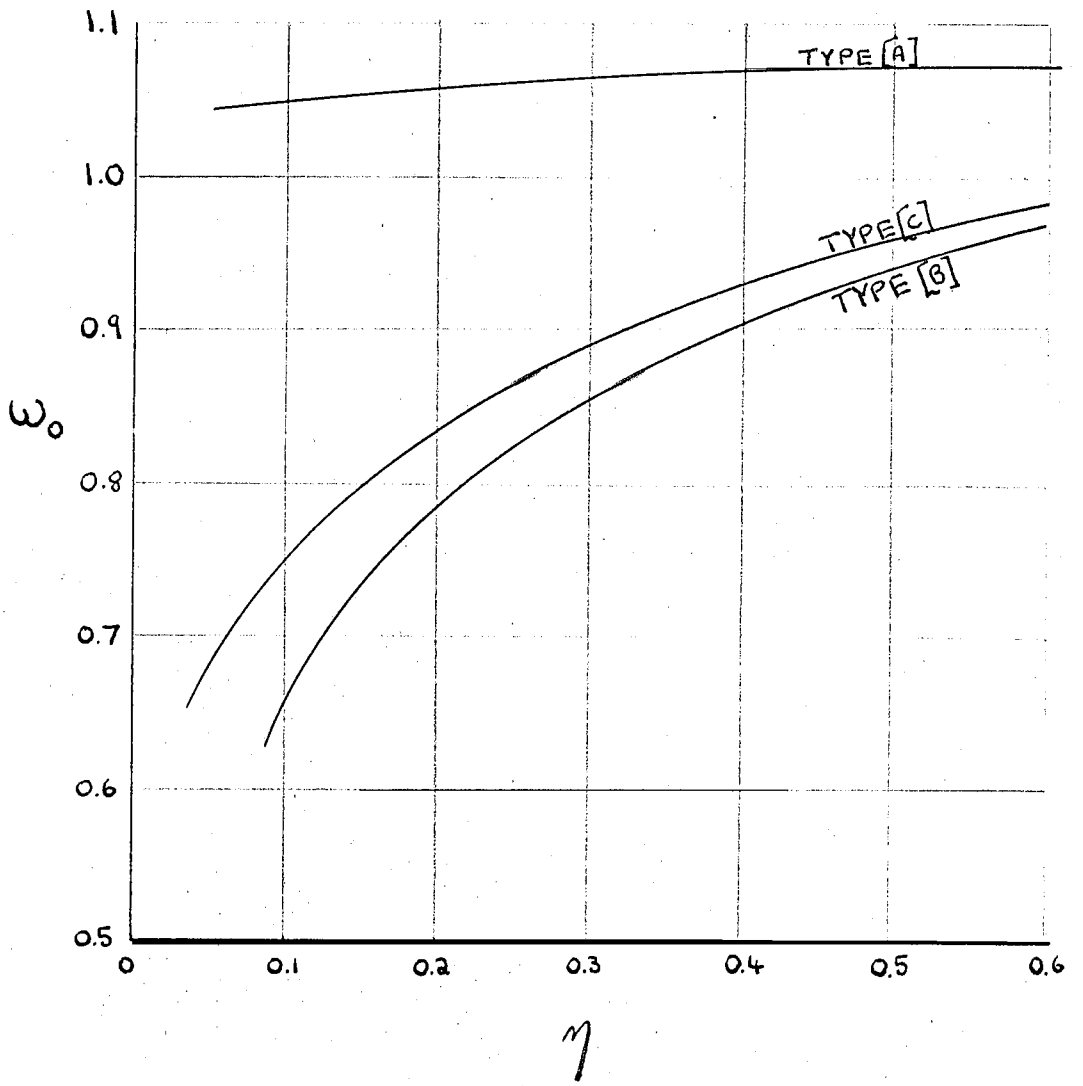

larger than those calculated from [5.5] for Laplace and Poisson fields.

From this graph we can draw the conclusion that the worst convergence rate occurs at the maximum η present in the problem ; that is to say in the region of minimum n*. For the disc , $(\eta)_{MAX} = 36$ and for the sphere $(\eta)_{MAX} = 3.24$. The value of $(\lambda)_{MAX}$ varies little with J or the type used.

However in order to compare the convergence per unit time of the three types two additional factors must be taken into account.

[1] The ω which is , or must be , used.

[2] The computer time taken for one complete field iteration. This is clearly greater for type [A] since a larger number of points must be used for a given f_μ and same $(f_v)_{j=1}$.

We will use , N , suggested by Russell (Ref. 39) to denote the number of iterations required to reduce the errors , e , through a decade.

[5.6] $$N = \frac{\ln(0.1)}{\ln(|\lambda|)}$$

Clearly from figure 5.5 , type [C] is preferable to type [B]. This also follows from figure 5.6 where a smaller ω is required for [B] than for [C] , thus reducing the rate of convergence. Comparing [C] and [A] , it is apparent from figure 5.5 that $(|\lambda|)$ is virtually the same (0.957) in each case. However , it follows from figure 5.6 that a larger ω may be used in type [A] than in type [C]. Thus for example ; for $(\eta)_{MIN} = 0.2$, using figure 5.6 and equations [5.6] and [5.5] :

the number of iterations to reduce the error by 5 times

in type [A] = 35 (with ω = 1.05)
the number of iterations to reduce the error by 5 times
in type [B] = 45 (with ω = 0.80)
But the ratio of the times required for one iteration will be approximately in the ratio of the total number of mesh points , in this case 60 / 100 . Thus a much better convergence / unit time is acheived with type [C]. This is true throughout the range of $(\eta)_{MIN}$ given above and encountered in the actual solutions.

In view of the results of this investigation the number of internal iterations to be carried out between each external iteration could reasonably be of the order of 30. This number and the type [C] were therefore used in the actual solutions , the former since a reduction of the errors , $\{e\}$, by about 5 times gave significant changes in the ΔQ_k values. (See section 4.3.5)

5.2.5 Comparison of the Methods for the External Iteration.

Two approaches to the treatment of the ΔQ_k residuals and the consequent changes in the d'_k values were given in section 4.3.6. Both involved the use of unknown parameters for which suitable values could only be found by trial and error , though the value of β to be used with the first method , once found , could be used universally.

The number of external iterations which are required before the values on the wetted surface and free

streamline converge is , of course , dependent on the accuracy of the initial guess. It was found desirable for the initial general shape of the cavity to be correct ; that is to say for the identities of section 3.2.4 to hold throughout the solution.

For the sake of an example a fairly bad guess is taken to the problem $Q = 0.5$, $f_H = 256$ for the disc. The following were the results obtained in some of the trials of the various methods using this example. It is important to realize that the optimum value of either β or α_1 (equations [4.54] and [4.55]) may vary with the over-relaxation factor employed and the number of internal iterations used between each external, since , referring to section 4.3.5 , the internal process is not taken to complete convergence. In view of the results of section 5.2.4 all the trials employed 27 internal iterations / external iteration and an ω of 0.9 .

[1] Method of equation [4.54].

Simple initial tests showed that the value of β in this method had to be less than unity. With $\beta = 0.2$ the variations in f and Q_R on the free streamline for successive external iterations is shown in figures 5.7 and 5.8 respectively. [In these graphical representations only the initial iterations are shown for the sake of clarity. The successive iterations are numbered in the graphs.] From this and other tests , specifically with $\beta = 0.4$ and 0.1 , the following points emerged :

(A) That the values of f converged much more rapidly than the values of Q_R and the oscillations in the

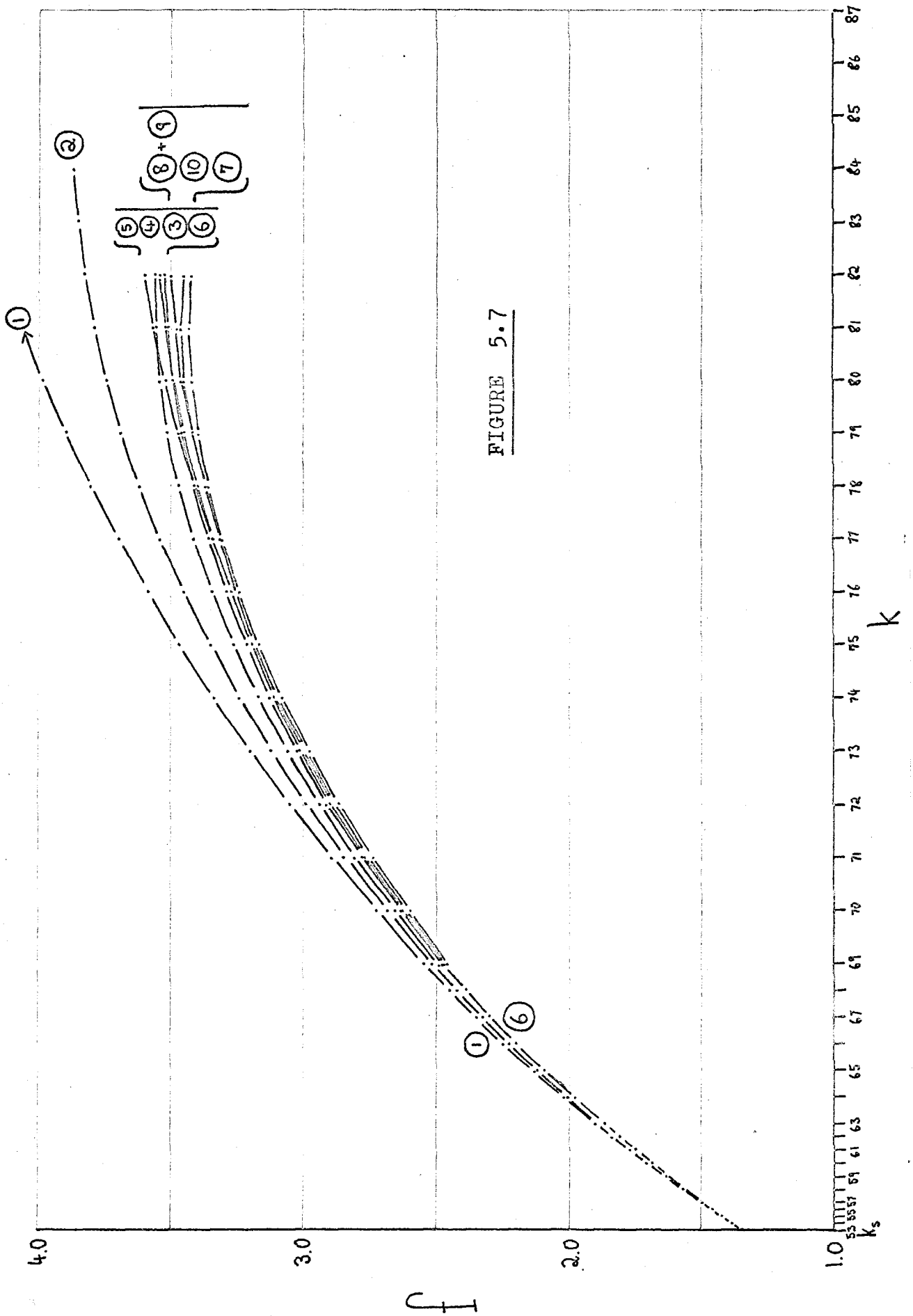

FIGURE 5.7

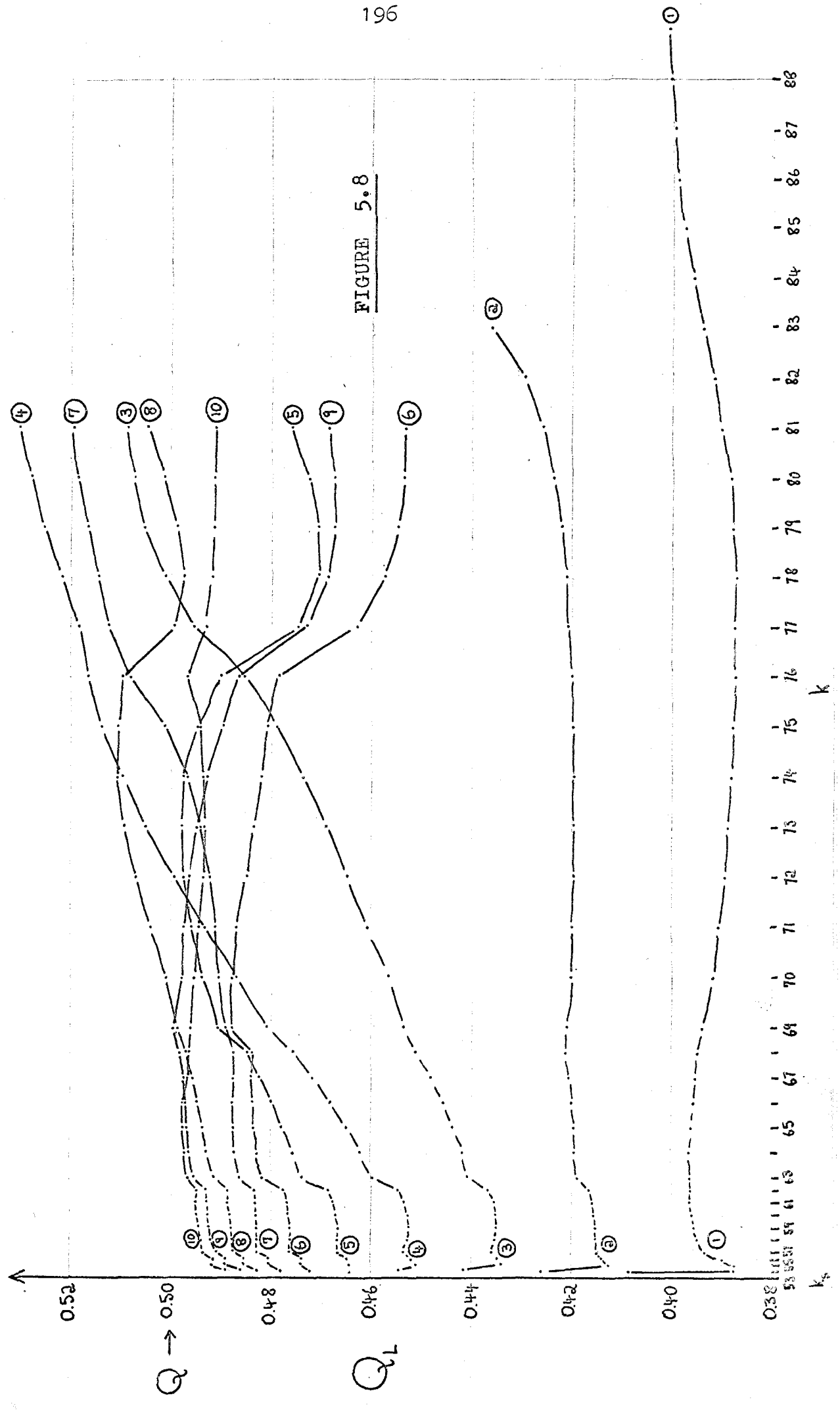

FIGURE 5.8

downstream Q_R values were only mirrored by small oscillations in the downstream f values. This is the whiplash effect mentioned in section 4.5.3 . The effect is damped considerably by the method outlined in that section and employed in all these trials.

(B) From figure 5.8 it is clear that for $\beta = 0.2$ the upstream values of Q_R are monotonically converging while the downstream values are oscillating about the required value. For larger β (0.4) the convergence of the upstream values was more rapid, but the downstream oscillations more dramatic with consequent deterioration in the rate of convergence. With smaller β (0.1) these trends were reversed.

(C) It was also found that , in general , the downstream values converged last , since change in the upstream values led to downstream changes as anticipated in section 4.3.6. It was therefore advisable to obtain reasonably rapid convergence of the upstream values in order to hasten the complete convergence.

In anticipation of tests on the second method of section 4.3.6 the converged values of $-\frac{\partial d'_R}{\partial \Omega Q_R}$ for each point are plotted against position on the φ axis in figure 5.9. (shown by dotted line)

[2] Method of equation [4.55].

Clearly one required modification of the first method would be to use different values of β along the free streamline ; thus β would take values larger at points upstream than at points downstream ,

FIGURE 5.9

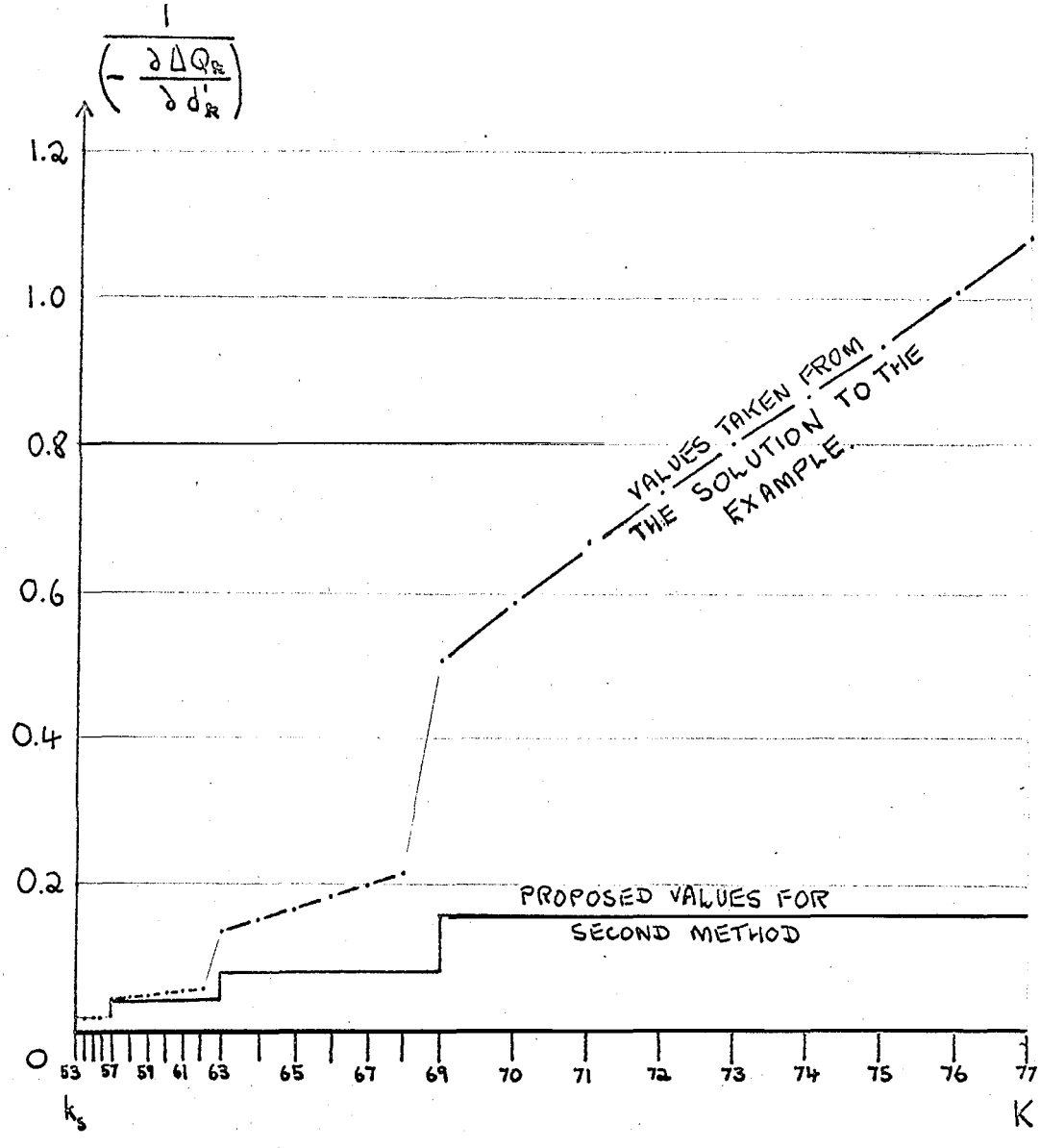
$\frac{1}{\left(-\frac{\partial \Delta Q_k}{\partial d'_k}\right)}$
1.2
1.0
0.8
0.6
0.4
0.2
0
VALUES TAKEN FROM THE SOLUTION TO THE EXAMPLE.
PROPOSED VALUES FOR SECOND METHOD
53 57 59 61 63 65 67 69 70 71 72 73 74 75 76 77
k_s
K
k

giving better overall convergence. The form of the curve plotted in figure 5.9 suggested that this could be done simply by replacing that curve by the function $\alpha_1 (n^*_k P)$, shown by full lines for $\alpha_1 = 0.02$. Comparison of equations [4.54] and [4.55] shows that the factor $-\beta\left(\frac{\partial d'_k}{\partial \Delta Q_k}\right)$ in the former method is replaced by $\alpha_1 (n^*_k P)$ in the latter ; hence the reason for the apparently more empirical second method. The value of α_1 which corresponds , in this example , to $\beta = 0.5$ would therefore be 0.01. Figures 5.10 and 5.11 show the resultant effect on the f and Q_k values of using the second method with $\alpha_1 = 0.007$. The following comments could be made :

(A) The upstream Q_k values can be made to converge much more rapidly than with the first method since the violent oscillations no longer occur in the downstream values.

(B) In comparing the two graphs 5.8 and 5.11 the following fact , which is difficult to represent there , must be taken into account. In further iterations , the oscillations of 5.8 persist for some time, whereas the ΔQ_k values of 5.11 converge to a better accuracy after a couple of slow oscillations ; this is the feature which makes the second method more efficient despite the relative sluggishness of the earlier iterations.

(C) This sluggishness in the downstream values is caused , presumably , by the carried-over effect of the upstream changes. Thus the upstream values converge first.

(D) Comparison of the figures 5.7 and 5.10 shows that there is little appreciable difference in the more

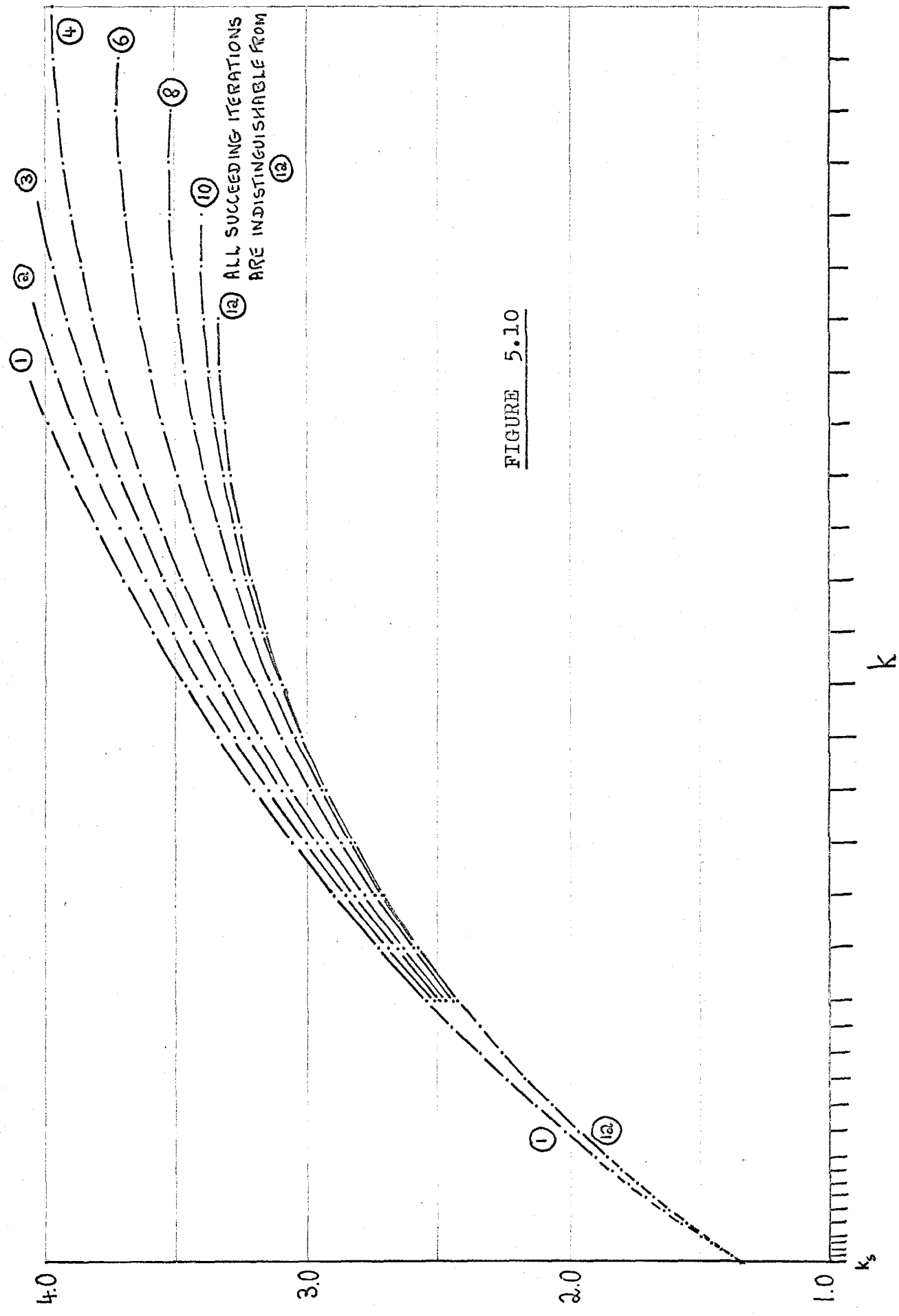
4.0
3.0
2.0
1.0
f
k
k_s
①
①a
②
③
④
⑥
⑧
⑩
⑫
⑫a ALL SUCCEEDING ITERATIONS ARE INDISTINGUISHABLE FROM

FIGURE 5.10

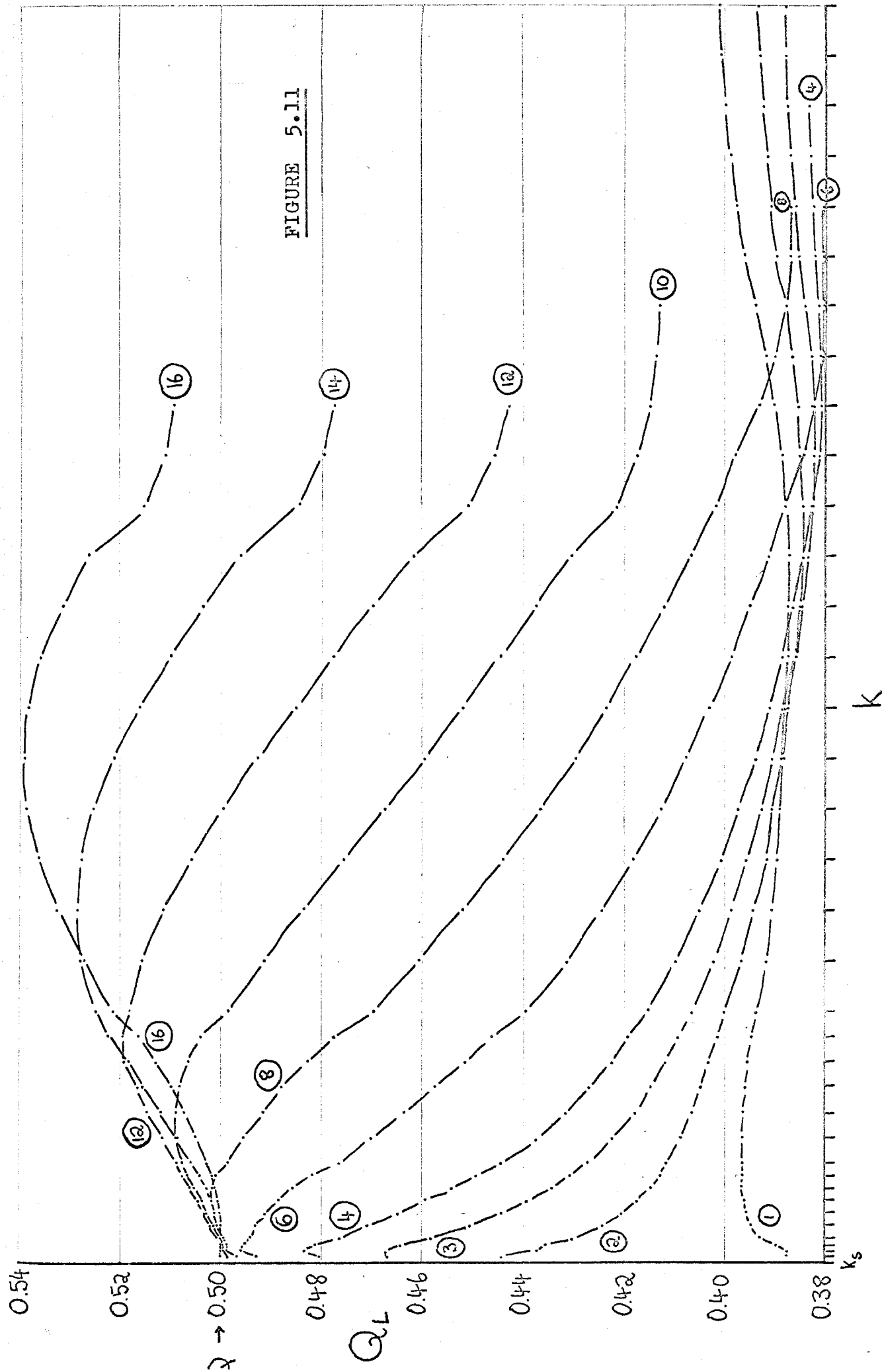

FIGURE 5.11

rapid convergence of the f values except for the whiplash effect in the former ; if anything , the convergence of the second method is more rapid and certainly more satisfactory.

(E) A limit on the value permitted for α_1 was discovered as follows. On increasing α_1 the convergence of the second method improved until an optimum value was reached above which the deleterious whiplash effect was again observed. The optimum value of α_1 varied with cavitation number and between the two types of solution carried out , for the disc and the sphere. Figure 5.12 shows the approximate optimum values used in the solutions.

Other more involved methods and functions giving β as a function of k were tried but failed to improve to any noticeable extent on the second method.

An incidental result of these tests was some correlation of the errors , ΔQ_k , to the errors in f. It is clear from both the tests presented that after the early iterations (say 10) further 10 per cent changes in the Q_k values produce less than one per cent change in the f values. A proper estimate of this correlation is however complicated by the fact that the internal iterations are not taken to complete convergence and the fact that an error , ΔQ_k , at an upstream point (where these are smallest in the final solution) may have a different effect than an error at a downstream point.

FIGURE 5.12

OPTIMUM VALUES OF α_1

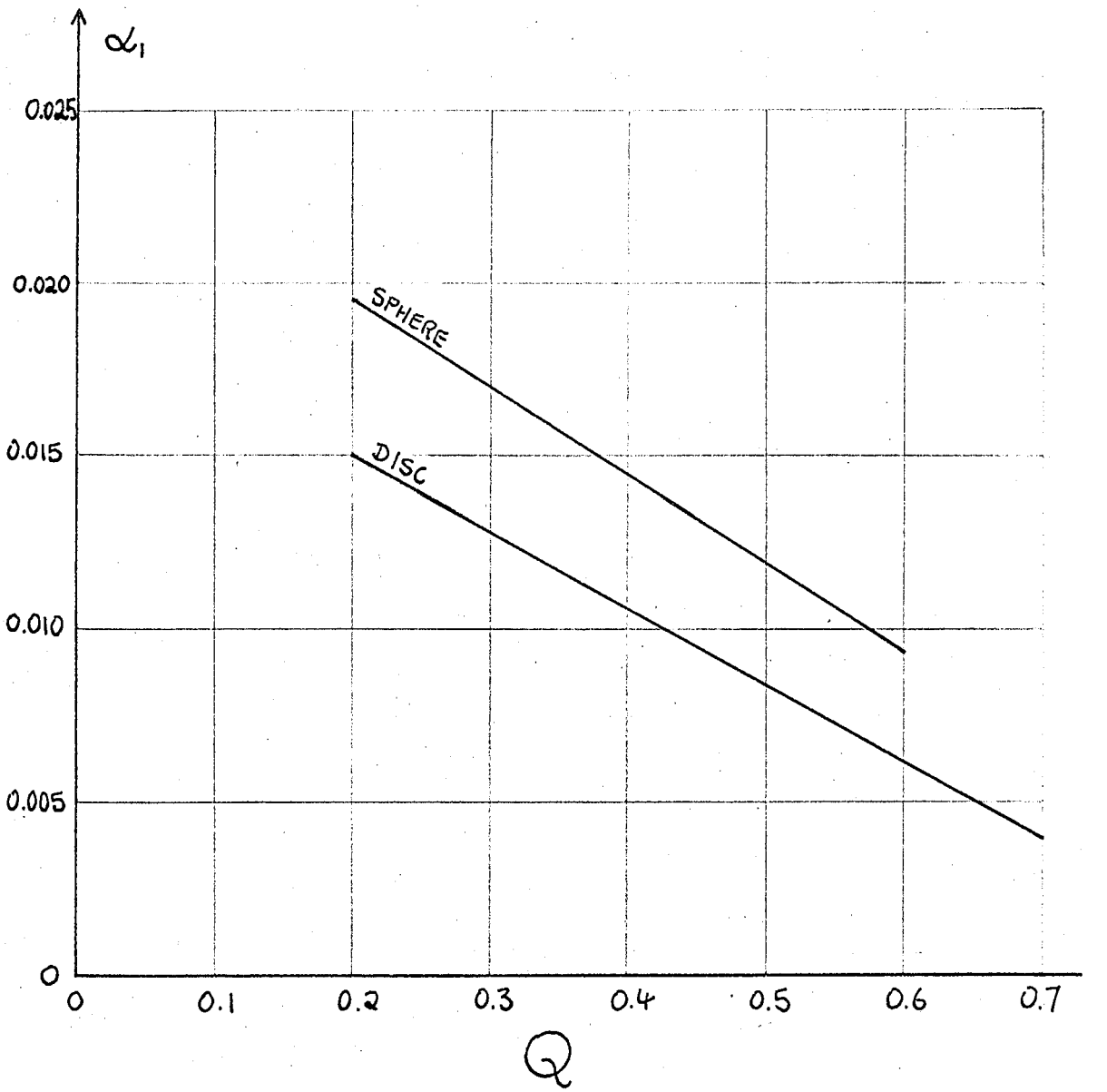

5.2.6 Conclusion of Overall Convergence.

In the last section a few of the many investigations carried out by the author were given for the sake of demonstration. One conclusion that must be drawn is that any of the methods attempted did not give very rapid convergence. In cases of this kind it is sometimes found that the required result converges more rapidly than the dependent variable values. This is true for some of the results required in this case , such as C_D , but not for others , such as L/C.

Since the variations occuring in the ΔQ_k values is greater than those in the f values , in determining the accuracy of the solution at a given moment it is best to concentrate on the former. The criterion , chosen by the author , for the conclusion of any solution was that all the Q_k values should be within 0.006 of the prescribed value of Q. At this point in the iterative process most of the required results had converged sufficiently for further iterations to have a negligible effect. The following are some rough observations on the number of external iterations required to achieve this objective :

[1] If the initial field was , in fact , a solution for one cavitation number different by 0.1 from the prescribed Q in the new problem , some 20 iterations were needed.

[2] If , however , the initial field had the same Q but a different value of f_H then the number required was of the order of 12.

[3] The average length of time required for one external iteration with its associated internal iterations was 1.2 minutes on the KDF9 computer. Thus , on average ,

one solution for the disc took 15 minutes. The time required for a sphere solution is dependent on the factors outlined in the next section.

A final comment must be made on the behaviour of the method when a problem with no real solution is attempted ; that is to say a problem whose solution lies "below" the choked flow condition. In this case the f values on the free streamline continued to rise indefinitely since the values of Q_R could never be reduced to the prescribed Q ; hence divergence took place.

5.2.7 Separation Angle for the Sphere.

The basic method employed to find the additional result , the separation angle (θ_S), in the case of the solutions with the sphere was discussed in sections 4.2.6 and 4.3.7. The question which will now be dealt with is how the guessed value , θ_S, and the test value , θ_S^* , are made to converge to one and the same.

Initially , the programmes were written so that the input value , θ_S, did not vary throughout the computations. The computed value of θ_S^* was printed out every external iteration. However , some eight external iterations were required before this test value converged. Thus it was most convenient to carry out the adjustment of θ_S using personal observation by terminating the programme , printing out the final field and restarting with a different according to the final value of θ_S^*. (See section 5.3.2) A rough formula was thus arrived at by trial and error for

the appropriate adjustment of

[5.7] $$(\theta_s)_{new} = \theta_s + 2(\theta_s^* - \theta_s)$$

The number of solutions which had to be carried out to achieve a small error , $\theta_s^* - \theta_s$, was dependent on the initial guess for θ_s and on the accuracy required. Reference to figure 5.18 shows that the total variation in θ_s in the final solutions for all Q and H/C (Q from 0.2 to 0.6) was a mere 8^0. The attainable objective , fixed by the author for the maximum final values of $(|\theta_s^* - \theta_s|)$ was 0.07^0.

As more complete solutions were obtained the initial guessed value of θ_s became progressively better. However , to give an estimate , the number of ,say, eight external iteration solutions required to attain the chosen accuracy , given the initial starting value of θ_s one degree different from the correct value , was of the order of 5. This number was however smaller for lower cavitation numbers and larger for higher Q. The sphere solutions took on average three times as long as their disc counterparts.

5.3 PROGRAMMING.

5.3.1 The simple results required.

Before the programmes themselves are included it is convenient to discuss the main results which will be required from the final field solution. Two of the chapters in the programme are devoted to calculating

the following results.

[1] The ratios of the overall dimensions of the cavity , the maximum radius and the half-length , to the typical dimension of the body. The half length is obtained using equation [3.10] where the derivative $\frac{\partial f}{\partial \psi}$ is calculated in the usual way , using extra-residuals at points near the singularity at separation. In the case of both the disc and the sphere this half-length is calculated as the length from the front stagnation point to the point of maximum radius. The maximum radius is estimated from the value of the fractional mesh length , c , and the f values surrounding the point , k = K , j = 0 .

[2] At every point on the wetted surface the coefficient of pressure is found by means of the formulae [3.39] and [3.40]. Then the integration of equation [3.41] is carried out to give a value for the coefficient of drag , C_D.

[3] Using these results the values of $\left(\frac{B}{C}\right)_{max}$ and $(C_D)_{max}$ are calculated according to section 3.3.1.

Thus at the conclusion of the set number of external iterations the programmes printed the following :

[A] For every point on the wetted surface ,

<u>For the disc</u> C_p , r

<u>For the sphere</u> C_p , r , $\frac{\pi}{2} - \theta$, x

the origin of the last being the stagnation point. In the case of the sphere , since the radius , R , is dependent on the value of θ_s (equation [4.30a]) , two sets of values are printed ; one for the set value

and the other for the final test value , θ_s^*. These give some estimate of accuracy.

[B] The values of C_D and $C_D/(1 + Q)$ which result.

[C] For every point on the free streamline

$$Q_k \ , \ r \ , \ x \ ;$$

the last two are also printed for the point of maximum radius as in [1] above.

The basic parameters , against which it is intended to plot the important results , are Q and H/C. The resulting curves , it can be anticipated , will be of the same form as the plane flow results given in Appendix A , with similar types of choked flow lines , obtained in the same manner. The cavitation numbers for which series of solutions for different H/C were obtained were as follows :

[1] For the disc from Q = 0.2 to 0.7 in steps of 0.1 .

[2] For the sphere from Q = 0.2 to 0.6 in steps of 0.1 .

Higher Q would be outside the range of fully developed cavities in each case.

Difficulties were experienced when an attempt was made to consider cavitation numbers lower than 0.2. These difficulties arose from the fact that the length of the cavities increased so rapidly with lower Q that the fields became too large to be dealt with by the present programme. However the author hopes to rewrite part of the programmes to overcome the storage difficulties and thus produce solutions for Q = 0.1.

For each cavitation number the range of H/C values for which solutions were obtained is limited as follows.

[A] Choked Flow limits the minimum H/C. The values of $(H/C)_{MIN}$ can only be guessed initially , appearing as results.

[B] Some maximum limit on H/C is provided by the time and space required for the computations. The f_H values were increased until little change occured in the required results for each cavitation number.

5.3.2 The Final Field.

The programmes are designed so that on a restart the control moves to a different section of the programme from the initial start and the final field of f values is printed out on paper tape. The form of this print out coincides precisely with the form to be read in as the initial guessed field of f except for a small number of essential parameters which can be tacked on the end. This final field print out can then be used in the following ways.

[1] With an ancillary programme to calculate further results such as the position of every mesh point in the physical plane.

[2] With an ancillary programme to carry out an error analysis of any of the types outlined in section 5.5 .

[3] As initial guessed field for a problem with different parameters. Thus in the case of the sphere it is required to re-input with an adjusted value of θ_s (see section 5.2.7).

The final field is printed in the form :

[A] K

[B] n^*_k ; k = 1,2 .... K.

[C] (J - 1) and J*. (See section 4.5.5)

[D] For j = 0,1 .... J ; (1) $(f_v)_j$

; (2) $f_{j,k}$, k = 1,2 ..... K.

[E] The reference f_{E*} for the stagnation point extra-residuals.

[F] Those extra-residuals and the gradients $\frac{\partial Z}{\partial f_{E*}}$ for the reference value , f_{E*} . These values are calculated by an initial ancillary programme.

[G] An additional print out of the final d_k values on the free streamline boundary , preceded by K and followed by the final value of c. This is to assist re-input.

Since it may be required to alter the geometry of this field before a new solution is started , the essential parameters mentioned above , include the means by which the programme will do this. A set of these parameters may include

(A) K , (J - 1) , J* . These may be different from the values inputed with the initial field. The field is , however , adjusted to this new geometry before the start of the main computations.

(B) The number of internal iterations to be carried out before the first external.

(C) X

(D) Q

[(Da) The initial value of $\frac{\pi}{2} - \theta_s$ in the case of the sphere.]

(E) ω

(F) The number of external iterations to be carried out.

(G) The number of intervening internal iterations.

(H) β or α_1. (See section 5.2.5)

(I) α_2. (See section 4.5.6)

(J) The value of K_L. (See section 4.5.3)

The next section gives one sample programme (in this case for the sphere) with comments inserted to describe each part. The programme is written in C203 Autocode.

5.3.3 A Typical Programme for the Problem of the Sphere.

The following is a typical programme used for the sphere solutions. Comments are inserted in square brackets to describe the particular task of each part of the programme. Symbols used in the programme could not , in many cases , be the same as those used in the text. In the comments , where a text symbol is referred to , it is followed by the programme symbol in brackets.

```
TITLE
FAEAA 52 A      SPHERE.TUBE.
CHAPTER1                          [Chapter 1 contains all the
F:99                               operations carried out during
B:99                               an external iteration.]
C:99
G:99
E:50
A:13
D:8

21)×6(300)C54,46
×6(400)F0,100
×6(500)G0,100
JUMP3,U↑>0.1
READ(E↑)
READ(Y↑)                  [Before the first external iteration , this
NEWLINE                    short list of parameters is read in. These
NEWLINE                    correspond to (F) → (J) of the last list
K=1(1)2                    of the section 5.3.2]
READ(AK)
PRINT(AK)1,5
REPEAT
READ(M)
PRINT(M)2,0

3)×6(653)D1,1
D2=5.65685425G53-D1-4.65685425F53-0.41421356W↑W↑/F53
D2=0.2734591D2/W↑
JUMP12,1>D2               [This section calculates the test value of
CAPTION                    π/2 - θ_ε (D3) and the new values of K*_1 (A5)
THETA UNREAL-              and K*_2 (A7) to be used for the separation
JUMP11                     point extra-residuals.]
12)D4=×SQRT(1-D2D2)
D3=90-180×ARCTAN(D2,D4)/£
NEWLINE
NEWLINE
CAPTION
THETA  TEST
PRINT(D3)2,5
NEWLINE
11)NEWLINE
A7=G53-F53-D↑W↑-0.25W↑W↑/F53
D1=×SQRT(F53)
A5=×LOG(F52/F53)+C↑/D1+0.25Z↑Z↑/F53
PRINT(A5)1,8
PRINT(A7)1,8
S=0
NEWLINE
NEWLINE
```

```
NEWLINE                [This calculates all the ΔQ_k values on
PRINT(F53)1,5           the free streamline (F9).]
K=1(1)12
SPACE
REPEAT
PRINT(C54)3,7
K=54(1)N
Q=K+1
R=K-×INTPT(BK/B(K-1)+0.6)
H=XGO/BK
×6(600+K)D5,1
JUMP32,K≠54
D2=×LOG(F54/F53)
D3=0.4375Z↑Z↑/F53+3.75D2-3.75C↑/D1
F3=HHD3+4GK-0.5D5-3.5FK
D4=-1.5C↑/D1+0.125Z↑Z↑/F53+2.5D2
F1=HD4F54
JUMP33
32)JUMP30,K=N
JUMP30,B(K+1)>BK+0.000001
F1=6FQ-F(K+2)-2FR-3FK
JUMP31
30)F1=-6FR+F(K-2)+2FQ+3FK
31)F1=0.16666666666HF1
F2=1/FK
F3=HH×LOG(FRFQF2F2)+4GK-0.5D5-3.5FK
33)F3=0.3333333333F3
F4=F1F1/FK+F3F3
F9=GOGO/F4-1-Z

NEWLINE
PRINT(FK)1,5
PRINT(F9+Z)1,7

D2=BK/B52
D1=A1F9D2
JUMP2,A2>×MOD(D1)   [This alters the d'_k values (C(K+1)) on the
CAPTION              free streamline according to the ΔQ_k values
M                    and the second method ( in this case ) of
D1=A2×SIGN(D1)       section 5.2.5 .  It also contains the G
2)D3=C(K+1)+D1       and M constraints referred to in section
JUMP6,57>K           4.5.6.]
JUMP6,K-2=R
JUMP6,CK>D3
D4=C(K-1)
JUMP14,B(K-2)>B(K-1)-0.0 01
D4=D4+C(K-2)
14)D4=2CK-D4
C(K+1)=D4
CAPTION
G
JUMP7
6)c(K+1)=D3
7)JUMP8,S≠0
JUMP8,C(K+1)>0
S=K
8)PRINT(C(K+1))3,7
JUMP28,K≠M-1
CAPTION
LIN.
28)REPEAT
```

```
NEWLINE
PRINT(F(K+1))1,5

JUMP9,S=0
JUMP10,0.1>×FRPT(0.5S+0.001)
N=S
JUMP9                  [This section linearizes the d  differences
10)N=S-1                from the points k=K_L (M) to k=K (N).  It
9)JUMP27,N≥M+2          also adjusts the value of K (N).]
M=N-4
27)D1=0
K=M(1)N
D1=D1+BK
REPEAT
D2=CM-C(N+1)
D3=0
K=M(1)N
D3=D3+BK
C(K+1)=CM-D2D3/D1
REPEAT

C=D1C(N+1)/D2
D4=D1+C                [Calculates the new value of c (C) and the
D4=FM+0.5CMD4/BN        approximate maximum f of the free stream-
C=C/BN+0.5              line (D4).]
JUMP5,C>-0.3
N=N-2
C=C+2
5)JUMP26,30>C
C=30
26)NEWLINE

×7(300)C54,46

CAPTION
   N       C       =FM
NEWLINE
PRINT(N)2,0
PRINT(C)2,5
PRINT(D4)2,5
NEWLINE
NEWLINE

U↑=U↑+1
ACROSS22/2

CLOSE
```

```
CHAPTER2                [Chapter 2 contains all the operations
VARIABLES1               carried out during an internal iteration.]

22)V↑=0
2)×6(400)F0,100
×6(500)G0,100
×6(600)C0,100

F30=0.6666666666666667YD-0.1111111111111111DD
K=31(1)52
R=K-×INTPT(BK/B(K-1)+0.6)
Q=K+×INTPT(B(K-1)/BK+0.6)     [Relaxes all the wetted surface
H=XG0/B(2K-Q+1)                points except the separation
D6=0                           point.  (D6) is the extra-
JUMP31,K>32                    residual for any point.]
×6(115+K)D6,1
31)JUMP30,K≠52
D6=-0.09314575HHA5
30)JUMP32,K>41
JUMP32,K=36
33)D1=6FQ-F(K+2)-2FR-3FK
JUMP34
32)JUMP33,K=46
JUMP35,K=52
D1=-6FR+F(K-2)+2FQ+3FK
JUMP34
35)D1=3FK×LOG(F53/F51)+1.97056272A5FK
34)D2=1/FK
D3=×SQRT(YY-FK)
D3=1/D3
D4=HH×LOG(FRFQD2D2)+4GK-0.5CK-3.5FK-0.5HD1D3-D6
D5=2HHD2+3.5+0.25HD3D3D3D1
FK=FK+FD4/D5
REPEAT

D1=×SQRT(F53)
D2=5.65685425×LOG(F52)-×LOG(F51)+3.65685425C↑/D1+0.41421356Z↑Z↑/F53
F53=×EXP(0.2147372D2)
D1=×SQRT(F53)
Y=D1/D↑
D2=×LOG(F55/F54)+3.65685425C↑/D1-0.41421356Z↑Z↑/F53
D3=F53×EXP(0.2147372D2)-F53
×7(300)D3,1                   [Calculates new values for f_s (F53),
                               R(Y) and (f_{k_{s+1}} - f_{k_s}) (D3) according
                               to section 4.3.7 [2].]
×6(300)C54,46
R=N+1
D1=1-G0/E                     [Applies the d'_R values to generate
K=54(1)R                       the f values on the free stream-
E(K-53)=F(K-1)+CK-FK            line according to section 4.5.2.]
FK=F(K-1)+CK
GK=GK+D1E(K-53)
REPEAT

×7(400)F0,100
×7(500)G0,100

D1=Y-V                        [Alters the stagnation residuals
140=×13(120,D1,100,8)          according to section 4.4.3.]
```

```
NEWLINE
PRINT(F31)1,5
PRINT(F53)1,5
PRINT(FN)1,5                          [Internal Iteration print out.]
PRINT(G31)1,5
PRINT(GN)1,5
PRINT(Y)1,5

D1=2C+1
A=4C/D1
B=A-1
O=1
J=1(1)I
JUMP19,J>2
×6(400)C0,100
JUMP25
19)×6(100J+300)F0,100
×6(100J+200)C0,100
K=1(1)99
CK=16CK-14FK
REPEAT
25)×6(100J+400)F0,100
×6(100J+500)G0,100
G=G0-F0                               [Relaxes all other points.]
JUMP18,J≠L
O=2
D1=1+C
A=2C/D1
B=A-1

18)D1=F(O+1)-F0
D2=F0+A(O+10)
D3=F0+A13
D4=D2/D3
F1=F0+D1D4×SQRT(D4)
D6=1-G0/E
T=O+1
K=T(O)N                               [Points on k = 1.]
JUMP20,53≥K
JUMP20,J=I
GK=GK+D6D6E(K-53)

20)S=×INTPT(B(K-1)/BK-0.4)
Q=K+OS+O
H=OB(K-S)                             [Points using the field equation
H=XG/H                                 [4.21].]
D5=F
JUMP26,H>0.9
D5=1.1111111HF
26)R=K-O×INTPT(BK/B(K-1)+0.6)
D1=1/FK
JUMP6,2≥J
D2=5.25HH×LOG(FRFQD1D1)+CK+5GK-7FK
D3=10.5HHD1+10.5
FK=FK+D5D2/D3
JUMP9,J≠L
F(K-1)=0.5FK+0.5F(K-2)
JUMP9
```

```
6)D3=0
JUMP11,K>30
JUMP29,28>K                          [Points using the field equation
×6(109+K+3J)D3,1                      [4.18].]
11)JUMP29,K≠53
D3=-0.09314575A7
JUMP29,J≠2
D3=5.65685425D3
29)D2=HH×LOG(FRFQD1D1)+GK+CK-2FK-D3
D3=2+2HHD1
FK=FK+D5D2/D3

9)JUMP10,K≠N-0
F(K+20)=AFQ-BFK
10)REPEAT

×7(100J+500)G0,100
×7(100J+400)F0,10

REPEAT

8)V↑=V↑+1
JUMP2,Y↑≥V↑
JUMP23,U↑>E↑
ACROSS21/1
23)ACROSS20/5

CLOSE
```

```
CHAPTER3                  [Chapter 3 contains the instructions for
VARIABLES2                 the final field print out referred to in
                           section 5.3.2.]
24)R=0(1)200
PUNCH(0)
REPEAT

NEWLINE
PRINT(N)2,0
NEWLINE
R=×INTPT(0.125N+0.01)
J=0(1)R
NEWLINE
K=1(1)8
Q=K+8J
JUMP1,Q>N
PRINT(BQ)1,4
1)REPEAT
REPEAT
NEWLINE
PRINT(I)2,0
PRINT(L)2,0
NEWLINE

R=0(1)50
PUNCH(0)
REPEAT
```

```
Q=XINTPT(0.2N+0.19)
R=I+1
O=1
J=O(1)R
NEWLINE
X6(100J+400)FO,100
JUMP2,J≠L+1
Q=XINTPT(0.1N+0.19)
O=2
2)NEWLINE
PRINT(FO)2,5
P=O(1)Q
NEWLINE
K=O(1)4
S=OK+5OP+1
JUMP3,S>N
PRINT(FS)2,7
3)REPEAT
REPEAT
REPEAT

R=O(1)100
PUNCH(O)
REPEAT

NEWLINE
NEWLINE
PRINT(V)1,3
NEWLINE
X6(120)FO,8
K=O(1)7
PRINT(FK)1,6
REPEAT
NEWLINE
X6(100)FO,8
K=O(1)7
PRINT(FK)1,6
REPEAT
NEWLINE

R=O(1)100
PUNCH(O)
REPEAT
NEWLINE
PRINT(N)2,O
NEWLINE
X6(30 )C53,46
K=53(1)N
NEWLINE
PRINT(CK)1,7
REPEAT
NEWLINE
NEWLINE
PRINT(C)2,6
NEWLINE

R=O(1)100
PUNCH(O)
REPEAT

I=O
ACROSS20/O
CLOSE
```

```
CHAPTER4                [Chapter 4 contains the instructions for
VARIABLES3               the initial adjustment of the guessed
                         field according to section 5.3.2.  Also
17)READ(N)               prints out some information concerning
READ(I)                  this initial adjusted field.]
READ(L)

JUMP18,I=S
JUMP19,I>S
×6(100I+500)F0,100
D1=1/F0
D1=D1D1
K=1(1)99
GK=D1F0-D1FK
FK=F0
REPEAT
E=F0
×7(100I+500)F0,100
J=1(1)I
×6(100J+400)F0,100
K=1(1)99
FK=FK+F0F0GK
REPEAT
×7(10 J+400)F0,100
REPEAT
JUMP18

19)×6(100I+300)F0,100
D1=1/E
D1=0.54D1D1
K=1(1)99
GK=-D1F0+D1FK
FK=4F0
REPEAT
F0=4F0
×7(10 I+50 )F0,100
E=F0
J=1(1)I
×6(10 J+40 )F0,100
K=1(1)99
FK=FK+F0F0GK
REPEAT
×7(100J+400)F0,100
REPEAT

18)JUMP9,T≥N
D1=CT-C(T+1)
Q=T+1
K=Q(1)N
C=C-1
C(K+1)=CK-D1
REPEAT
9)×7(300)C54,46

NEWLINE
CAPTION
C.START
PRINT(C)2,5
CAPTION
N.I.L.
PRINT(N)2,0
```

```
PRINT(I)2,0
PRINT(L)2,0
NEWLINE
NEWLINE

ACROSS21/0
CLOSE



CHAPTER5                [Chapter 5 contains the instructions for
VARIABLES4               calculating the results for the wetted
                         surface.]

20)×6(400)F0,100
×6(500)G0,100
E18=0
NEWLINE
NEWLINE
CAPTION
VALUES FOR SURFACE OF SPHERE
21)NEWLINE
NEWLINE
CAPTION
   R  PHi/2 - THETA        X    -CP(POT.FLOW)     -CP     D.CD
NEWLINE
NEWLINE
CAPTION
 0.00 00    00.0000    0.0 00    -1.00000  -1.000 0

D1=1+2C
D2=1-2C
D3=4C/D1
D4=D2/D1
F(N+1)=D3FN+D4F(N-1)
G(N+1)=D3GN+D4G(N-1)

E10=0
E7=1+Z
K=30(1)53
E1=×SQRT(FK)
E2=×SQRT(YY-FK)
E3=180×ARCTAN(E2,E1)/£
E4=Y-E2
R=K-×INTPT(BK/B(K-1)+0.6)
Q=K+×INTPT(B(K-1)/BK+0.6)
H=XG0/B(2K-Q+1)

JUMP1,K≠30
E5=0.66666666667HYD-0.2222222222HDD
JUMP2
1)JUMP13,K>41
JUMP13,K=36
18)E5=6FQ-F(K+2)-2FR-3FK
JUMP14
13)JUMP15,K≠53
E6=0
JUMP17
```

```
15)JUMP16,K≠52
E5=0.5HF52×LOG(F53/F51)+0.32842712A5XF52
JUMP2
16)JUMP18,K=46
E5=-6FR+F(K-2)+2FQ+3FK
14)E5=0.166666666667HE5
2)E5=YYE5E5
E6=-FKE2E2GOGO/E5+1+Z
17)E8=E6+E7
E7=E6
E9=FK-F(K-1)
E9=E9/Y
E10=E10+0.5E8E9/Y
E15=1.5E1/Y
E15=E15E15-1
NEWLINE
PRINT(E1)1,5
PRINT(E3)2,4
PRINT(E4)1,5
PRINT(E15)1,5
PRINT(Z-E6)1,5
PRINT(E10)1,5
REPEAT

NEWLINE
NEWLINE
CAPTION
  CD(Q)     CD(O)     CD(Q).RR/F53      CD(O).RR/F53
NEWLINE
D1=1+Z
E16=E10/D1
PRINT(E10)1,5
PRINT(E16)1,5
PRINT(YYE10/F53)1,5
PRINT(YYE16/F53)1,5
NEWLINE
NEWLINE

JUMP19,E18>3
×6(653)D5,1
D2=5.65685425G53-D5-4.65685425F53-0.41421356W↑W↑/F53
D2=0.2734591D2/W↑
D4=×SQRT(1-D2D2)
D3=90-180×ARCTAN(D2,D4)/£
NEWLINE
CAPTION
TEST THETA
PRINT(D3)2,5
NEWLINE
NEWLINE
CAPTION
SURFACE WITH TEST RADIUS
Y=×SQRT(F53)/D2
E18=5
JUMP21

19)NEWLINE
NEWLINE

ACROSS20/6

CLOSE
```

[This calculates r , $\pi/2 - \theta$ and x for each mesh point. It also calculates C_p and the C_p for the same point in the equivalent Dirichlet flow and by integrating the former values arrives at the coefficient of drag. This is carried out for both the input and test values of θ_s and therefore R. (See section 5.3.1)]

[Prints out the final value of C_D in all forms. NB. CD(O) refers to $C_D/(1+Q)$.]

```
CHAPTER6                [Chapter 6 calculates the results required
VARIABLES 5              from the final free streamline values.]

20)CAPTION
VALUES ON F.S.
NEWLINE
NEWLINE
CAPTION
   R       CAV.NO.(L)       X
NEWLINE
NEWLINE
PRINT(E1)1,5
K=1(1)12
SPACE
REPEAT
CAPTION
 0.0 00
J=N+1
C53=W↑D↑
D1=E4
K=54(1)J
F11=×SQRT(FK)
Q=K+1
R=K-×INTPT(BK/B(K-1)+0.6)
H=XG0/BK
×6(600+K)D5,1
JUMP32,K≠54
D3=×SQRT(F53)
D2=-1.5C↑/D3+0.125Z↑Z↑/F53+2.5×LOG(F54/F53)
F1=HD2F54
JUMP33
32)JUMP30,K=N
JUMP30,B(K+1)>BK+0.000001    [Calculates r,x and Q, for every
F1=6FQ-F(K+2)-2FR-3FK         mesh point.]
JUMP31
30)F1=-6FR+F(K-2)+2FQ+3FK
31)F1=0.1666666666HF1
33)F2=1/FK
F3=HH×LOG(FRFQF2F2)+4GK-0.5D5-3.5FK
CK=0.3333333333F3
F4=F1F1/FK+CKCK
F9=G0G0/F4-1
JUMP5,K=54
D2=72H
JUMP3,B(K-1)>B(K-2)+0.0001
F10=24C(K-1)-3CK+15C(K-2)
JUMP4
3)F10=10.5C(K-1)+8C(K-2)-0.5CK
4)JUMP7,K=R+1
D2=144H
7)D1=D1+F10/D2
PRINT(D1)2,5
5)JUMP6,K=J
NEWLINE
PRINT(F11)1,5
PRINT(F9)1,6
6)REPEAT
```

```
D5=FJ-F(N-1)
D2=2FN-FJ-F(N-1)
D6=FN+0.5CD5-0.5CCD2
D6=xSQRT(D6)
D3=xSQRT(1+Z)                    [Calculates the values of r and
D4=GO/D3+CN                       x at the point of maximum dia-
D5=0.25D4C/H+D1                   meter.]
NEWLINE
CAPTION
CL.VALUES
NEWLINE
PRINT(D6)1,5
K=1(1)11
SPACE
REPEAT
PRINT(D5)2,5
NEWLINE
NEWLINE
NEWLINE

K=0(1)2
CAPTION
 B/C     L/C          CC/BB       C/L
JUMP22,K=0
CAPTION
C=TEST R
JUMP25
22)JUMP23,K≠1                    [Print out of required ratios.]
CAPTION
C=MAX R↑
Y=E1
JUMP25
23)CAPTION
C=REAL R
Y=E1/D1↑
25)NEWLINE
NEWLINE
D7=Y/D6
PRINT(D6/Y)1,4
PRINT(D5/Y)2,4
PRINT(D7D7)1,5
PRINT(Y/D5)1,5
NEWLINE
NEWLINE
REPEAT
D7=xSQRT(E)
CAPTION
H/C  =
PRINT(D7/Y)4,4
NEWLINE
NEWLINE

ACROSS20/0
CLOSE
```

```
CHAPTER0                [Control and initial input chapter]
F:99
B:99
C:99
G:99
E:50
A:13
D:8

JUMP6,I=0
ACROSS24/3

6)READ(P)
×10(0,P)
×6(0)B1,98
K=P(1)99
BK=BP
REPEAT
READ(S)
READ(M)                 [Initial field input.  See section 5.3.2.]
I=S+1
0=1
J=0(1)I
JUMP2,J/M+1
0=2
2)READ(F0)
K=1(0)P
READ(FK)
JUMP8,0=1
JUMP8,K=1
F(K-1)=0.5FK+0.5F(K-2)
8)REPEAT
K=P(1)99
FK=FP
REPEAT
×7(100J+400)F0,100
REPEAT
E=F0

READ(V)
×10(120,8)              [Stagnation residual input.]
×10(100,8)
140=×15(120,8)

READ(T)
K=53(1)T                [Initial free streamline difference input.]
READ(C(K+1))
REPEAT
READ(C)
ACROSS17/4

21)READ(Y↑)
READ(X)                   [X]   [Parameter input corresponding to (A)
READ(Z)                   [Q]    → (E) of the second list of section
READ(U)                [I½ -θ6]  5.3.2.]
READ(F)                   [ω]
NEWLINE
```

```
CAPTION
   X        Q     Pi/2 - Θs     O.R.F.
NEWLINE
PRINT(X)1,3
PRINT(Z)1,3
PRINT(U)2,3
PRINT(F)1,3
NEWLINE

D1=0
K=2(1)28
D1=D1+B(K-1)
REPEAT
D2=0.5D1/X
A13=D2D2                          [Some other quantities required
D3=D2-0.5B1/X                      throughout the programme.]
D4=D3-0.5B2/X
A11=D3D3
A12=D4D4

U=90-U
U=0.00555555555555555£U
D=B29/X
D↑=×COS(U)
D1=×SQRT(Z+1)
W=1/D1
Z↑=WB52/X
C↑=Z↑×SIN(U)
×6(452)F52,2
×6(50 )G0,1
×6(553)G53,1
D1=×SQRT(F53)
Y=D1/D↑
W↑=G0W
READ(A5)
READ(A7)

U↑=0

5)ACROSS22/2

20)END
CLOSE
→→
```

5.4 CAVITATING FLOW SOLUTIONS.

5.4.1 Wetted surface results for the Disc.

Figure 5.13 shows a typical pressure distribution which resulted from the solutions of the cavitating flow behind a disc. That particular solution was for $Q = 0.3$, $H/C = 13.47$ and the figure shows the result of plotting the value of C_p obtained at each mesh point. The author drew many curves of this type and found that for a particular cavitation number the distributions obtained for different H/C were indistinguishable on the scale of figure 5.13.

The variation with Q was also very small and figure 5.14 shows C_p plotted against r/r_s for $Q = 0.3$ and $Q = 0.7$. The curves for other cavitation numbers are not inserted for the sake of clarity but lie regularly between the two (in the case of $Q = 0.4, 0.5, 0.6$). It is thus anticipated that there will be little variation of the function $C_D/(1 + Q)$ with either Q or H/C.

Rouse and Mc Nown (Ref. 38) produce experimental pressure distributions ; however , their interest lies more in the cavity pressure distributions so that at only four points on the surface of the disc is a pressure measurement made. The author has reproduced one set of their measurements [for $(C_p)_s = -0.24$] and this is shown by the points in figure 5.14. The agreement is close , though in view of the lower drag coefficients given by experiment , it is a little surprising that the values are not below those of theory. (See section 5.4.3) Some error may , however , have occured in reproduction due to the small size of this region in the graphs of Rouse and

FIGURE 5.13

A Pressure Distribution for the Disc showing the positioning of the Mesh Points.

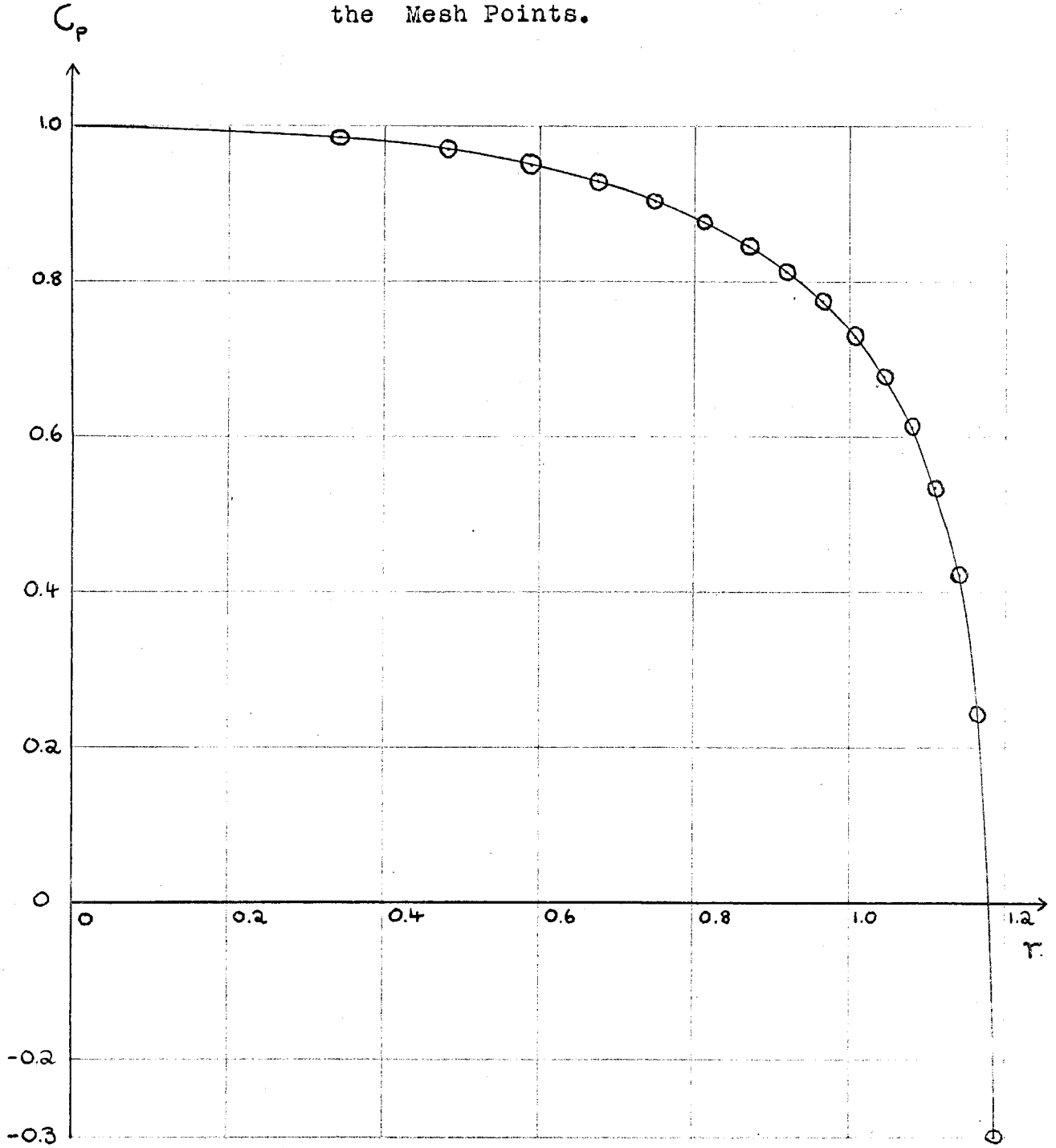

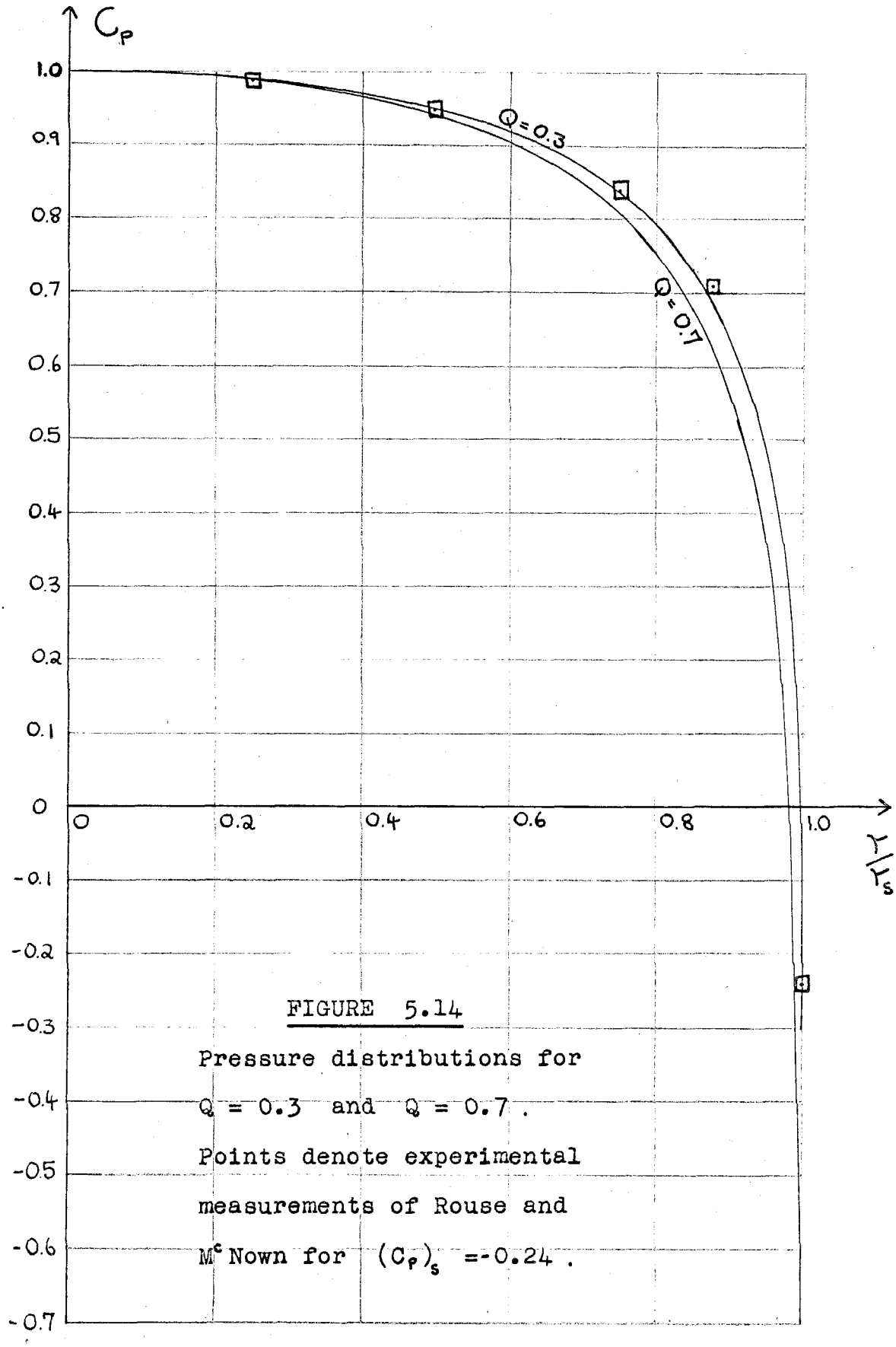

FIGURE 5.14

Pressure distributions for $Q = 0.3$ and $Q = 0.7$.
Points denote experimental measurements of Rouse and McNown for $(C_p)_s = -0.24$.

Mc Nown.

Figure 5.15 shows all the values obtained for $C_D/(1+Q)$ plotted against H/C ; the total variation is under 2.5 per cent. Despite the magnified scale , the results show the regular behaviour of the drag coefficient as the choked flow condition is approached. In accordance with the results of Appendix A , the drag falls off as $H/C \rightarrow (H/C)_{MIN}$.

With the results obtained , the value of $C_D/(1+Q)$ at $H/C = \infty$ is accurately defined for each cavitation number. It is true for most of the results to follow , that best definition is obtained for H/C remote from $(H/C)_{MIN}$.

Corresponding to the curve in figure 5.15 for each cavitation number , there is the intersecting line of $(C_D)_{MAX}/(1+Q)$; these are calculated from equation [3.44d] knowing H/C and Q. However the scale of figure 5.15 is such that these lines appear as the verticals indicated in the lower left hand corner of the figure. For example , for $Q = 0.4$, $H/C = 5.8$ leads to $(C_D)_{MAX}/(1+Q) = 0.8066$ and $H/C = 6.0$ gives $(C_D)_{MAX}/(1+Q)$ as 0.8632.

As a consequence of this we will make an assumption which proves extremely useful in tentatively constructing later choked flow lines. This assumption is that the choked flow condition occurs , for each Q , at the values of H/C indicated by the vertical lines in figure 5.15. This is a reasonable assumption since the two curves , for $(C_D)/(1+Q)$ and $(C_D)_{MAX}/(1+Q)$, will , presumably , not intersect at values of $C_D/(1+Q)$ very far below those in the figure 5.15, if the plane flow

FIGURE 5.15

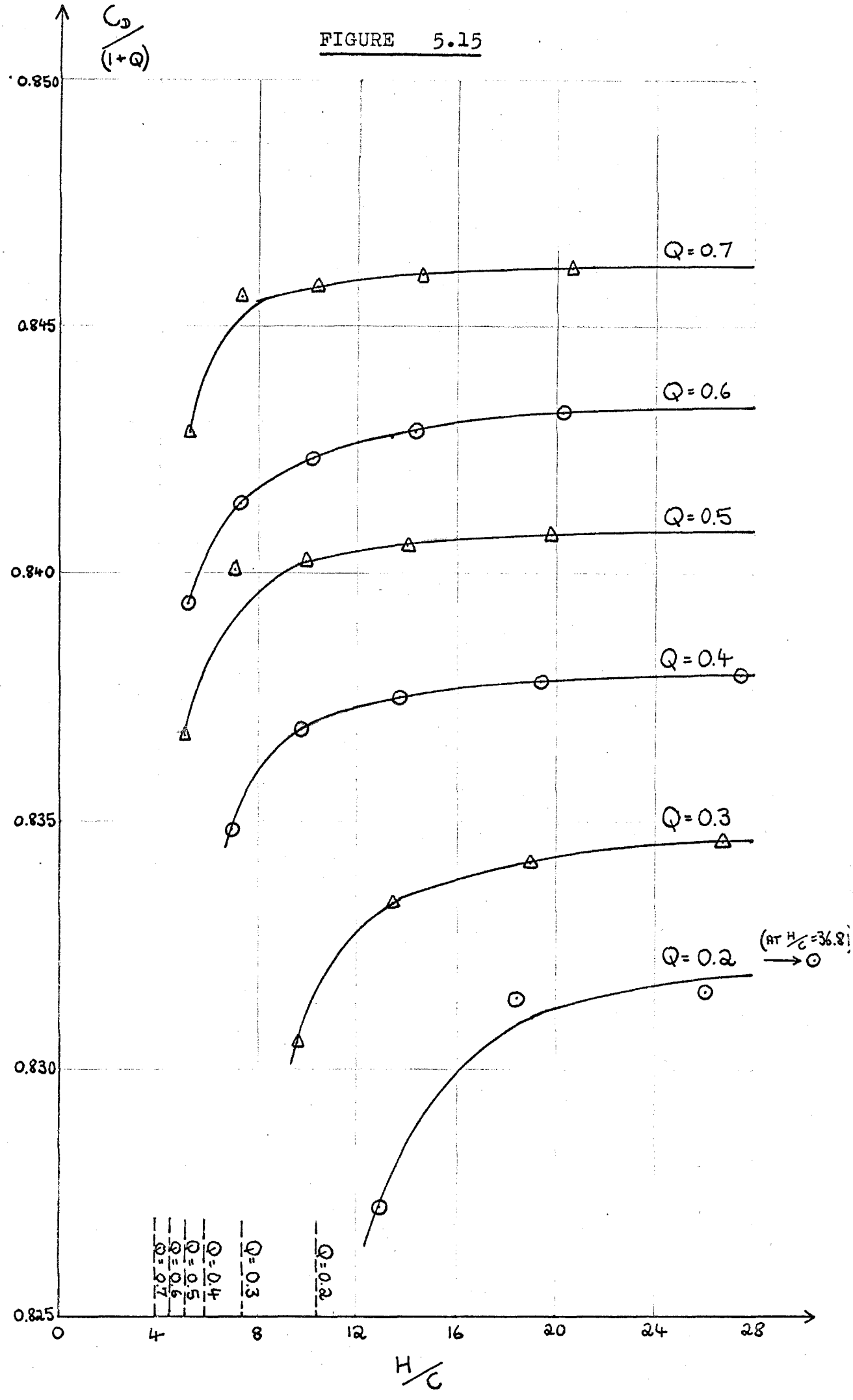
$C_D/(1+Q)$
0.850
0.845
0.840
0.835
0.830
0.825
Q = 0.7
Q = 0.6
Q = 0.5
Q = 0.4
Q = 0.3
Q = 0.2
(AT H/C = 36.8)
Q = 0.7
Q = 0.6
Q = 0.5
Q = 0.4
Q = 0.3
Q = 0.2
0
4
8
12
16
20
24
28
H/C

results are any guide.

This assumption does not help in constructing the choked flow line in that figure , however , since the two curves will clearly intersect at a small angle.

Figure 5.16 shows the result of plotting $C_D/(1+Q)$ against Q for various fixed values of H/C (these being written on each line). The line for $H/C = \infty$ has been tentatively produced to cut the axis at $Q = 0$, giving a value of $(C_D)_{Q=0}$ of 0.8263.

In figure 5.17 the line $H/C = \infty$ is replotted to compare with similar results given by Armstrong and Dunham (Ref. 1) , Fisher (Ref. 11) and Plesset and Shaffer (Ref. 33). (See sections 2.3.2 and 2.4.1.) Clearly the author's results are in very good agreement with all but the latter , whose method is outlined in section 2.3.2. The author's value of $(C_D)_{Q=0}$ of 0.8263 is extremely close to that of Garabedian (Ref. 13 and section 2.4.2) of 0.8272 and is well within Garabedian's estimate of error. However, Garabedian's other result , of $C_D/(1+Q) = 0.865$ at $Q = 0.22$ would seem a little high in comparison with other results.

Experimental measurements of C_D for the disc have been made by Reichardt (Ref. 34) and Eisenberg and Pond (Ref. 10) ; these sets of results both indicate a constant value of $C_D/(1+Q)$, any deviation being within experimental error. The values of $(C_D)_{Q=0}$ so obtained are 0.79 and 0.80 respectively , values which are substantially lower than those of theory. A comment on this is found in section 5.4.3.

FIGURE 5.16

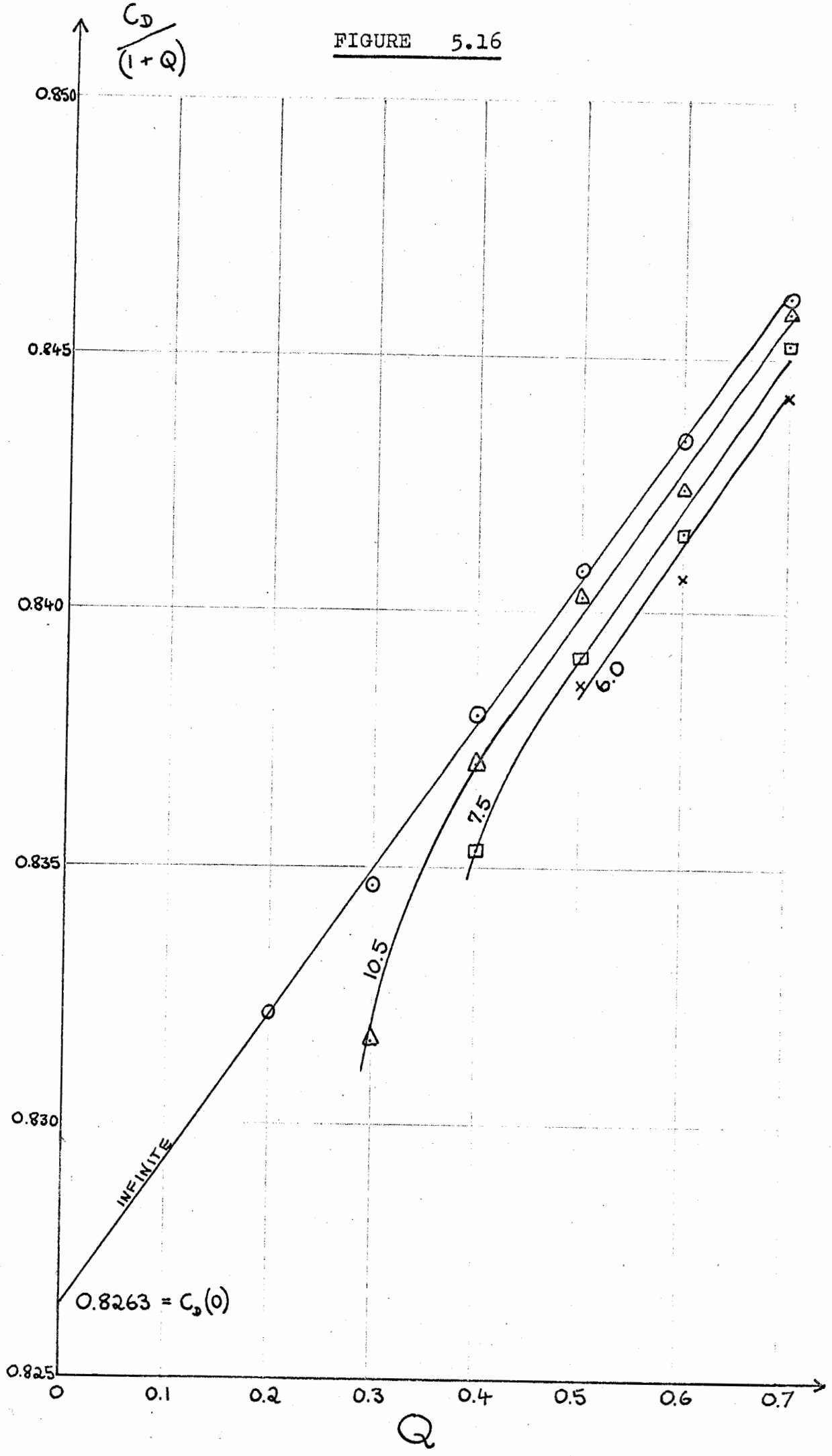
$C_D/(1+Q)$
0.850
0.845
0.840
0.835
0.830
0.825
0
0.1
0.2
0.3
0.4
0.5
0.6
0.7
Q
INFINITE
0.8263 = $C_D(0)$
10.5
7.5
6.0

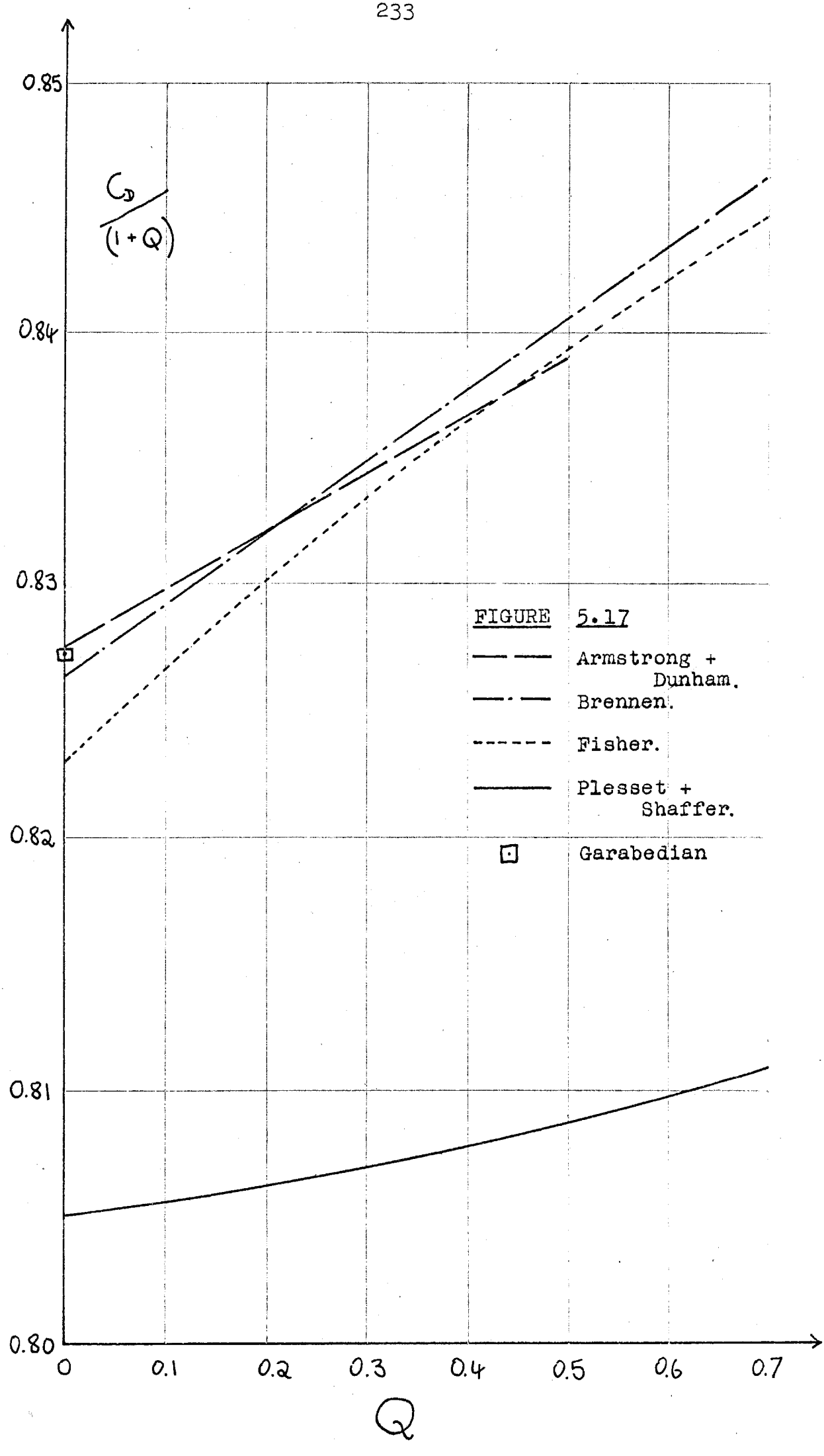
0.85
0.84
0.83
0.82
0.81
0.80
$\frac{C_D}{(1+Q)}$
0
0.1
0.2
0.3
0.4
0.5
0.6
0.7
Q
FIGURE 5.17
Armstrong + Dunham.
Brennen.
Fisher.
Plesset + Shaffer.
Garabedian

5.4.2 The Angle of Separation from the Sphere.

As mentioned in section 5.2.7 , the separation angle solutions are terminated when $|\theta_s^* - \theta_s| < 0.07$. Figure 5.18 shows the results for $\pi/2 - \theta_s$ and $\pi/2 - \theta_s^*$ in the final solutions. Within each ring there are two points ; a square indicates that $\frac{\pi}{2} - \theta_s^* < \frac{\pi}{2} - \theta_s$ and a circle the reverse. The approximate relation of that section would show the errors in the final value of θ_s to be little greater than $+ 2 (\theta_s^* - \theta_s)$. In view of this the difference of behaviour in the results for $Q = 0.2, 0.3$ and those for $Q = 0.4, 0.5, 0.6$ near the choked flow condition would seem to be outside the margin of error.

In figure 5.19 the variation of $\pi/2 - \theta_s$ with Q is shown for certain fixed values of H/C (marked on the curves). In both 5.18 and 5.19 any choked flow line constructed would be extremely tentative but the author has drawn a rough estimate in 5.19 based on the assumption of the last section and the results of the next.

The clearly defined line for $H/C = \infty$ is reproduced in figure 5.20 on a much larger scale. This figure also shows the results of Armstrong and Tadman (Ref. 3) for both a cylinder and a sphere. The author finds it very surprising that their results show $\theta_s \to 0$ as $Q \to \infty$ in both cases. Since the Dirichlet flow around a sphere exhibits a minimum C_p of -1.25 at $\theta = 0$, it would seem more likely for $\theta_s \to 0$ as $Q \to 1.25$. The Dirichlet flow is identical with a Riabouchinsky flow for $Q = 1.25$, the length of the cavity being zero. (This identity extends to the second derivative of

FIGURE 5.18

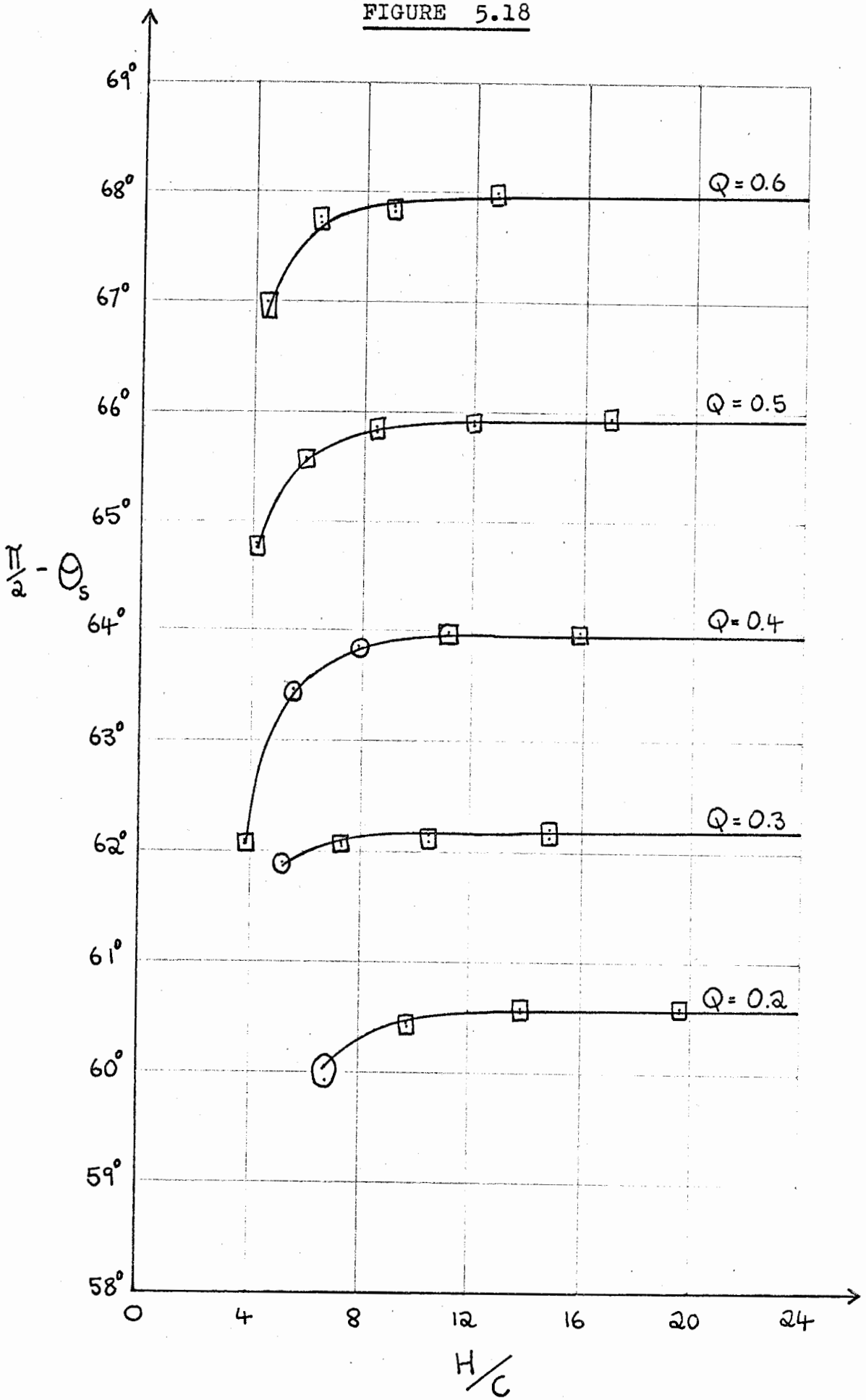
69°
68°
67°
66°
65°
64°
63°
62°
61°
60°
59°
58°
$\frac{\pi}{2} - \theta_s$
Q = 0.6
Q = 0.5
Q = 0.4
Q = 0.3
Q = 0.2
0
4
8
12
16
20
24
H/C

FIGURE 5.19

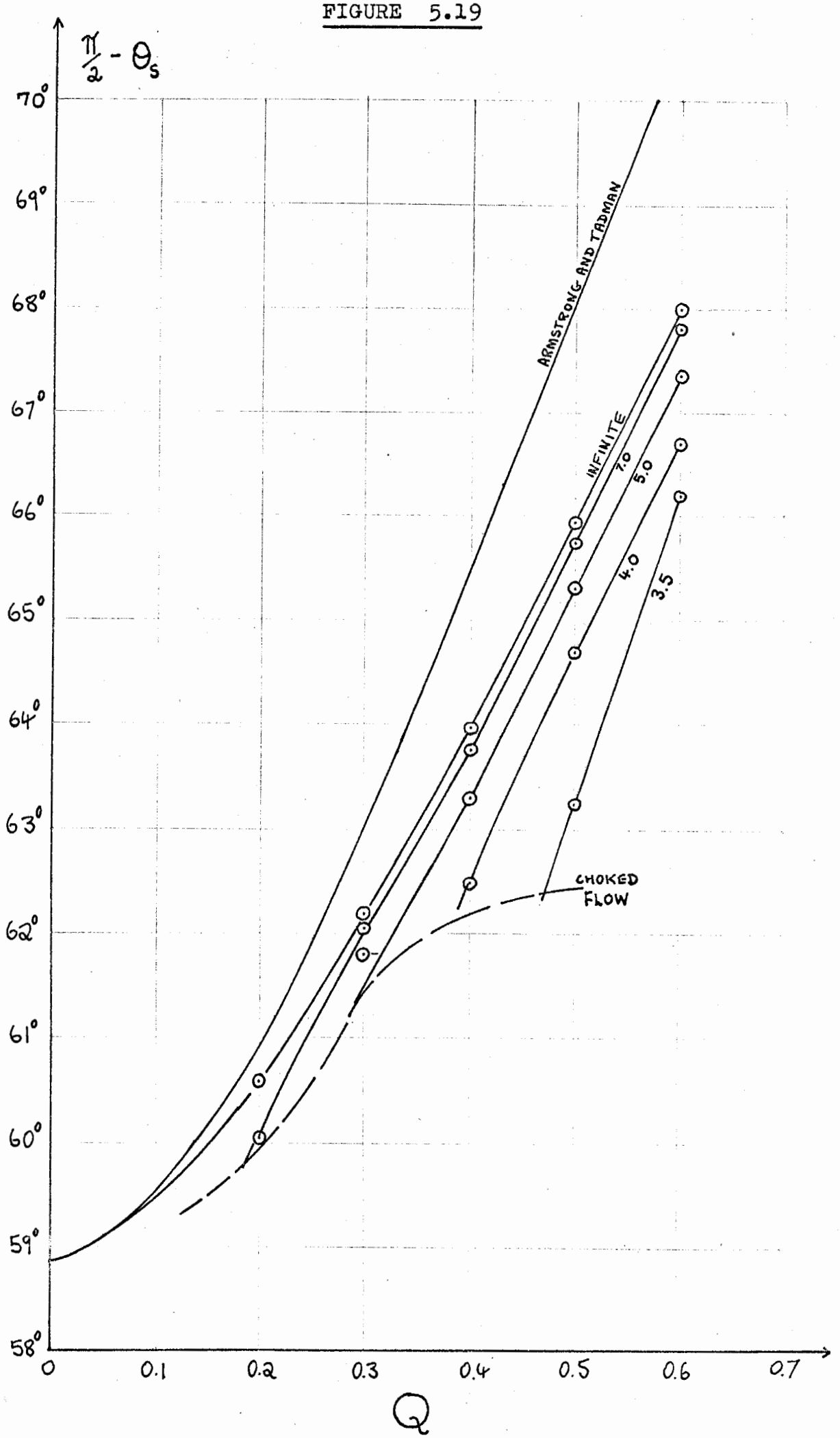
$\frac{\pi}{2} - \theta_s$
70°
69°
68°
67°
66°
65°
64°
63°
62°
61°
60°
59°
58°
0
0.1
0.2
0.3
0.4
0.5
0.6
0.7
Q
ARMSTRONG AND TADMAN
INFINITE
7.0
5.0
4.0
3.5
CHOKED FLOW

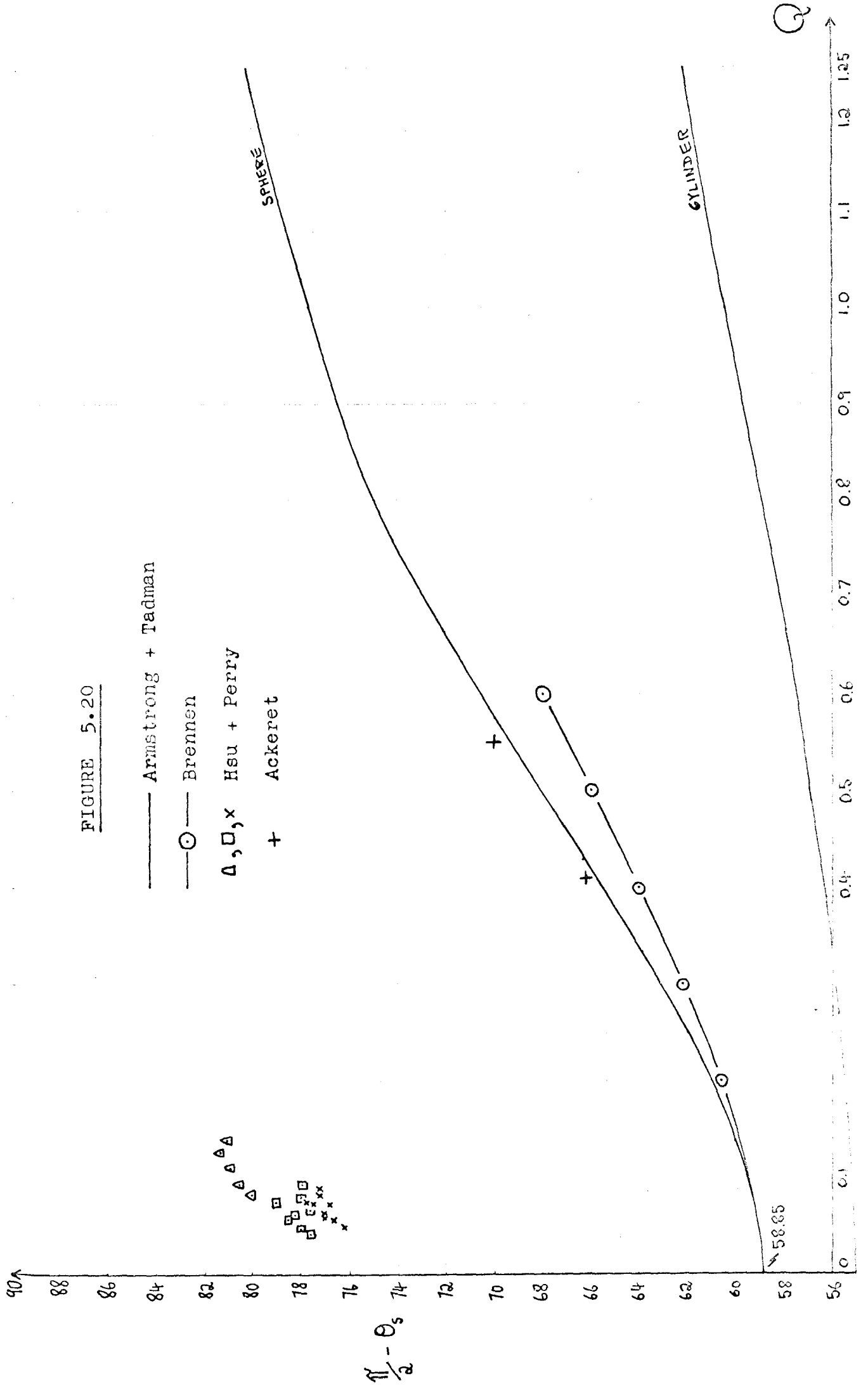
FIGURE 5.20
Armstrong + Tadman
Brennen
Δ, □, × Hsu + Perry
+ Ackeret
SPHERE
CYLINDER
58.85
$\frac{\pi}{2} - \theta_s$
Q
90
88
86
84
82
80
78
76
74
72
70
68
66
64
62
60
58
56
0
0.1
0.4
0.5
0.6
0.7
0.8
0.9
1.0
1.1
1.2
1.25

section 3.4.4 as well as the velocity as can easily be shown from the Dirichlet solution.) In the case of the cylinder , the same reasoning gives $\theta_s \to 0$ as $Q \to 1.5$.

In figure 5.19 the authors results are tentatively produced to $Q = 0$ and would seem to be closest to the results of Armstrong and Tadman at lower Q .

Some experimental results given by Hsu and Perry (Ref. 19) are included in figure 5.20. These show marked disagreement , not only with the theoretical results but also with the following observations.

Reichardt (Ref. 34 , quoting results of experiments by Ackeret) includes pressure distributions for the cavitating flow past a sphere. From these the separation angles would seem to be roughly as indicated in figure 5.20. Similarly the experimental distributions of Rouse and Mc Nown (Ref. 38) would seem to display values of $\pi/2 - \theta_s$ varying from 60^o at $Q = 0.2$ to 80^o at $Q = 0.7$.

Konstantinov (Ref. 24) gives experimental pressure distributions for the cavitating flow past a cylinder ; these show fair agreement with the results of Armstrong and Tadman with values between 60^o and 70^o for Q from 0.5 to 1.2 .

Hsu and Perry conclude , however , that their measurements , based on the observance of a scalloped line of demarcation (due , in their opinion, to surface tension) , may be a little high.

Finally , of course , a remark of section 1.4.6 must be repeated. In the flow of a viscous fluid the point of smooth separation will be determined by the boundary layer and the pressure distribution just

outside the layer. A comparison with the ideal fluid results is , nevertheless , interesting.

5.4.3 Wetted surface results for the Sphere.

Figure 5.21 shows the type of wetted surface pressure distribution obtained for the sphere , the mesh point values being marked ; also plotted on that graph is the pressure distribution for the equivalent Dirichlet or non-cavitating flow (dotted line).

As in the case of the disc , distributions for different H/C , same Q were indistinguishable , except , in this case , for a very small portion near separation , giving slightly different separation angles.

The distribution variation with Q is shown in figure 5.22 and seems regular. Also plotted is one of the experimental distributions of Rouse and Mc Nown (Ref. 38) , in this case with Q = 0.3 ; the same comments apply as in the case of the disc.

The values obtained for C_D are shown in figure 5.23. These exhibit the same difference in behaviour near choked flow between Q = 0.2,0.3 and Q = 0.4,0.5,0.6 as does the separation angle.

Plotting the values of C_D for $H/C = \infty$ against Q gives the result shown in figure 5.24. Both Hsu and Perry (Ref. 19) and Eisenberg and Pond (Ref. 10) give numerous experimental results and the mean line through each set is shown in figure 5.24. Also shown for the sake of demonstration , are the theoretical results of Armstrong and Tadman (Ref. 3) and the experimental results of Waid (Ref. 45) for C_D of the plane flow past

FIGURE 5.21

A Pressure Distribution on the Surface of the Sphere showing the Positioning of the Mesh Points. —⊖—

Dirichlet Flow – – – – –

Rouse and M^{c} Nown ⊡

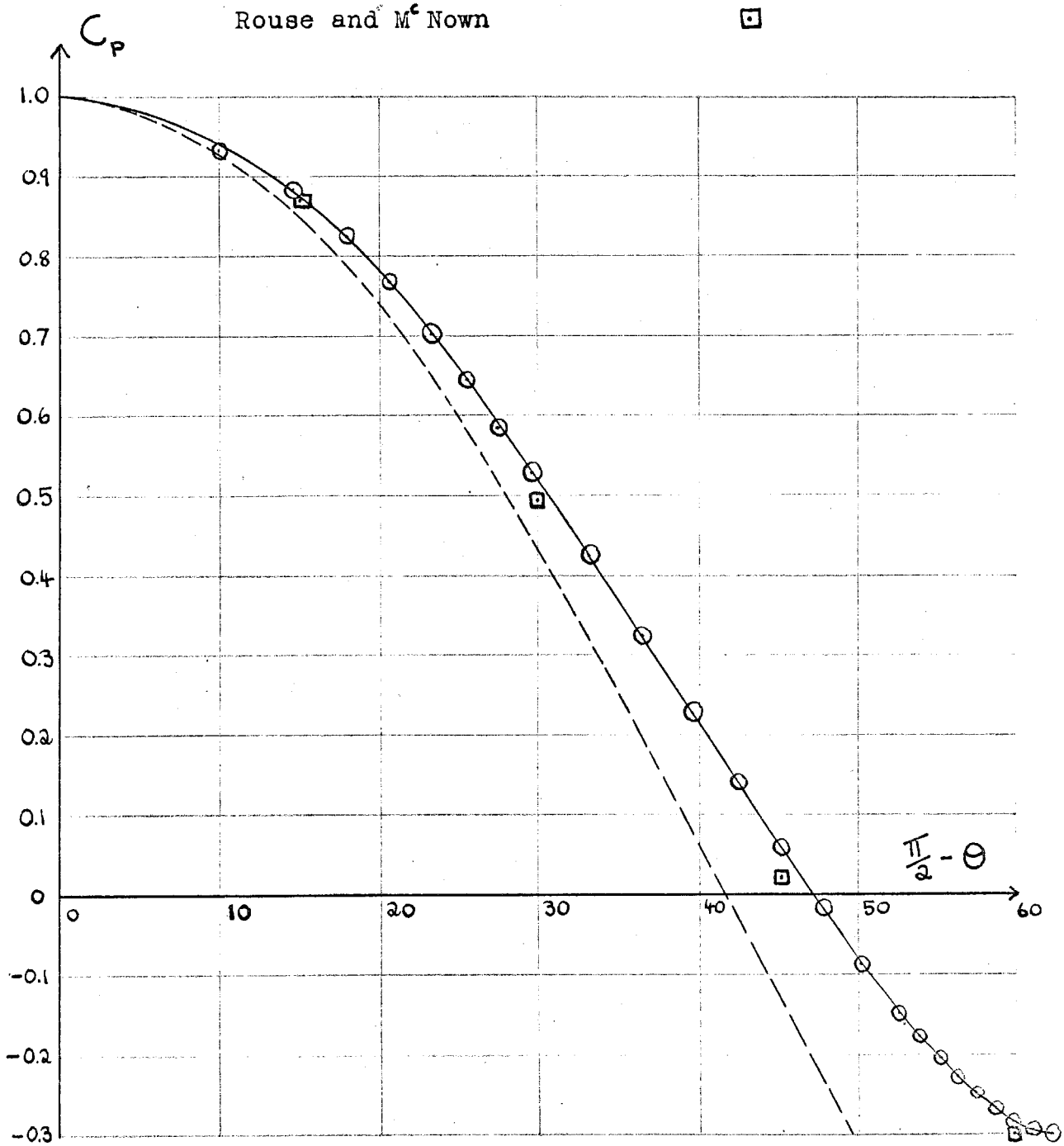

FIGURE 5.22

Pressure Distribution Variation with Cavitation Number. Sphere.

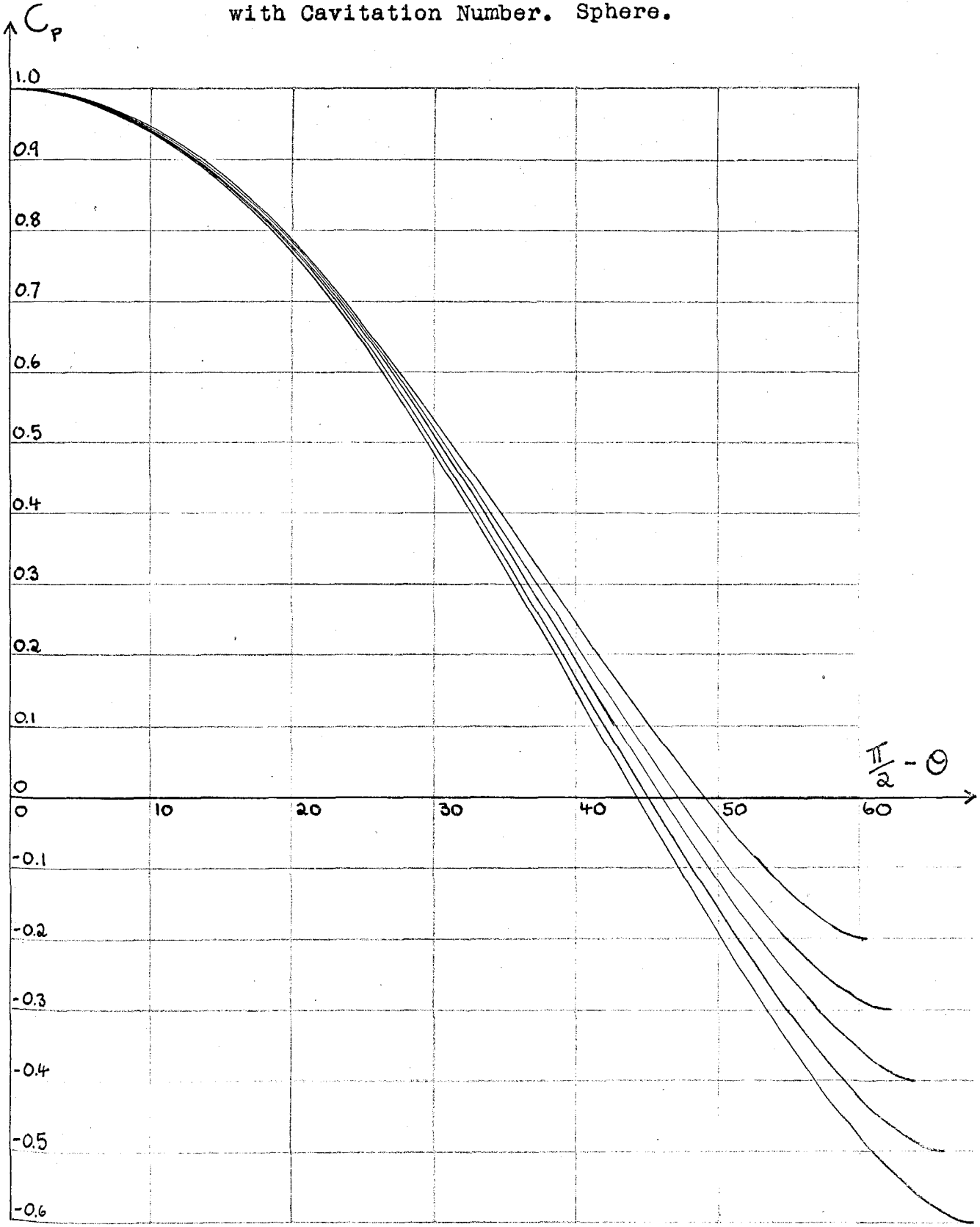

FIGURE 5.23

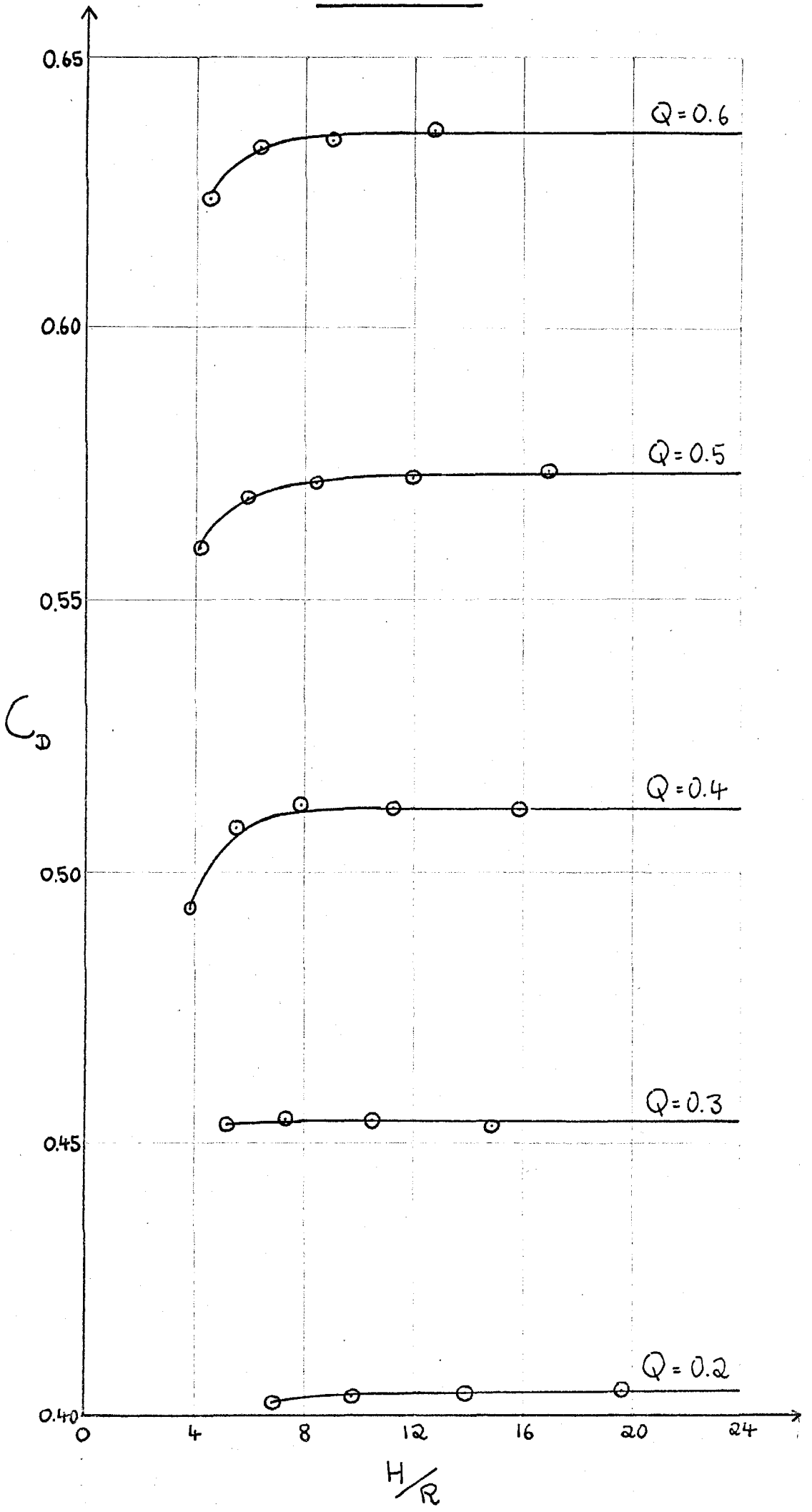

FIGURE 5.24

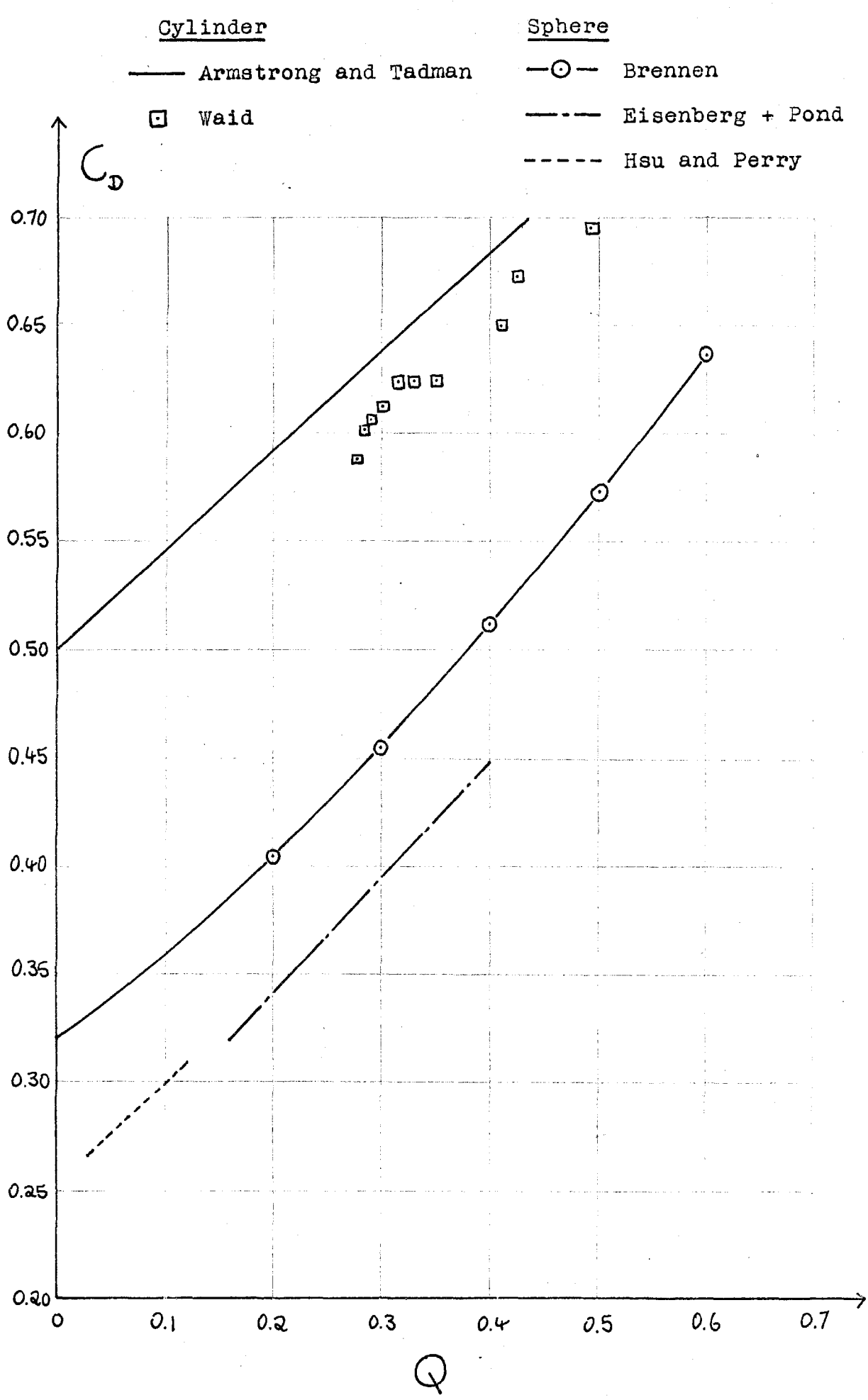
Cylinder
Armstrong and Tadman
Waid
Sphere
Brennen
Eisenberg + Pond
Hsu and Perry
C_D
0.70
0.65
0.60
0.55
0.50
0.45
0.40
0.35
0.30
0.25
0.20
0
0.1
0.2
0.3
0.4
0.5
0.6
0.7
Q

a cylinder.

An interesting observation , based on the results of this section and 5.4.1 , that can be made is that the experimentally measured drags are invariably substantially below the theoretical. This is , presumably , due to the presence of the boundary layer which produces a lower pressure gradient at separation, thus "flattening" the pressure distribution for a given cavitation number and producing a lower C_D. This is corroborated by the comparison of the pressure distributions of figure 5.21 , though not of figure 5.14.

In figure 5.25 the authors results for $C_D/(1+Q)$ at $H/C = \infty$ would seem to compare favourably with those of Armstrong and Tadman (Ref. 3). As is widely recognized , the variation of $C_D/(1+Q)$ with Q for smoothly separating flow (sphere) is very much greater than that for abruptly separating flow (disc). Thus the accuracy of equation [2.1] in the case of the sphere is very limited for both experimental and theoretical results.

5.4.4 Cavity Dimension Results for the Disc.

Figure 5.26 shows all the results obtained for $(C/B)^2$ for the disc. Also presented are most of the values of $(C/B)^2_{MIN}$ corresponding to the points for $(C/B)^2$. Where each pair of curves intersect , that point should give the choked flow condition for that particular Q .

The behaviour of the two curves in each set near the choked flow condition is not very well defined by the results obtained. However , with the aid of the

FIGURE 5.25

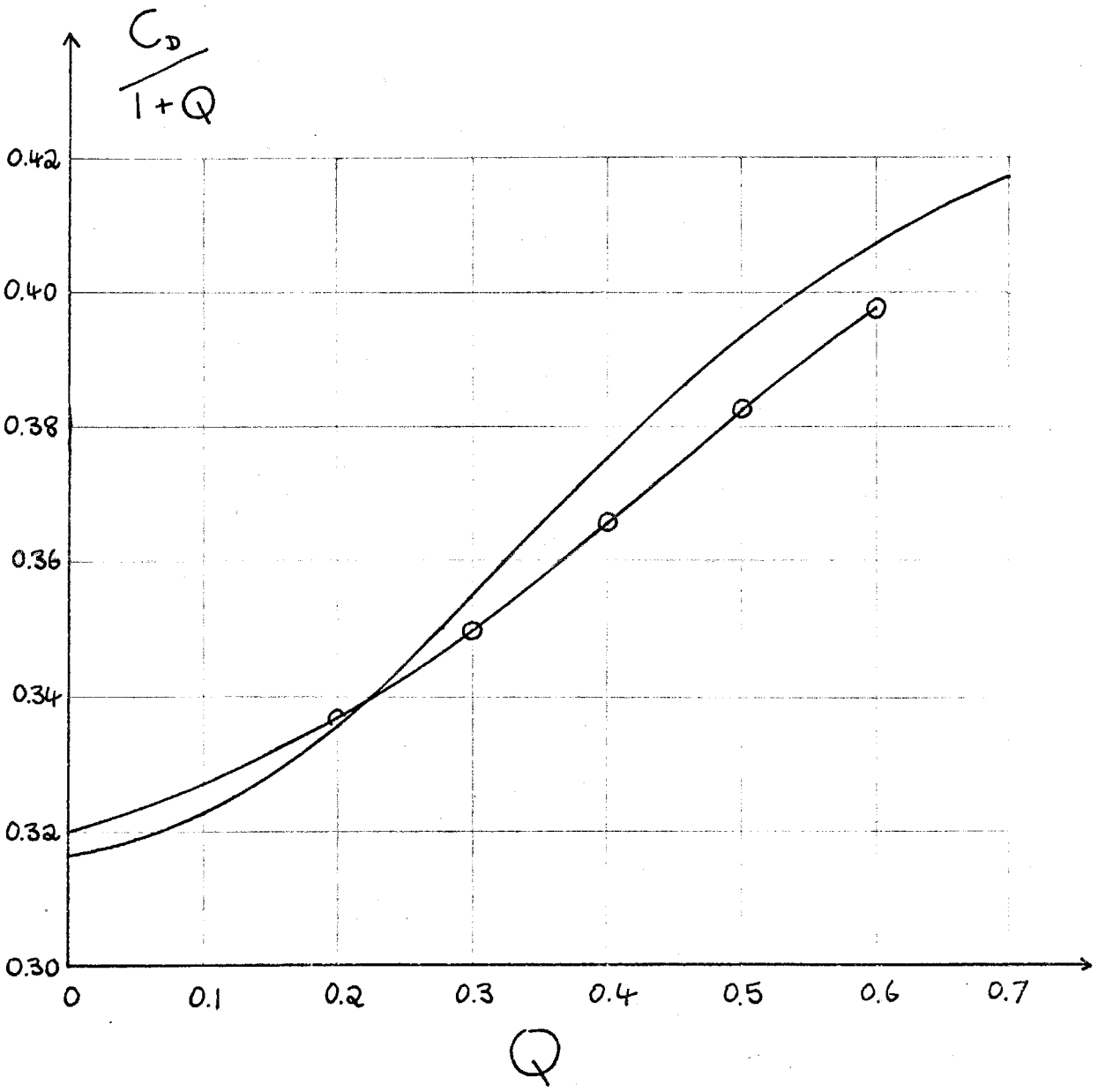
Armstrong and Tadman (Sphere).
Brennen.
$\frac{C_D}{1+Q}$
0.42
0.40
0.38
0.36
0.34
0.32
0.30
0
0.1
0.2
0.3
0.4
0.5
0.6
0.7
Q

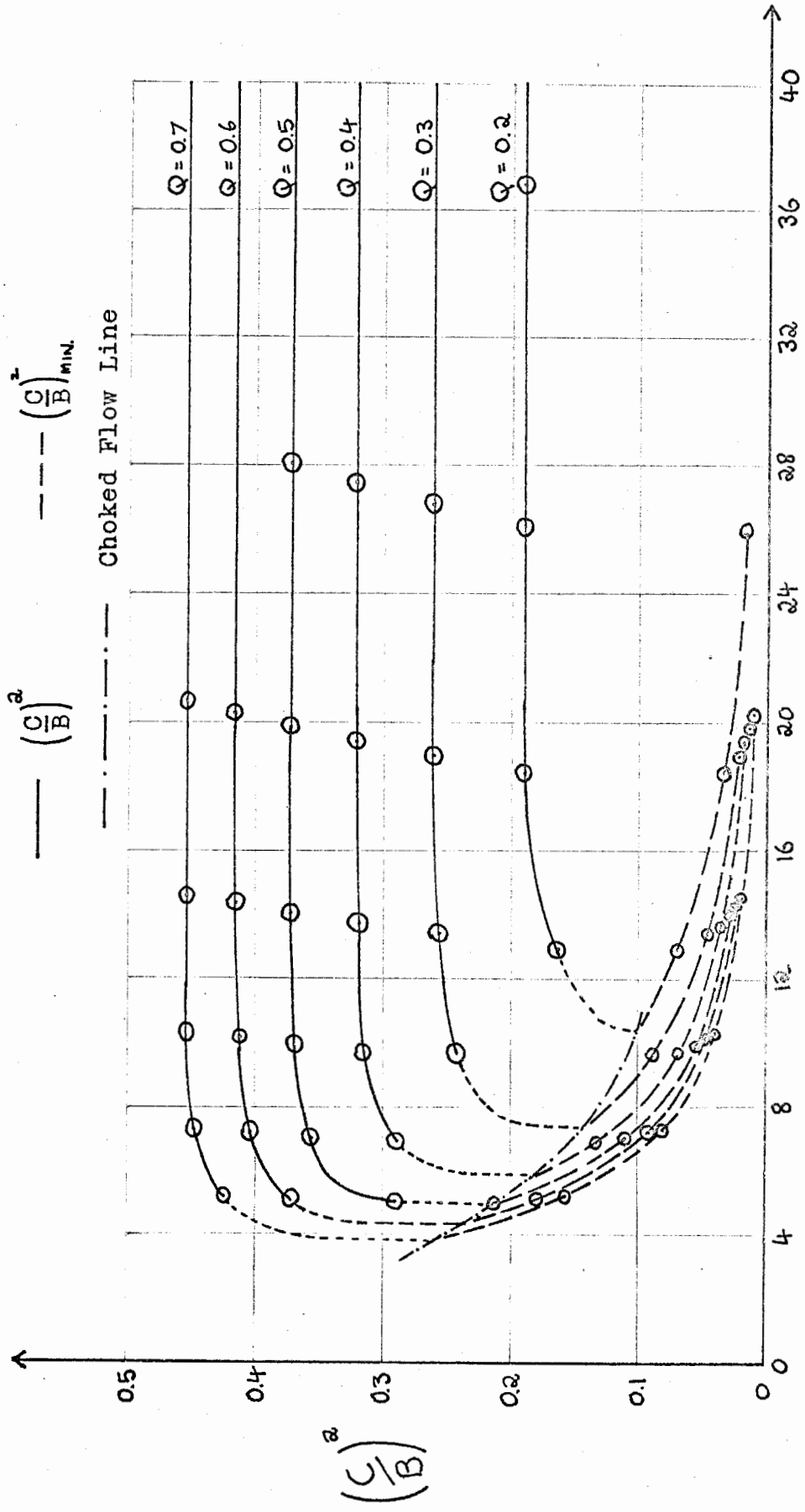

FIGURE 5.26

Results for the Disc.

$\left(\frac{C}{B}\right)^2$ ——— $\left(\frac{C}{B}\right)^2_{MIN.}$ — · — · —

FIGURE 5.27

Results for the Disc.

——— $\left(\frac{C}{B}\right)^2$ for various $\frac{H}{C}$

—·— Choked Flow Line.

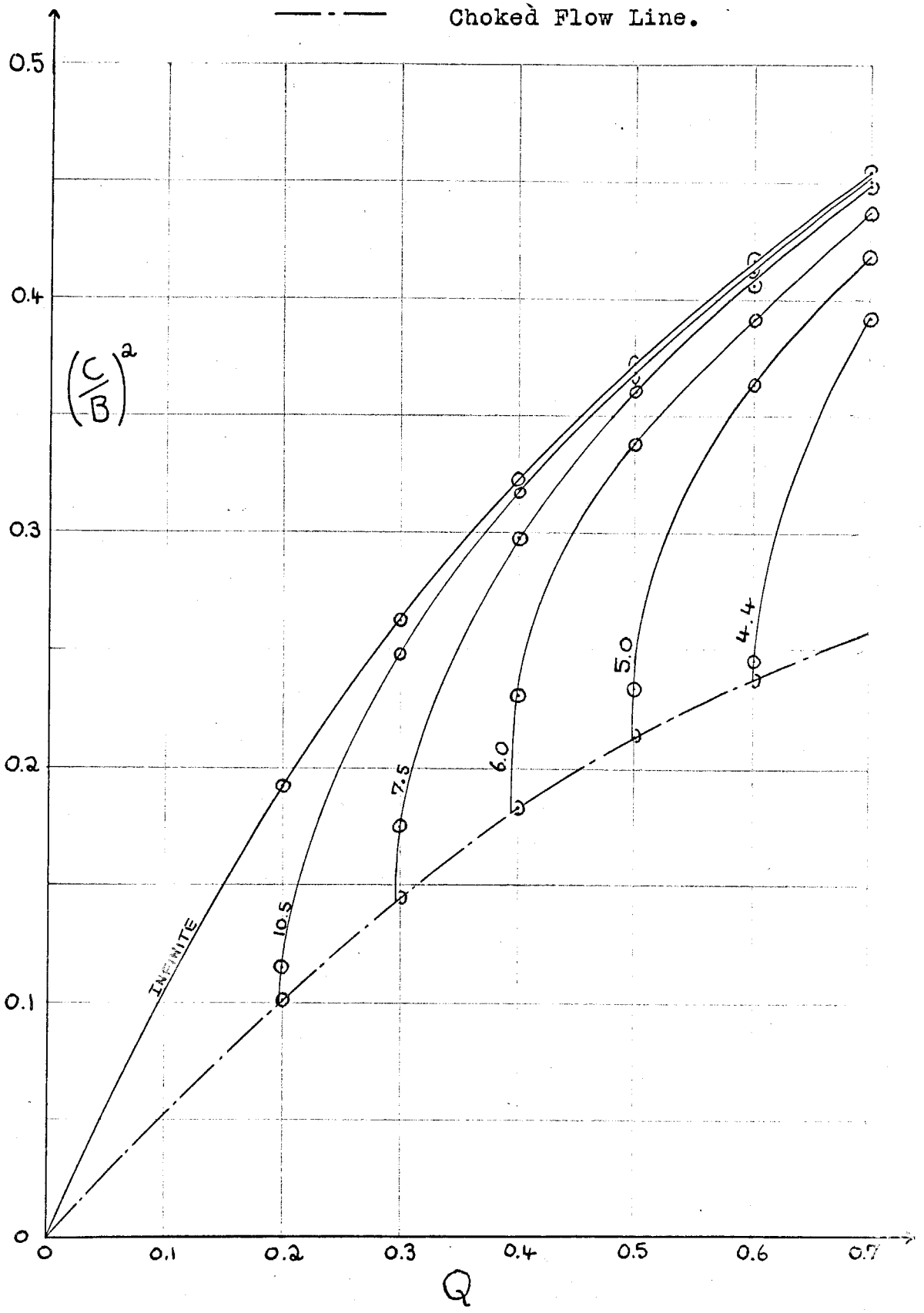

FIGURE 5.28 Results for the Disc.

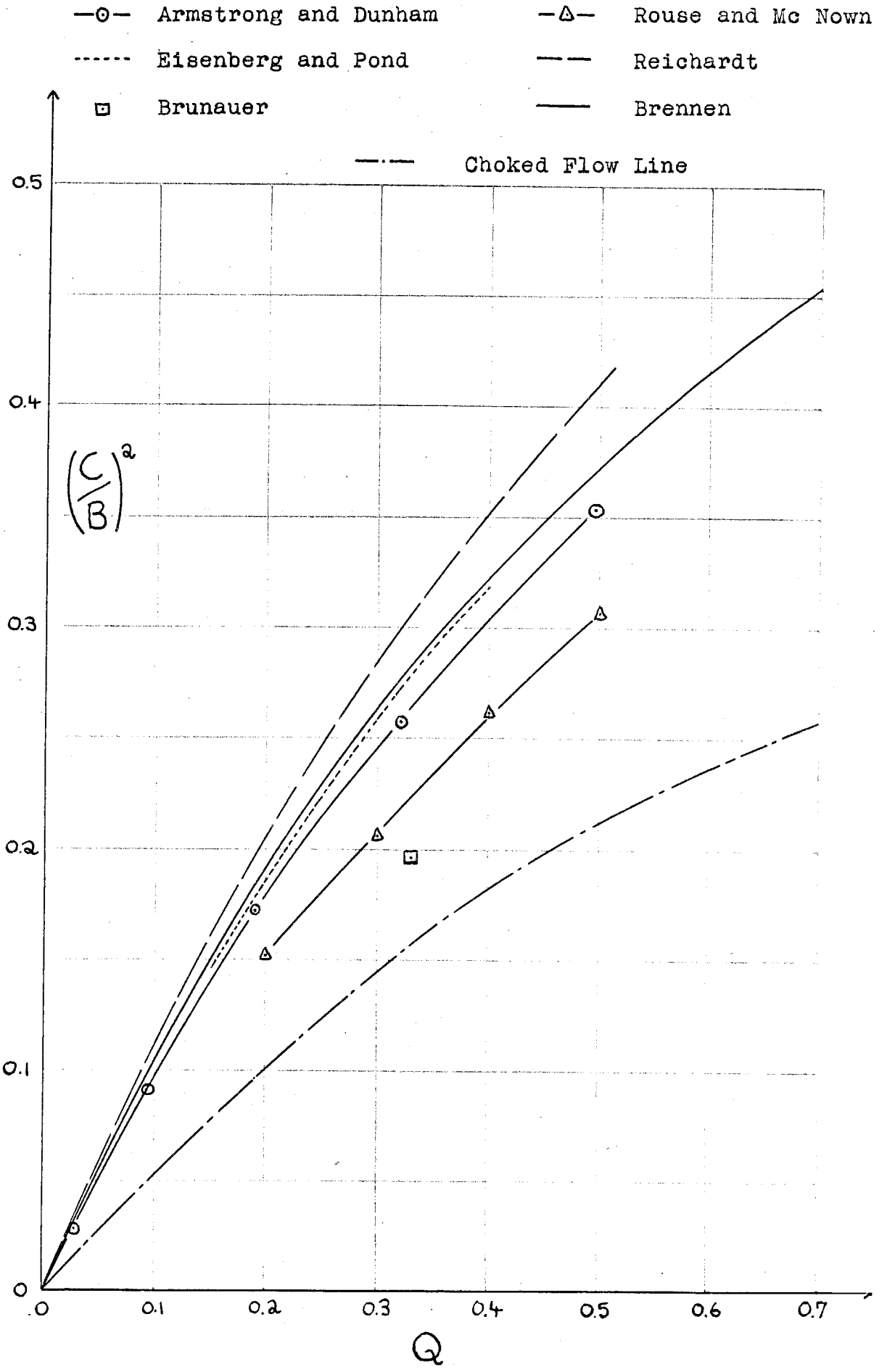

assumption given in section 5.4.1 , that the choked flow condition occurs at those values of H/C shown in figure 5.15 , the choked flow points can be obtained with fair accuracy in figure 5.26 . They must be the points where the three lines intersect in each case.

The line joining the choked flow points , the choked flow line , is therefore constructed and shown in figure 5.26.

The corresponding graphs of $(C/B)^2$ against Q for various values of H/C is shown in figure 5.27 ; the choked flow line is also transcribed to this graph. The latter exhibits a smoothness in both 5.26 and 5.27 which would seem to indicate that the tentative construction has given fairly accurate results. The reader is reminded that the choked flow line is independent of the mathematical model chosen.

Clearly the most accurate definition of results is obtained at larger H/C. The line , $H/C = \infty$, is reproduced in figure 5.28 for the sake of comparison. Also shown there are the theoretical results of Armstrong and Dunham (Ref. 1) and Brunauer (Ref. 9) ; the experimental results of Rouse and Mc Nown (Ref. 38) , Eisenberg and Pond (Ref. 10 , a mean line) and the results of Reichardts empirical formula (equation [2.10]). The last is , of course , only designed for the range $0 < Q < 0.1$ .. The authors results would seem a little higher than others though close to those of Armstrong and Dunham and Eisenberg and Pond.

The authors results for C/L are shown in figure 5.29 . A similar tentative construction to that for $(C/B)^2$ is made in that graph , being simpler in this case since

FIGURE 5.29

Results for the Disc

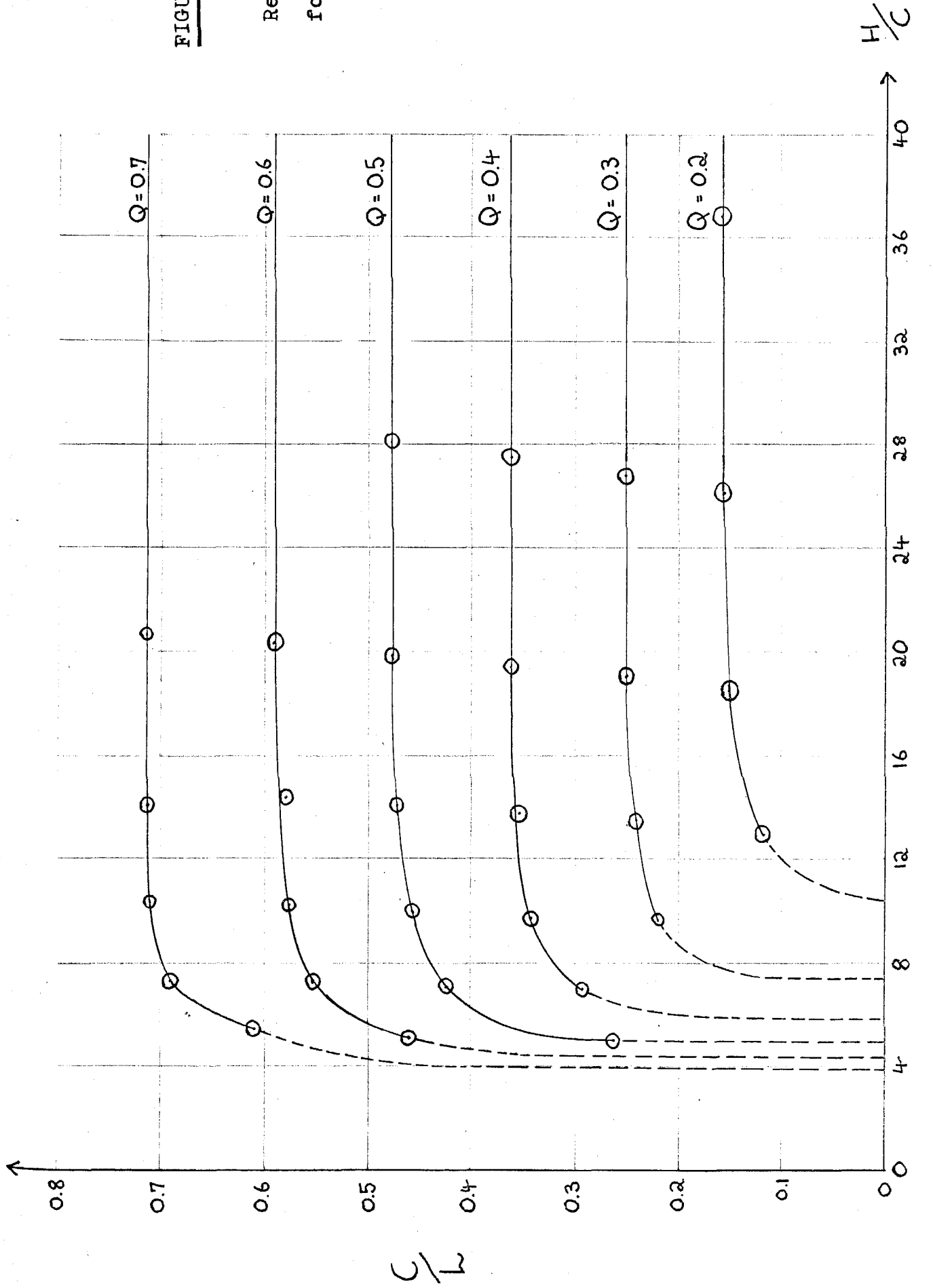

the choked flow condition is $L = \infty$.

Figure 5.30 presents the graphs of C/L against Q for the particular values of H/C shown.

In figure 5.31 the curve for $H/C = \infty$ is reproduced to compare again with results by some of the authors mentioned above. Also presented are some experimental results given by Gadd and Grant (Ref. 15, a mean line).

The experiments of Gadd and Grant were carried out in a fixed walled channel with H/C = 14.67 ; those of Rouse and Mc Nown in both fixed and free channels with H/C = 12.94 ; the experimental results of Reichardt are for a free jet ; Eisenberg and Pond do not give details of H/C ; the theoretical results of Armstrong and Dunham are , of course , for an infinite stream.

The result given by Brunauer (Ref. 9) in both figure 5.31 and figure 5.28 would seem to agree less well with other values. However , a knowledge of his value of H/C may bring his results into line with those of figures 5.30 and 5.27.

5.4.5 Cavity Dimension Results for the Sphere.

Figures 5.32,5.33,5.34,5.35 present the authors results for the dimensions of a cavity behind a sphere ; these figures are parallel to 5.26,5.27,5.29 and 5.30 for the disc so little further comment on their construction is required.

Figure 5.33 shows the appropriate sort of

FIGURE 5.30

Results for the Disc

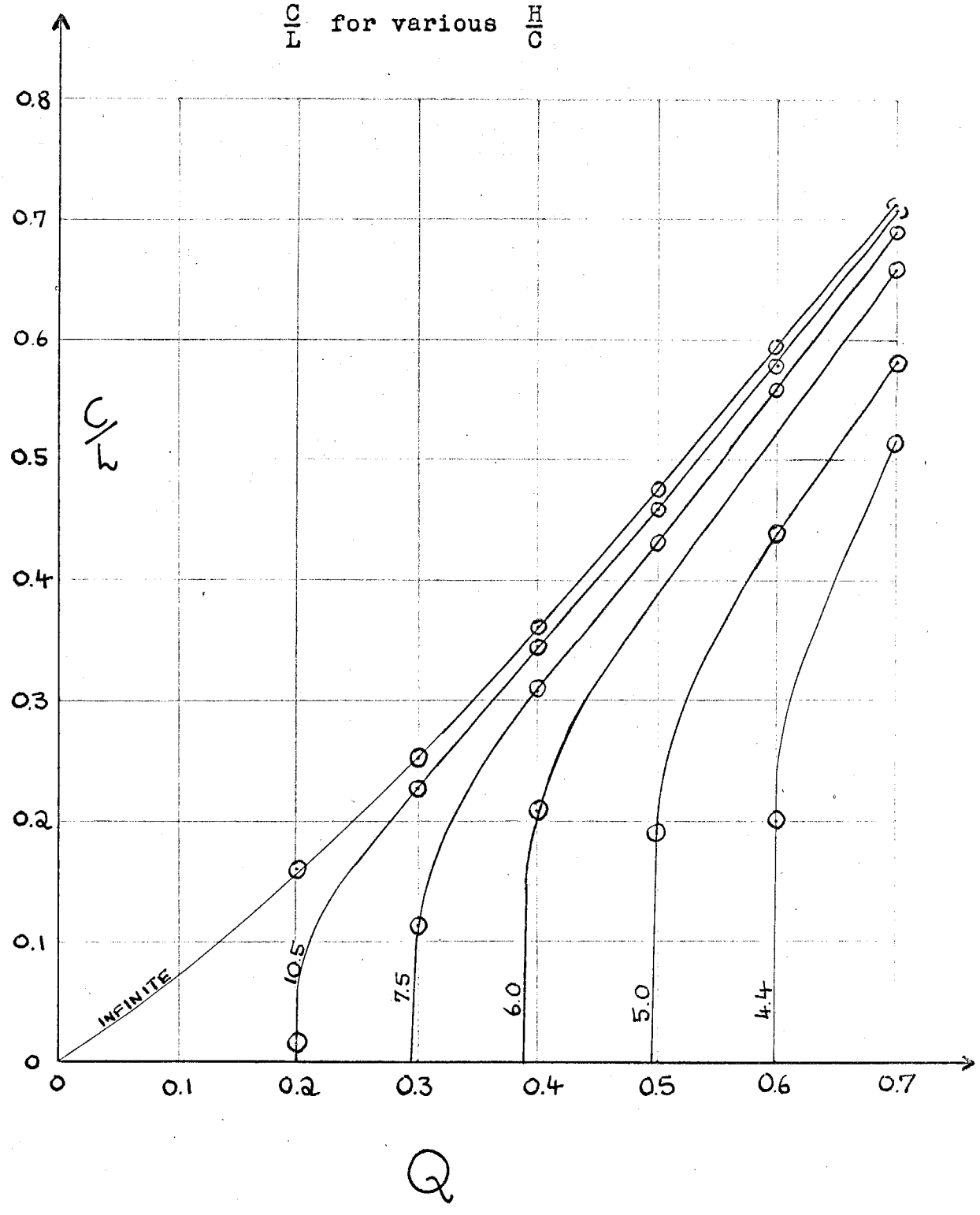

FIGURE 5.31 Results for the Disc

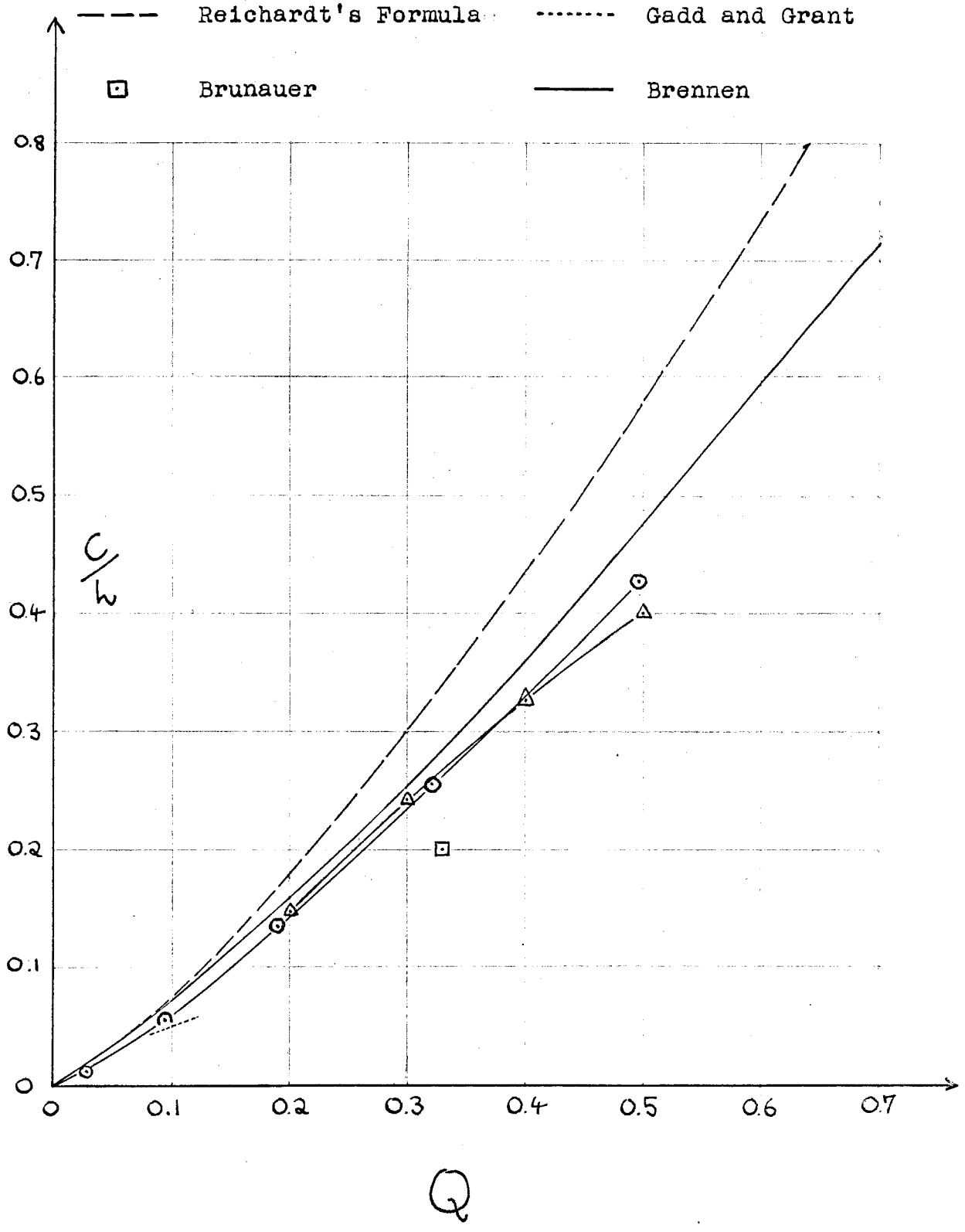

FIGURE 5.32 Results for the Sphere

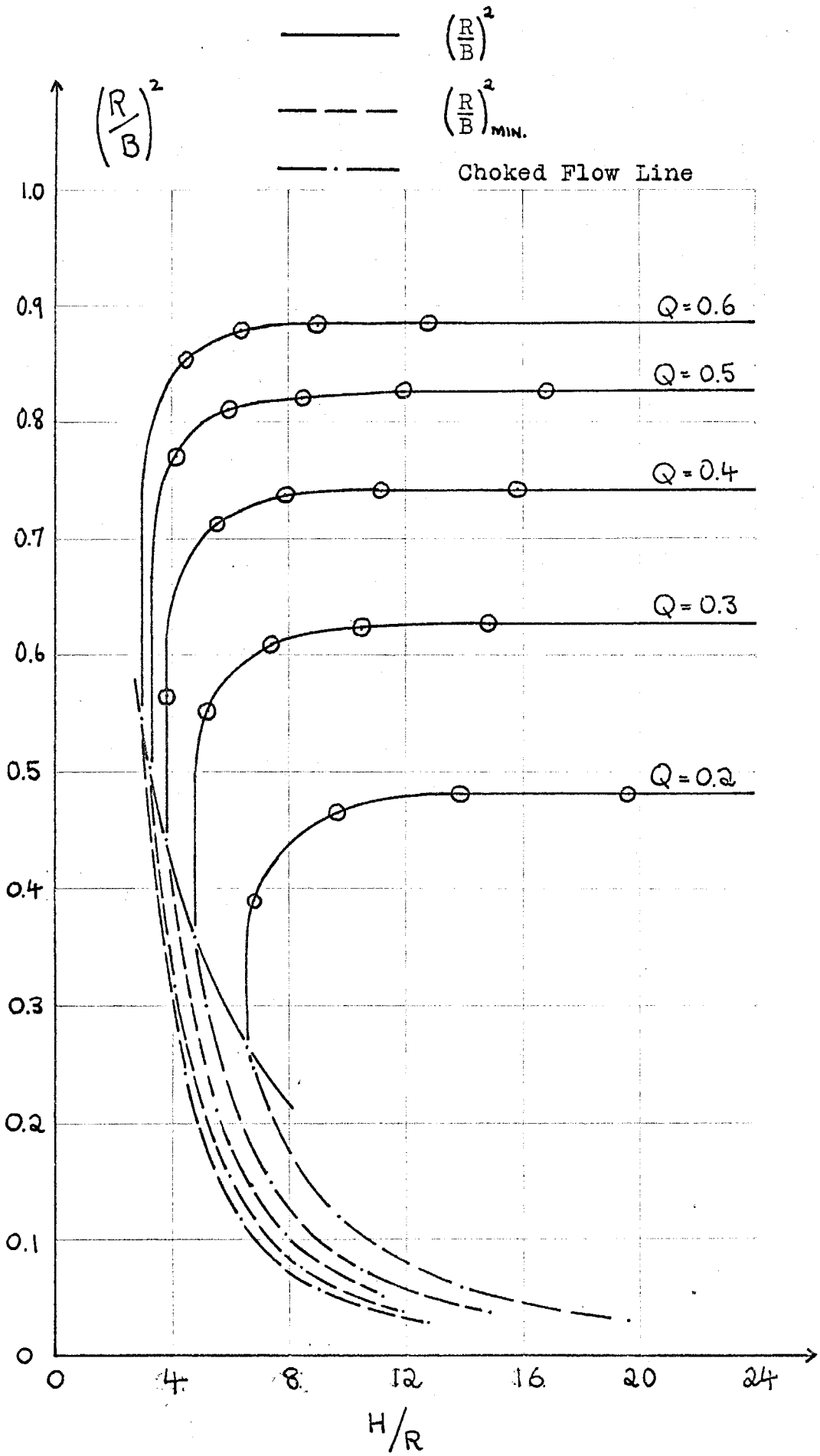

FIGURE 5.33 Results for the Sphere

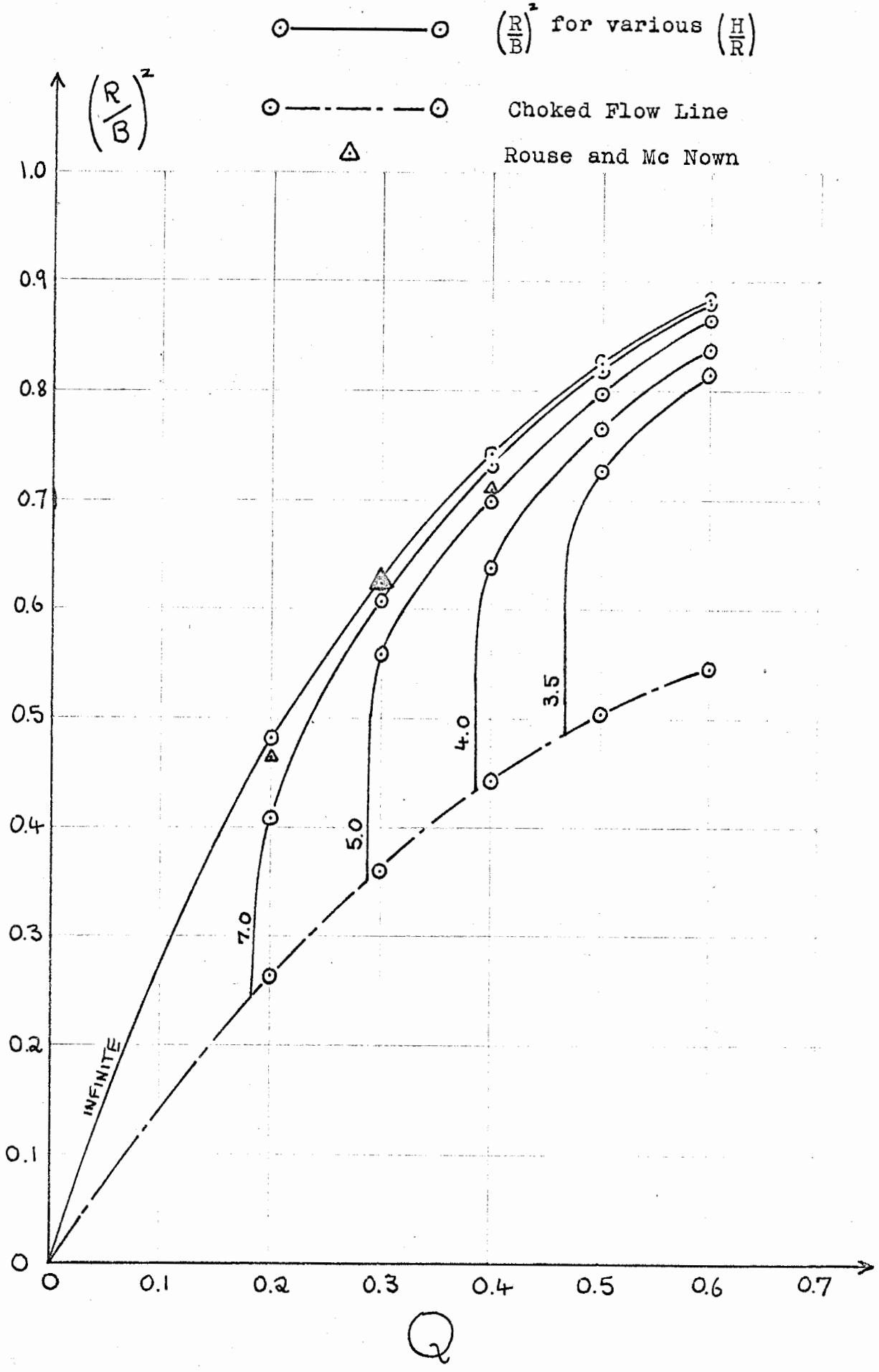

FIGURE 5.34

Results for the Sphere

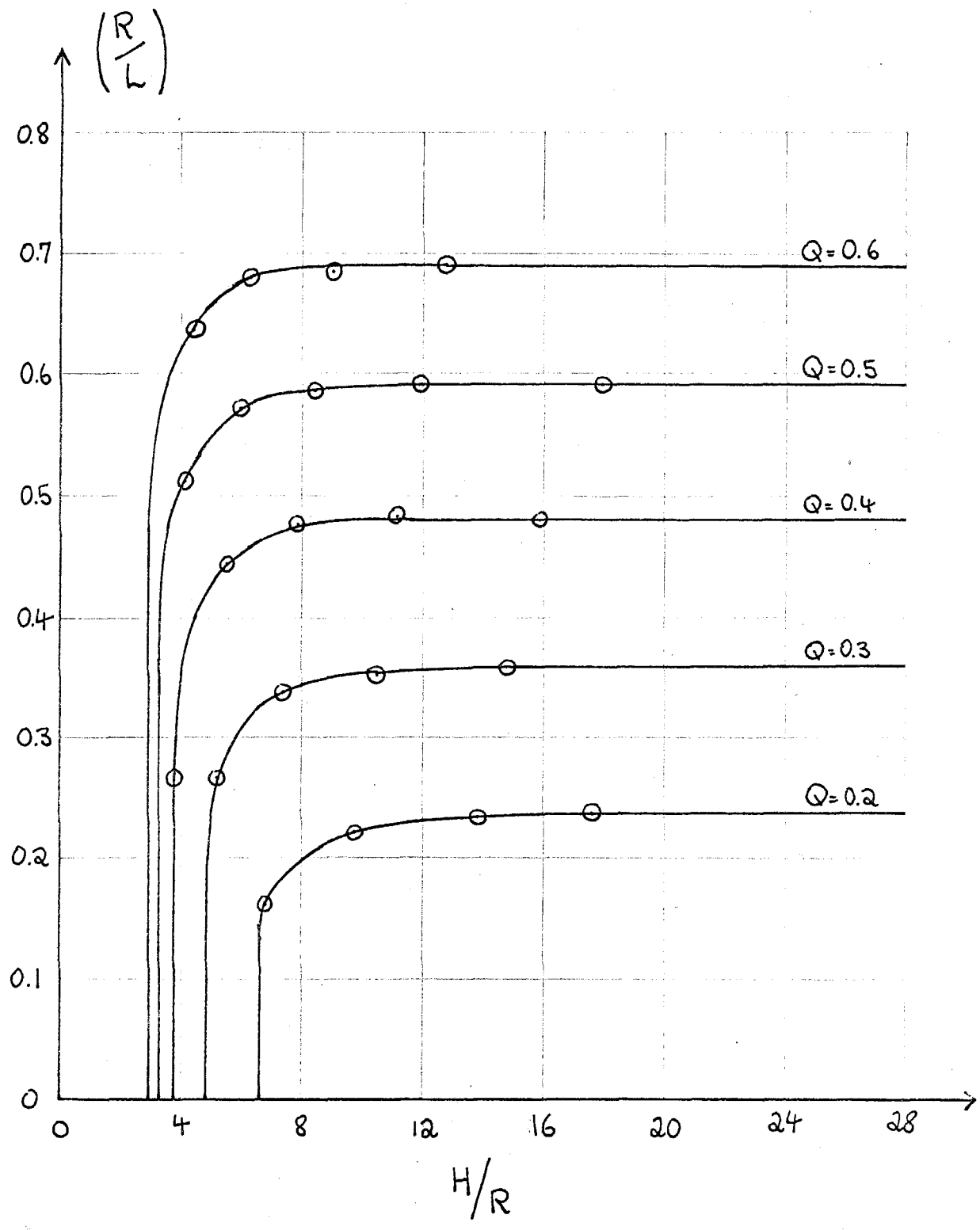

FIGURE 5.35

Results for the Sphere

—⊙— $\left(\frac{R}{L}\right)$ for various $\left(\frac{H}{R}\right)$

△ Rouse and Mc Nown

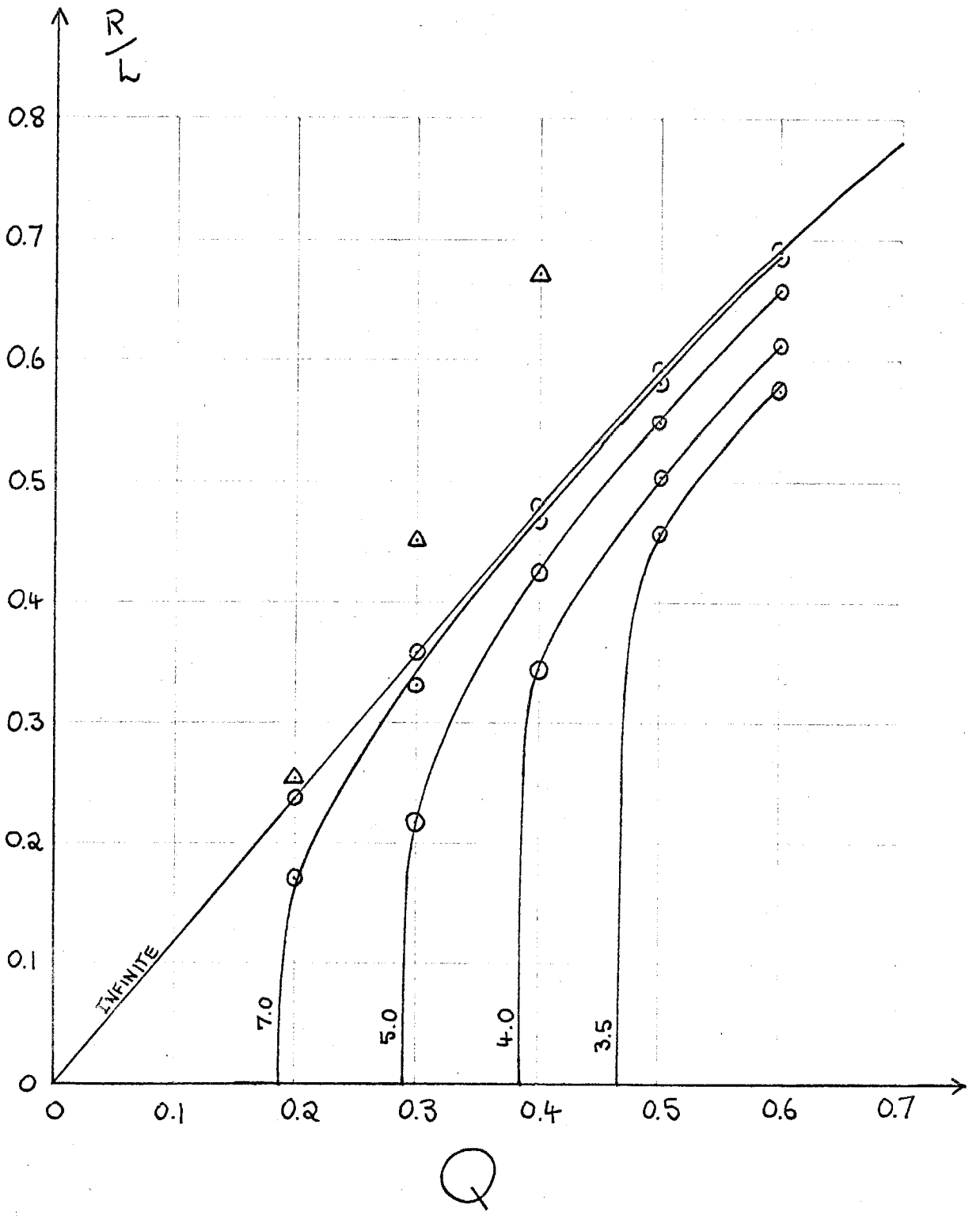

tendency ; that is , $(R/B)^2 \rightarrow 1$ as $Q \rightarrow 1.25$. Also presented in that figure (as well as figure 5.35) are the experimental results taken from cavity profiles given by Rouse and Mc Nown (Ref. 38) . Those profiles are rather small which may have led to inaccuracies in the authors measurements from them. This applies less to the results presented as from Rouse and Mc Nown for the disc , the cavities being much larger. However , it applies more in the results of figure 5.35 ,which may account for the rather larger discrepancy than in 5.33 , since the cavities at higher Q are very small.

5.4.6 Separation Singularity Results.

The results given in the final solutions for the unknowns , $K_2, K_3, K_1^*, K_2^*, K_3^*$,in the expansions of section 4.3.7 , are now discussed. All these quantities were seen to converge to steady values before the termination of any solution.

The quantities are not dimensionless as defined in section 4.3.7 ; the author therefore transferred for reasons of compatibility to dimensionless equivalents as follows :

<u>Disc</u>

$$\text{DIM.}(K_2) = \left(\frac{q_c f_s}{m_{j=0}}\right)^{\frac{3}{2}} \frac{K_2}{f_s}$$

$$\text{DIM.}(K_3) = \left(\frac{q_c \sqrt{f_s}}{n_{k_s}}\right)^{\frac{3}{2}} K_3$$

<u>Sphere</u>

$$\text{DIM.}(K_1^*) = \left(\frac{q_c \sqrt{f_s}}{n_{k_s}}\right)^{\frac{5}{2}} K_1^*$$

$$\text{DIM.}(K_2^*) = \left(\frac{q_c f_s}{m_{j=0}}\right)^{\frac{5}{2}} \frac{K_2^*}{f_s}$$

$$\text{DIM.}(K_3^*) = \left(\frac{q_c\sqrt{f_s}}{n_{k_s}}\right)^{\frac{5}{2}} K_3^*$$

The results for the disc are presented in figures 5.36 and 5.37. These exhibit the same type of behaviour as the majority of the other results and were clearly defined in their converged state. It is interesting to note that the relation $\text{DIM.}(K_2) = -1.26 \times \text{DIM.}(K_3)$ holds fairly closely for all pairs of values, indicating a definite strength of singularity in each case.

The magnitudes of the values in figures 5.36 and 5.37 are misleadingly large. The factors used in the conversion to dimensionless quantities (above) are large due to the small mesh lengths, $m_{j=0}$ and n_{k_s}, appearing in the denominators. Typical conversion multipliers are 256 for K_2 and 543 for K_3. Thus the quantities appearing in the expansions of section 4.3.7 are small in relation to the other terms since K_2 and K_3 are again multiplied by factors including the mesh lengths in the numerator.

The results for K_1^*, K_2^* and K_3^* in the solutions for the sphere were, however, less satisfactory. Only one set, namely that for K_3^*, is displayed (figure 5.38). The others showed similar results in which a pattern can barely be distinguished.

The main problem here was that the values were dependent on the smallest differences in $\theta_s^* - \theta_s$. Thus, though the K* values converged to a definite limit with no oscillation for one solution with a set θ_s, once this θ_s was altered, even fractionally, a relatively large

FIGURE 5.36 a

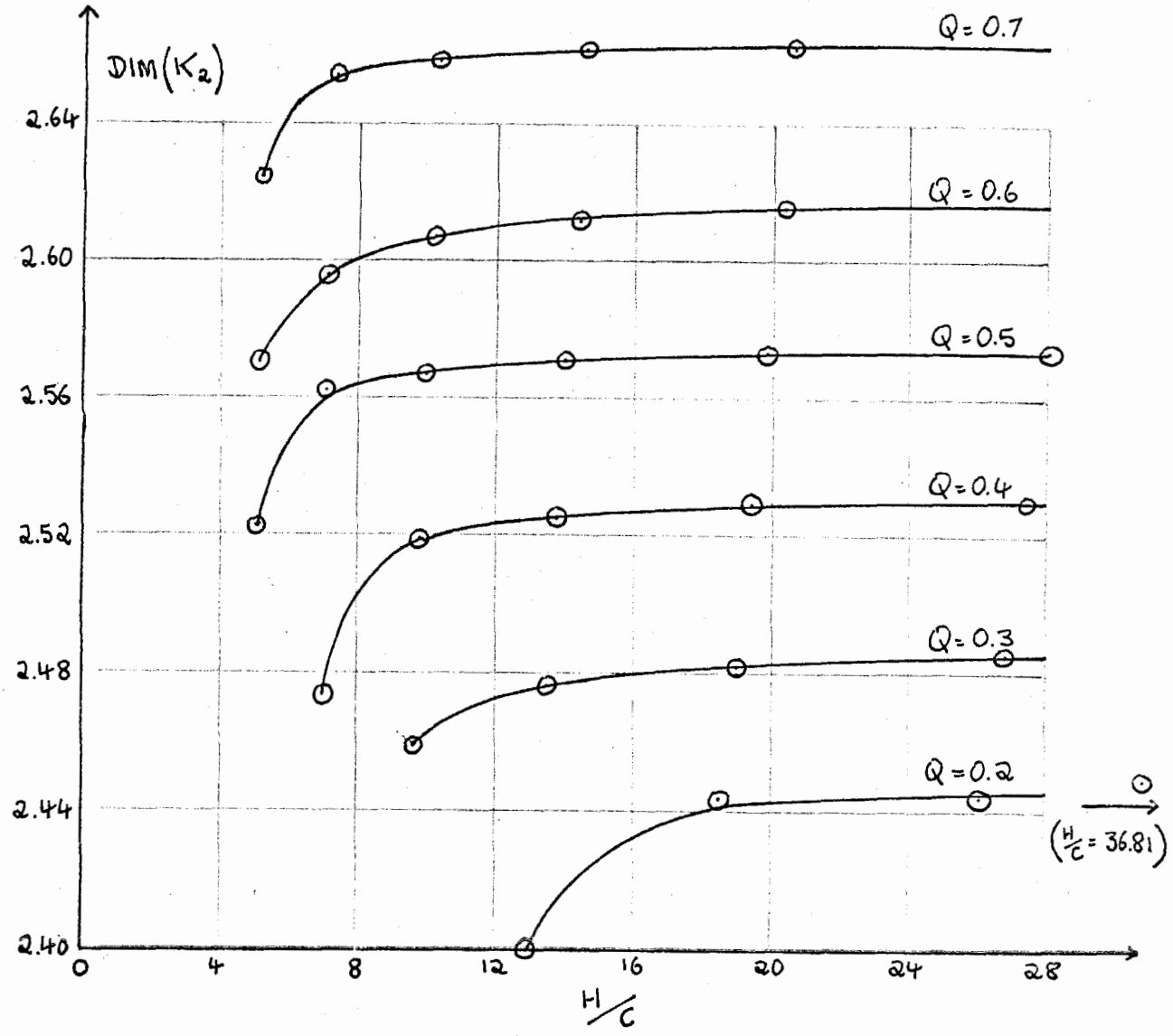

FIGURE 5.36 b

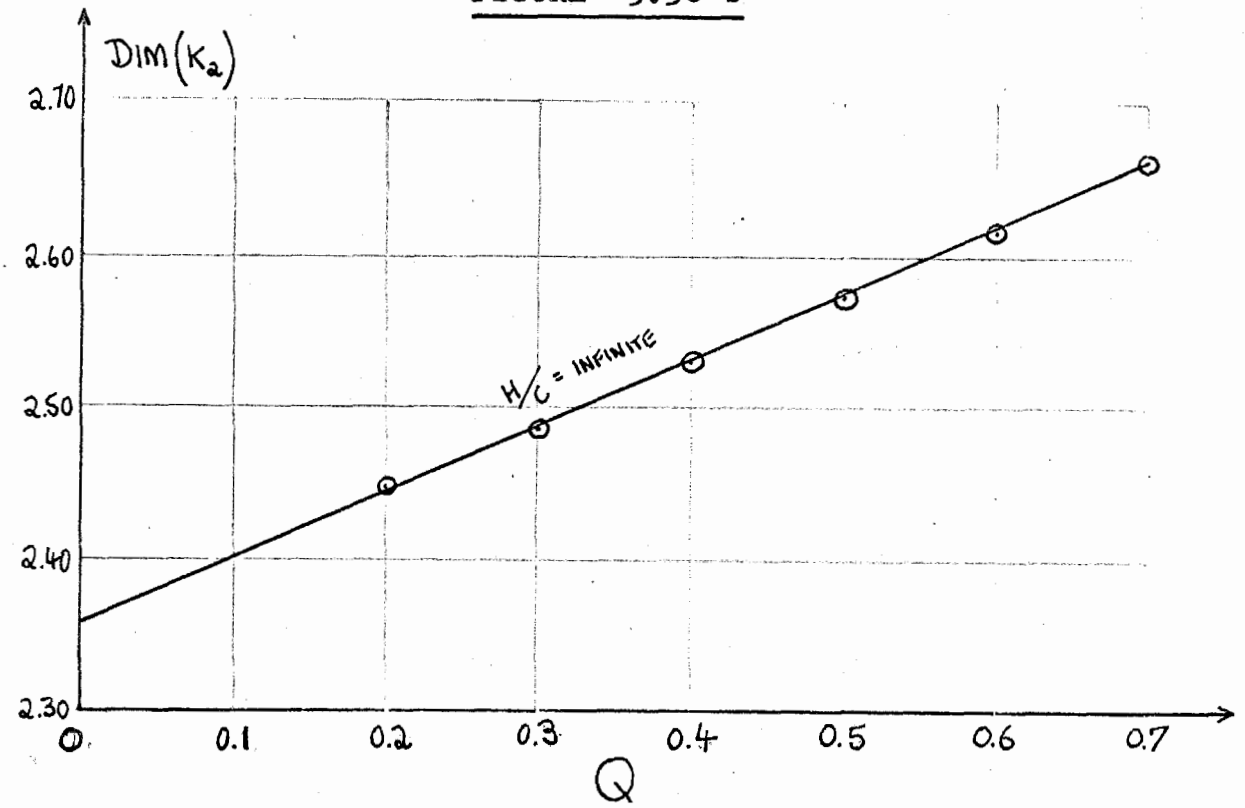

FIGURE 5.37 a

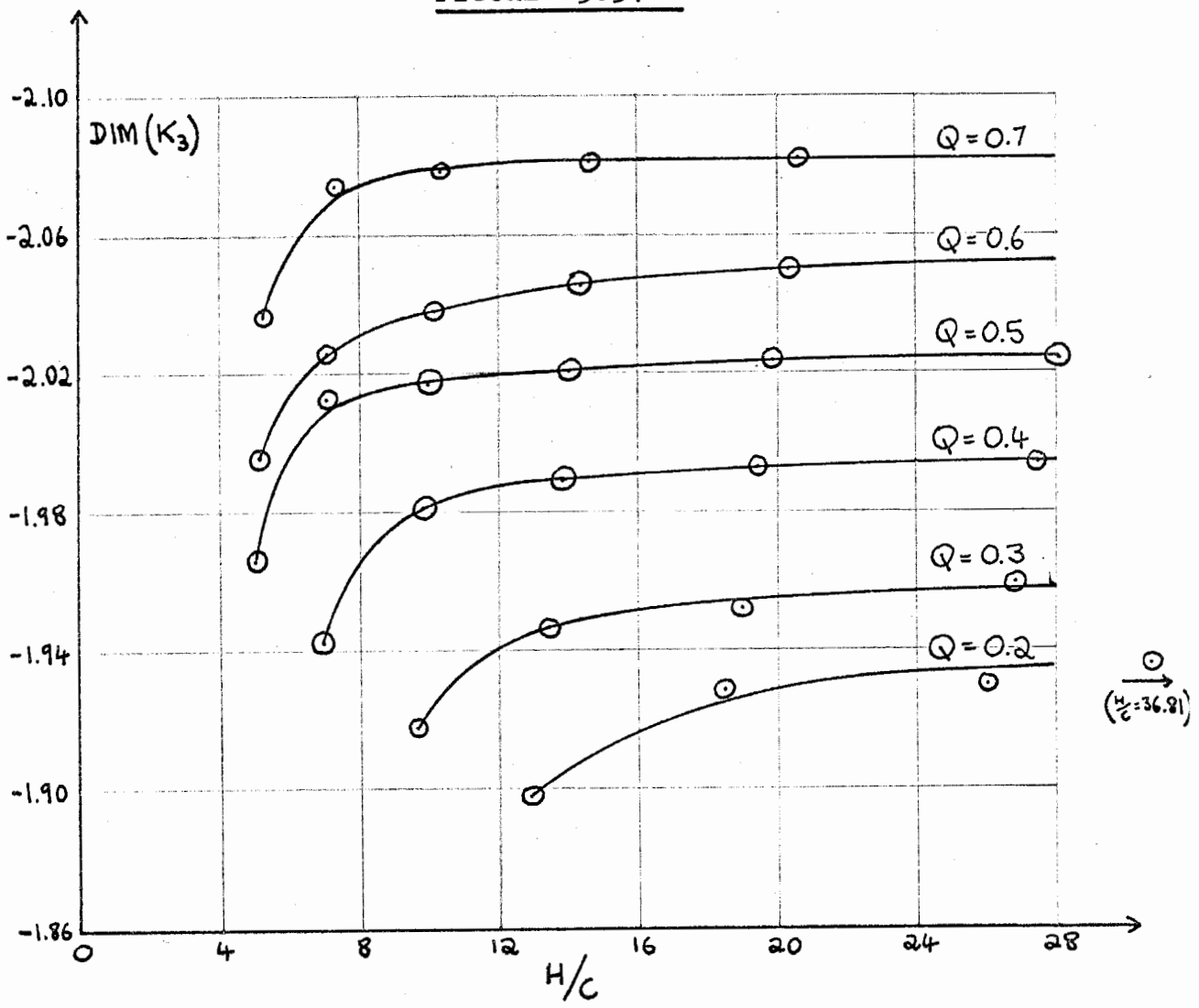

FIGURE 5.37 b

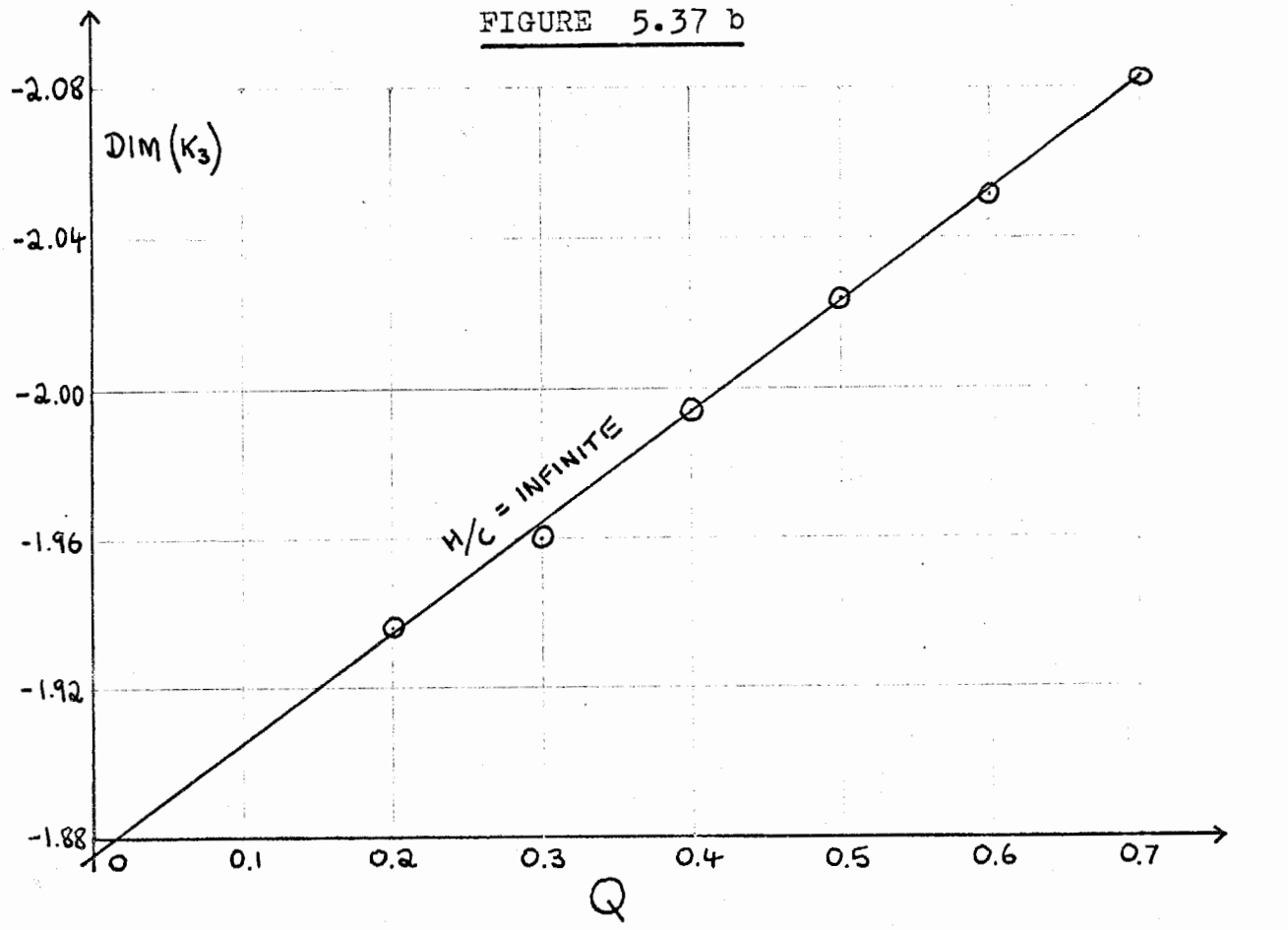

FIGURE 5.38

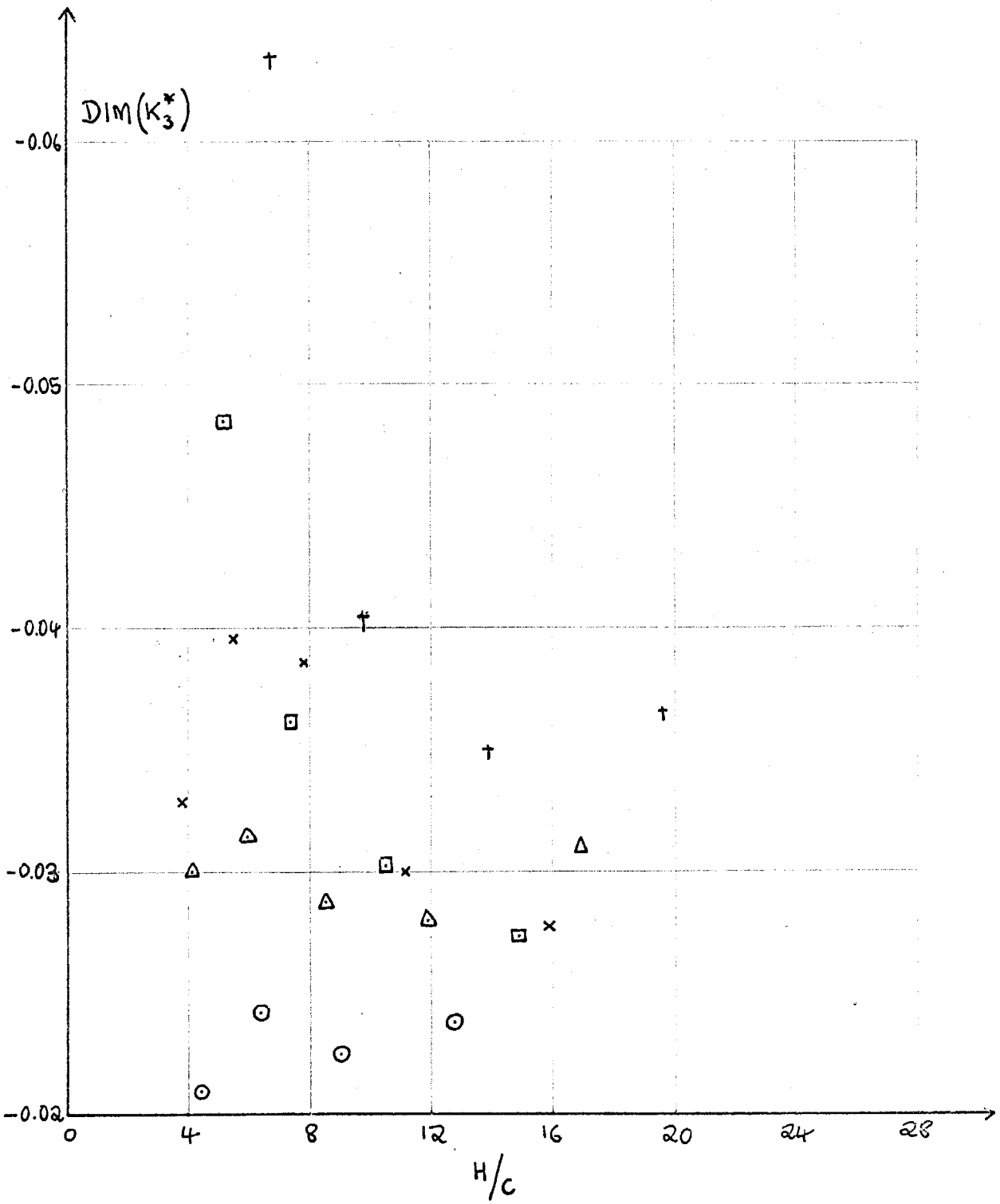

LEGEND – † Q = 0.2 △ Q = 0.5

⊡ Q = 0.3 ⊙ Q = 0.6

× Q = 0.4

change occured in the results of K^* from the second solution. This must , in part , be due to the minute magnitudes of those quantities since , as with the disc ,the dimensionless conversion multipliers were large. For example, for K_3^* , a typical value of this factor was 1200 , making the relevant term in expansion [4.64] almost negligible. This is an indication of the weakness of this singularity, and the fact that the introduction of the 5/2 power terms in the expansions of section 4.3.7 makes little difference in the region around separation.

5.4.7 Complete x,r Planes.

Two reconstructions of the x,r planes are presented for the sake of completeness ; these are constructed knowing the coordinates (x,r) of every mesh point in the Ψ, φ plane. Figure 5.39 shows the result of the disc solution for Q = 0.3 , H/C = 13.47 with all of the streamlines and some of the equipotentials sketched in. The two outermost streamlines , that for f_U = 128 and the channel wall , f_U = 256 , are omitted so that the disc may be of a reasonable size. The latter is precisely, and the former approximately a straight line.

The equipotentials are too closely bunched in the region of the wetted surface for presentation in figure 5.39 so figure 5.40 shows a magnification of the diagram near separation.

Figures 5.41 and 5.42 show the equivalent results for the solution of the sphere with Q = 0.3 and H/C = 7.389.

FIGURE 5.39

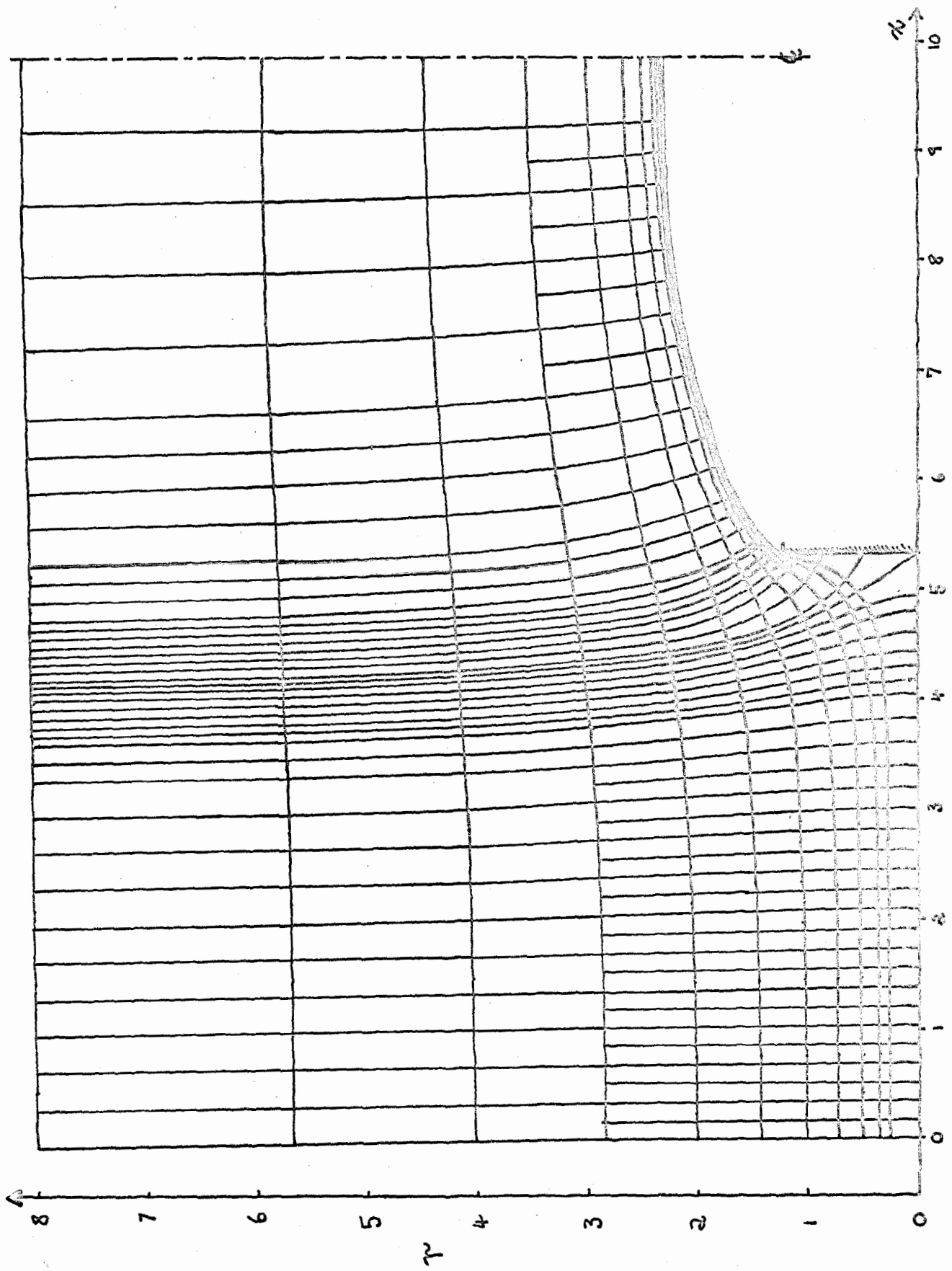

FIGURE 5.40

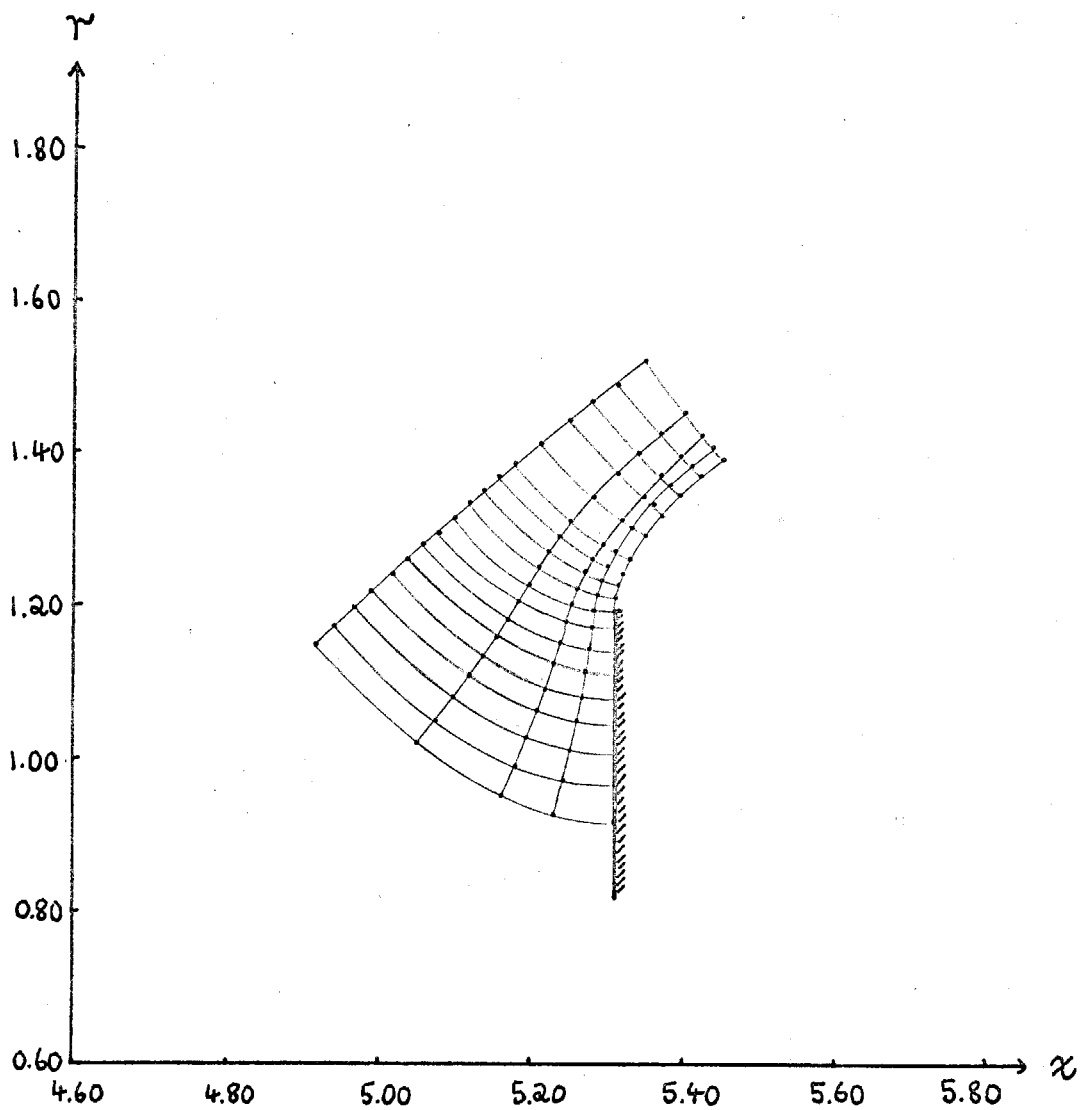

FIGURE 5.41

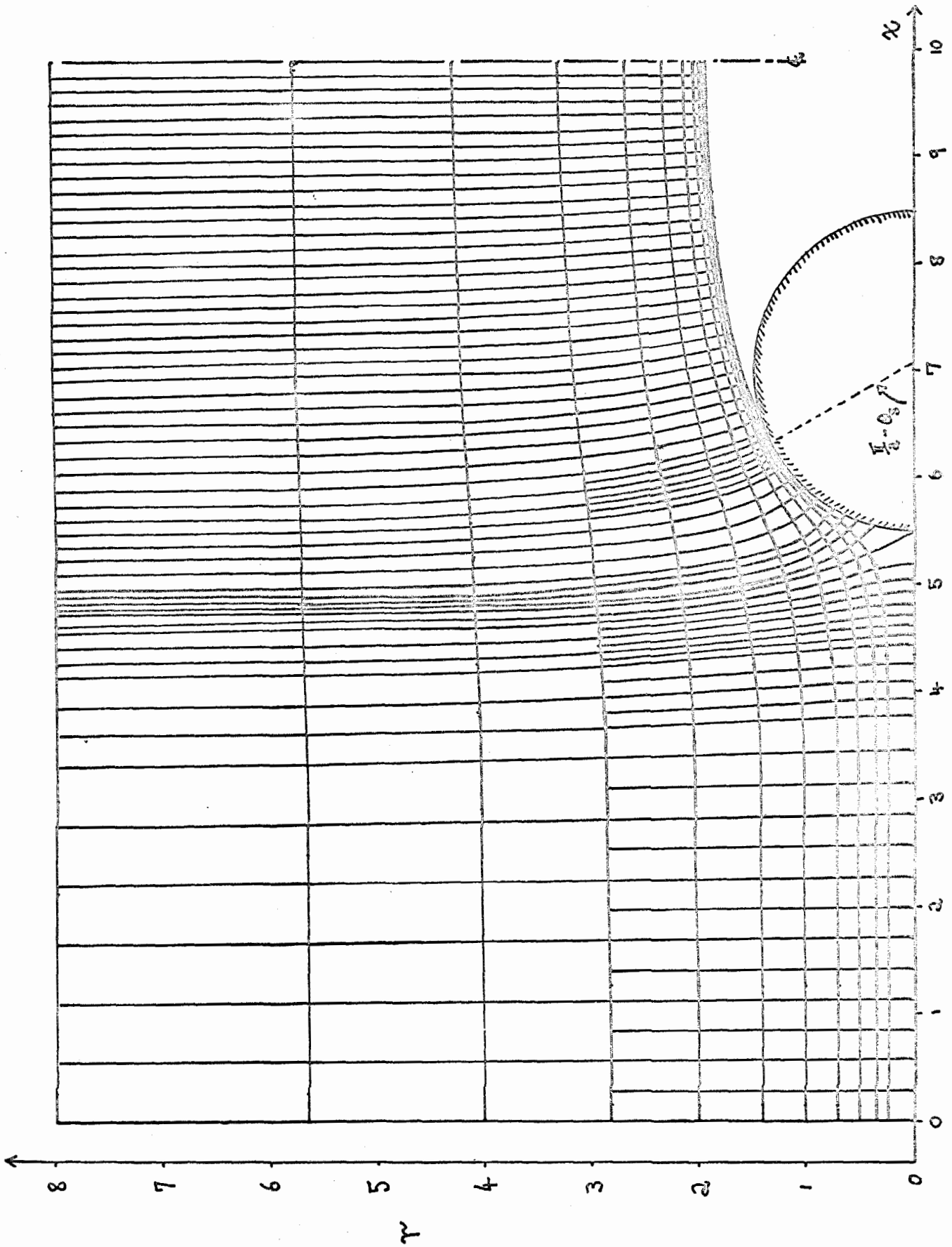

FIGURE 5.42

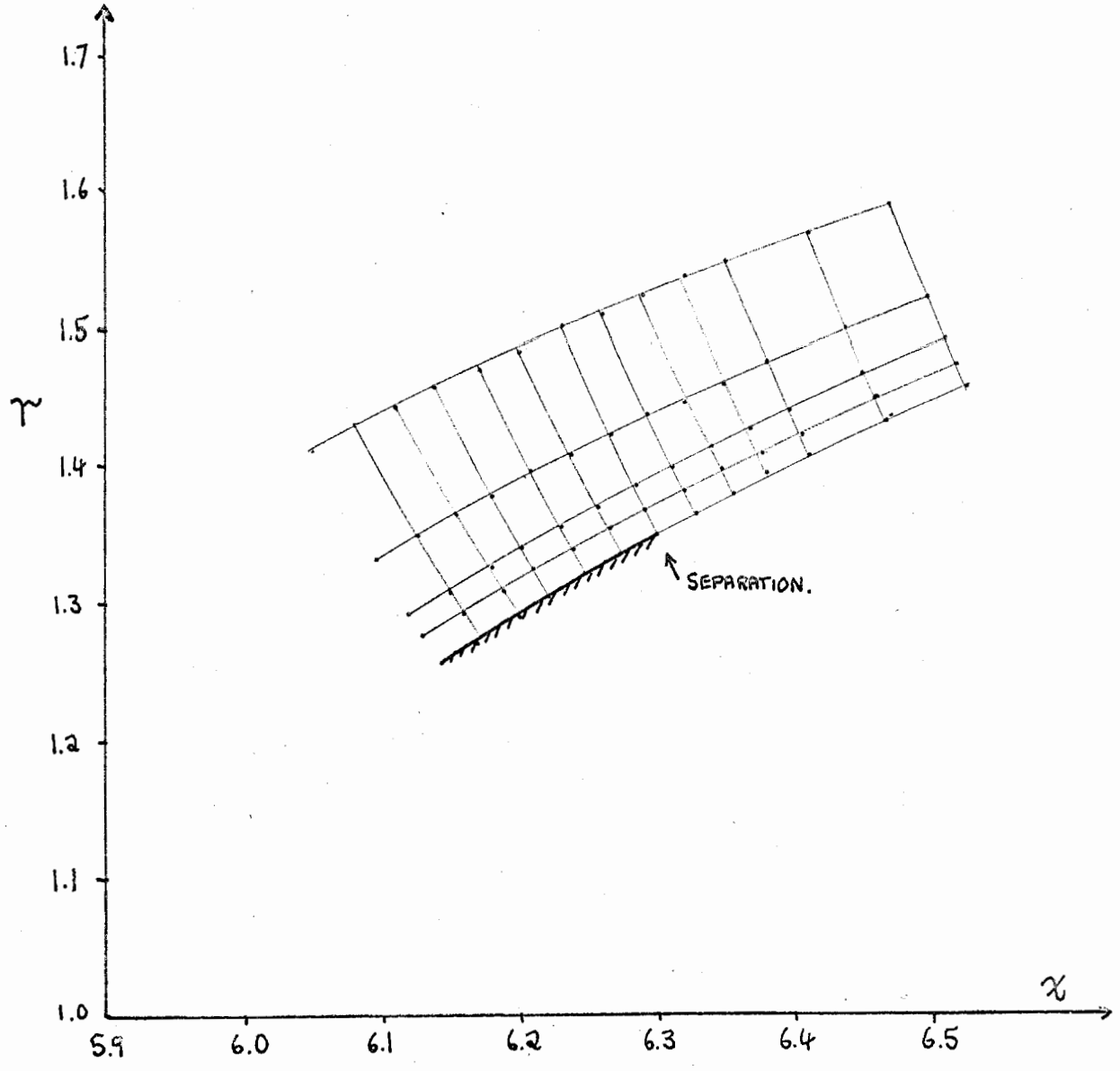

In both cases the flow in the region of separation exhibits the correct behaviour ; this is , in fact , ensured by the treatment of that point.

5.5 ERROR ANALYSIS.

5.5.1 Introduction.

Having obtained a solution and the final field of f values , an error analysis must be carried out to check the validity of that solution. In section 5.5.2 the major error analysis is outlined and the subsequent sections describe the results of some additional tests which can be applied.

5.5.2 Evaluation of error terms.

Clearly the essential aspect of an error analysis is that the errors in the field equation substitution by the finite difference forms be negligible or within an acceptable tolerance. This can be checked by an estimation of the first terms in the expansions [4.19] or [4.22]. However , if the equations [4.18] or [4.21] are multiplied through by a factor , which makes no difference to their application , the equivalent E will also be changed by this same factor. Thus the magnitudes of the values obtained by computing the first terms , say E* , in expansions [4.19] or [4.22] are not significant in themselves. They must be converted to some meaningful error in the values of f , the dependent variable.

This is done by considering the change in f at each point which would be produced by a residual of magnitude E* at that point if the values of f at surrounding points are unaltered. Thus the value of $E^*_o \Big/ \left(-\frac{\partial Y_o}{\partial f_o}\right)$ is is computed at each point. The fourth derivatives required are estimated using finite difference formulae. Thus the values obtained are for changes in f . These are then converted to fractional changes , denoted by E**, at every point. Hence , in fact , the value of

$$E^{**} = - \frac{E^*_o}{f_o \left(\frac{\partial Y_o}{\partial f_o}\right)}$$

is computed at each point.

Table 5.1 shows the result of such a computation with the final solution for a disc at Q = 0.4 , f_H = 256. The numbers are given in floating decimal form. Only the results for the lines j = 1 to j = 6 are presented . In this case the channel wall is j = J = 13 but the values for all lines above j = 6 fall off gradually to the order of 10^{-7} on j = 12. Thus , in general , a slight peak occurs in the values around j = 4.

As expected the values rise markedly in the region of the stagnation point. Since extra-residuals are applied within the region shown by the dotted lines , any results obtained there would be meaningless in view of the above analysis , since those extra-residuals are meant to counteract the error due to the larger values of the fourth and higher derivatives in that region. Also , the results on the borders of that region are suspect since , in their estimation , f values within the dotted region must be used. A better estimation of the errors in this region is provided in section 5.5.3.

TABLE 5.1

Values computed for the fractional errors , E^{**} , in f in the solution for the disc with Q = 0.4 , f_H = 256 .

The stagnation point is marked , E .

The separation point is marked , D .

k	E^{**}					
	j = 1	j = 2	j = 3	j = 4	j = 5	j = 6
3			4.7, -8	7.9, -8	6.3, -8	-1.1, -7
4			1.3, -7	1.1, -7	4.5, -8	-7.6, -8
5			2.3, -7	2.2, -7	9.0, -8	-3.2, -7
6			2.3, -7	2.1, -7	9.4, -8	-2.8, -7
7			3.4, -7	3.0, -7	8.5, -8	-6.5, -7
8			4.7, -7	4.2, -7	1.1, -7	-6.9, -7
9			6.0, -7	5.4, -7	7.8, -8	-1.3, -6
10			8.1, -7	6.7, -7	6.3, -8	-1.5, -6
11			1.1, -6	9.0, -7	-4.0, -8	-2.5, -6
12			1.5, -6	1.1, -6	-1.6, -7	-3.2, -6
13			2.0, -6	1.5, -6	-4.5, -7	-5.1, -6
14			2.8, -6	2.0, -6	-9.4, -7	-6.9, -6
15			4.0, -6	2.6, -6	-1.9, -6	-1.1, -5
16			5.9, -6	3.5, -6	-3.7, -6	-1.5, -5
17			8.9, -6	4.7, -6	-6.9, -6	-2.4, -5
18			1.4, -5	6.0, -6	-1.3, -5	-3.7, -5
19			2.3, -5	7.4, -6	-2.5, -5	-5.9, -5
20			5.6, -5	3.4, -5	3.7, -6	-1.8, -5
21			1.1, -4	5.7, -5	-3.8, -7	-3.1, -5
22			3.5, -4	2.8, -4	1.7, -4	7.6, -5
23			-2.6, -6	-3.2, -5	-6.6, -5	-6.9, -5
24			-8.0, -6	-5.1, -5	-9.5, -5	-9.0, -5
25			-2.1, -5	-8.6, -5	-1.4, -4	-1.2, -4
26			3.1, -5	-1.9, -5	-4.8, -5	-3.9, -5
27			4.0, -5	-4.2, -5	-7.4, -5	-5.2, -5
28			3.8, -4	2.0, -4	5.5, -5	6.9, -6
29			-1.3, -4	-1.4, -4	-1.2, -4	-6.8, -5
30			-2.1, -4	-1.9, -4	-1.5, -4	-7.8, -5

(Continued overleaf)

TABLE 5.1 (continued)

	31					-3.5, -4		-2.7, -4		-1.9, -4		-8.9, -5		
	32					-1.4, -4		-9.6, -5		-5.8, -5		-2.5, -5		
	33					-2.8, -4		-1.4, -4		-7.1, -5		-2.8, -5		
	34					2.3, -7		9.6, -6		-1.1, -5		-8.1, -6		
	35					-5.7, -4		-1.9, -4		-7.8, -5		-2.9, -5		
	36					-3.5, -4		-2.2, -4		-7.9, -5		-3.0, -5		
E	37					-3.9, -4		-2.3, -4		-7.7, -5		-3.0, -5		
	38					-4.1, -4		-2.1, -4		-7.1, -5		-2.8, -5		
	39	1.1, -2	3.1, -3			-2.1, -5		-1.5, -4		-5.9, -5		-2.6, -5		
	40	3.6, -3	1.1, -3			2.8, -4		-7.2, -5		-4.3, -5		-2.3, -5		
	41	1.4, -3	3.8, -4			4.3, -4		1.2, -5		-2.4, -5		-2.0, -5		
	42	4.8, -4	2.5, -5			4.8, -4		8.7, -5		-4.9, -6		-1.5, -5		
	43	9.5, -5	-1.7, -4			4.6, -4		1.4, -4		1.4, -5		-1.0, -5		
	44	-4.1, -5	-2.6, -4			4.1, -4		1.8, -4		3.1, -5		-5.0, -6		
	45	-7.0, -5	-3.0, -4			3.4, -4		2.0, -4		4.6, -5		1.3, -7		
	46	-6.4, -5	-3.0, -4			2.8, -4		2.1, -4		5.8, -5		5.1, -6		
	47	-5.0, -5	-2.8, -4			2.2, -4		2.0, -4		-6.8, -5		9.8, -6		
	48	-3.7, -5	-2.6, -4			1.7, -4		1.9, -4		7.5, -5		1.4, -5		
	49	-2.9, -5	-2.4, -4			1.3, -4		1.8, -4		8.0, -5		1.8, -5		
	50	-2.2, -5	-2.2, -4			1.1, -4		1.6, -4		8.2, -5		2.1, -5		
	51	-1.3, -5	-1.9, -4			9.1, -5		1.5, -4		8.2, -5		2.3, -5		
	52	4.7, -5	-1.5, -4			8.2, -5		1.3, -4		7.9, -5		2.5, -5		
D	53	4.6, -5	-1.2, -4			3.8, -5		1.1, -4		7.4, -5		2.6, -5		
	54	-5.4, -5	-1.3, -4			9.7, -6		8.1, -5		6.8, -5		2.7, -5		
	55	-3.3, -5	-9.9, -5			-1.4, -5		5.8, -5		6.1, -5		2.7, -5		
	56	-6.7, -5	-3.2, -4			-2.5, -4		4.1, -5		1.7, -4		9.7, -5		
	57	-2.7, -5	-1.8, -4			-1.0, -4		1.1, -4		1.9, -4		1.0, -4		
	58	-9.1, -6	-1.1, -4			-8.2, -5		4.6, -5		1.4, -4		9.5, -5		
	59	-4.3, -6	-8.0, -5			-5.9, -5		1.3, -5		1.1, -4		8.6, -5		
	60	-2.4, -6	-6.1, -5			-4.1, -5		-3.3, -6		8.2, -5		7.7, -5		
	61	-1.5, -6	-4.9, -5			-2.8, -5		-1.0, -5		6.1, -5		6.9, -5		
	62	-1.8, -5	-1.2, -4			-2.1, -4		-2.3, -4		5.1, -5		1.9, -4		
	63	-2.6, -6	-6.4, -5			-5.8, -5		-6.0, -5		1.3, -4		2.1, -4		
	64	-1.4, -6	-4.7, -5			-3.0, -5		-4.6, -5		7.4, -5		1.6, -4		
	65	-8.1, -7	-3.6, -5			-1.7, -5		-3.2, -5		4.0, -5		1.3, -4		
	66	-5.1, -7	-2.8, -5			-1.0, -5		-2.1, -5		2.2, -5		9.7, -5		
	67	-3.4, -7	-2.3, -5			-6.6, -6		-1.4, -5		1.2, -5		7.5, -5		
	68	-4.9, -6	-3.9, -5			-8.6, -5		-1.9, -4		-1.8, -4		8.5, -5		
	69	-6.7, -7	-2.0, -5			-1.4, -5		-3.6, -5		-1.9, -6		1.7, -4		
	70	-3.7, -7	-1.5, -5			-7.5, -6		-1.8, -5		-4.5, -6		1.1, -4		
	71	-2.2, -7	-1.1, -5			-4.2, -6		-1.0, -5		-2.7, -6		7.0, -5		
	72	-1.4, -7	-8.7, -6			-2.6, -6		-5.8, -6		-8.1, -7		4.6, -5		
	73	-9.0, -8	-7.0, -6			-1.6, -6		-3.4, -6		5.7, -7		3.4, -5		
	74	-6.2, -8	-5.8, -6			-1.1, -6		-2.1, -6		1.3, -6		2.4, -5		
	75	-4.4, -8	-4.9, -6			-7.5, -7		-1.3, -6		1.7, -6		1.9, -5		
	76	-3.3, -8	-4.3, -6			-5.4, -7		-8.3, -7		1.8, -6		1.5, -5		
	77	-2.5, -8	-3.7, -6			-4.1, -7		-5.5, -7		1.8, -6		1.3, -5		
	78	-2.0, -8	-3.3, -6			-3.2, -7		-3.8, -7		1.7, -6		1.0, -5		
	79	-1.6, -8	-3.0, -6			-2.5, -7		-2.6, -7		1.6, -6		9.8, -6		
	80	-1.4, -8	-2.7, -6			-2.2, -7		-2.0, -7		1.5, -6		7.7, -6		
	81	-1.2, -8	-2.5, -6			-1.7, -7		-1.0, -7		1.6, -6		8.1, -6		
	82	-7.7, -9	-2.4, -6			-1.0, -7		4.7, -8		1.7, -6		6.6, -6		
	83	-4.6, -9	-2.2, -6			-3.5, -8		2.2, -7		1.9, -6		7.3, -6		
	84	1.1, -8	-2.1, -6			1.5, -7		4.9, -7		1.9, -6		5.8, -6		
	85	-2.3, -8	-2.1, -6			-3.1, -7		-3.8, -7		9.8, -7		6.1, -6		
	86	-4.5, -9	-2.0, -6			-7.7, -8		-1.0, -8		1.1, -6		4.7, -6		
	87	-3.7, -9	-1.9, -6			-4.3, -8		1.1, -7		1.4, -6		5.6, -6		

TABLE 5.2

Values computed for the fractional errors , E^{**}, in f in the solution for the sphere with Q = 0.3 , f_H = 128.

The stagnation point is marked , E .

The separation point is marked , D .

k	E^{**}					
	j = 1	j = 2	j = 3	j = 4	j = 5	j = 6
3			2.6, -7	3.5, -7	3.0, -7	-1.5, -7
4			5.3, -7	5.9, -7	5.5, -7	5.0, -7
5			7.9, -7	8.5, -7	7.7, -7	-3.5, -7
6			1.3, -6	1.4, -6	1.2, -6	5.0, -7
7			1.5, -6	2.1, -6	1.6, -6	-1.0, -6
8			2.9, -6	3.2, -6	2.4, -6	-1.9, -7
9			4.6, -6	5.0, -6	3.1, -6	-3.3, -6
10			7.7, -6	8.0, -6	4.5, -6	-3.8, -6
11			1.4, -5	1.3, -5	5.6, -6	-1.2, -5
12			4.0, -5	3.5, -5	2.2, -5	5.9, -6
13			8.3, -5	6.7, -5	3.5, -5	3.2, -6
14			2.0, -4	1.9, -4	1.6, -4	9.9, -5
15			8.3, -6	-2.4, -6	-2.1, -5	-3.6, -5
16			1.2, -5	-6.7, -6	-3.6, -5	-5.2, -5
17			1.6, -5	-1.7, -5	-6.2, -5	-7.7, -5
18			5.9, -5	1.5, -5	-1.7, -5	-2.7, -5
19			1.1, -4	2.2, -5	-3.7, -5	-4.3, -5
20			3.6, -4	2.3, -4	1.0, -4	3.8, -5
21			-5.6, -5	-3.7, -5	-1.0, -4	-7.0, -5
22			-1.1, -4	-1.3, -4	-1.4, -4	-8.7, -5
23			-2.1, -4	-2.1, -4	-1.9, -4	-1.1, -4
24			-7.9, -5	-8.3, -5	-6.5, -5	-3.4, -5
25			-2.2, -4	-1.5, -4	-9.0, -5	-4.1, -5
26			8.5, -5	5.4, -5	2.5, -6	-4.7, -5
27			-6.6, -4	-2.5, -4	-1.1, -4	-4.7, -5
28			-4.9, -4	-3.0, -4	-1.2, -4	-4.9, -5
E 29			-5.0, -4	-3.4, -4	-1.2, -4	-5.0, -5
30			-6.6, -4	-3.2, -4	-1.1, -4	-5.0, -5
31	1.0, -2	3.2, -3	3.6, -5	-2.1, -4	-9.2, -5	-4.6, -5
32	9.2, -3	1.1, -3	4.3, -4	-6.3, -5	-6.4, -5	-4.1, -5
33	1.0, -3	2.9, -4	5.7, -4	-3.4, -5	-3.3, -5	-3.4, -5
34	3.0, -4	-6.9, -5	5.7, -4	1.6, -4	-3.3, -6	-2.6, -5
35	5.3, -5	-2.3, -4	5.0, -4	2.1, -4	2.2, -5	-1.3, -5

(Continued overleaf)

TABLE 5.2 (continued)

36	-4.1,	-4	-1.3,	-3	1.1,	-3	8.6,	-4	2.0,	-4	-1.5,	-5
37	-9.4,	-5	-6.8,	-4	1.2,	-3	9.2,	-4	2.4,	-4	-7.8,	-6
38	-6.2,	-5	-5.8,	-4	6.7,	-4	7.8,	-4	3.1,	-4	4.6,	-5
39	-3.2,	-5	-4.3,	-4	3.3,	-4	5.9,	-4	3.3,	-4	8.5,	-5
40	-1.7,	-5	-3.1,	-4	1.5,	-4	4.1,	-4	3.1,	-4	1.1,	-4
41	-9.3,	-6	-2.2,	-4	6.6,	-5	2.8,	-4	2.8,	-4	1.2,	-4
42	-5.4,	-6	-1.7,	-4	2.6,	-5	1.9,	-4	2.3,	-4	1.3,	-4
43	-3.3,	-6	-1.3,	-4	9.4,	-6	1.2,	-4	2.0,	-4	1.3,	-4
44	-5.8,	-6	-5.5,	-5	-3.6,	-6	2.2,	-5	4.3,	-5	3.1,	-5
45	-3.5,	-6	-4.5,	-5	-3.9,	-6	1.4,	-5	3.4,	-5	2.8,	-5
46	-7.4,	-5	-1.7,	-4	-1.6,	-4	-1.1,	-4	-3.1,	-5	9.5,	-6
47	-1.7,	-7	-3.3,	-5	6.0,	-7	9.7,	-6	2.6,	-5	2.6,	-5
48	-1.7,	-7	-3.0,	-5	5.8,	-7	8.1,	-6	2.4,	-5	2.4,	-5
49	-1.2,	-7	-2.8,	-5	6.7,	-7	6.9,	-6	2.1,	-5	2.3,	-5
50	-5.5,	-8	-2.6,	-5	8.4,	-7	6.0,	-6	1.9,	-5	2.2,	-5
51	8.4,	-6	-2.4,	-5	1.0,	-6	5.1,	-6	1.7,	-5	2.0,	-5
52	5.0,	-7	-2.1,	-5	1.4,	-6	4.4,	-6	1.5,	-5	1.9,	-5
53	1.8,	-7	-1.9,	-5	5.3,	-8	2.8,	-6	1.2,	-5	1.7,	-5
54	-7.5,	-7	-1.6,	-5	-1.2,	-6	1.3,	-6	1.0,	-5	1.6,	-5
55	-2.9,	-7	-1.5,	-5	-1.3,	-6	5.6,	-7	8.7,	-6	1.5,	-5
56	-7.4,	-6	-4.7,	-5	-5.4,	-5	-5.6,	-5	-1.4,	-5	3.3,	-5
57	-5.1,	-7	-2.4,	-5	-5.1,	-6	-2.0,	-6	2.4,	-5	5.0,	-5
58	-2.9,	-7	-2.0,	-5	-3.4,	-6	-2.3,	-6	1.7,	-5	4.2,	-5
59	-1.9,	-7	-1.7,	-5	-2.3,	-6	-1.9,	-6	1.2,	-5	3.5,	-5
60	-1.3,	-7	-1.5,	-5	-1.5,	-6	-1.4,	-6	9.2,	-6	3.0,	-5
61	-9.7,	-8	-1.3,	-5	-1.1,	-6	-9.5,	-7	7.1,	-6	2.5,	-5
62	-3.5,	-6	-2.7,	-5	-5.1,	-5	-8.9,	-5	-7.4,	-5	1.9,	-5
63	-2.2,	-7	-1.3,	-5	-3.5,	-6	-4.8,	-6	1.4,	-5	7.0,	-5
64	-1.5,	-7	-1.1,	-5	-2.1,	-6	-2.5,	-6	1.3,	-5	5.2,	-5
65	-9.8,	-8	-8.9,	-6	-1.3,	-6	-1.2,	-6	8.0,	-6	4.0,	-5
66	-6.6,	-8	-7.5,	-6	-8.7,	-7	-4.1,	-7	6.8,	-6	3.1,	-5
67	-4.6,	-8	-6.4,	-6	-5.7,	-7	2.4,	-8	5.9,	-6	2.5,	-5
68	-3.5,	-8	-5.5,	-6	-3.9,	-7	2.6,	-7	5.2,	-6	2.0,	-5
69	-2.6,	-8	-4.8,	-6	-2.7,	-7	3.3,	-7	4.6,	-6	1.7,	-5
70	-2.0,	-8	-4.3,	-6	-1.9,	-7	4.2,	-7	4.1,	-6	1.4,	-5
71	-1.0,	-8	-3.8,	-6	-1.4,	-7	4.0,	-7	3.6,	-6	1.2,	-5
72	-1.4,	-8	-3.4,	-6	-1.2,	-7	3.6,	-7	3.1,	-6	1.0,	-5
73	-1.2,	-8	-3.1,	-6	-1.2,	-7	2.8,	-7	2.6,	-6	9.2,	-6
74	-1.2,	-8	-2.8,	-6	-1.2,	-7	2.0,	-7	2.2,	-6	7.7,	-6
75	-1.2,	-8	-2.6,	-6	-1.3,	-7	1.2,	-7	1.9,	-6	7.0,	-6
76	-1.1,	-8	-2.4,	-6	-1.3,	-7	6.0,	-8	1.6,	-6	6.0,	-6
77	-1.1,	-8	-2.2,	-6	-1.2,	-7	4.6,	-8	1.6,	-6	5.9,	-6
78	-9.4,	-9	-2.1,	-6	-1.0,	-7	3.5,	-8	1.5,	-6	5.2,	-6
79	-7.0,	-9	-2.1,	-6	-6.1,	-8	1.8,	-7	1.7,	-6	5.6,	-6
80	-3.8,	-9	-2.0,	-6	-1.8,	-9	3.4,	-7	1.9,	-6	5.3,	-6
81	-4.0,	-10	-1.9,	-6	6.7,	-8	5.4,	-7	2.3,	-6	5.9,	-6
82	3.3,	-9	-1.9,	-6	1.6,	-7	6.5,	-7	2.6,	-6	5.6,	-6
83	5.7,	-8	-1.7,	-6	7.2,	-7	1.5,	-6	2.9,	-6	5.6,	-6
84	-5.2,	-9	-1.9,	-6	-5.5,	-7	-5.3,	-7	9.9,	-7	4.3,	-6
85	-3.6,	-9	-1.7,	-6	-8.3,	-8	-2.0,	-8	1.0,	-6	4.3,	-6
86	-2.3,	-9	-1.6,	-6	-1.3,	-8	1.5,	-7	1.1,	-6	3.7,	-6
87	-1.7,	-9	-1.6,	-6	2.2,	-9	2.1,	-7	1.2,	-6	4.1,	-6
88	-1.6,	-9	-1.6,	-6	6.2,	-9	2.3,	-7	1.2,	-6	3.6,	-6
89	-1.6,	-9	-1.6,	-6	7.5,	-9	2.3,	-7	1.3,	-6	4.0,	-6

It is a little surprising that the values in the region of separation are not more sharply peaked. This is perhaps due to the fineness of the mesh in that region.

In general these results show that the streamline distribution of mesh points could be more drastically graded than that used by the author, shown in section 5.1.1. The equipotential distribution of points would seem to be adequate.

Some estimate of the accuracy of the f values obtained on the free streamline could be obtained by totaling the results for E** for all j at k = constant. This leads , on average , to total changes never greater than 0.05 per cent. The author feels , however , that this would be a very optimistic assumption , the final values of the local cavitation number giving , perhaps , a better estimation of accuracy.

Table 5.2 shows the results for the final field for a sphere at $Q = 0.3$, $f_H = 128$ ($J = 12$). This displays the same characteristics.

These results are encouraging provided another method , given in section 5.5.3 , shows the invalidity of the results obtained near the stagnation point.

5.5.3 A Test at the Stagnation Point.

Figure 5.43 shows the graph of the functions $f(\phi)$ for $f_U = 0$, 0.0625 , 0.125 and 0.25 in the region of the stagnation point for the disc solution , $Q = 0.5$, $f_H = 128$. The fuller lines present the actual values obtained and the broken the solution for the Dirichlet

FIGURE 5.43

Stagnation Point Test .

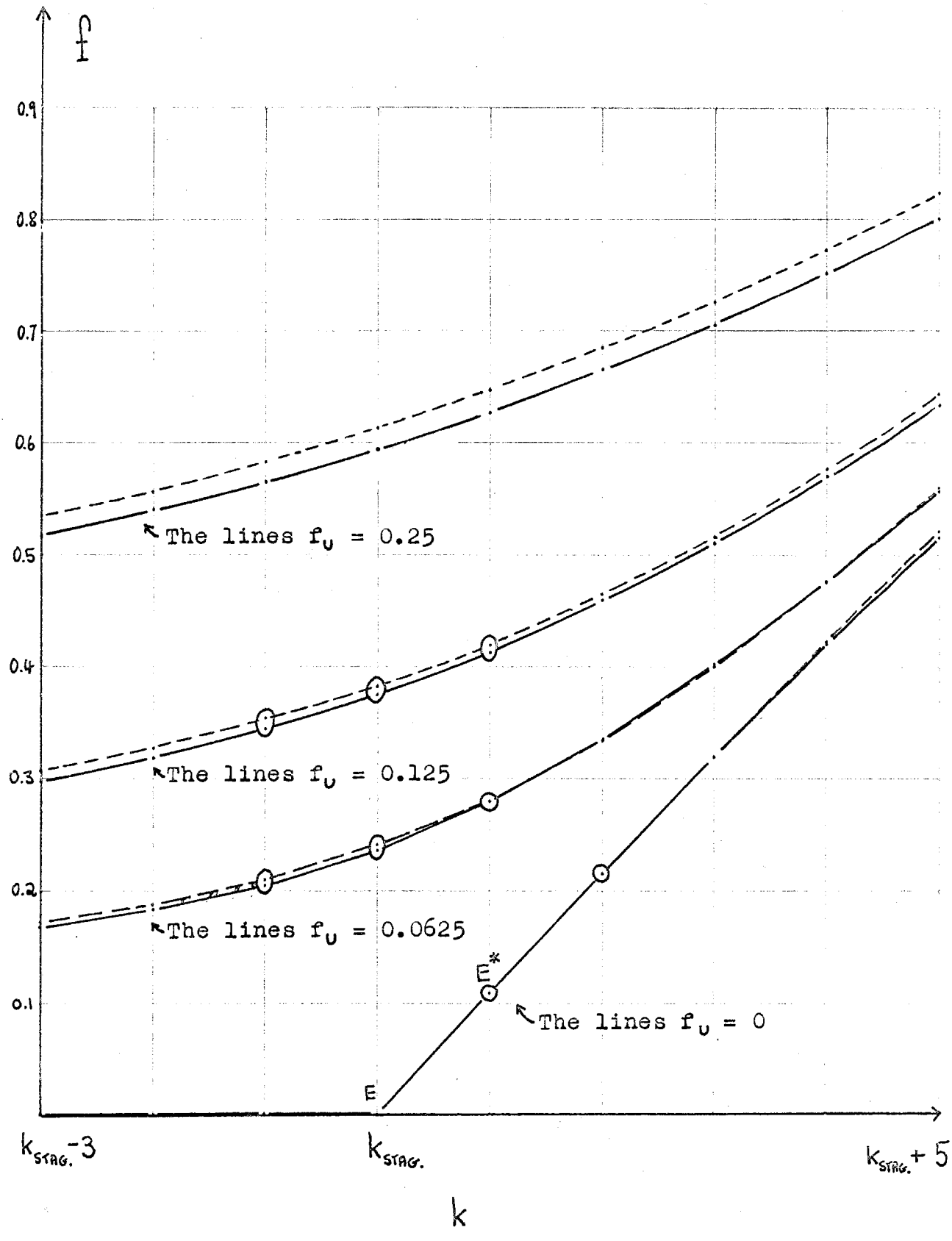

flow which has the same upstream velocity and the same value at the point E*. That is to say , referring to section 4.4.3 , the function used to find the extra-residuals in this region , f' . Naturally the solutions diverge with distance from the stagnation point but , in the close proximity of that point , the difference between the functions f and f' (see sections 4.4.1,4.4.2) is very small.

In order to judge the limit of application required of the extra-residuals , Z , the changes which these would produce in the values of f at each point were estimated from computations of $Z_0 / \left[- \frac{\partial Y_0}{\partial f_0} \right]$. For the same solution depicted in figure 5.43 these values are shown in figure 5.44. Both these figures give results which are typical of those for the disc.

It is clearly sufficient to treat the points ringed in figure 5.44 and , correspondingly , in figure 5.43 with extra-residuals. This range was used for the solutions with both the disc and the sphere , the latter giving very similar results in this region.

5.5.4 The Upstream Test.

Figure 5.45 shows some results of the upstream test , mentioned in section 4.2.3, on the solution for the disc with $Q = 0.4$, $f_H = 512$. The values of $f - f_U$ are plotted for points near the upstream boundary for the actual solution (solid lines) and for the values given using [4.27] at points downstream of k = 1 . The curves for $f_U = 0.0625$ (j = 1) , 0.50 (j = 4) and 32 (j = 10)

FIGURE 5.44

Stagnation Point Residual Test.

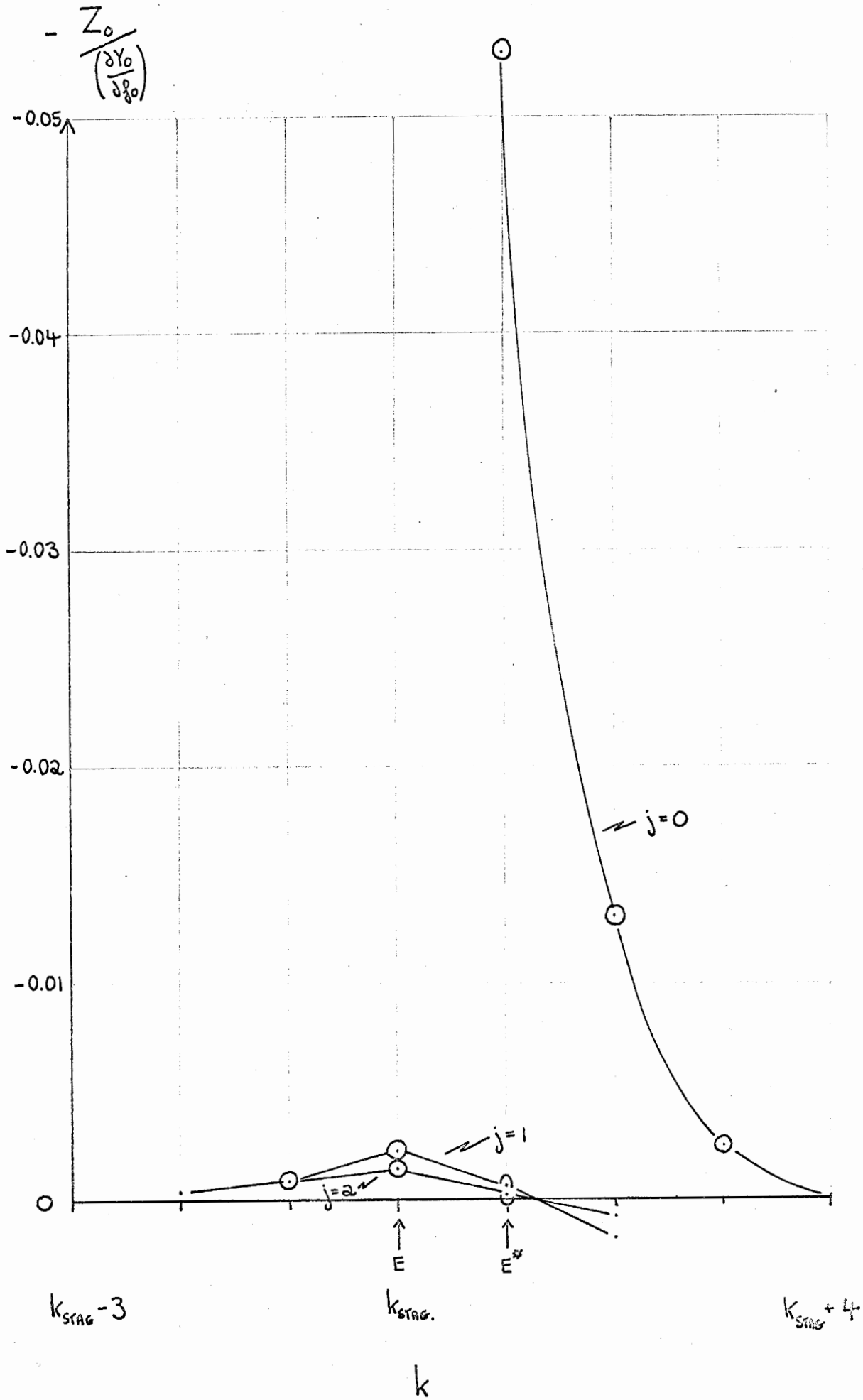

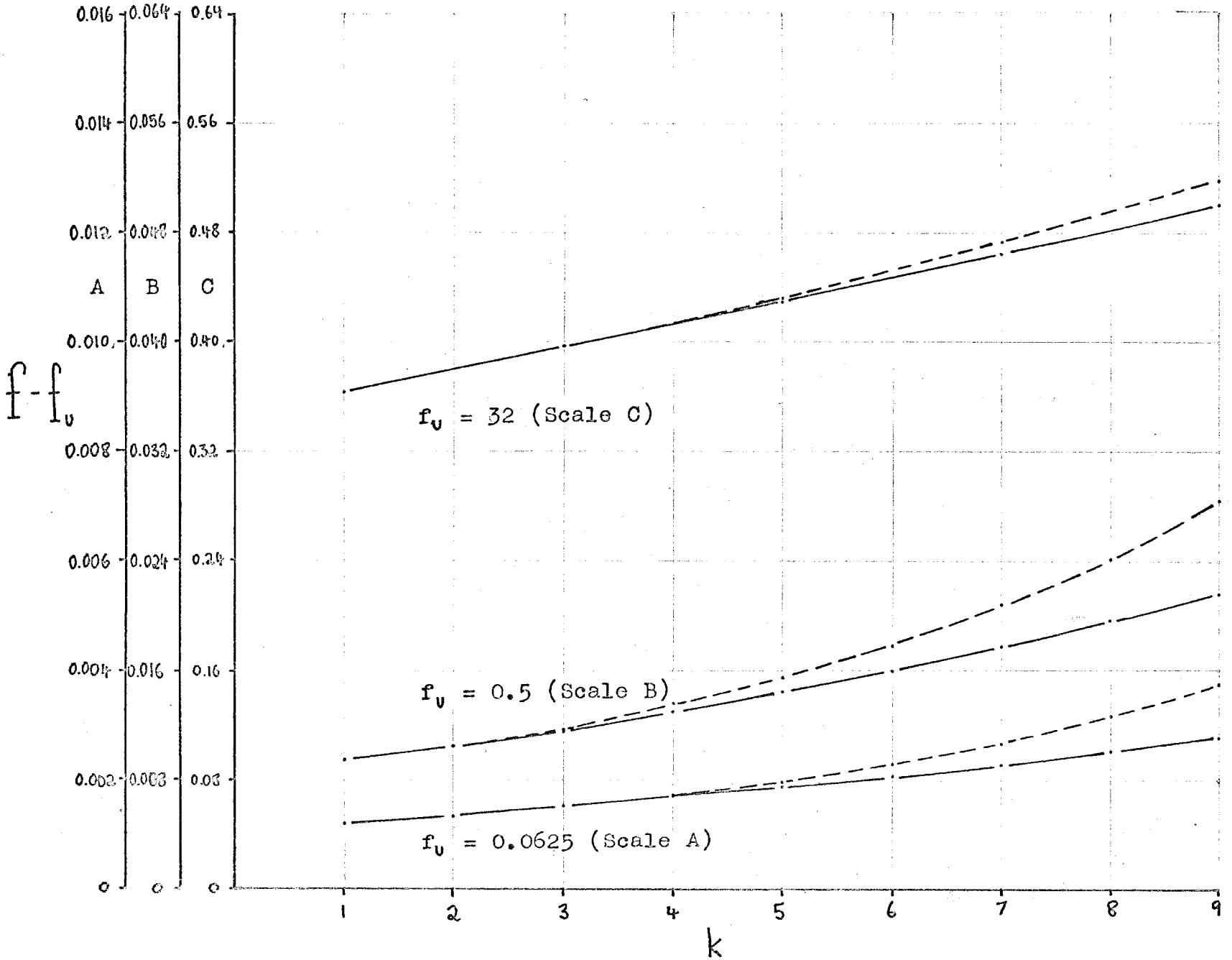

FIGURE 5.45

Upstream

Test.

are neccessarily presented on different scales.

The results of these tests substantiated the results of section 5.5.2 in showing a slight peak in the errors around $j = 4$ or 5. Thus the greatest relative difference between the two curves for all streamlines occured at $j = 4$ or $f_U = 0.5$ in this test. To show this two other sets are presented in figure 5.45 , one for a streamline above and one for a streamline below $j = 4$.

The results of this test are difficult to comment on. They are not , perhaps , as satisfactory as might be wished. Accordingly the author carried out a couple of major solutions with a larger value of φ_L , but no significant changes took place in the results ; that is to say none that could be assigned to this alteration in φ_L. The conclusion was therefore reached that the upstream solution was satisfactory. This was partially ensured by the analysis of section 4.1.6 [3].

5.4.5 Tests by Integration to find x Differences by Several routes.

This provides a demonstration of the accuracy of the final f field. Using equation [3.10] , we can integrate the relevant first derivative of f along either a streamline or an equipotential to find the difference in axial distance , x , between two mesh points. Thus the same distance can be estimated by several routes.

However , any errors which occur cannot be

simply analysed since they may be due to either or both of errors in the f values and errors in the numerical integration carried out. Some examples are given below from the solution for the disc with $Q = 0.4$, $f_H = 256$.

[A] To find the distance from (0,25) (on the stagnation streamline) to (0,45) (on the wetted surface),

(i) by integration along the line $j = 0$, travelling through the stagnation point , $x = 1.23217$,

(ii) by the route , $(0,25) \rightarrow (2,25) \rightarrow (2,45) \rightarrow (0,45)$, $x = 1.21590$.

Thus , despite the presence of the singularity , we find an error of less than 2 per cent.

[B] Between two points on the free streamline :

(i) $(0,61) \rightarrow (0,67)$, $x = 0.28918$,

(ii) $(0,61) \rightarrow (2,61) \rightarrow (2,67) \rightarrow (0,67)$, $x = 0.28925$,

giving a negligible error.

[C] Between the same two points :

(iii) $(0,61) \rightarrow (6,61) \rightarrow (6,67) \rightarrow (0,67)$, $x = 0.28733$.

This is a long way round in comparison with the actual x difference and yet gives an error of less than one per cent.

However , due to the difficulty in analysis of these errors , this section is merely presented as a confirmation of accuracy. In fact , in any test of this sort , it was found that the errors were rarely greater than one per cent , except when the front stagnation point was included , when the errors rose to around 2 per cent.

5.6 CONCLUSION.

The method of solving axisymmetric cavity flows , developed in this thesis has the great advantage of flexibility. Alternative types of flow which the method can be simply adapted to treat are , for example , those in which the outer boundary takes any axisymmetric form , or in which it is a free jet. Besides this , the author is considering the possibility of adaptation to unsteady cavity flow.

Both the previous significant methods , those of Garabedian and of Armstrong and Dunham , are limited to the infinite stream case.

Another advantage of this method is that it solves the complete flow field. Thus the author is considering the problem of diffusion of absorbed air in a cavity flow , using these solutions as a framework.

It is difficult to compare the computational work required in the three methods , though that of Garabedian must be the most complex.

The method has been employed to solve the steady state cavitating flows behind a sphere and a disc , demonstrating the behaviour of those cavities and drag on the body as the condition of choked flow is approached ; the solutions also provide values for the separation angle in the case of the sphere.

APPENDIX A

APPENDIX A

A.1 Computations on the Riabouchinsky Planar Flow past a Flat Plate set normal to a Uniform Stream in a Channel.

One of the results of this thesis is an attempt to discover the behaviour of the cavity behind a disc in a channel for varying Q and H/C, a blockage ratio. It is clearly of interest to compare the results obtained with those for the equivalent planar flow , for a flat plate in a channel. The solution to this problem was given in section 1.5.5.

Although the numerical results for the infinite stream case are often quoted (e.g. Ref.1) , the author could not find similar results for non-infinite H/C. A programme was therefore written for the purpose of computing the main dimensions , B/C and L/C , and the coefficient of drag , C_D , for various values of Q and H/C. Equations [1.36] to [1.40] contain the two parameters u_0 and k. Since the simplest of these equations is that for Q , the results B/C , L/C , H/C and C_D were calculated from those equations for sets of the parameters u_0 and k where all pairs within a set gave a prescribed value of Q.

Bearing in mind the "choked" flow phenomenon investigated in section 3.3.1 , the results $(B/C)_{MAX}$ and $(C_D)_{MAX}$ were also computed for each result using the values of Q and H/C.

The results of these computations are shown in graphs [A1],[A2] and [A3] , being plotted against Q

for various H/C. The values of H/C chosen were those which gave choked flow close to Q = 0.1,0.2,0.3,0.4,0.5 and 0.6.

Graph [A1] shows the values obtained for C/B (solid lines) , the particular value of H/C being written in on each line. For each of these values the corresponding values of $(C/B)_{MIN}$ are also plotted (evenly dotted lines). Thus the point of intersection of the curves for C/B and $(C/B)_{MIN}$ marks the choked flow point for that particular value of H/C. Joining these choked flow points produces a choked flow line.(unevenly dotted) Thus any result for C/B must lie between this choked flow line and the infinite H/C line. The position of the choked flow line will be independent of the mathematical model chosen as was pointed out in section 3.3.1 since in a choked flow condition the cavity becomes infinitely long.

In the case of the cavity length parameter, $(C/L)^{\frac{1}{2}}$, the choked flows gave this parameter as zero for all H/C,as anticipated. These results are shown in graph [A2].

Finally a modified coefficient of drag , $C_D/(1 + Q)$, is shown plotted against Q in graph [A3]. The corresponding values of $[C_D/(1 + Q)]_{MAX}$ are also plotted for each H/C (evenly dotted lines) , the intersection points giving the choked flow line (unevenly dotted). Thus all values of $C_D/(1 + Q)$ must lie between this choked flow line and the infinite H/C line. It is noticeable that the variation of this modified coefficient with either Q or H/C is negligible for any practical purposes. The drag at given Q is reduced by decreasing H/C. The choked

PLANAR FLOW. GRAPH [A1]

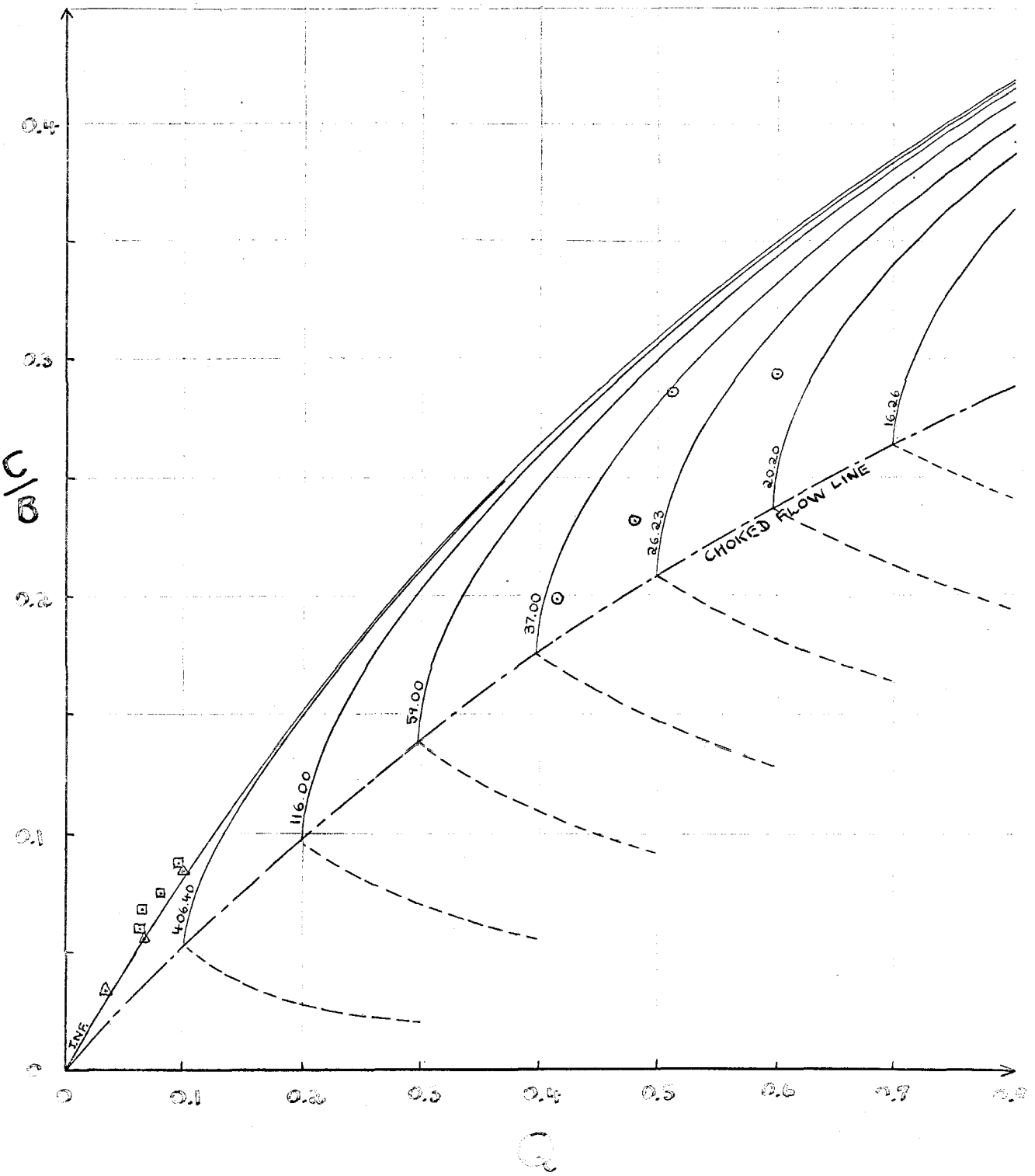

⊙ Waid. ⊡, Δ Reichardt.

Planar Flow. Graph [illegible]

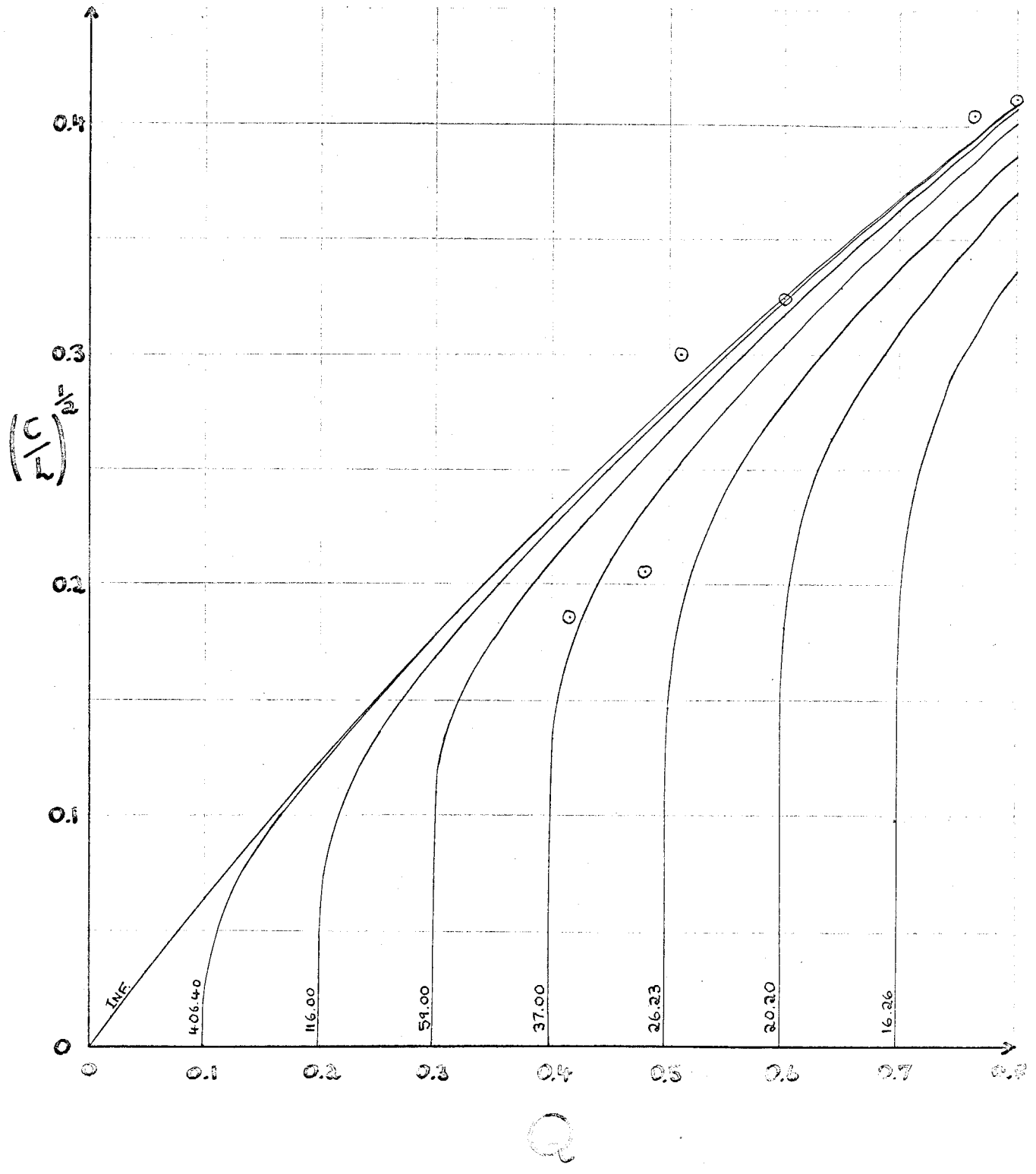

⊙ Waid.

PLANAR FLOW. GRAPH [A5]

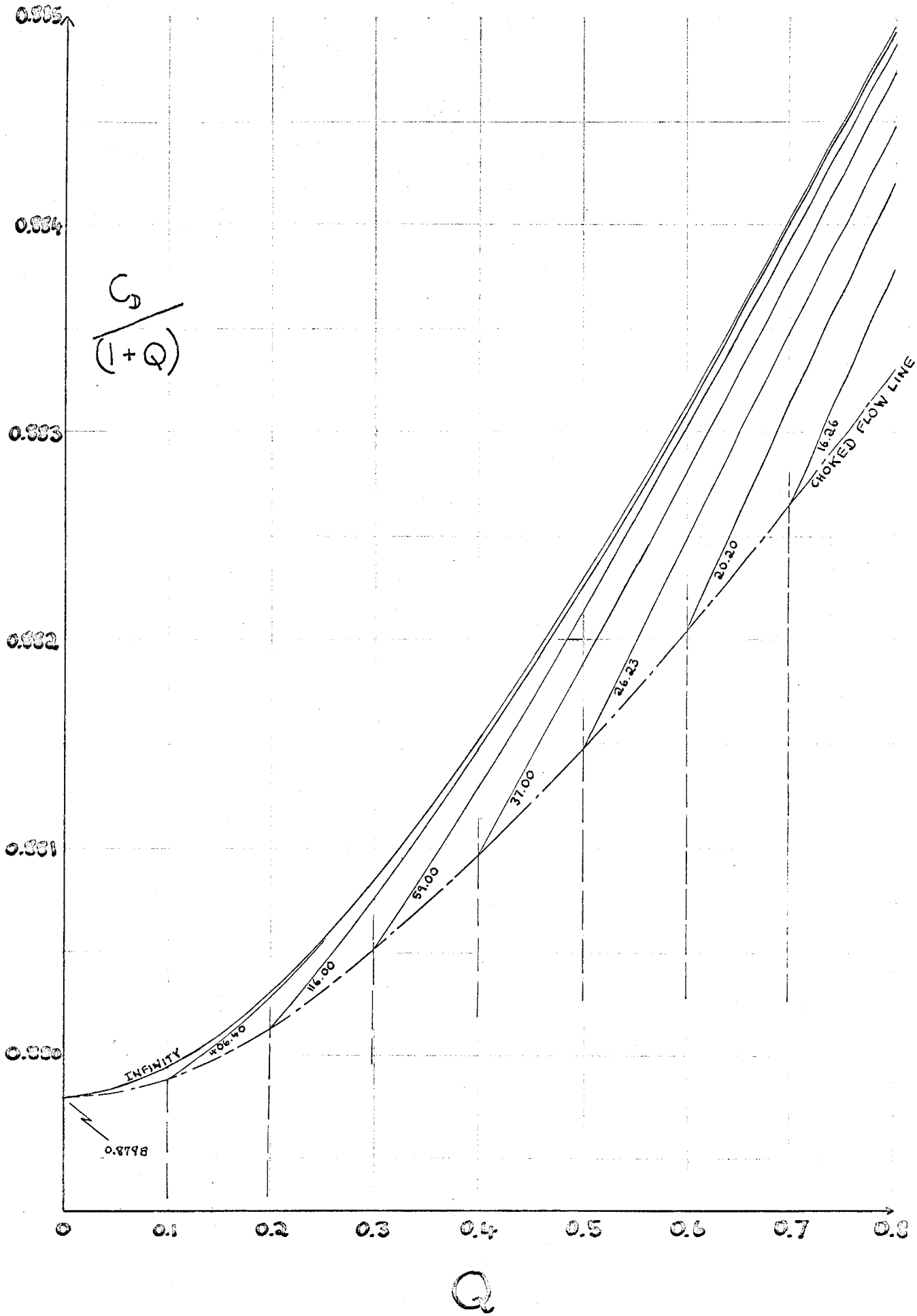

flow line is better defined in this graph than in the first.

As Gadd (Ref. 14) points out there is a marked lack of experimental data for this problem. Graphs [A1] and [A2] show some results given by Waid (Ref. 45) for a normal plate in a channel. These experiments were carried out with H/C = 37.3. It is noticeable that his results are at least better fitted to the theoretical results for H/C = 37.00 than to the other H/C in those graphs. Some other results quoted by Reichardt (Ref. 34) are shown in graph [A1]. These were , however , for experiments in which the outer boundary was a free jet.

A.2 A Note on Choked Flow.

Birkhoff,Plesset and Simmons (Ref. 7) have investigated wall effects in plane cavity flow.

In that paper , they consider plane flows in a choked condition for various stream limiting boundaries including a straight wall and a free jet. In the former case , they find C_D and Q as functions of H/C using an infinite cavity model in all cases. Their results therefore show $C_D \to \infty$ as $H/C \to 1$, as does graph [A3]. This is , however , misleading since Q also tends to infinity in their case. They do not give results for the transition region between infinite stream flow and choked flow , which shows the drag falling , at a given Q , as the flow nears the choked condition.

NOTATION

The following is the notation used in this thesis. The author has attempted as far as possible to adhere to a single universal notation , but in some sections a common symbol may have a localized meaning different from that given below. When that occurs the definition is given in the text.

a	Equal to $f - f_U$.
B	The maximum radius or half-height of the cavity.
c	The fractional mesh length which locates , with $k = K$, the boundary of symmetry of the Riabouchinsky flow.
C	The radius of the disc or half-height of the flat plate.
C_p	The coefficient of pressure.
C_D	The coefficient of drag.
d^1_k d^2_k d^3_k	The differences in the values of f between a point on the free streamline boundary and the surrounding mesh points.
e^i	The error after i iterations between the value of f at a mesh point and the final , converged value at that point.
$[E]$	The matrix of e .
E	The error involved in the substitution for a differential equation of its finite difference equivalent.
E* E**	Two other error terms which are functions of E.
f	The value of r^2, where r is the radial variable in the physical plane.
f_U	The asymptotic , upstream value of f on a particular streamline.
f**	The exact solution of the differential equation at a particular mesh point.
f*	The solution of the finite difference equations.

f' The analytic function used in the neighbourhood of a singularity.

Fr The Froude number.

g The acceleration due to gravity. When subscripted it refers to the difference in the value of f_U on the streamlines $j = j + 1$ and $j = j$.

H The radius or half-height of the channel.

i Either the complex quantity or the number of iterations.

j The mesh line streamline numbering integer in the φ, Ψ plane.

J The value of j for the channel wall streamline.

J* A mesh size change-over value of j.

k The equipotential mesh line numbering integer in the φ, Ψ plane.

K The value of k for the equipotential just upstream of the plane of symmetry of the Riabouchinsky flow.

K_4 A special value of k, referring to a point on the free streamline at which linearization of the d_k' differences commences.

K_2
K_3 Quantities describing the singular behaviour of the flow at the point of flow separation from the disc.

K_1^*
K_2^*
K_3^* Quantities describing the singular behaviour of the flow at the point of flow separation from the sphere.

L_1 The axial distance between the upstream boundary and the stagnation point in the physical plane.

L The half-length of the cavity.

m The mesh length in the Ψ direction.

m* The relative mesh length in the Ψ direction.

M^p As a differential operator, $\frac{\partial^p}{\partial \Psi^p}$

$[M]$ To denote a matrix of f values.

n The mesh length in the φ direction. In section 3.4 it denotes the coordinate perpendicular to the body streamline at separation.

n* The relative mesh length in the φ direction.

N^P	As the differential operator , $\frac{\partial^P}{\partial \varphi^P}$.
N	When subscripted in section 3.4 , it refers to a coefficient in the expansion for n.
p	Pressure.
p_v	Vapour pressure.
P_j^n	Used to denote an unknown constant where n is any integer.
P	The number of equal intervals on the wetted surface.
q	Fluid velocity magnitude.
Q	Cavitation number.
Q_i	Incipient cavitation number or index.
Q_k or Q_{kk}	The local cavitation number , calculated at a mesh point on the free streamline boundary.
ΔQ_k	The residual , $Q_{kk} - Q$.
r	The radial variable measured from the axis in axisymmetric problems.
r*	Equal to $r - r_s$.
R	The radius of the sphere or cylinder.
Re	The Reynolds number.
s	The arc length measured along a streamline. In section 3.4 , it denotes the coordinate parallel to the tangent to the body streamline at separation.
S	When subscripted , this refers to a coefficient of the expansion of s in section 3.4 .
t_1 , t_2	Coordinates of a transformed plane in section 3.4 .
t	Time, except in section 3.4 and section 1.5 .
u, v, w	Components of velocity in the directions Ox , Oy or Or , Oz .
U	The uniform stream velocity.
w	The complex potential function , $\varphi + i\psi$. In section 3.4 it denotes the perturbation velocity potential , $-\varphi + s$.
W	A coefficient in the expansion for the perturbation velocity potential , w , in section 3.4 .

x	The coordinate measured parallel to the uniform stream direction.
X	The special parameter , $\frac{\psi_H}{\varphi_s f_H}$.
y	The coordinate measured perpendicular to the uniform stream direction.
Y	The residual at a mesh point. In section 3.4 , it refers to a coefficient in the expansion for φ .
z	The complex variable , $x + iy$, or the third dimensional coordinate.
Z	The extra-residual applied at mesh points near a singularity. In section 3.4 , it refers to a coefficient in the expansion for ψ .

GREEK SYMBOLS.

α_1	The parameter used in the second free streamline method.
α_2	The maximum movement parameter in the free streamline methods.
β	The parameter used in the first free streamline method.
λ	The eigenvalue of the error matrix with the largest spectral radius. Or , in section 4.1 a function of Q .
Ψ	Stokes stream function.
φ	Velocity potential.
φ_L	The difference in potential between the upstream boundary and the stagnation point.
φ_s	The difference in potential between the stagnation and separation points.
φ_F	The difference in potential between the separation point and the point of maximum radius of the cavity.
Ω	The complex quantity , $\ln (U/q)$.
ρ	Density.
ω	The over-relaxation factor.

θ	The angle between the direction of the flow velocity vector and the uniform stream direction.
Υ	$\Omega + i\theta$.

SUBSCRIPTS.

a	A value at a reference point.
c	A value on the free streamline or within the cavity.
E^*	A value at the mesh point just downstream of stagnation.
H	A value on the channel wall.
j,k	A value at a mesh point using the field system of identification.
$0,1,2,3,\cdots$	A value at the points 0,1,2 ... in the local system of identification.
k	Used as j,k when j = 0.
j	Used as j,k when the value is the same for all k.
S	A value at the separation point.
STAG OR E	A value at the stagnation point.

REFERENCES

(1) Armstrong,A.H.and Dunham,Miss J.H. (1953). Axisymmetric Cavity Flow. Report.Res.Est.,Gt.Br. No. 12/53.

(2) Armstrong,A.H. (1953). Abrupt and smooth separation in plane and axisymmetric cavity flow. Memor.Arm.Res. Est.,Gt.Br. No. 22/53.

(3) Armstrong,A.H. and Tadman,K.G. (1954). Axisymmetric Cavity Flow about Ellipsoids. Proc.Jt.Adm.-U.S.N. Meet. on Hydroballistics.

(4) Arnoff,E.L. (1951). Re-entrant jet theory and cavity drag for symmetric wedges. U.S.Navord.Rep.1298 NOTS 368.

(5) Birkhoff,G. (1950). Hydrodynamics. Princeton Univ. Press.

(6) Birkhoff,G. and Zarantonello,E.H. (1957). Jets,wakes and cavities. Acedemic Press,N.Y.

(7) Birkhoff,G.,Plesset,M.and Simmons,N. (1950). Wall effects in cavity flows,I. Quart.Appl.Math. 8. Ibid. II. Quart.Appl.Math. 9 (1952).

(8) Brillouin,M. (1911). Les surfaces de glissement de Helmholtz et la resistance des fluides. Ann.de Chim. Phys. 23.

(9) Brunauer,E.A. (1951). Axially symmetric free streamline flows about tandem discs. Illinois Inst.Tech.

(10) Eisenberg,P.and Pond,H.L. (1948). Water tunnel investigations of steady state cavities. David Taylor Model Basin Rep.No. 668.

(11) Fisher,J.W. (1944). The drag on a circular plate generating a cavity in water. Underwater Ball.Committee No. 17.

(12) Fox,L. (1962). Numerical Solution of Ordinary and Partial Differential Equations. Pergamon Press,Oxford.

(13) Garabedian,P.R. (1955). Calculation of axially symmetric cavities and jets. Pacif.J.Math.,6.

(14) Gadd,G.E. (1962). Two dimensional separated or cavitating flow past a flat plate normal to the stream. N.P.L. Ship Rep.No. 38.

(15) Gadd,G.E.and Grant,S. (1966). Some experiments on cavities behind disks. N.P.L.Ship Rep.No. 78.

(16) Gilbarg,D. (1960). Jets and Cavities. Enc.Phys., Vol. 9 , Berlin.

(17) Gilbarg,D.and Rock,D.H. (1945). On two theories of plane potential flows with finite cavities. Memor. U.S.Naval Ord.Lab.Rep.No. 8718.

(18) Gurevich,M.I. (1965). Theory of jets in ideal fluids. Acedemic Press,N.Y.and London.

(19) Hsu,E-Y.and Perry,B. (1954). Water tunnel experiments on spheres in cavity flow. Hydro.Lab.,Cal.Inst.of Tech.,Rep.No. E-24.9.

(20) Helmholtz,H.von (1868). Uber discontiniuerliche Flussigkeitsbewegungen. Mber.Ber.Akad.Wiss.23.

(21) Holl,J.W. (1960). An effect of air content on the occurence of cavitation. Trans.ASME,Jnl.Basic Engg., Vol. 82.

(22) Holl,J.W.and Wislicenus,G.F. (1961). Scale effects on cavitation. Trans.ASME.,Jnl.Basic Engg.,Vol. 83.

(23) Kirchhoff,G. (1869). Zur Theorie freier Flussigkeitsstrahlen. J.Reine Angew.Math. 70.

(24) Konstantinov,V.A. (1950). Influence of Reynolds number on the separation (cavitation) flow. David Taylor Model Basin,Trans. 233.

(25) Lamb,H. (1932). Hydrodynamics. 6th ed.,Camb.Univ. Press.

(26) Landweber,L. (1951). The axially symmetric potential flow about elongated bodies of revolution. David Taylor Model Basin,Rep. 761.

(27) Levi-Civita,T. (1907). Scie e leggi di resistenzia. Rend.cir.mat.,Palermo 23.

(28) Levinson,N. (1946). On asymptotic shape of cavity behind an axi-symmetric nose moving through an ideal fluid. Ann.Math., 47.

(29) Lighthill,M.J. (1949). A note on cusped cavities. Rep.Memor.Aero.Res.Coun.,London,No. 2328.

(30) Milne-Thomson,L.M. (1949). Theoretical Hydrodynamics. (2nd ed.),Macmillan,London.

(31) Munk,M. (1935). Fluid Mechanics. Vol. 1 , Part 2, Berlin.

(32) N.P.L. (1961). Modern Computing Methods. 2nd Ed., H.M.S.O.,London.

(33) Plesset,M.S.and Shaffer,P.A. (1948). Cavity drag in two and three dimensions. Jnl.Appl.Phys. 19,No. 10.

(34) Reichardt,H. (1945). The physical laws governing the cavitation bubbles produced behind solids of revolution in a fluid flow. Kaiser Wilhelm Inst.Hyd.Res., Gottingen. TPA3/TIB. Trans. Acsil/49/1499.

(35) Reichardt,H.and Munzner,H. (1950). Rotationally symmetric source-sink bodies with predominantly constant pressure distributions. Arm.Res.Est.Trans.No. 1/50.

(36) Riabouchinsky,D. (1920). On steady fluid motion with free surfaces. Proc.Lond.Math.Soc. 19.

(37) Ripken,J.F.and Killen,J.M. (1959). A study of the influence of gas nuclei on scale effects and acoustic noise for incipient cavitation in a water tunnel. St.Anthony Falls Hyd.Lab.,Univ.Minnesota,Tech. Paper 27,Ser. B.

(38) Rouse,H.and McNown,J.M. (1948). Cavitation and pressure distribution : headforms at zero angles of yaw. State Univ. Iowa,Stud.in Engg.,Bull. 32.

(39) Russell,D.B. (1963). The numerical solution of problems in fluid flow. Thesis submitted for D.Phil., Oxford.

(40) Silverleaf,A. (1963). A survey of some recent basic studies of cavitation phenomenon. Note presented to 10th Int.Towing Tank Conf.,London. N.P.L. Ship Rep. T.M.29.

(41) Silverleaf,A.and Berry,L.W. (1962). Propellor cavitation as influenced by the air content of the water. Int.Assn.of Hyd.Res.,Sendai,Japan. N.P.L. Ship Rep. 31.

(42) Southwell,R.V. (1948). Relaxation methods in mathematical physics. O.U.P.

(43) Southwell,R.V.and Vaisey,G. (1946). Fluid motions characterized by free streamlines. Phil.Trans.240.

(44) van der Walle,F. (1962). On the growth of nuclei and the related scaling factors in cavitation inception. 4th ONR Symp.Naval Hyd.,Wash.D.C.

(45) Waid,R.L. (1957). Water tunnel investigations of two dimensional cavities. Hyd.Lab.,Cal.Inst.of Tech., Rep.No. E-73.6.

(46) Woods,L.C. (1951). A new relaxation treatment of flow with axial symmetry. Quart.Jnl.of Mech.and Appl.Math. 4,3.

(47) Woods,L.C. (1951). The relaxation treatment of singular points in Poissons equation. Quart.J. Mech. and Appl.Math.,6,2.

(48) Woods,L.C. (1961). The theory of subsonic plane flow. Camb.Univ.Press.